

**From cell penetrating peptides to peptoids and polyamines as novel
artificial molecular transporters**

(Entwicklung neuer *Delivery*-Strategien für siRNAs
Von zellpenetrierenden Peptiden zu Peptoiden und Polyaminen
als neuartige molekulare Transporter)

Dissertation

zur

Erlangung des Doktorgrades (Dr. rer. nat.)

der

Mathematisch-Naturwissenschaftlichen Fakultät

der

Rheinischen Friedrich-Wilhelms-Universität Bonn

vorgelegt von

Katja Schmitz

aus

Andernach

Bonn 2005

Angefertigt mit Genehmigung der Mathematisch-Naturwissenschaftlichen Fakultät
der Rheinischen Friedrich-Wilhelms-Universität Bonn

1. Referent: Prof. Dr. K. Sandhoff
2. Referent: Prof. Dr. S. Bräse

Tag der Promotion: 18.02.2005

Diese Dissertation ist auf dem Hochschulschriftenserver der ULB Bonn
http://hss.ulb.uni-bonn.de/diss_online elektronisch publiziert.

Erscheinungsjahr: 2005

Hiermit versichere ich, dass ich diese Arbeit selbstständig und ohne jede unerlaubte Hilfe angefertigt habe, dass diese oder eine ähnliche Arbeit noch keiner anderen Stelle zur Prüfung vorgelegen hat und dass sie an den nachstehend aufgeführten Stellen auszugsweise veröffentlicht worden ist.

Ort, Datum

Katja Schmitz

Auszugsweise Veröffentlichung:

Diallo, M; Schmitz, K; Schepers, U (2004) *“RNA Interference: RNAid for Future Therapeutics?”* The Oncogenomics Handbook: *Understanding and Treating Cancer in the 21 st Century*. Eds. LaRochelle, W., Shimkets, A., Humana Press.

Noch nicht erschienene Veröffentlichungen:

Schmitz, K; Schepers, U (2004) *“Cell penetrating peptides in siRNA delivery”* Expert Opin. Biol. Ther. *im Druck*,

Schmitz, K; Schepers, U *“Silencio: RNA interference – the tool of the new millennium?”* Biol. Chem. *eingereicht*,

Schmitz, K; Diallo, M; Mundegar, R; Schepers, U *„pepsiRNAs for RNAi in mammals“*, *eingereicht*,

Schmitz, K; Hahn, F; Balaban TS; Bräse, S; Schepers, U *“Covalent coupling of porphyrins with novel molecular transporters enhance their antitumor activity”*, *eingereicht*,

Schmitz, K, Hahn, F, Schepers, U *„Modification of 2´,3´-O,O-isopropylidene guanosine leads to an improved yield in the synthesis of 5´-deoxy-5´-thioguanosine-monophosphorothioate“*, *eingereicht*.

Für meine Eltern
und
für Oma Lucia

Acknowledgement

I thank Dr. Ute Schepers for her excellent support in all aspects of this work, for her commitment, for hours of fruitful discussions and for teaching me all the essentials of scientific life. Thanks for enabling me to attend all these interesting meetings, to work on these exciting projects and for encouraging me to surpass my own limits.

I thank Prof Sandhoff for his generous support of this work and for his advice.

I thank Prof. Dr. Bräse for the collaboration on novel peptoid and polyamine transporters and for kindly assuming the correferate.

Many thanks to my lab fellows for their scientific support, refreshing coffee breaks, and bench-to-bench chats. I thank all my colleagues for the friendly atmosphere in lab.

Thanks to Dr. Rustam Mundegar and Margit Zweyer for providing murine GFP-myocytes and for fruitful discussions. Thanks also to Prof. Dr. A. Wernig, permitting me to carry out the experminets on these cells in the Institute of Physiologie II.

Many thanks to Miqiang Chai (DKFZ Heidelberg) for his enthusiastic collaboration during the first tests of enzymatically generated pepsRNAs.

Thanks to Heike Hupfer for measuring the MALDI-TOF mass spectra.

I am grateful to Claus Schmidt and Ulrike Weynand for their advice and support with the NMR experiments. Many thanks to Volkmar Fieberg for his friendly support with the work on the ÄKTA FPLC.

Thanks to Tina Schröder and Yvonne Schmidt for their collaboration and for kindly providing the fluorescently labeled peptoid transporters and the spermine derivatives.

I want to thank all my students who participated in this work during their practicals. My special thanks goes to Henning Breyhan for his work on the Tat vectors and test expression experiments and for his commitment in the establishment of the synthesis lab 2.132, to Frank Hahn who joined me in the search for improved guanosine derivatives for GSMP synthesis, and to Timo Mack for his work on the GSMP synthesis and siRNA preparation.

Thanks to the Fonds der Chemischen Industrie, who financially supported me by a doctorate scholarship, which greatly helped me to focus on my research work and permitted me to attend many scientific meetings that have been a good motivation for my work.

I thank the Bonner Forum für Biomedizin for the two poster prizes, that allowed me to take part in some motivation scientific meetings. Thanks also to the German Scholarship foundation for the idealistic doctorate fellowship by which I got to meet many people, who inspired my work.

I am grateful to all of my friends for the gorgeous time I could spent in Bonn with all its Sneak Preview nights, visits to Cologne, opera visits and long nights of chatting and celebrating.

Special thanks to Jan, Vanessa and Jenny for never getting tired of reminding me that there is indeed a life outside the lab. Thanks also to the neuroscience reading group for the inspiring excursions into the world of cognition processes. Many thanks to all those who encouraged me so much during the last part of this work.

Finally, this work would not have been possible without the support of my parents who greatly helped me through the dark times of this work and always found some ways to cheer me up. Thank you very much for the unforgettable journeys we undertook together, for all these relaxing weekends and long chats on the phone.

Table of contents

| | |
|---|-----|
| Table of contents..... | 1 |
| Abbreviations..... | 5 |
| 1 Introduction | 8 |
| 1.1 RNA interference | 8 |
| 1.1.1 The study of gene function | 8 |
| 1.1.2 The discovery of RNAi | 10 |
| 1.1.3 RNAi is a highly conserved eukaryotic mechanism | 10 |
| 1.1.4 The molecular basics of RNAi | 12 |
| 1.1.5 The many roles of small endogenous RNAs | 15 |
| 1.1.6 RISC is responsible for mRNA cleavage and transcriptional repression..... | 17 |
| 1.1.7 The role of RNA dependent RNA polymerases (RdRps)..... | 22 |
| 1.1.8 RNAi in mammalian cells..... | 22 |
| 1.1.9 Stable RNAi in mammalian cells..... | 24 |
| 1.1.10 Viral vectors to trigger RNAi | 26 |
| 1.1.11 Cure for diseases..... | 27 |
| 1.1.12 Non-specific effects of siRNAs | 32 |
| 1.1.13 Modifications of siRNAs for in vivo applications | 33 |
| 1.1.14 The delivery issue..... | 36 |
| 1.2 Cell-penetrating peptides and their small molecule analogs..... | 38 |
| 1.2.1 The delivery issue..... | 38 |
| 1.2.2 Cellular uptake mechanisms..... | 38 |
| 1.2.3 Passive transport by diffusion..... | 38 |
| 1.2.4 Active transport by transmembrane transporters..... | 39 |
| 1.2.5 Active transport by endocytosis | 40 |
| 1.2.6 Common methods of delivery | 41 |
| 1.2.7 Membrane penetration by peptides and proteins | 46 |
| 1.2.8 The discovery of protein transduction..... | 46 |
| 1.2.9 Cell-penetrating peptides..... | 50 |
| 1.2.10 Modifications to optimize CPPs | 53 |
| 1.2.11 Synthetic molecules to mimic CPPs | 56 |
| 1.2.12 The versatility of CPPs | 59 |
| 1.2.13 The mechanism of peptide-based delivery | 65 |
| 2 Aims of this work | 74 |
| 3 The concept of pepsirNAs | 74 |
| 3.1 Design and synthesis of thiol-modified siRNAs | 78 |
| 3.1.1 Synthesis of GSMP..... | 82 |
| 3.1.2 Purification of GSMP | 91 |
| 3.1.3 <i>in vitro</i> transcription of siRNAs from T7-DNA-oligonucleotides..... | 93 |
| 3.1.4 Coupling of 5'-thiol modified siRNAs to Penetratin™ | 96 |
| 3.1.5 Gel electrophoresis with pepsirNAs | 97 |
| 3.1.6 MALDI-TOF mass spectrometry of pepsirNAs | 98 |
| 3.2 Test of pepsirNAs for their potential to trigger RNAi <i>in vivo</i> | 100 |

| | | |
|-------|--|-----|
| 3.2.1 | Targeting recombinant genes with pepsirNAs..... | 100 |
| 3.2.2 | pepsirNAs to knock out Lamin A/C in HeLa cells | 101 |
| 3.2.3 | PepsirNAs to knock out proteins of the sphingolipid metabolism in fibroblasts 102 | |
| 3.2.4 | Test of pepsirNAs in various mammalian cell lines | 104 |
| 3.3 | Recombinant expression of CPPs in <i>E. coli</i> | 105 |
| 3.3.1 | Generation of a recombinant expression vector for modified CPPs | 106 |
| 3.3.2 | Expression of GST-CPPs in <i>E. coli</i> | 108 |
| 3.3.3 | Purification of GST-CPP fusion proteins by affinity chromatography | 109 |
| 3.3.4 | Refining of the purification protocol for GST-fusion proteins for GST-CPPs .. | 111 |
| 3.4 | Expression of TEV protease in <i>E. coli</i> | 113 |
| 3.4.1 | Expression of GST-TEV-protease in <i>E. coli</i> | 114 |
| 3.4.2 | Expression of His ₆ -TEV-protease from <i>E. coli</i> | 117 |
| 3.4.3 | Cleavage of GST-CPP fusion proteins with TEV protease..... | 120 |
| 3.5 | Novel cell-penetrating molecules for the delivery of siRNAs | 122 |
| 3.5.1 | Preliminary tests of polyamines | 123 |
| 3.5.2 | Spermine-coupled porphyrin for photodynamic therapy | 124 |
| 3.5.3 | Solid phase synthesis of peptoid transporters | 130 |
| 3.5.4 | Cellular uptake of fluorescein-labeled peptoids | 134 |
| 4 | Discussion..... | 145 |
| 5 | Materials and methods..... | 156 |
| 5.1 | Bacteria culture | 156 |
| 5.1.1 | Culture conditions | 156 |
| 5.1.2 | Storage | 156 |
| 5.1.3 | Generation of competent cells | 156 |
| 5.1.4 | Transformation and selection | 156 |
| 5.2 | Cell culture techniques for mammalian cells..... | 157 |
| 5.2.1 | General procedures | 157 |
| 5.2.2 | Storage of mammalian cells in liquid nitrogen | 157 |
| 5.2.3 | Preparation of FCS-coated cover slips | 157 |
| 5.2.4 | Treatment of adherent cells with pepsirNAs..... | 157 |
| 5.2.5 | Transfection of adherent cells with siRNAs | 158 |
| 5.2.6 | Treatment of suspension cultures with pepsirNAs | 158 |
| 5.2.7 | Treatment of adherent cells with novel cell permeating molecules | 158 |
| 5.2.8 | Fixation of cells for microscopy..... | 159 |
| 5.2.9 | Preparation of cells grown on cover slips for immunofluorescence microscopy 159 | |
| 5.3 | DNA-Techniques..... | 160 |
| 5.3.1 | Photometric measurement of nucleic acid concentration | 160 |
| 5.3.2 | Separation of DNA by agarose gel electrophoresis..... | 160 |
| 5.3.3 | Extraction of DNA from agarose gels | 160 |
| 5.3.4 | Synthetic gene cloning..... | 160 |
| 5.3.5 | Enzymatic restriction of plasmids | 160 |
| 5.3.6 | Ligation of DNA-fragments | 161 |

| | | |
|--------|--|-----|
| 5.3.7 | Plasmid isolation from recombinant bacteria cells | 161 |
| 5.3.8 | PCR : <i>in vitro</i> amplification of DNA | 161 |
| 5.3.9 | Mutagenesis-PCR..... | 162 |
| 5.4 | RNA techniques | 163 |
| 5.4.1 | Isolation of RNA | 163 |
| 5.4.2 | Separation of dsRNA | 163 |
| 5.4.3 | RT-PCR | 163 |
| 5.4.4 | <i>In vitro</i> generation of 5'-thiol-modified siRNAs with T7-polymerase | 164 |
| 5.4.5 | Reduction of homodimers of 5'-thiol-modified siRNAs | 164 |
| 5.4.6 | Coupling of synthetic siRNA and CPP..... | 164 |
| 5.4.7 | Coupling of enzymatically synthesized siRNA and CPP | 165 |
| 5.4.8 | Radiolabelling of siRNAs | 165 |
| 5.4.9 | Analysis of siRNAs on sequencing gels | 165 |
| 5.5 | Protein techniques | 165 |
| 5.5.1 | Preparation of protein samples..... | 165 |
| 5.5.2 | SDS-PAGE | 166 |
| 5.5.3 | Protein staining with Coomassie Brilliant Blue R250 | 166 |
| 5.5.4 | Silver staining of protein gels..... | 166 |
| 5.5.5 | Western blot..... | 166 |
| 5.5.6 | Quantitative measurement of protein concentrations | 167 |
| 5.5.7 | Protein expression in bacteria | 167 |
| 5.5.8 | Preparation of native GST-fusion proteins (pGEX protocol)..... | 168 |
| 5.5.9 | Preparation of native GST-fusion proteins (modified protocol)..... | 168 |
| 5.5.10 | Preparation of native TEV-protease | 168 |
| 5.5.11 | Preparation denaturing of TEV-protease from inclusion bodies | 169 |
| 5.5.12 | Purification of GST-fusion proteins on glutathione-sepharose | 169 |
| 5.5.13 | Preparation of sepharose beads..... | 169 |
| 5.5.14 | Regeneration of GST-sepharose beads | 169 |
| 5.5.15 | Native preparation of His ₆ -TEV from <i>E. coli</i> | 170 |
| 5.5.16 | Denaturing preparation of His ₆ -TEV from <i>E. coli</i> | 170 |
| 5.5.17 | Purification of His ₆ -fusion proteins on Ni-NTA-sepharose | 170 |
| 5.5.18 | Dialysis | 171 |
| 5.5.19 | Cleavage of GST-fusion peptides with TEV | 171 |
| 5.5.20 | Handling of Penetratin TM | 171 |
| 5.6 | Chemical syntheses..... | 172 |
| 5.6.1 | Thin layer chromatography | 172 |
| 5.6.2 | NMR spectroscopy | 172 |
| 5.6.3 | Long-term NMR measurements | 172 |
| 5.6.4 | Mass spectroscopy | 173 |
| 5.6.5 | Anion exchange chromatography | 173 |
| 5.6.6 | Reversed phase HPLC | 174 |
| 5.6.7 | 2',3'-O,O-Isopropylidene-guanosine, (10) | 174 |
| 5.6.8 | 2',3'-O,O-Isopropylidene-5'-deoxy-5'-iodoguanosine, (11) | 175 |
| 5.6.9 | <i>N,N</i> -Dimethylaminomethylene-2',3'-O,O-isopropylidene-guanosine (12) | 175 |

| | | |
|--------|---|-----|
| 5.6.10 | <i>N,N</i> -Dimethylaminomethylene-2',3'- <i>O</i> , <i>O</i> -isopropylidene-5'-deoxy-5'-iodoguanosine (13): | 176 |
| 5.6.11 | 5'-Deoxy-5'-iodoguanosine (14): | 177 |
| 5.6.12 | 5'-Desoxy-5'-thioguanosine-monophosphorothioate (GSMP) (15): | 177 |
| 5.6.13 | 2',3'- <i>O</i> , <i>O</i> -Isopropylidene- 3,5'- <i>C</i> - cycloguanosine (20) | 178 |
| 5.6.14 | <i>N,N</i> -dimethylaminomethylene-2',3'- <i>O</i> , <i>O</i> -isopropylidene-3,5'- <i>C</i> -cycloguanosine (21) | 178 |
| 5.7 | Buffers and solutions | 179 |
| 5.7.1 | Cell culture | 179 |
| 5.7.2 | Protein expression | 179 |
| 5.7.3 | Protein purification | 180 |
| 5.7.4 | Gel electrophoresis | 181 |
| 5.7.5 | Western blotting | 182 |
| 5.7.6 | DNA/RNA techniques | 182 |
| 5.7.7 | Synthesis | 182 |
| 5.8 | Material | 183 |
| 5.8.1 | Apparatus | 183 |
| 5.8.2 | Consumables | 184 |
| 5.8.3 | Antibodies | 184 |
| 5.8.4 | Purification kits | 185 |
| 5.8.5 | Enzymes and markers | 185 |
| 6 | Oligonucleotides and Peptides | 185 |
| 6.1.1 | Radioactivity | 185 |
| 6.1.2 | Bacterial Strains | 185 |
| 6.1.3 | Cell Lines | 185 |
| 6.1.4 | Vectors | 186 |
| 6.1.5 | Chemicals | 187 |
| 7 | References | 188 |
| | Summary | 221 |

Abbreviations

| | |
|---------|--|
| µg | microgramm |
| µl | microliter |
| µM | micromolar |
| aa | amino acid |
| AA | acrylamide |
| AB | antibody |
| AntP | antennapedia (3 rd helix) peptide |
| Antp-HD | antennapedia-homeodomain |
| APS | ammonium persulfate |
| as | antisense |
| ATP | adenosine triphosphate |
| BMP | bis(monoacyl)glycerophosphate |
| bp | base pairs |
| BSA | bovine serum albumine |
| CAPS | 3-(cyclohexyl)amino-1-propansulfonic acid |
| CD | circular dichroism |
| cDNA | copy- deoxyribonucleic acid |
| CF | carboxyfluorescein |
| CH | cyclohexane |
| CIP | calf intestinal phosphatase |
| CNEt | cyanoethyl |
| CPP | cell-penetrating peptide |
| CV | column volume |
| Cys | cysteine |
| Cyt | cytohesin |
| dATP | deoxy-adenosinetriphosphate |
| DCM | dichloromethane |
| dCTP | deoxy-cytosinetriphosphate |
| DEAE | 2-(diethylamino)ethyl |
| ER | endoplasmic reticulum |
| dGTP | deoxy-guanosinetriphosphate |
| DIPEA | <i>N,N</i> -diisopropylethylamine |
| DMEM | Dulbeccos modified Eagle medium |
| DMF | <i>N,N</i> -dimethylformamide |
| DMSO | dimethylsulfoxide |
| DNA | deoxyribonucleic acid |
| dNTP | deoxy-nucleotidetriphosphate |
| ds | doublestranded |
| dsRBD | dsRNA binding domain |
| DTDP | dithiodipyridine |
| DTT | dithiothreitol |
| dTTP | deoxy-thymidinetriphosphate |

| | |
|-------------------|---|
| EDTA | ethylenediaminetetraacetate |
| EE | ethyl acetate |
| FACS | fluorescence activated cell sorting |
| FCS | fetal calf serum |
| FITC | fluorescein isothiocyanate |
| GaCS | galactosylceramide synthase |
| GCS | glucosylceramide-synthase |
| GFP | green fluorescent protein |
| GSMP | 5'-deoxy-5'-thioguanosine monophosphorothioate |
| GST | glutathione-S-transferase |
| h | hour |
| HEPES | [4-(2-hydroxyethyl)-piperazino]-ethanesulfonic acid |
| HOBt | 1-hydroxybenzotriazole |
| HOX | homeobox protein |
| HRP | horse radish peroxidase |
| Hz | Hertz (1/s) |
| IPTG | isopropyl-thiogalactopyranoside |
| k.o. | knock-out |
| kDa | kilodalton |
| LB | Luria Bertani medium |
| LCAA | long chain alkyl amino |
| LTR | long terminal repeat |
| LUV | large unilamellar vesicle |
| mA | milliampere |
| MCS | multiple cloning site |
| MEM | minimum essential Eagle medium |
| min | minute |
| ml | milliliter |
| mM | millimolar |
| MOI | multiplicity of infection |
| MPM | membrane permeable motif |
| mRNA | messenger RNA |
| NLS | nuclear localization sequence |
| nM | nanomolar |
| NTA | nitrilo acetic acid |
| OD ₆₀₀ | optical density measured at 600 nm |
| ODN | oligodeoxyribonucleotide |
| ORF | open reading frame |
| ori | origin of transcription |
| PA | polyacrylamide |
| PAGE | polyacrylamide-gelelectrophoresis |
| PBS | phosphate buffered saline |
| PCR | polymerase chain reaction |
| PFA | paraformaldehyde |

| | |
|--------|---|
| pGEX | plasmid for glutathion-S-transferase expression |
| PKR | proteinkinase R |
| PNA | peptide nucleic acid |
| PolH | polyhedrin promoter |
| PorSp | porphyrin-labeled spermine |
| ppm | parts per million |
| pSAP | precursor of sphingolipid activator protein |
| PTD | protein transduction domain |
| PyBrOP | bromo-tris(pyrrolidino)phosphonium-hexafluoro-phosphate |
| RNA | ribonucleic acid |
| RNase | RNA-cleaving enzyme |
| rpm | revolutions per minute |
| RT | room temperature |
| SAP | sphingolipid activator protein |
| SDS | sodium dodecyl sulfate |
| SFM | serum free medium |
| siRNA | short interfering RNA |
| SLDB | science lab database |
| SPS | solid phase synthesis |
| ss | single stranded |
| SUV | small unilamellar vesicle |
| TAE | Tris acetate EDTA |
| Tat | transactivator of transcription |
| TBAB | tetrabutylammoniumborohydride |
| TBS | Tris-buffered saline |
| TEA | triethylamine |
| TEAA | triethylamine acetate buffer |
| TEAB | triethylamine bicarbonate buffer |
| TEMED | N, N, N', N'-tetramethylenediamine |
| TEV | tobacco etch virus |
| TFA | trifluoroacetic acid |
| THAP | trihydroxyacetophenone |
| THF | tetrahydrofuran |
| TLC | thin layer chromatography |
| Tris | tris(hydroxymethyl)-aminomethane |
| u | units |
| V | volt |
| X-Gal | 5-chloro-4-bromo-3-indolyl- β -D-galactoside |

1 Introduction

1.1 RNA interference

The finding that double-stranded RNA (dsRNA) triggers the degradation of homologous mRNA is one of the most important recent discoveries. Since the first reports about this phenomenon in the late nineties, RNA interference (RNAi) has been broadly recognized by many disciplines ranging from functional genomics over biological chemistry to pharmacology. Today, the application of dsRNA to specifically silence genes at a posttranscriptional level (Posttranscriptional Gene Silencing, PTGS) has become a standard technique in the study of gene function, and it is on its best way to become a new weapon to combat disease triggered by RNA viruses, parasites or even mutations of the genome, like cancer or inherited diseases (Arenz and Schepers 2003; Schepers and Kolter 2001).

1.1.1 The study of gene function

Only half a century ago, Watson and Crick postulated the helical structure of DNA and its significance as the carrier of the hereditary information in all forms of life. Since then, large efforts were undertaken to understand the translation of genetic information into gene function and the sophisticated coordination of the mechanisms that govern life at a molecular level. The expression of genes in each individual cell needs to be highly regulated to activate the appropriate subset of genes for specific cellular functions or as responses to environmental changes.

At the turn of the millennium, the publication of the first draft version of the complete sequence of the human genome was a scientific milestone (Lander et al. 2001; Venter et al. 2001). The task resulting from this achievement is much greater: correlating approximately 30,000 open reading frames with the function of about 100,000 human proteins resulting from posttranslational modifications and alternative splicing of the RNA transcripts. This task is tackled by functional genomics or functionomics. Its solution is the prerequisite for an understanding of complex physiological functions and the key to the development of drugs against diseases.

Traditionally, functional genomics had to trace back inherited diseases from the protein defect to the responsible gene in a time consuming process. The generation of knock-out animals permitted the specific study of gene defects and their related phenotypes. However, the generation of knock-out animals is time consuming and laborious, defects in essential genes lead to lethality at early embryonic stages preventing phenotypic studies and not all results obtained in model organisms can be transferred to related species, which is especially true for humans and mice (Kolter and Sandhoff 1999).

The combination of large chemical libraries, high throughput screening and elaborate screening assays together with findings of classical genetics brought forth the field of "chemical genetics", holding high promises for drug development and functional genomics (Frank-Kamenetsky 2001; Stark et al. 1998).

By means of rationally designed synthetic inhibitors loss of function phenotypes can be generated in a short time. Although the lead structures can be optimized to binding

efficiencies in the nanomolar range and below (Frank-Kamenetsky 2001), they may also bind to unexpected sites on different molecules where they exhibit off-target effects. A recent example is the anti-inflammatory drug celecoxib, that was designed to selectively target cyclooxygenase (COX) 2 while sparing inhibition of COX-1, but exhibited an unexpected nanomolar binding affinity for members of the totally unrelated carbonic anhydrase family (Weber et al. 2004). Combinatorial chemistry and the use of chemical evolution allowed the development of aptamers as an important tool for gene function studies. These synthetic RNAs adopt a specific secondary structure by which they bind to either DNA, RNA, or proteins and thus down-regulate protein function (Famulok 1999; Sullenger et al. 1990). The free availability of genomic sequencing data opened the door to a rational design of synthetic inhibitors to any target gene and generating the corresponding loss-of-function phenotype in a straightforward fashion. The first step into this direction was taken in the early 1990s by antisense technology, in which complementary antisense-oligonucleotides bind to the target mRNA-sequence and thereby prevent its translation to the corresponding gene product (Brantl 2002). At first, single stranded RNA (ssRNA) was used, which is unstable toward degradation by ribonucleases. Many efforts have been made to improve the stability of the RNA ranging from protection groups on the ssRNA, thiol-modifications to stabilize the ribophosphate backbone, or peptide nucleic acids (PNAs) in which the nucleobases are bound to a peptide backbone. Antisense DNAs are not only more stable than RNA, but also form hybrid strands with mRNA that are degraded by RNase H. All these approaches require a saturation of all targeted mRNA strands with corresponding antisense agents to obtain the desired knock-down phenotype. This implies the use of more than stoichiometric amounts of antisense agent to inactivate present as well as newly transcribed mRNA until all remaining protein has been degraded. However, antisense techniques are a common method in the study of gene function and some specific modifications have made their way to clinical studies as potential drugs to suppress tumor function.

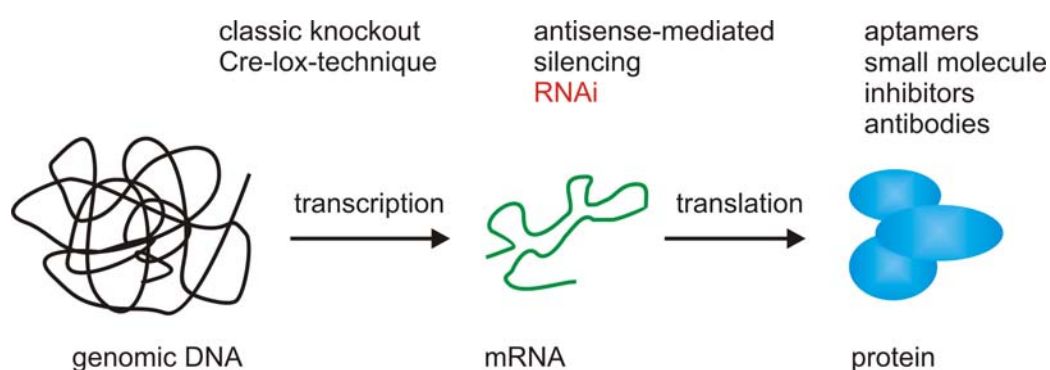


Figure 1-1 Dissecting the expression of gene products at different stages. Knock-out organisms and naturally occurring mutations alter the information stored in the DNA, protein inhibitors and aptamers bind to gene products and inhibit protein functions, antisense agents and RNAi act on the level of transcripts by preventing ribosomal binding or triggering its degradation. Naturally occurring or synthetic small molecules can be selected to target any of the three stages by high throughput screening.

1.1.2 The discovery of RNAi

New possibilities were opened up with the discovery of RNA interference that combines the advantages of rational design with a much higher efficiency in down-regulating the targeted gene-product. Therefore, it was soon adopted as the tool of choice in reverse genomics to study gene-protein relations in almost all eukaryotic organisms.

First hints at this phenomenon had come from antisense experiments in *C. elegans*, in which the sense control exhibited an unusually strong effect (Guo and Kemphues 1995). Assuming a contamination with asRNA in the sense control, Fire and Mello demonstrated that the simultaneous injection of two complementary RNA strands, and likewise the use of dsRNA, could specifically silence the corresponding gene product with an at least 10fold higher efficiency than conventional antisense reagents (Fire et al. 1998). Following this key discovery, it was shown that RNAi takes place at the posttranscriptional level where a dsRNA triggered molecular machinery causes the degradation of homologous mRNA (Montgomery and Fire 1998; Montgomery et al. 1998) identifying RNAi as a form of posttranscriptional gene silencing (PTGS).

In *C. elegans*, RNAi could not only be induced by injecting the dsRNA into the gut (Fire et al. 1998; Grishok et al. 2000), but also by soaking the worms in dsRNA solution (Tabara et al. 1998), introduction of transgenes that code for double stranded RNA (Tabara et al. 1999b; Tavernarakis et al. 2000) or feeding bacteria that recombinantly express double-stranded RNA constructs to the worms (Timmons and Fire 1998). Moreover, a systemic spread of the silencing effect was observed and it was even inherited to the progeny (Fire et al. 1998; Sijen et al. 2001b). Cultured cells transfected with dsRNA could keep up the silencing phenotype for up to 9 cell divisions (Tabara et al. 1998). However, the most important features of RNAi are its high specificity and efficiency: Substoichiometric amounts of dsRNA are sufficient to significantly reduce the amount of homologous mRNA within a few hours in a highly sequence specific manner (Fire et al. 1998). Other mRNAs, even those with point mutations, remain unaffected (Bosher and Labouesse 2000; Fire et al. 1998; Hunter 1999).

1.1.3 RNAi is a highly conserved eukaryotic mechanism

Posttranscriptional gene silencing (PTGS) had been previously reported in plants. In *Arabidopsis thaliana* the attempt to express an endogenous gene from a recombinant vector had led to a complete downregulation of the respective gene and the phenomenon had been termed cosuppression (Napoli et al. 1990). A related mechanism was found in the fungus *Neurospora crassa* where it became known as quelling (Cogoni and Macino 1997). In plants, the infection with RNA viruses expressing dsRNA was discovered to lead to immunity that limits the spread of the virus and prevents a second infection with the same virus, a phenomenon termed virus-induced gene silencing (Baulcombe 1999). Today, these related phenomena are often summarized as RNA silencing.

With a growing interest in RNAi, dsRNA triggered gene silencing was also found to be functional in *Drosophila melanogaster* (Kennerdell and Carthew 2000; Misquitta and Paterson 2000), plants (Hamilton and Baulcombe 1999) and *Trypanosoma brucei* (Ngo et al. 1998). It appeared that dsRNA-induced gene silencing is a highly conserved phenomenon. It

is assumed to be an ancient defense mechanism against RNA viruses (Ruiz et al. 1998; Voinnet 2001) and transposable elements (Ketting et al. 1999; Tabara et al. 1999a). Both produce dsRNA in the course of their replication. It may also be involved in the elimination of defective mRNAs by degradation (Plasterk 2002) and in the regulation of protein levels in response to environmental stimuli (McManus et al. 2002). In the course of evolution, organisms have developed alternative strategies to fulfil the same tasks, so that the main function of the dsRNA triggered silencing machinery varies from species to species.

The most prominent, and for RNAi scientists most troublesome, alternative mechanism was the induction of an interferon response upon the introduction of dsRNA into mammalian cells. Increased levels of β -interferon lead to an activation of RNase L, that non-specifically degrades all mRNAs, and of RNA-dependent protein kinase R (PKR), which in turn phosphorylates and thereby inactivates the transcription factor eIF2 α . This results in a shutdown of the global protein biosynthesis and thereby in apoptosis (Clemens 1997; Clemens and Elia 1997). Therefore, it was doubted that RNAi could be used to study mammalian organisms and the question arose whether the molecular machinery for RNAi was actually present in mammals.

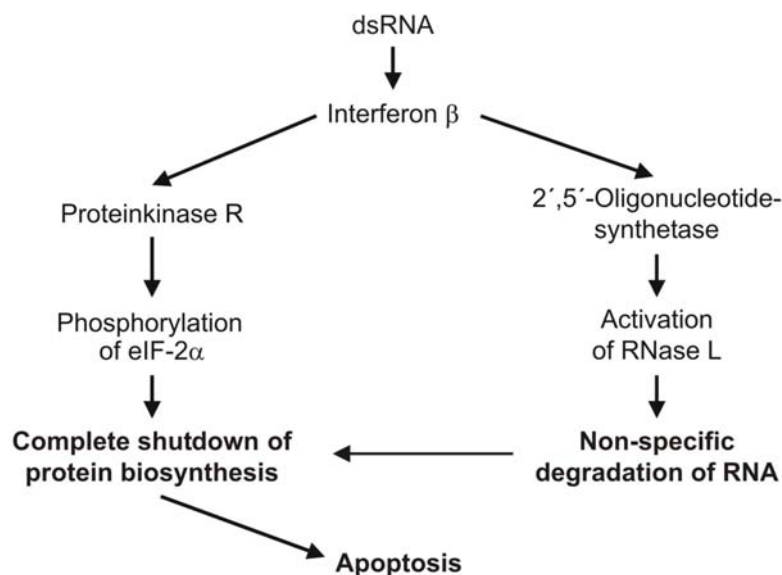


Figure 1-2 dsRNA triggers an interferon response in mammals. The different events triggered by interferon- β finally lead to apoptosis (Sledz et al. 2003).

Studies in mice oocytes and murine embryonic cancer cell lines, in which the innate defense mechanisms are not yet functional, proved that, indeed, RNAi works in mammalian cells (Billy et al. 2001; Wianny and Zernicka-Goetz 2000).

The milestone experiment was published by the Tuschl group (Elbashir et al. 2001a). They showed that RNAi could be induced in adult mammalian cells if the trigger dsRNA is short enough to omit the interferon response. dsRNAs of 21-25 nt exhibited the highest efficiency, whereas shorter dsRNAs were no longer recognized.

This opened the door to a broader application of RNAi. Not only could RNAi be utilized to link the genomic data from humans, mice, and other mammals to protein function, it also

constituted a new technique to combat diseases caused by viruses, parasites or genomic mutations as in inherited diseases and cancer.

1.1.4 The molecular basics of RNAi

The existence of an RNAi machinery in almost all eukaryotic organisms allowed the mutual exchange of results to elucidate its mechanism and thereby greatly enhanced the rate with which the insights into the molecular requirements grew.

The most intensively studied organisms in the quest for the mechanism of RNAi are *C. elegans* (Plasterk 1999; Smardon et al. 2000), *Arabidopsis* (Mourrain et al. 2000), *N. crassa* (Cogoni and Macino 1997, 1999b), *Drosophila* (Kennerdell and Carthew 2000), and mammals (Elbashir et al. 2001a). The fact that RNAi takes place in the cytosol greatly facilitated the experimental setup as cell extracts from flies or worms mimic the conditions of the cytosol (Hutvagner and Zamore 2002b; Kawasaki and Taira 2003; Zeng and Cullen 2002). This introduction focuses on the findings and developments in animals. Results obtained in plants are only cited if they contributed to the understanding of the molecular processes in animals.

The mechanism of RNAi can be divided into two steps. In the initiator step, dsRNA is cleaved into 21-25 nt long fragments. In the effector step, these so-called short interfering RNAs (siRNAs) are incorporated into a ribonucleotide protein complex (RNP) and serve as a molecular template to recognize homologous mRNA that is cleaved.

Discrete 21-25 nt small dsRNAs with a sequence complementary to the target sequence were first observed in transgene or virus-induced PTGS and co-suppression in plants (Hamilton and Baulcombe 1999) and it was assumed that these small dsRNAs constituted the active component in the examined silencing phenomena. The degradation of long dsRNA into 21-23-nt short dsRNAs was also found in *Drosophila* extracts (Zamore et al. 2000) and intact *Drosophila* embryos (Yang et al. 2000), Schneider 2 (S2) cells (Hammond et al. 2000) and *C. elegans* (Parrish et al. 2000). The Hannon group demonstrated that the short dsRNA species is associated with the nuclease activity that leads to the cleavage of the target mRNA (Hammond et al. 2000; Hutvagner et al. 2000). These findings suggested that the sequence specificity of RNAi was conveyed by the 21-23 nt dsRNA fragments cleaved from the trigger dsRNA, that became known as siRNAs (Zamore et al. 2000).

Closer examination of these short dsRNAs showed that functional siRNAs bear characteristic 3'-overhangs of 2 nucleotides on both strands (Hamilton and Baulcombe 1999) with nonphosphorylated hydroxyl groups (Elbashir et al. 2001c) that are essential for their recognition by the RNAi machinery.

At the same time, these features correspond to the characteristic cleavage pattern of nucleases of the RNase III family that specifically cleave dsRNA (Robertson et al. 1968). Indeed, proteins with homology to RNase III family members could be identified by homology screens of genomic data from *Drosophila*, *C. elegans*, and humans (Bass 2000; Bernstein et al. 2001; Billy et al. 2001; Ketting et al. 2001). In *Drosophila* two such homologs were found, that both comprise two RNase III domains (Bernstein et al. 2001). Tests upon their role in RNAi showed that cells deficient of either one of the two RNases exhibited neither RNAi activity nor did the cell extracts produce siRNAs from dsRNA. This confirmed that dsRNA is

indeed processed by an enzyme of the RNase III family. As it cleaves dsRNA into equally sized fragments it was named Dicer (Bernstein et al. 2001; Ketting et al. 2001). First studies, suggested that Dicer is loosely associated with ribosomes at the interface endoplasmic reticulum-cytosol (Billy et al. 2001; Provost et al. 2002).

Corresponding to the widespread occurrence of RNAi in nature, homologs of *Drosophila* Dicer have been found in all eukaryotic organisms ranging from *C. elegans* (Grishok et al. 2001; Hutvagner et al. 2001) and *Arabidopsis* (Jacobsen et al. 1999) to mammals (Zhang et al. 2002) and *Schizosaccharomyces pombe* (Volpe et al. 2002), with baker yeast *Saccharomyces cerevisiae* constituting the only known exception. In plants like *Arabidopsis*, up to 4 Dicer like enzymes (DCL) have been found (Schauer et al. 2002), while in vertebrates like mice or humans only one single homolog could be identified (Bernstein et al. 2003; Nicholson and Nicholson 2002). In general, Dicer-deficiency leads to developmental phenotypes (Carrington and Ambros 2003; Schauer et al. 2002) or even to lethality as in mice or zebrafish (Bernstein et al. 2003; Wienholds et al. 2003). In *Arabidopsis*, the action of different DCL enzymes leads to siRNAs of either 21 or 25 nt of which the shorter species is responsible for dsRNA cleavage while the longer species ascertains the systemic spread (Hamilton et al. 2002). Similarly, in wheat germ extracts, 21mers are cleaved from exogenous dsRNA while 24-25mers are derived from transgene derived dsRNA by a distinct Dicer ortholog (Tang et al. 2003). Likewise, the two Dicer homologs in *Drosophila*, Dicer-1 and Dicer-2 are specialized on the processing of endogenous dsRNA and the degradation of exogenous dsRNA triggers, respectively (Lee et al. 2004c). In organisms with only one Dicer, associated proteins may convey task specificity.

As depicted in Figure 1-3, the RNase III family is constituted by three groups of endoribonucleases that specifically cleave dsRNA. Class 1 occurs in bacteria and fungi and contains only one RNase III domain adjacent to a dsRNA-binding domain (dsRBD). As shown for the archaebacterium *Aquifex aeolicus* this species acts as a homodimer and produces 9-10 nt fragments (Blaszczyk et al. 2001).

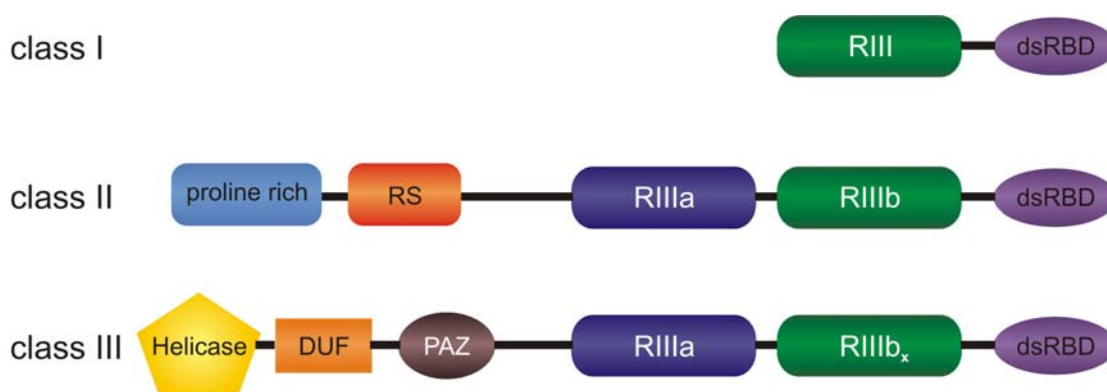


Figure 1-3 Subgroups of the RNase III family sharing the RNase III domain as a common motif. This motif is duplicated in classes II and III that are characterized by proline and arginine-serine (RS)-rich domains or ATPase/helicase, PAZ-domain and DUF283, respectively (Carmell and Hannon 2004).

Class 2 encompasses metazoan RNases III like the nuclear RNase Drosha in *Drosophila* (Wu et al. 2000). These enzymes comprise two RNase III domains, an N-terminal dsRBD and a C-terminal proline-rich and arginine-serine-rich domain (Filippov et al. 2000; Fortin et al. 2002; Lee et al. 2003b). *Drosophila* Dicer I comprising 2249 amino acids is a typical representative of an RNase III class 3 enzyme. It contains two RNase III domains arranged as an antiparallel dimer (Mian 1997; Rotondo and Frendewey 1996), a dsRNA binding domain (dsRBD) (Aravind and Koonin 2001), an amino-terminal DExH/DEAH RNA helicase/ATPase domain and a Piwi/Argonaute/Zwille (PAZ) domain (Cerutti et al. 2000).

PAZ domains have been found in several proteins involved in RNA silencing where they play an important role in the recognition of the characteristic dsRNA termini generated by Dicer (Lingel et al. 2003; Song et al. 2003b; Yan et al. 2003).

The existence of an ATPase/helicase domain may explain the finding from S2 cell extracts and recombinant enzymes from *C. elegans* and *Drosophila* that Dicer activity is greatly stimulated upon the addition of ATP (Bernstein et al. 2001; Ketting et al. 2001; Nykänen et al. 2001). However, common RNase III enzymes do not require ATP for their catalytic activity so that it was assumed that ATP is needed for structural rearrangements of the RNA or for translocation of the enzyme along the dsRNA template (Bernstein et al. 2001; Hutvagner et al. 2001; Ketting et al. 2001; Myers et al. 2003; Provost et al. 2002; Zhang et al. 2002). It is also thought that ATP is required to release readily cut siRNAs from the active site and prepare Dicer for the following round of cleavage, a process that is moreover regulated by Mg²⁺ ions (Zhang et al. 2002).

Human Dicer does not require ATP as it cleaves dsRNA into 22mers from its terminus but exhibits a lower activity than its *Drosophila* homolog (Zhang et al. 2002). Possibly the energy requirements of Dicer differ according to species.

The generation of recombinant Dicer homologs from *Drosophila* (Paddison et al. 2002a) and humans (Provost et al. 2002; Zhang et al. 2002) as well as recombinant bacterial RNase III from *A. aeolicus* and *E. coli* (Blaszczyk et al. 2001; Zhang and Hua 2004) helped to understand the mechanism of the RNAi initiator step. Remarkably, these enzymes showed dsRNA cleavage activity *in vitro* but failed to undergo multiple cycles of cleavage apparently due to a lack of associated proteins that take over the nascent siRNAs to the effector complex (Zhang et al. 2004a)

According to the size of the cleavage fragments, it was assumed that Dicer aggregates to an anti-parallel dimer, in which only 2 of 4 active sites are involved in dsRNA cleavage leading to ~22mers whereas the activity of all four centers would lead to the production of 11mers (Blaszczyk et al. 2001).

Mutagenesis studies replacing the putative catalytically active residues in human Dicer and *E. coli* RNase III demonstrated that all RNase domains comprise only one active center, which can only cleave one RNA strand. Upon the formation of homodimers or intramolecular dimerization of the two RNase III domains, the two active sites are brought into close proximity and can thus produce the characteristic staggered cut in the RNA double strand. Sedimentation analysis showed that recombinant Dicer occurs only in its monomeric form, that cleaves dsRNA at the interface of its dimerized RNase III domains (Zhang et al. 2004a).

The PAZ domain that is highly conserved in all Dicer homologs plays an important role in dsRNA recognition. In general, the binding affinity of the PAZ domain for nucleic acids is low,

but it is able to recognize the 3'-terminal 2nt overhangs of siRNAs and the base-paired terminus of siRNAs as confirmed by the X-ray structure (Lingel et al. 2003; Song et al. 2003b; Yan et al. 2003). The distance between the PAZ bound terminus of the dsRNA and the cleavage site on the adjacent RNase III domain b (see Figure 1-4) determines the size of the double stranded cleavage fragments to 20-22 nt. (Castro-Obregon et al. 2004).

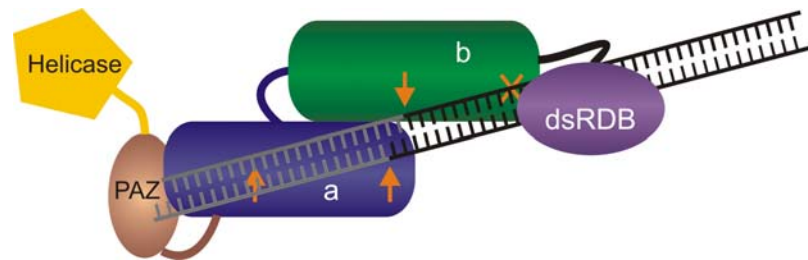


Figure 1-4 Schematic representation of dsRNA cleavage by Dicer. The two RNase III domains RIIIa and RIIIb form an intramolecular dimer that brings the active sites in position to produce the characteristic 3'-2nt overhangs. The dsRNA terminus is recognized by the PAZ domain, that interacts with RIIIb to determine the length of the cleavage fragments (Zhang et al. 2004a).

1.1.5 The many roles of small endogenous RNAs

The mechanistic studies on RNA interference aroused the interest in endogenous small RNAs that had been long neglected for being too short to be translated into a protein. Soon after siRNAs had been identified as the active species, small RNAs of 21-22 nt in length were discovered as Dicer cleavage products from endogenous substrates. It soon became clear that these now called micro RNAs (miRNAs) played an important role regulating the expression of gene products. Until today, about a hundred miRNAs have been found in *Drosophila* and *C. elegans* (Aravin et al. 2003; Lai et al. 2003; Lau et al. 2001; Lee and Ambros 2001; Lim et al. 2003; Llave et al. 2002; Mourelatos et al. 2002; Park et al. 2002; Reinhart et al. 2002; Smalheiser et al. 2001), and up to 250 in vertebrates (Lagos-Quintana et al. 2001; Lagos-Quintana et al. 2003; Lagos-Quintana et al. 2002).

The first miRNAs, lin-4 and let-7, were found in *C. elegans*, where mutation of these loci led to a developmental phenotype (Grishok et al. 2001; Ketting et al. 2001; Knight and Bass 2001; Reinhart et al. 2000). The ~70 nt non-protein coding RNAs transcribed from these loci adopt a secondary structure with double-stranded regions with one or two mismatches and serve as substrates for a Dicer-homolog (Hutvagner et al. 2001). Many more of these short-temporal RNA precursors (stRNAs) have been found, which need to be cleaved by Dicer and play an essential role in germline development (Grishok et al. 2001; Hutvagner et al. 2001; Ketting et al. 2001; Knight and Bass 2001; Reinhart and Bartel 2002).

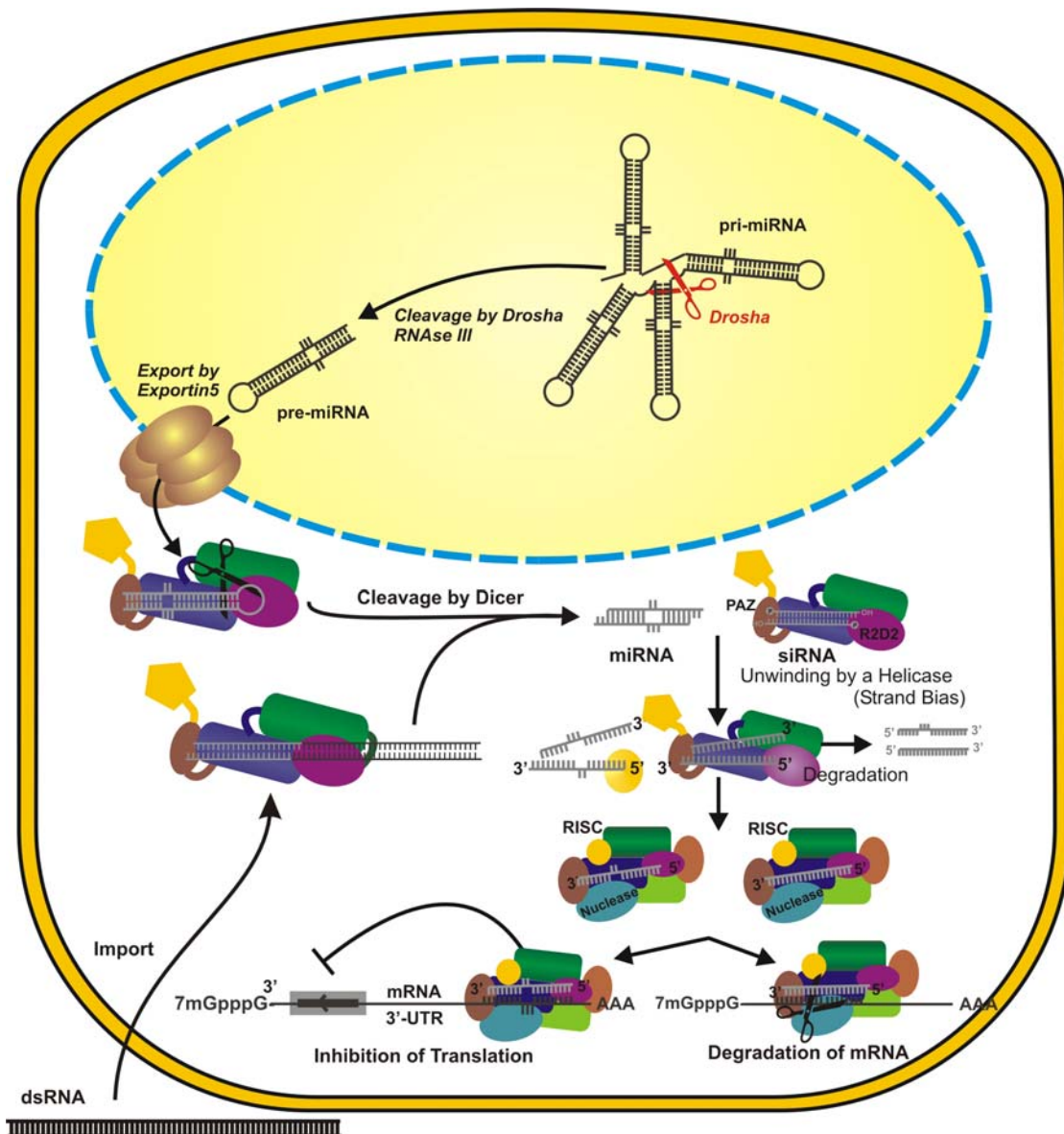


Figure 1-5 Schematic representation of miRNA and siRNA action. MiRNAs originate from long pri-miRNA precursors that are cleaved to pre-miRNAs by Drosha and exported to the cytosol for further processing by Dicer to yield miRNAs. siRNAs are generated by Dicer from exogenous dsRNA. Both species are incorporated into RISC. Perfectly homologous mRNAs are cleaved, while for partially homologous mRNAs the translation is inhibited by RISC binding.

Many long stem loop precursors (pri-miRNAs) are encoded by highly conserved genes. They are cleaved into hairpin shaped pre-miRNAs by Drosha, another enzyme of the RNase III family, to yield pre-miRNAs (Lee et al. 2003b; Wu et al. 2000). These hairpin-shaped molecules with characteristic 2-nt 3'-overhangs are transferred to the cytosol by exportin-5 (Lund et al. 2003), where they are cleaved by Dicer into their final shape that resembles an siRNA with several mismatches. These miRNAs frequently target regions in the 3'-untranslated regions (3'-UTR) of mRNA, to which they bind with imperfect homology. As a consequence, the mRNA is not cleaved but translation of the open reading frame (ORF) is suppressed (Olsen and Ambros 1999; Seggerson et al. 2002; Slack et al. 2000).

Today, it is known that siRNAs and miRNAs use common components of the same molecular machinery. In animals, it is the homology to the target sequence that determines the mode of action: If synthetic siRNAs bear a sufficiently low degree of complementarity, target translation will be inhibited without mRNA degradation (Ambros et al. 2003). Also, miRNAs will lead to mRNA degradation, if a target with perfect complementarity is provided (Doench et al. 2003; Hutvagner and Zamore 2002a; Zeng and Cullen 2003). The imprecise pairing between animal miRNAs and their targets implies a large number of putative binding sites for every miRNA and therefore a huge regulatory potential (Ambros 2004).

By means of databases and homology search algorithms it is now attempted to identify putative target regions of the known miRNAs. However, the targets found for the same miRNA differ depending on the applied algorithm (Kiriakidou et al. 2004; Lewis et al. 2003; Rajewsky and Socci 2004; Stark et al. 2003). This indicates that the mechanisms of miRNA function are still poorly understood and the search engines to identify putative binding sites need more refining.

As for gene silencing triggered by exogenous dsRNA, several functions could be assigned to endogenous short RNAs. Apparently, they are not only responsible for developmental control of gene expression, but also for long-term modifications of gene expression patterns.

In *Schizosaccharomyces pombe* (Reinhart and Bartel 2002; Volpe et al. 2003; Volpe et al. 2002) and *Tetrahymena* (Mochizuki et al. 2002; Taverna et al. 2002) a role for small dsRNAs in chromatin remodelling, chromosome dynamics (Hall et al. 2003), and heterochromatin silencing (Martienssen 2003) was established. In plants, dsRNA is also involved in DNA methylation that leads to transcriptional gene silencing (TGS) if promoter sequences are methylated (Jones et al. 2001; Mette et al. 2001; Pal-Bhadra et al. 2002; Wassenegger et al. 1994). And also in *C. elegans*, mutations in *mut-7* and *rde-2*, that play a role in RNAi, lead to a reorganization of chromatin and a release of transgene repression (Dudley et al. 2002; Hannon 2002; Tabara et al. 1999b). Recently, a connection between RNA silencing and mRNA turnover was found in plants (Belostotsky 2004; Gazzani et al. 2004).

1.1.6 RISC is responsible for mRNA cleavage and transcriptional repression

In the effector step, both siRNAs and miRNAs are incorporated into a ~360 kDa ribonuclear protein complex (RNP) to either direct sequence specific cleavage of mRNA or translational repression. The RNP with the nuclease activity required for RNAi was first observed in *Drosophila* embryo lysates and became known as RNA induced silencing complex (RISC) (Hammond et al. 2000).

As siRNA containing Dicer was found to associate with proteins, it was thought that the siRNA was handed over to a dsRNA binding protein that transfers the active species to the effector complex (Nykänen et al. 2001). The first of these siRNA binding components was a 36 kDa protein in *Drosophila* that associates with Dicer-2, that processes exogenous dsRNA, but not with Dicer-1. With reference to its tandem dsRBD and Dicer-2 binding domains it was named R2D2 (Liu et al. 2003b). *C. elegans* Rde-4 was soon recognized as an R2D2 homolog (Grishok and Mello 2002; Tabara et al. 2002). Both proteins are required to stabilize the siRNAs and provide their transfer to RISC (Liu et al. 2003b). R2D2 is capable of binding both siRNAs cleaved *in vivo* and transfected synthetic siRNAs.

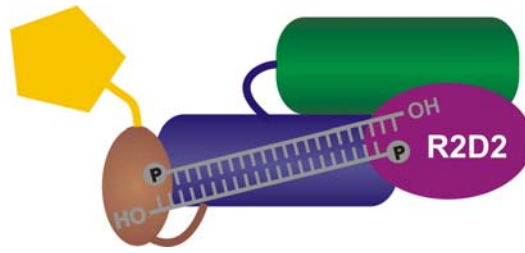


Figure 1-6 R2D2 forms a complex with Dicer2 and siRNAs and helps in the verification of the siRNA identity.

In an ATP dependent step, Dicer-2 and R2D2 and some unidentified proteins assemble to form the RISC loading complex (RLC) (Tomari et al. 2004). In RLC, Dicer helps to transfer the siRNA to RISC, a role distinct from its dsRNA cleavage task (Schwarz et al. 2004). Dicer is required for the RISC incorporation of both native and synthetic siRNAs (Pham et al. 2004). The siRNA is unwound in an ATP-dependent process (Nykänen et al. 2001) inside the RLC, which was confirmed by the finding of RLC associated with single-stranded siRNA (Tomari et al. 2004). Duplex unwinding determines the fate of the siRNA strands (Bernstein et al. 2001; Nicholson and Nicholson 2002). The so-called passenger strand is expelled from the complex and destroyed (Schwarz et al. 2003), while the guide strand serves as a template for the recognition of homologous mRNA by conventional Watson-Crick base-pairing (Martinez et al. 2002a; Tijsterman et al. 2002).

Statistical analysis of naturally occurring siRNAs, miRNAs and efficient synthetic siRNAs revealed a decreased thermodynamic stability at the 5'-ends and to a lesser extent between base pairs 9-14 of the strand that is incorporated into RISC as a guide strand (Khvorova et al. 2003; Schwarz et al. 2003). This indicated that the RLC helicase is biased towards unwinding the less stable 5'-terminus, so that the thermodynamic stability of the siRNA or miRNA precursor gives rise to strand selectivity by RISC. Thus, it became clear that artificial siRNAs are most efficient if the antisense strand is designed to be unequivocally incorporated as the guide strand, while randomly chosen target sequences bear the risk that the sense strand is incorporated into the effector complex. Indeed, the silencing efficiency of artificial siRNAs could be increased by about two orders of magnitude by designing stability patterns in which the 5'-end of the antisense strand is flexible due to mismatches and the sense-5'-terminus is tightly bound via C-G interactions (Schwarz et al. 2003). Naturally occurring miRNA precursors have evolved to match this stability pattern. If siRNAs are cleaved from artificial long dsRNAs or long hairpin shaped RNA transcripts from artificial expression vectors, a large fraction of these statistically generated siRNAs will meet the requirements to have the antisense strand incorporated into RISC.

The stability of an siRNA 5'-end is sensed by R2D2. It also detects the presence of a 5'-phosphate group to verify the identity of the siRNA as an authentic Dicer cleavage product (Tomari et al. 2004) confirming early assumptions on 5'-phosphorylation serving as a licensing function in RNAi (Nykänen et al. 2001). It is assumed that R2D2 orients the Dicer-2/R2D2 heterodimer on the siRNA inside the RLC. The orientation of the siRNAs then determines the guide strand for target cleavage (Liu et al. 2003b). The 5'-terminus of the

strand that enters RISC is located near Dicer-2, while the 5'-terminus of the passenger strand is bound in the proximity of R2D2 (Tomari et al. 2004).

Ago-2, a core component of RISC (Hammond et al. 2001), is essential for siRNA unwinding (Okamura et al. 2004). By crosslinking studies it was found that the 5'-terminus of the guide strand is bound by Ago-2 (Tomari et al. 2004). Therefore, unwinding only takes place if RISC can be assembled to incorporate the guide strand. The ~130 kDa protein Ago-2 is a member of the Argonaute (Ago) family. This class of proteins was first linked with RNAi by screening of Argonaute mutants in plants, *C. elegans* and *N. crassa* (Cerutti et al. 2000). The number of homologs found in RNA silencing organisms ranges from one in *S. pombe* (Verdel et al. 2004) to over 8 in humans (Sasaki et al. 2003) to twenty in *C. elegans* (Carmell et al. 2002; Grishok et al. 2001). Like Dicer, Ago proteins contain a highly conserved PAZ domain that is involved in siRNA recognition and binding (Carmell et al. 2002). The PIWI domain comprised by some Argonaute proteins mediates the interactions of Dicer and RISC and facilitates the transfer of the guide strand (Doi et al. 2003; Pham et al. 2004; Tahbaz et al. 2004).

It was proposed that the active effector complex is assembled around the Dicer-2/R2D2 initiator complex to form a large holo-RISC (Pham et al. 2004). In the same study, an instable intermediate R2 was detected. Since all three complexes contain Dicer, R2 may be formed by interaction of RLC (R1) with a pre-associated protein complex or a single large factor (Pham et al. 2004). As Dicer-2 is specialized on exogenous dsRNAs (Lee et al. 2004c), miRNAs may be incorporated into RISC in a similar mechanism involving Dicer-1 (Pham et al. 2004).

Apart from Ago-2 and Dicer, the fully assembled RISC also contains a DEAD-box helicase and Tudor-staphylococcal nuclease (Caudy et al. 2003). More recently, dFXR1, the *Drosophila* homolog to FMR, an RNA binding protein responsible for fragile X mental retardation, that associates with translating ribosomes, was identified as a component of RISC along with VIG (vasa intronic gene) (Caudy et al. 2003; Caudy et al. 2002; Ishizuka et al. 2002). For long, the ATP-dependent helicase was thought to unwind the siRNA from its 5'-end and thereby convert RISC into its active form RISC* (Hammond et al. 2000). However, the action of a RISC nuclease is incongruent with the finding that the siRNA is already unwound inside RLC, unless unwinding takes place in the process of guide strand transfer to Ago-2 and leaves behind RLC with the single-stranded passenger strand.

For a long time it was thought that RISC associated Tudor-staphylococcal nuclease (TSN) was responsible for the endonuclease or "Slicer" activity of RISC (Callebaut and Morion 1997; Caudy et al. 2003; Ponting 1997). TSN comprises a Tudor domain and five repeats of a nuclease domain known from staphylococcus bacteria. However, the cleavage pattern of this nuclease did not match mRNA fragments generated by RISC that generates a 5'-phosphate and a 3'-hydroxyl-terminus (Caudy et al. 2003). Purification of RISC activity from HeLa cells indicated that mRNA cleavage was correlated with either an Argonaute family member or a non-identified component of the active fraction (Martinez et al. 2002a). Studies with affinity-tagged recombinant Ago homologs and knockout of different Ago family members revealed that the Ago-2 is responsible for mRNA cleavage (Meister et al. 2004). Purification of RISC associated to biotin-labeled siRNAs under more stringent conditions and proteolysis of the residual siRNA-protein complex confirmed these findings (Rand et al. 2004). Considering the sequence conservation of the Argonaute family, the question for the

domain responsible for these unique cleavage properties arose. Recently, several groups could elucidate this question by bioinformatics revealing a homology between the PIWI-domain of the Ago proteins from *P. furiosus* and RNase H (Song et al. 2004) and between *Drosophila* Ago-2 protein with endonuclease V (Rand et al. 2004). Moreover, mutagenesis on the predicted active sites abolished RISC activity in murine cells (Liu et al. 2004).

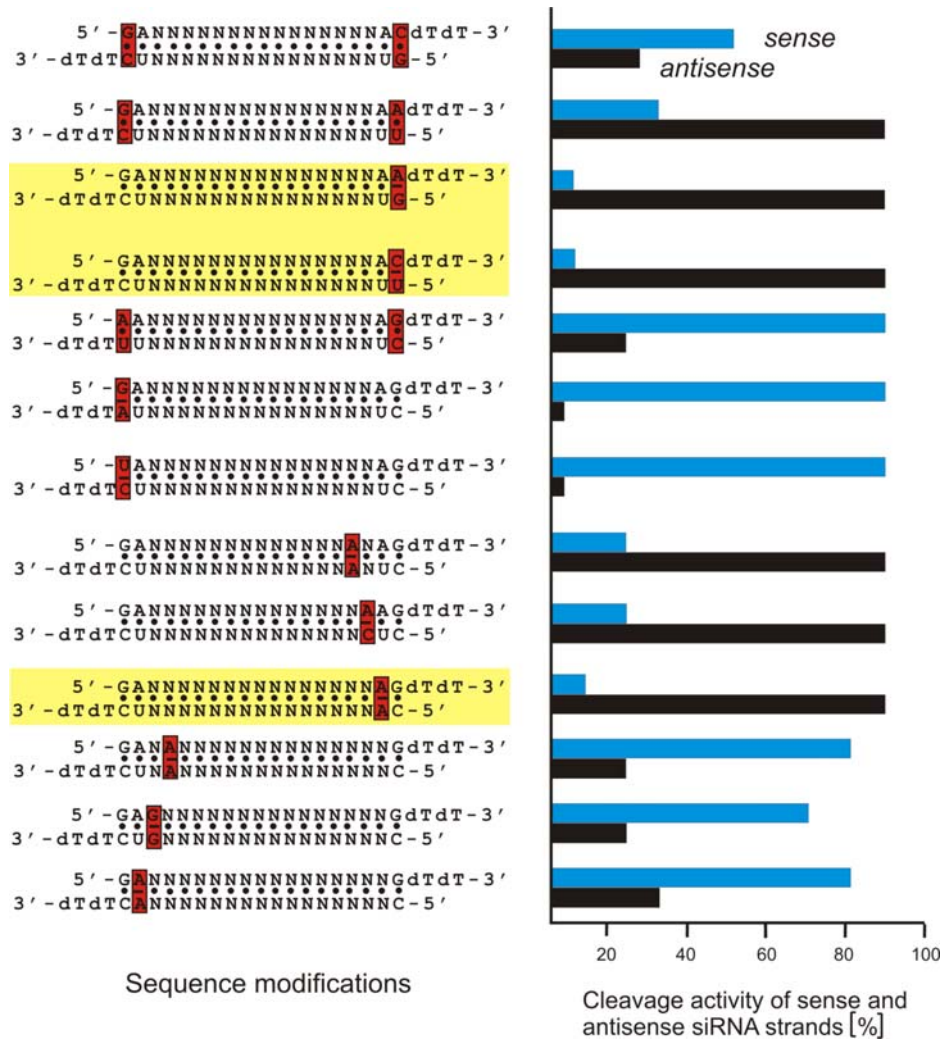


Figure 1-7 Asymmetry of strand incorporation into RISC. The thermodynamic stability of the 5'-ends determines which strand is preferentially incorporated. If the antisense-strand (black) is exclusively incorporated, the siRNA is highly efficient in silencing its target. Preferential incorporation of the sense strand (blue) leads to off-target effects.

The antisense-strand incorporated into RISC hybridizes with the target mRNA to an A-form helix (Chiu and Rana 2003). In this process, the 5'-nucleotides of the siRNA contribute more to target binding than the 3'-nucleotides. However, the 3'-region of the guide strand must pair with the target for effective target cleavage (Haley and Zamore 2004). The mRNA is cleaved between the 9th and 10th base pair from the 5'-end of the guide strand in an ATP-independent step (Haley and Zamore 2004; Tomari et al. 2004). The formation of at least one turn of a contiguous A-form RNA-RNA helix surrounding the scissile phosphate may

serve as a means of quality control to decide whether the target-mRNA matches the siRNA guide strand (Chiu and Rana 2003; Haley and Zamore 2004)

The decreased stability between base pairs 9-14 found in the statistical analysis of siRNA and miRNA stability (Khvorova et al. 2003; Schwarz et al. 2003) might facilitate target cleavage.

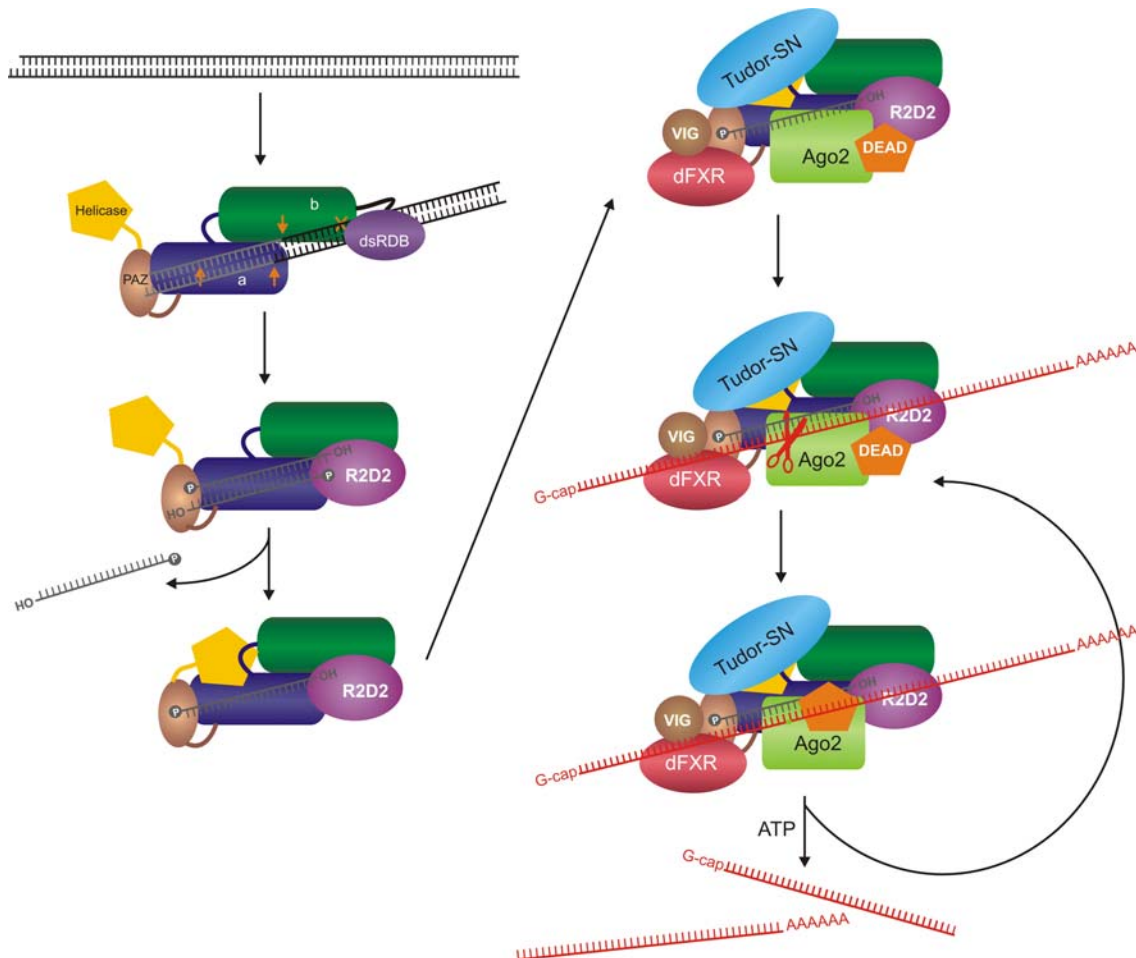


Figure 1-8 Mechanism of dsRNA triggered mRNA degradation. In the initiator step (left column), the dsRNA is cleaved into siRNAs by Dicer. R2D2 helps in strand recognition and selection. The Dicer/R2D2 complex loaded with the guide strand recruits numerous other proteins to form RISC. In the effector step (right column), RISC recognizes homologous mRNA and Ago-2 cleaves the target in the middle of the homology region. An ATP-dependent helicase helps to unwind the siRNA-mRNA hybrid. The cleavage fragments are released for non-specific degradation and RISC can undergo multiple rounds of catalysis.

It may also help in the release of the mRNA fragments for their degradation by non-specific RNases (Hutvagner and Zamore 2002a). This rate-determining step requires ATP and is essential to restore the RISC activity for further cycles of cleavage (Haley and Zamore 2004). Possibly, the function of the DEAD box helicase lies in the mRNA dissociation step, as the described instability between base pairs 9-14 would facilitate the dissociation-association reaction of DEAD helicase (Nykänen et al. 2001). Further, the action of ATP-dependent DEAD helicase would explain the energy requirements of the last step and the activity of siRNAs within a broad range of GC content (Reynolds et al. 2004).

Due to its large size of 80S (Pham et al. 2004; Zhang et al. 2004a), holo-RISC was suggested to be bound to ribosomes. This assumption is based on reports that RISC components from *Drosophila* were also found to precipitate together with ribosomes (Caudy et al. 2003; Caudy et al. 2002; Hammond et al. 2001), and Ago-2 and dFMR1 were detected in complex with 5S rRNA and ribosomal proteins L5 and L11 (Ishizuka et al. 2002). siRNAs conjugated to cell-penetrating peptides (CPPs) were found to localize in the perinuclear region for interactions with RISC (Chiu et al. 2004b).

Ribosomal association of RISC would explain why mRNAs undergoing translation are more susceptible to RNAi than untranslated mRNAs. This picture could also explain the action of RISC in translational repression (Pham et al. 2004)

1.1.7 The role of RNA dependent RNA polymerases (RdRps)

For a long time it was debated whether a catalytic mechanism was sufficient to provide the high efficiencies observed in *C. elegans* (Fire et al.) or whether an additional amplification mechanism was involved.

Such amplification could be attributed to RNA dependent RNA polymerases that are thought to transcribe aberrant RNA transcripts or long dsRNAs into the corresponding antisense RNA that hybridizes with its template. The resulting dsRNA can then be cleaved by Dicer to form siRNAs that lead to the degradation of the mRNA. The first RdRp found in context with RNA silencing was the *Arabidopsis* gene locus *sgs2/sde2* that is essential for transgene suppression (Dalmay et al. 2000; Mourrain et al. 2000). It was followed by EGO-1, RRF-1 and RRF-2 in *C. elegans* (Sijen et al. 2001a; Simmer et al. 2002; Smardon et al. 2000) and QDE-1 in *Neurospora* (Cogoni and Macino 1999a, 2000). Findings in *C. elegans* (Sijen et al. 2001a) and *Drosophila* (Lipardi et al. 2001) suggest that siRNAs function as primers in the RNA synthesis from mRNA templates by RdRps. In this process, called random degradative PCR (Lipardi et al. 2001), the regions upstream of the primary dsRNA sequence are also amplified yielding a set of secondary siRNAs that do not show homology to the primary dsRNA sequence. In wheat germ extracts, ssRNA originating from transgenes is amplified by an RdRP even if no corresponding siRNAs are present (Tang et al. 2003).

Despite the existence of an RdRp in flies, no secondary siRNAs were found in *Drosophila* (Roignant et al. 2003; Zamore et al. 2000). Mammals are completely deficient of RdRps (Stein et al. 2003) so that the high efficiency of RNAi can only be accounted for by the catalytic nature of RISC. In fact, it was shown that the siRNA guiding strand remains intact so that the active RISC can undergo up to 50 cycles of dsRNA cleavage (Haley and Zamore 2004).

1.1.8 RNAi in mammalian cells

Since the discovery of RNAi, many attempts have been made to transfer this technique to mammalian cells not only to understand gene function but also to develop therapies against human diseases. Understanding the molecular basics of RNAi has played a key role in its development into a powerful tool for functional genomics and therapeutic approaches.

The first successful attempt to trigger RNAi in mammalian cells with synthetic siRNAs (Elbashir, 2001a) was followed by careful studies of siRNA features that are required for their recognition by RISC and their efficiency in gene silencing.

Short RNAs of less than 21 or more than 25 bp have been shown to be significantly less efficient than the 21-23 bp species, while more than 30 bp trigger an interferon response. 3'-overhangs as generated by Dicer play a crucial role in the recognition of the siRNAs, as does the phosphorylation of the 5'-hydroxy groups. Uridine overhangs enhance the efficiency of siRNAs, and deoxythymidine on both 3'-ends additionally enhances the stability (Elbashir et al. 2001c). 2'-Deoxynucleotides in the 3'-2nt overhangs are generally tolerated, whereas O-methylated deoxynucleotides abolish the RNAi efficiency completely.

In chemically modified siRNAs, minor modifications at the 5'-terminus of the sense-strand are generally tolerated, such as the addition of fluorescent probes. However, small changes of the antisense-strand lead to a dramatic loss of efficiency (Chiu and Rana 2002). As the target mRNA is cleaved at the 10th nucleotide counting from the 5'-terminus of the guide strand, mispairing is more crucial for the first 10 nucleotides from the 5'-end of the antisense strand than for the 3'-terminal sequence (Amarzguioui et al. 2003; Chiu and Rana 2002; Elbashir et al. 2001c). As has been discussed above, the efficiency of siRNA strongly depends on the flexibility of the antisense-5'-terminus and can be greatly enhanced by destabilizing the 5'-terminus of the antisense strand with sequence mismatches and choosing stable base pairings for the sense-5'-terminus (Schwarz et al. 2003).

Besides, mRNA and siRNAs can adopt a secondary structure that inhibits the binding recognition of the target mRNA, which reduces the silencing efficiency of the chosen siRNA sequence. Regions of high secondary structure can be detected experimentally or computationally revealing suitable target sequences that are free from secondary structure or protein binding sites.

Of the different means to generate siRNAs *in vitro*, solid phase synthesis is the most versatile one, as it allows chemical modifications of the individual building blocks and leads to uniform siRNAs of high purity. Larger amounts of siRNAs of a defined sequence are generated by the *in vitro* transcription of DNA templates with T7 RNA polymerase (Donze and Picard 2002; Milligan et al. 1987; Sohail et al. 2003; Yu et al. 2002). Both complementary strands can be transcribed individually and then hybridized. Likewise, short inverted repeats that fold back to a hairpin structure are recognized by Dicer and fulfil the same function as siRNAs.

To generate a pool of siRNAs covering different regions of a target gene, dsRNA comprising several hundred base pairs of the gene sequence are digested by active *Drosophila* embryo lysates (Holen et al. 2002; Nykänen et al. 2001; Zhang et al. 2002). These endoribonuclease-prepared short interfering RNAs (esiRNAs) have been successfully tested in mouse embryos (Calegari et al. 2002). Recombinant human Dicer (r-Dicer) was found to be well suitable for the *in vitro* generation of siRNAs (Myers et al. 2003) and is now commercially available (Gene Therapy Systems, Invitrogen). Also, artificial ribozymes were generated that mimic the Dicer activity and exceed the efficiency of the recombinant proteins (Sohail et al. 2003). In this context, allosterically controllable ribozymes, so-called maxizymes, have been devised to recognize and specifically cleave mRNAs in a RISC-like fashion (Oshima et al. 2003).

To further scale up the production of siRNAs in a cost-efficient manner, recombinant tobacco plants (*Nicotiana tabacum*) were generated that express long hairpin-shaped RNA that is processed to siRNAs by the PTGS machinery in the living plant. It could be shown that siRNAs purified from plants could induce RNAi in mammalian cells with an efficiency similar to that of synthetic siRNAs targeting the same endogenous or viral genes (Zhou 2004).

Without an amplification mechanism, the siRNA concentration in mammalian cells decreases in the process of cell division. After 8-10 cycles mRNA levels return to their normal values so that siRNA-triggered RNAi in mammalian cells is only transient. Only proteins with a sufficiently short half-life time can be targeted so that the remaining protein can be fully degraded before the mRNA levels recover. Otherwise, the cells have to be treated repeatedly to keep the level of mRNA low.

Transient methods help to study the function of developmentally important genes in grown-up organisms where a stable knockout would induce an embryonically lethal phenotype.

1.1.9 Stable RNAi in mammalian cells

To increase the persistence and efficiency of RNAi in mammals, dsRNA may be generated inside the cells. This is achieved by the transfection of plasmids employing siRNA or short hairpin RNA (shRNA) expression cassettes under the control of an RNA polymerase III promoter. In early experiments, these vectors expressed separate 21nt short RNAs corresponding to the target sequence and its complementary sequence that could hybridize to form siRNAs (Lee et al. 2002; Miyagishi and Taira 2002). It turned out to be much more efficient to express both sequences in one transcript. These so-called inverted repeats fold back to form short hairpin RNAs (shRNAs) that resemble pre-miRNAs and undergo processing by Dicer (Brummelkamp et al. 2002b; Paddison et al. 2002a; Paul et al. 2002; Sui et al. 2002; Yu et al. 2002). The shRNA approach is commonly used due to its higher efficiency.

The amount of siRNA/shRNA generated under the RNA polymerase III promoter allows the generation of persistent phenotypes and the down-regulation of gene-products with long half-life times. However, the generation of the inverted-repeat and the selection of cells exhibiting the RNAi phenotype is a time-consuming process. Therefore, an efficient silencing sequence needs to be carefully selected as described for the transient approach. Despite many attempts to predict the RNAi efficiency of a given sequence, the efficiency is often probed by transfecting synthetic siRNAs covering a set of convenient sequences and measuring the knock-down rate (Lee et al. 2002). Using a set of siRNAs corresponding to different regions of the target sequences leads to cooperative silencing effects (Ji et al. 2003; Zhang et al. 2002).

The first stable expression of shRNA *in vivo* was performed with a pSUPER vector containing a human polymerase-III H1-RNA promoter (Brummelkamp 2001). To date, RNA polymerase III promoters such as human H1 and murine U6 are commonly used to control the expression of shRNAs (Brummelkamp et al. 2002b; Kwak et al. 2003; Lee et al. 2002; Miyagishi and Taira 2002; Paddison et al. 2002b; Paul et al. 2002; Sui et al. 2002) as it was known from antisense and ribozyme experiments that these systems are highly stable and efficient (Ilves et al. 1996; Jennings and Molloy 1987; Sullenger et al. 1990). Transcripts

driven by an RNA polymerase III (pol III) promoter terminate with 1-6 uridine residues that are readily recognized as a 3'-overhang by the RNAi machinery. Transcription via an RNA pol II promoter leads to transcripts with an m7G 5'-cap and a 3'-poly-A tail, that are more efficiently exported to the cytosol. More recent approaches make use of tRNA^{Met} (Boden et al. 2003b) and tRNA^{Val} derived promoters that lead to an up to 60% higher rate of expression and enhance the export rates (Kawasaki and Taira 2003).

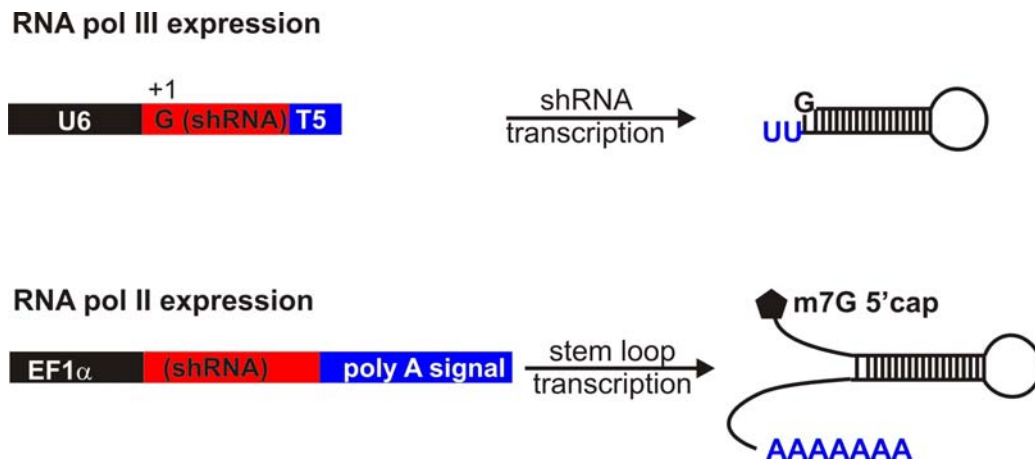


Figure 1-9 Expression of short hairpin RNAs. The choice of the promoter determines the features of the RNA transcript.

Minimal siRNA expression units comprising a U6 promoter can be easily obtained by PCR. If transfected into mammalian cells, this short stretch of DNA is transcribed into functional siRNA. This technique is of special interest for the validation of different siRNA sequences and for the screening of siRNA gene libraries (Michienzi et al. 2003).

siRNAs generated from long hairpin RNAs (lhRNAs) *in vivo* are likely to be more efficient than shRNAs as they cover different regions of the target mRNA. Cleavage of long dsRNA by Dicer leads to the binding of the siRNAs to R2D2 facilitating their recruitment by RISC (Zamore 2001). Somatic transgenic cell lines expressing lhRNA of up to 800 bp exhibit a high degree of RNA silencing and a persistent knock-out phenotype that allows extensive studies of metabolic changes (Diallo et al. 2003a; Paddison 2002; Yi et al. 2003). As opposed to transfected long dsRNAs, no interferon response was detected in cells endogenously expressing lhRNAs. Possibly, transfection and selection is only survived by cells producing small amounts of dsRNA or by cells deficient in some component of the interferon pathway.

By means of electroporation, an shRNA expressing vector was successfully transferred into murine somatic cells (Brummelkamp et al. 2002b) and even into embryonic stem cells establishing cell-lines with a stable phenotype (Kunath et al. 2003). However, the phenotype is only transient if the cells are not subjected to an antibiotic selection procedure.

First reports of transgenic mice and rats expressing siRNAs displaying stable phenotypes have already been published (Hasuwa et al. 2002) and it was reported that dsRNA expressing transgenic vectors are passed on to progeny (Carmell et al. 2003).

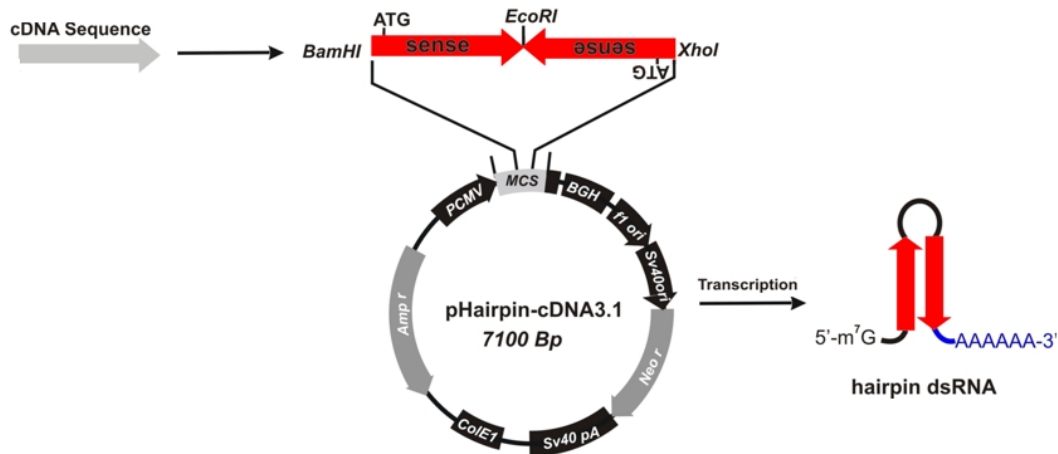


Figure 1-10 DNA-vector for the expression of long hairpin RNA. The up to 800 bp cDNA sequence is cloned twice in sense and inverse orientation. Transcripts from this inverted repeat fold back onto themselves to form a long hairpin-shaped RNA (Schepers 2004).

By this method, genes that are essential in early stages of development can be silenced in fully-grown animals, if the shRNA expression cassette is preceded by an inducible promoter. Thus, shRNA production can be triggered by an external clue such as change in temperature or the application of a specific drug (Blochlinger et al. 1991; Gonzalez-Reyes and Morata 1990). The expression of shRNAs could be also controlled by the Cre/loxP recombination system in which the expression vector is switched on by the action of Cre-recombinase that is added to the medium and enters the cells due to a cell-penetrating fusion tag (Kasim et al. 2004).

All these approaches allow triggering the gene silencing at different stages of development. The down-regulation of target genes can be restricted to one tissue, if tissue specific promoters are used to control the expression of the hairpin RNA (Brand and Perrimon 1993; Giordano et al. 2002; Lee et al. 2003a; Parkhurst et al. 1990).

1.1.10 Viral vectors to trigger RNAi

Applications of RNAi in mammalian cells are limited as some cell lines and especially primary cells are difficult to transfect and cannot be grown in culture for longer periods. Therefore, retroviral vectors have been applied to deliver plasmids into cells (Brummelkamp et al. 2002a; Hemann et al. 2003; Paddison 2002).

The Moloney murine leukemia virus (MoMuLV) vector was modified by incorporation of a U6 expression cassette into the long terminal repeat (LTR), which resulted in a duplication of the U6 cassette during reverse transcription of the viral genomic RNA. The viral expression of the shRNA induced the silencing of the targeted p53 tumor suppressor in murine hematopoietic stem cells (Paddison et al. 2002a). The same was achieved with an H1 expression cassette against p53 that was virally transfected into human fibroblasts (Barton and Medzhitov 2002).

A self-inactivating murine stem cell virus (MSCV) vector was successfully used to express shRNAs targeting nuclear Dbf2-related (NDR) kinase (Devroe and Silver 2002) and to generate siRNAs directed against a mutated form of Ras that down-regulated the Ras

oncogene without affecting the wild-type form in human bladder cancer cells (Brummelkamp et al. 2002a).

Retroviral vectors bear an oncogenic potential and require active cell division for gene transduction. To overcome these limitations, adeno-associated viral vectors (AAVs) have been employed to efficiently deliver siRNAs and down-regulate genes in dividing and non-dividing cells (Tomar et al. 2003). Lentiviruses are even more efficient in delivering siRNAs into cells. They can infect both dividing and post-mitotic cells (Abbas-Terki et al. 2002; Banerjea et al. 2003; Bonci et al. 2003; Scherr et al. 2002; Tiscornia et al. 2003; Tomar et al. 2003). Lentiviruses have been successfully applied in cultured primary dendritic cells, where they led to the expression of shRNAs targeting transgenic green-fluorescent protein (GFP) (Stewart et al. 2003) and the pro-apoptotic Biml (Rubinson et al. 2003). The same approach was functional in primary T-cells (Rubinson et al. 2003). Despite their enormous potential to transfer vectors for siRNA and shRNA expression into cells, retroviruses randomly insert new sequences into the host genome which may disrupt genes leading to the formation of tumors or leukemias (Hacein-Bey-Abina et al. 2003a; Hacein-Bey-Abina et al.). The same is true for adeno-associated viral vectors (AAVs) (Tomar et al. 2003) indicating that the use of viral vectors *in vivo* generally constitutes a considerable risk. Therefore, the application of viral vectors may remain limited to analytical applications.

1.1.11 Cure for diseases

With its establishment in mammalian cells, RNAi became interesting for therapeutic approaches. Due to its high specificity and efficiency it bears a high potential to silence RNA viruses, interfere with the metabolism of parasites, inhibit the growth of tumor cells, or cure the effects of inherited genetic defects. The approaches vary from the mere attempts to understand the underlying mechanism to the fight against infectious diseases and cancer. Most of the studies clearly show that RNAi will hold its promise to become an efficient tool in the treatment of viral and other infectious diseases in human. However, before RNAi can make its way to therapeutic applications, an appropriate siRNA delivery system is required to guide the active species to the target organs, a problem that is far from being solved. In spite of the great excitement created by those studies, it has to be kept in mind that most of the experiments were performed in cell culture or model animals using laboratory strains of viruses that are well characterized.

As the human immunodeficiency virus (HIV) constitutes a major threat to people all over the world, many groups have started to develop RNAi-based strategies to fight the virus and almost all of the viral genome has been targeted by RNAi approaches.

The first promising attempt to inhibit HIV-infection aimed at the HIV-1 cellular receptor CD4 and HIV-1 nef (Novina et al. 2002). In the following, siRNAs and shRNAs have been successfully applied to inhibit HIV1 replication in human cell lines and primary lymphocytes by targeting Rev and Tat (Coburn and Cullen 2002; Dave and Pomerantz 2003; Lee et al. 2003a), Gag (Capodici et al. 2002; Novina et al. 2002), Env (Park et al. 2003), gp41, nef (Dave and Pomerantz 2003), and LTR (long terminal repeat) (Yamamoto et al. 2002). Lentiviral vectors have successfully inhibited HIV-1 infection in mice and primary macrophages (Banerjea et al. 2003; Lee et al. 2003a) and in human T-cells (Qin et al. 2003).

However, the high mutation rate of HIV limits these approaches: HIV-1 has already been observed to escape from RNAi by point mutations in the targeted sequence (Boden et al. 2003a). DNA-vectors expressing a variety of siRNAs may be used to overcome viral resistance, and sequences of highly conserved regions of the viral genome have to be chosen as targets (Anderson et al. 2003; Boden et al. 2004a; Boden et al. 2003b; Boden et al. 2004b; Dunn et al. 2004; Jacque et al. 2002; Lee et al. 2002; Martinez et al. 2002b; Michienzi et al. 2003; Novina et al. 2002; Yamamoto et al. 2002). As an alternative, T-cell receptors of the host cells essential for viral entry such as CCR5 (Arteaga et al. 2003; Lee et al. 2003a; Qin et al. 2003), CXCR4 (Martinez et al. 2002c), and CD4 (Novina et al. 2002) can be down-regulated to prevent the infection of new cells. In this context, human lysyl-tRNA synthetase was down-regulated to prevent the incorporation of the tRNA-Lys iso-acceptors into the HIV 1 particle, which lead to a decrease in infectivity (Guo et al. 2003).

More striking results were obtained on hepatitis B virus (HBV). RNAi could inhibit the production of HBV replicative intermediates in cell culture and in immunocompetent and immunodeficient mice transfected with an HBV plasmid (McCaffrey et al. 2003). Upon siRNA delivery to mice by hydrodynamic injection, substantially reduced (up to 90%) levels of HBV RNAs and replicated HBV genomes were found in mouse liver. In these studies, most of the targets are genes that are relatively conserved between different viral strains and exhibit a low mutation activity as it is found for the genes essential for replication. The transfection of siRNAs also inhibited the replication of hepatitis B virus in hepatic cell lines (Hamasaki et al. 2003; Shlomai and Shaul 2003; Ying et al. 2003). Likewise, host genes that are required for viral entry or that play an essential role in the viral life cycle are also potential targets (Lieberman et al. 2003). The downregulation of Fas-protein expression in hepatocytes by transfected vectors that express siRNAs has turned out to prevent fulminant hepatitis in mice (Song et al. 2003a).

Like hepatitis B, hepatitis C is rapidly spreading and has been in the focus of RNAi-based therapeutical approaches (Shlomai and Shaul 2004). Transfected and vector derived siRNAs inhibited the protein expression of the hepatitis C virus (HCV) in hepatocytes without affecting endogenous genes (Kapadia et al. 2003; Kronke et al. 2004; Sen et al. 2003). In mice, transgenic HCV proteins were degraded by the hydrodynamic injection of siRNAs and plasmids expressing shRNAs (McCaffrey et al. 2002).

The effective silencing of proteins from the respiratory syncytial virus by synthetic siRNAs at low nanomolar concentrations in A549 cells was the first report about the use of RNAi to combat human viruses (Bitko and Barik 2001). In the meantime a broad range of viruses has been targeted comprising γ -herpes virus (Jia and Sun 2003), human papilloma virus (Butz et al. 2003; Hall and Alexander 2003; Milner 2003), rotavirus (Dector et al. 2002), influenza (Ge et al. 2003), herpes simplex virus (Godfrey et al. 2003), Epstein-Barr virus (Li et al. 2004) and human T-cell leukemia virus-1 (Stewart et al. 2003). Attempts to cure the SARS (severe acute respiratory syndrome) with siRNA techniques are on their way (He et al. 2003; Qin et al. 2003; Wu et al. 2003; Zhang et al. 2004c).

Soon after the first report that replication of poliovirus in HeLa cells could be reduced by silencing a polio-specific capsid protein (Gitlin et al. 2002), it was found that poliovirus can also escape from RNAi selection by mutation of the target sequence, indicating that viral escape through sequence mutation is a common obstacle in RNAi based viral therapies.

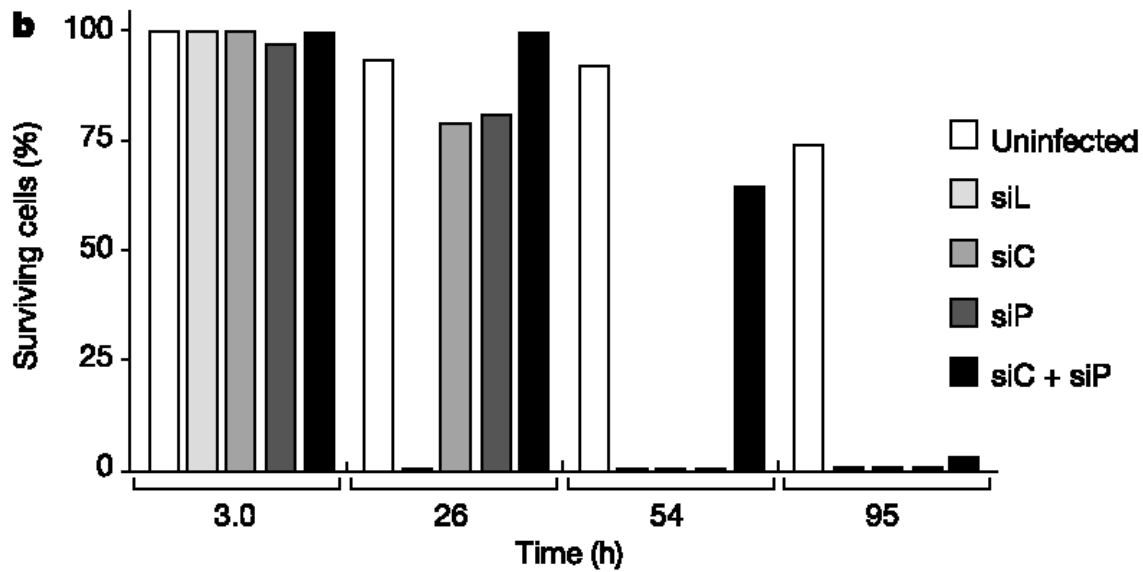


Figure 1-11 Cell viability in the presence of siRNA, determined by trypan blue staining at various times after infection. The graph indicates the number of surviving infected cells after infection with poliovirus and treatment with different siRNAs: one corresponding to a capsid sequence (siC), another to a viral polymerase sequence (siP), and an unrelated siRNA corresponding to a firefly luciferase coding sequence (siL). The graph demonstrates that the downregulation of the viral particles is not complete, which is probably due to several problems such as transfection efficiency, efficacy of the siRNA, and viral behavior (source Gitlin et al. 2003).

To overcome this obstacle, siRNA double expression (SiDEx) vectors are being developed to simultaneously target several viral genes and prevent viral escape (Boden et al. 2003a). Moreover, adenovirus VA1 possesses a non-coding RNA that can inhibit shRNAs and miRNA biogenesis. Remarkably, RNAi triggered by exogenous siRNAs was not affected. However, nuclear export of shRNAs and miRNAs is impaired. Thus, viruses can actively block the RNAi mechanism rather than simply escaping specific target sequences (Lu and Cullen 2004).

At the same time, RNAi studies help to understand the functions of viral genes, revealing new drug targets, as has been shown for the arenavirus (Perez and White 2003).

The study of gene function in parasites such as the nematode *Brugia malayi* (Aboobaker and Blaxter 2003), the sporocyst *Schistosoma mansoni* (Skelly et al. 2003), and the protozoa *Leishmania* (Robinson and Beverley 2003) by RNAi will help to develop new antiparasitic drugs based on RNAi or on lead structures derived from insights obtained by RNAi. Studies on host organisms that transfer parasites to humans, such as anophelid mosquitoes (Brown et al. 2003; Jayachandran and Fallon 2003) may aid in the development of drugs to specifically and efficiently reduce the host population and thereby stall the spread of diseases among humans. Several *in vitro* studies have already demonstrated the potential use of RNAi in cancer treatment. Cancer cells usually differ from normal cells by their uncontrolled growth and the ability to escape programmed cell death (apoptosis). For nutrition supply, they assemble a network of blood vessels around tumors, and to evade chemotherapy, they may

change surface composition. Targets for a possible RNAi treatment are therefore genes that are either involved in cell division and proliferation such as growth factors, tumor suppressor genes, transcription factors, and apoptosis inhibitors (Adams et al. 2001; Aza-Blanc et al. 2003; Brummelkamp et al. 2003; Chatterjee 2003; Chen et al. 2002b; Cioca et al. 2003; Duxbury et al. 2003; Dzitoyeva et al. 2003; Grzmil et al. 2003; Jiang and Milner 2003; Lin et al. 2001; Milner 2003; Subramanian and Chinnadurai 2003; Tanaka et al. 2003; Wall and Shi 2003; Wang et al. 2004; Wilda et al. 2002; Zangemeister-Wittke 2003) or proto-oncogenes that take part in many regulatory events and signaling cascades such as Ras and Bcl-2 (Tanaka et al. 2003), as well as viral oncogenes, such as from human papilloma virus (HPV). Another characteristic feature of cancer cells is their uncontrolled growth. Therefore, genes that are involved in cell division and proliferation such as growth factors, tumor suppressor genes, transcription factors, and apoptosis inhibitors have been targeted by RNAi (Aza-Blanc et al. 2003; Brummelkamp et al. 2003; Chatterjee 2003; Chen et al. 2002b; Cioca et al. 2003; Duxbury et al. 2003; Dzitoyeva et al. 2003; Grzmil et al. 2003; Jiang and Milner 2003; Lin et al. 2001; Milner 2003; Subramanian and Chinnadurai 2003; Tanaka et al. 2003; Wall and Shi 2003; Wang et al. 2004; Wilda et al. 2002; Zangemeister-Wittke 2003). Similarly, mutated forms of proto-oncogenes like Ras (Tanaka et al. 2003), c-myc (Rutz and Scheffold 2004), and PKA (Farrow et al. 2003), that play a role in signaling cascades, or genes participating in cell-cycle regulation like p53 (Hemann et al. 2003) are common targets in the search for cancer therapeutics.

In many tumors anti-apoptotic proto-oncogenes are overexpressed or mutated to a constitutively active form, so that apoptosis is impaired. These cells become resistant to chemotherapy and apoptosis triggered by the death receptor pathway (Zangemeister-Wittke 2003). Downregulation of other proto-oncogenes and apoptosis inhibitors, such as cdk-2, mdm-2, pkc- α , tgf- β 1, h-Ras, and vegf, effectively suppressed the proliferation of cancer cells to different extents leading to the conclusion that chemically synthesized and vector-driven siRNAs can inhibit the growth and proliferation of cancer cells (Yin et al. 2003a; Yin et al. 2003b). Ras is a powerful regulator of several interconnected receptor-signalling pathways. In its mutated form it is constitutively active and acts as an oncogene. Oncogenic k-Ras (h-Ras) is responsible for the early onset of tumors and the maintenance of tumor viability. It is thought to contribute to malignant transformation in many cell types, which makes elements of this signalling-pathway attractive targets for inhibition by RNAi (Cunningham and Weinberg 1985). Previous attempts to silence the k-Ras oncogene with phosphorothioate oligonucleotides succeeded in stabilizing the disease. Silencing of crucial effectors in the Ras signaling like the Raf-c kinase by oligonucleotides show low to moderate effects *in vitro* and in an *in vivo* tumor-xenograft model, while treatment with siRNAs can specifically silence expression of oncogenic k-Ras in tumor cells leaving the non mutated wild type k-Ras untouched (Brummelkamp et al. 2002a; Duursma and Agami 2003). Although the silencing of the mutated mRNA was only 95%, the protein level was completely reduced. This led to a complete loss of tumorigenicity (Brummelkamp et al. 2002a).

The RNAi mediated inhibition of these oncogenes has helped to recover the normal apoptosis pathways (Konnikova et al. 2003; Lima et al. 2004; Yin et al. 2003a). A common example for this class of genes is the B-cell lymphoma protein 2 (Bcl-2), which is discussed to convey resistance to chemotherapy and to prevent apoptosis in its constitutively active

form (Cioca et al. 2003; Futami et al. 2002; Jiang and Milner 2003; Lima et al. 2004; Subramanian and Chinnadurai 2003).

Cancer cells often develop transporters for the export of chemotherapeutics, which leads to multidrug-resistance. Tumors also produce factors that trigger angiogenesis (blood vessel formation) to provide their own supply with nutrients for further growth. Both classes of proteins are potential RNAi targets (Ameri et al. 2004; Bachelder et al. 2003; Deroanne et al. 2003; Jarad et al. 2002; Liu et al. 2003a; Nagashima et al. 2002; Niu et al. 2004; Riss et al. 2003; Schafer et al. 2003; Sun et al. 2003; Tien et al. 2004; Zhang et al. 2003; Zippo et al. 2004). RNAi experiments on cancerogenous targets have been carried out in a number of different cells many of which are difficult to target by other therapeutic means like murine hematopoietic stem cells (HSC) (Hemann et al. 2003), pancreatic cell-lines (Brummelkamp et al. 2002a), lung adenocarcinoma cells (July et al. 2004) and even epithelial lung cultures (Sunaga et al. 2004). In a comparative study, single siRNAs and combinations of siRNAs were transfected into HeLa cells, lung adenocarcinoma cells, hepatoma cells, ovarian carcinoma cells, and melanoma cells. A major drawback for the application of RNAi in therapy remains the issue of site- and tissue-specific delivery. Although proto-oncogenes can be specifically targeted without affecting the wild type gene, many of the other target proteins play their essential role in non-proliferating cells and healthy organs so that their systemic knockout would lead to severe side effects. For the down-regulation of such targets, techniques for direct delivery to the tumor are required.

RNAi approaches are also applied to study the mechanisms of cardiovascular diseases, that cause the highest mortality in the western world beside cancer and infectious diseases (Lorenz et al. 2003; Schafer et al. 2003; Wolff and Herweijer 2003). The first step towards prophylactic therapies seems to be the systemic application of siRNAs targeting apolipoprotein B, a protein not amenable to inhibition by conventional small-molecule therapeutics (Soutschek et al. 2004) in order to decrease the risk of coronary artery disease. With the increase of life expectancy in western countries, the number of patients suffering from Alzheimer's disease is steadily increasing. First approaches were already ongoing to elucidate possible candidate genes responsible for Alzheimer's disease (Asai et al. 2003; Francis et al. 2002; Kao et al. 2004; Marlow et al. 2003; Mattson 2003; Miller et al. 2003; Takasugi et al. 2003). Also, mechanisms of Parkinson's disease have been investigated with RNAi (Kiehl et al. 2000; Love 2004; Yang et al. 2003), and dominant disease alleles such as mutations in the Cu, Zn superoxide dismutase (SOD1) gene resulting in myotrophic lateral sclerosis (Ding et al. 2003; Maxwell et al. 2004; Xia et al. 2003) have been used as targets. dsRNA mediated gene silencing finally helped to decrease the spread of prion proteins in bovine spongiform encephalopathy (BSE) (Tilly et al. 2003).

However, neurons in culture are sensitive to invasive procedures and transfection efficiencies by conventional methods are poor. *In vivo*, the blood brain barrier prevents the uptake of drugs from the vascular system with exception of small (less than 500 Da), lipid-soluble molecules preventing the intravenous application of oligonucleotides to the brain (Trulzsch et al. 2004). Even though it is possible to treat primary neurons and neuronal cell lines with siRNAs (Krichevsky and Kosik; Omi et al. 2004; Trulzsch et al.) *in vivo* studies in mice are just at the beginning and still have their drawbacks. Adenoviral vectors successfully

passed the blood brain barrier and were expressed in the brain after intravenous application (Moon et al. 2003) and direct injection of siRNA expressing adenoviral vectors into the brain lead to a decent RNAi phenotype (Xia et al. 2002).

The large number of results gathered in hardly four years of RNAi research in mammals seems to promise a bright future for RNAi as a therapeutic tool. However, the rapid progress also revealed a number of drawbacks of RNAi, and many obstacles need to be overcome until RNAi can be applied in clinical studies ranging from siRNA stability *in vivo* to the delivery issue and questions of tissue selectivity.

1.1.12 Non-specific effects of siRNAs

When the first steps into the direction of RNAi therapy were taken, it was assumed that siRNAs or dsRNAs would specifically degrade homologous mRNA without affecting the expression of other genes. The specificity issue was put into doubt by the finding that point mutations are tolerated by the silencing machinery (Boutla et al. 2001; Holen et al. 2002) especially if the mismatches are located in the 3'-terminal half of the antisense strand (Chiu and Rana 2003). siRNAs with up to 5 mismatches at the 5'-end and nine mismatches at the 3'-end can still trigger target cleavage by Dicer albeit at a markedly lower rate (Haley and Zamore 2004). Like miRNAs, siRNAs with 3-5 mismatches targeting the 3'-UTR region of a gene impair the translation of the mRNA without triggering its degradation (Ambros et al. 2003; Jackson et al. 2003; Saxena et al. 2003). In this process, 5'-complementarity is essential as it provides most of the binding strength (Doench and Sharp 2004), while mismatches and wobble base pairs are accepted at the 3'-end. This allows a large number of non-specific sequences to suppress translation of the same gene, and *vice versa* a single siRNA can impair the translation of several genes.

Today, it is well-known that a single siRNA can affect whole cellular expression patterns, and that siRNAs targeting different regions of the same mRNA may have entirely different effects on expression patterns (Jackson et al. 2003). These off-target effects are attributed to mismatched binding of siRNAs leading to translational repression and thus to altered expression patterns (Ambros et al. 2003; Jackson et al. 2003). Sense strands with instable 5'-ends will be preferentially incorporated into RISC, but even if the antisense strand is preferred a small fraction of sense strands may be incorporated as guide strands. Therefore, when choosing RNAi target sequences, homology screens have to be carried out for the sense-sequence, too, to avoid off-target effects (Jackson et al. 2003).

In this context, the role of the interferon response has to be reconsidered. Although neither interferon response nor non-specific effects were found for siRNAs at doses around 100 nM (Elbashir et al. 2001a), recent experiments have shown the up-regulation of interferon-stimulated genes, such as the Jak-Stat pathway, in the nucleus upon the transfection with siRNAs or the transcription of shRNAs (Bridge et al. 2003; Sledz et al. 2003). This effect was markedly stronger for the transcription of shRNAs, which yields higher intracellular concentrations of siRNAs (Bridge et al. 2003). However, it has been long known that the transfection of almost all plasmids triggers the interferon response (Akusjarvi et al. 1987). Studies in living mice, on the other hand, failed to detect an interferon response triggered by Toll-like receptor 3 (TLR3) that recognizes dsRNA, or TLR9 that detects CpG motifs, and no

IL-12 or IFN- α responses could be detected (Heidel et al. 2004). It turned out that the interferon response was triggered by enzymatically-generated siRNAs, that contain 3'-triphosphates on both strands. Removal of the triphosphates by incubation of the transcripts with phosphatase abolished the interferon response (Kim et al. 2004).

Non-specific effects can be reduced by using sets of siRNAs that cover several regions of the target mRNA, and by avoiding near-homologous off-targets by conducting a BLAST search or a Smith-Waterman search with putative siRNA sequences. It was shown that effective targets exist in mice, *Drosophila* and *C. elegans* that are unlikely to accidentally silence other transcripts (Snove and Holen 2004). New design rules for siRNAs have been devised in order to increase the efficiency of siRNAs and reduce off-target effects (Khvorova et al. 2003; Reynolds et al. 2004; Schwarz et al. 2003; Yamada and Morishita 2004).

The original design rules for siRNAs were based on experimental findings from the Tuschl group (Elbashir et al. 2001a) and therefore became known as the "Tuschl rules". They predict good efficiency for 19 bp sequences with 2 nt overhangs that target an mRNA sequence of the form AA(N19)TT (with N as any nucleotide) or less favorable NA(N19)TT, where the sense strand corresponds to positions 3-23 and the antisense-strand to the complement of positions 1-21. Target sequences with a purine at position 3 and a pyrimidine at position 21 yield improved results.

For long it was thought, that the position of the target sequence on the mRNA was decisive for RNAi efficiency (Elbashir et al. 2001c). Recent experiments have shown that neither secondary structures in the target sequence nor the localization of this sequence along the mRNA strand are decisive. Only the target sequence itself, with different base pairings at specific sites determines the siRNA activity (Yoshinari et al. 2004).

The more recent rules also employ algorithms that account for the thermodynamic properties of siRNAs. The 5'-terminus of the antisense strand needs to be destabilized by A-U basepairs or single mismatches at positions 2-4, while the 5'-end of the sense strand needs to be stabilized by G-C pairings to obtain siRNAs with an exclusive RISC-incorporation of the antisense-strand (Schwarz et al. 2003). The difference in thermodynamic stabilities of sense and antisense strand directly correlates with the siRNA efficiency.

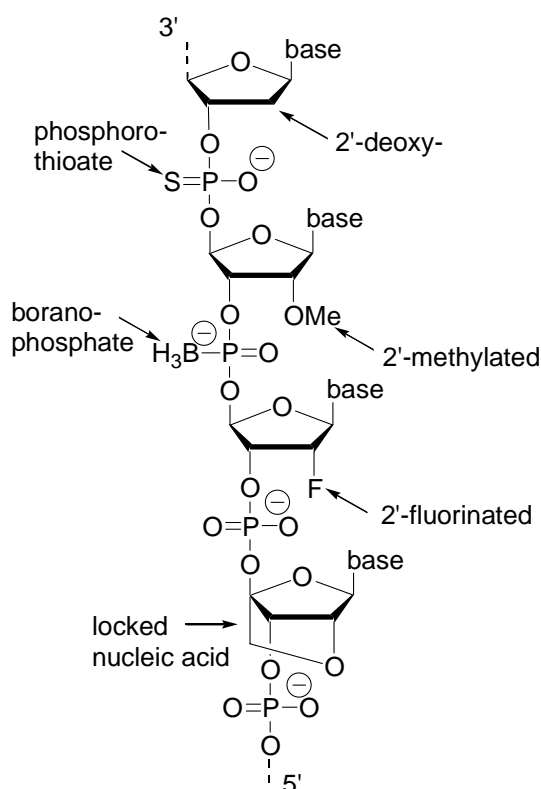
Furthermore, an accumulation of less stable A and T bases in the region around position 10 from the 5'-terminus of the guide strand helps in the unwinding of the siRNA-mRNA duplex for target cleavage. This is taken into account by a new algorithm that demands a sense strand with a T at position 10, no G at position 13, and no C or G at position 19, as well as an A at positions 3 and 19 with respect to the 5'-terminus. Moreover, the G/C content should be 30-52% and no internal repeats or palindromes should occur to avoid secondary structures (Reynolds et al. 2004).

As the rate of cleavage is low for mismatched siRNAs, off-target effects may be minimized by keeping the amount of loaded RISC as low as possible. This means that siRNA design has to balance the competing demands of efficacy and specificity (Haley and Zamore 2004).

1.1.13 Modifications of siRNAs for in vivo applications

Albeit more stable than single-stranded antisense RNA, siRNAs are subject to degradation by exonucleases which reduces their *in vivo* half-life time. Different means to stabilize

oligonucleotides for *in vivo* applications have been examined in context with antisense mediated gene silencing, but not all of them are functional in RNAi. In general, modifications on the sense strand are tolerated, while manipulating the antisense strand abolishes RNAi activity (Chiu and Rana 2002) apparently due to interference with its incorporation into RISC. As in antisense techniques, phosphorothioates increase the stability of siRNAs but at the same time enhance cytotoxicity.



Scheme 1-1 Summary of modifications that are tolerated by the RNAi mechanism.

In the process of nuclease-mediated cleavage, 2',3'-cyclophosphates are formed on the 5'-terminal fragment. So 2'-modifications that prevent cyclophosphate formations may help to stabilize siRNAs *in vivo*. Indeed, methylation of the 2'-hydroxyl groups leads to persistence of RNAi, and apart from allylation most modifications are tolerated (Amarzguioui et al. 2003). This also indicates that 2'-OHs are not essential for the recognition by Dicer or the incorporation into RISC (Chiu and Rana 2003). Early studies have already shown that substitution of the ribonucleotides in the 3'-overhangs by 2'-deoxyribonucleotides (especially by dUdU) leads to a stabilization of the siRNA (Elbashir et al. 2001c). Such modifications prolong the half-life of siRNAs in serum up to 2h (Heidel et al. 2004). However, 2'-deoxyribonucleotides and 2'-methylated nucleotides at other positions have been found to render siRNAs inactive.

In recent studies, 2'-fluoro-modifications not only increased the half-life span of siRNAs in plasma extracts but also prolonged the duration of the gene silencing (Chiu et al. 2004b).

The fact that the guide strand hybridizes with the target mRNA to an A-form helix (Chiu and Rana 2003) explains that siRNAs cannot be replaced by dsDNA (Elbashir et al. 2001c; Parrish et al. 2000) as a DNA-RNA hybrid would rather adopt an intermediate between A- and B-form helix (Cummins et al. 1995) that impairs RISC mediated target cleavage. At the same time, a combination of 2'-fluoro- and 2'-deoxy modifications on the same strand permits the formation of A-type helices upon mRNA binding and is therefore tolerated by the RNAi machinery (see 1.1.6).

In the meantime, companies have developed chemical modifications on siRNAs that not only lead to a stabilization towards nucleases but also decrease the interferon response. These siRNAs are now sold as Stealth™ siRNAs (Sledz et al. 2003).

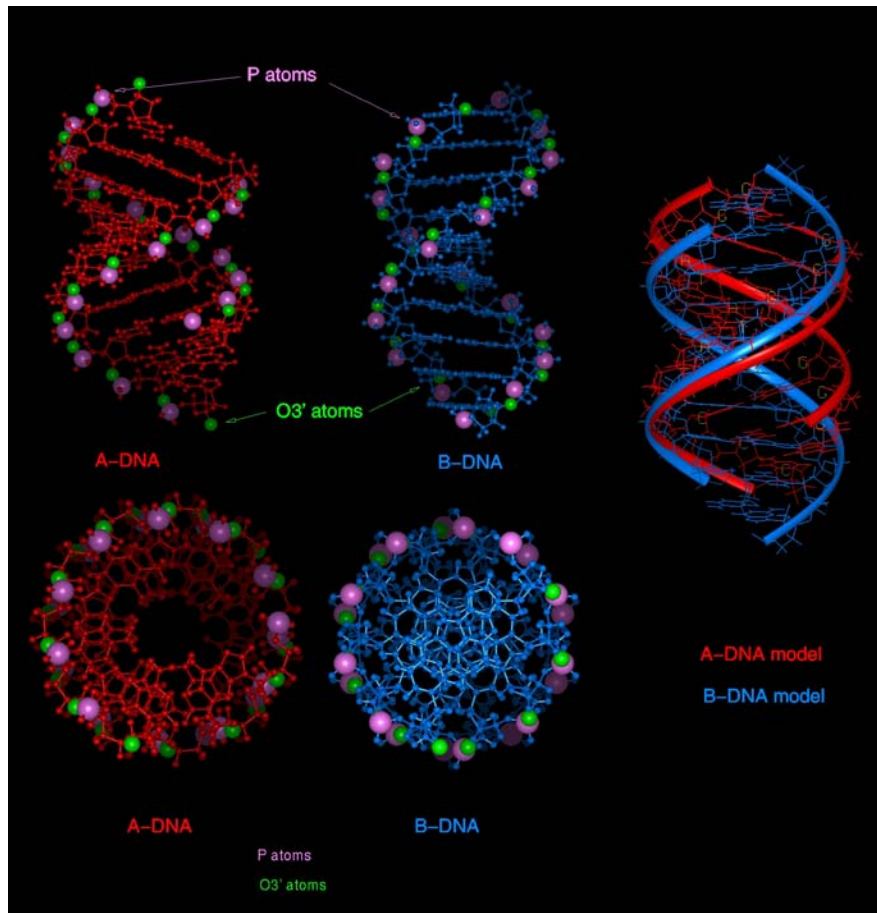


Figure 1-12 Conformations of DNA. Major and minor grooves in both helices are of different size. As opposed to dsDNA that preferentially adopts a B-form helix, dsRNA is found in an A-helical conformation. Hybrids of DNA and RNA adopt an intermediate conformation, that is not recognized by RISC (Schepers 2004).

Another recent strategy is the use of locked ribonucleotides (LNA), in which the 2'- and 5'-positions are bridged by a methylene group to fix the nucleotides conformation and protect the 2'-position from nuclease attacks (Braasch et al. 2003). Also, stereoregular boranophosphate siRNAs are not only stabilized against nuclease degradation but also significantly more effective and more potent than phosphorothioate siRNAs and native siRNAs (Hall et al. 2004).

Recent findings indicate that degradation by nucleases and dilution by cell division are not the only factors that limit siRNA efficiency in mammals. Adenosine deaminase acting on RNA (ADAR) is responsible for the editing of mRNA sequences, which regulates their nuclear export. It recognizes short double stranded regions of the target RNA, where it converts an adenosine into an inosine. ADAR-1 is localized to the cytosol, where it exhibits a markedly high binding affinity for siRNAs. RNAi efficiency is markedly increased in ADAR deficient cells (Yang 2004). Means to circumvent ADAR binding without affecting siRNA recognition by Dicer and RISC still need to be devised.

1.1.14 The delivery issue

The application of synthetic siRNAs *in vivo* is severely restricted by insufficient transfection efficiency and the limited persistence of the transient RNAi phenotype. As already described, vectors expressing short hairpin RNAs help to establish cell lines with a stable RNAi phenotype. However, like siRNAs, DNA expression vectors require classical methods such as liposome-mediated transfection (Caplen et al. 2001; Elbashir et al. 2001a; Gitlin and Andino 2003; Martins et al. 2002; Novina et al. 2002; Park et al. 2003), microinjection (Usui et al. 2003), and electroporation (Cioca et al. 2003; Siegmund et al. 2002) to reach the interior of the cells. Many cell lines are easy to transfect, and various cationic liposomal formulations were developed to increase transfection efficiency to up to 90% depending on the cell type. Without cell division, shRNA (DNA) constructs cannot enter the nucleus as required for DNA transcription, and most non-dividing cells are not susceptible to transfection as are primary cells and stem cells. Electroporation is an alternative for application of siRNAs and shRNA expression vectors in non-dividing cells or cells resistant to chemical transfection reagents (Dunne et al. 2003; Heidenreich et al. 2003; Scherr et al. 2003; Walters and Jelinek 2002). It has also been applied to living organisms such as chicken embryos (Pekarik et al. 2003) and mouse embryos (Calegari et al. 2002) where liposomal transfection is no longer feasible.

Many of the methods that are successfully used *in vitro* cannot be used in entire vertebrate animals. High toxicity of most cationic transfection reagents prohibits whole body application of siRNAs by liposomal or chemical approaches. The delivery of siRNAs or shRNA expression vectors by recombinant adenoviruses (Hemann et al. 2003; Rubinson et al. 2003; Tiscornia et al. 2003) reaches almost every cell or tissue, including stem cells and neurons, but goes along with an intolerable risk of leukemia and other cancers if applied systemically in fully-grown organisms (Hacein-Bey-Abina et al. 2003a).

Physical techniques like electroporation and the hydrodynamic injection method were successfully applied in mice. Naked siRNAs applied to mice via tail-vein injection accumulate in liver, kidney, spleen, lung, and pancreas where they knocked-down a reporter gene (Lewis et al. 2002; McCaffrey et al. 2002) as well as endogenous genes (Chang et al. 2001; Lewis et al. 2002; McCaffrey et al. 2003; Zhang et al. 1999). Also, naked siRNAs have been successfully applied to neurons by intrathecal bolus injection in mice to target TRP V1 and relieve chronic neuropathic pain (Dorn 2004), to the eyes of mice to inhibit neovascularization in the eye by downregulation vascular endothelial growth factor (VEGF) (Reich et al. 2003), and intranasally to target heme oxygenase-1 in lung epithelium (Zhang et al. 2004b).

Remarkably, naked siRNAs are taken up into tissues without any transfection reagents. Even fluorescently labeled siRNAs have been taken up into neurons by a yet unexplained mechanism (Grunweller et al. 2003). However, large concentrations and therefore high-pressure injections are required to achieve these effects. Clinical studies employing this technique are hardly thinkable if one considers that an siRNA solution corresponding to 10% of the patients body weight would have to be injected (Andino 2003). Moreover, changes in critical blood chemistry and liver enzyme levels were observed for high pressure tail vein injection in mice (Askjaer et al. 2002).

Yet, the first siRNA approaches have made their way into clinical trials. *Acuity Pharmaceuticals* and *Sirna Therapeutics* are both testing siRNAs stabilized by phosphorothioate bonds upon their potential to downregulate VEGF and VEGF receptor as a treatment of age-related macular degeneration. In this case, siRNAs are applied locally to the eye, and the lowest effective dose remains to be estimated in order to keep side effects as low as possible (Couzin 2004).

siRNAs injected into the bloodstream accumulate in liver and kidney where they are filtered for elimination. The tissue specificity can be altered by attaching small molecules to siRNAs. The modification of siRNAs with cholesterol led to an increased uptake of these siRNAs in the liver and jejunum, heart, kidney, lungs and more importantly fat tissue, where they acted to down-regulate apo-lipoprotein B (Soutschek et al. 2004). Apparently, specific ligands can mediate siRNA uptake by receptor-mediated endocytosis. As an additional advantage, the cholesterol-modification on siRNAs improves its *in vivo* pharmacokinetics: elimination half-life was increased from 6 min to 95 min, plasma clearance was decreased from 17.6 ml/min to 0.5 ml/min, and a broad biodistribution was found after 24 hours.

Nanoparticles may constitute an appropriate vehicle for the *in vivo* delivery of siRNAs. To this means ligand-targeted, sterically stabilized nanoparticles have been constructed from PEGylated polyethyleneimine modified with a specific peptide ligand to deliver siRNAs to tumors in the vascular endothelium. Intravenous application in mice resulted in an accumulation of the siRNAs in the tumor tissue where VEGF receptor-2 was down-regulated and angiogenesis inhibited. Thus, nanoparticles provide a promising tool for the delivery of siRNAs *in vivo* (Schiffelers et al. 2004).

Very recently, cell-penetrating peptides (CPPs) have been employed to deliver siRNAs. Due to their great versatility with respect to cargo and cell type (Derossi et al. 1998; Derossi et al. 1994; Prochiantz 1996; Schwarze and Dowdy 2000; Schwarze et al. 1999), these short, highly positively charged peptides have been recognized as a valuable tool for the introduction of siRNAs. The short MPG, a chimeric protein composed of gp41 (the HIV-1 fusion peptide domain) and the nuclear localization sequence (NLS) of SV40 large T-antigen, forms stable non-covalent complexes with nucleic acids. Mutations in its NLS prevent nuclear entry and distribute the siRNAs throughout the cytosol (Simeoni et al. 2003). Non-covalent complexes of siRNAs with Antennapedia peptide, also known as Penetratin (Derossi et al. 1996), and with an NLS derived β -sheet forming peptide (Deshayes et al. 2004) could be used as an alternative to liposomal complexes. However, comparatively large amounts of the CPP are required to transfect sufficient amounts of siRNA.

A consequent development following these techniques is the covalent coupling of such protein transduction domains (PTDs) derived from HIV-Tat or *Drosophila* Antennapedia protein (AntP) to deliver siRNAs to primary cells and non-dividing cells without the toxicity associated with transfection (Chiu et al. 2004a; Davidson et al. 2004; Muratovska and Eccles 2004; Schmitz et al. submitted). Interestingly, in cultured neurons, protein knock-down preceded the degradation of targeted mRNA suggesting that perfectly matched siRNAs lead to an early translational repression (Davidson et al. 2004).

Compounds that mediate rapid cellular uptake of siRNAs help to restrict the down-regulation of genes to the site of application. As CPPs strongly interact with the plasma membrane in a

receptor-independent fashion, conjugates of these peptides with siRNAs or pepsRNAs would be an important step towards the locally restricted application of siRNAs *in vivo*

1.2 Cell-penetrating peptides and their small molecule analogs

1.2.1 The delivery issue

Like RNAi, many modern biological techniques make use of bio-macromolecules to manipulate cellular functions in order to study gene function or interfere with pathological processes. Common examples are antisense mediated silencing, vector based vaccination, gene therapy, and therapeutic antibodies. As these effector molecules act with high efficacy, they also hold a great promise as potential cures for all kinds of diseases.

However, the design of new drugs has ever been limited by the question of bioavailability, target recognition, and clearance from the body. Depending on the mode of application, these molecules have to cross the epithelium of the intestine or the duodenum, the nasal mucosa or the lung epithelium to enter the bloodstream and the endothelium of the blood vessel to reach their destination. Unless the compound is directly injected at its site of action, more than one cellular membrane has to be overcome. The delivery issue is a major challenge, especially if it comes to *in vivo* applications of bio-macromolecules.

1.2.2 Cellular uptake mechanisms

As a first step to tackle this issue, one has to understand the mechanisms by which nutrients or messenger molecules enter the cell, and the pathways exploited by pathogens to penetrate the protective barrier of the cell.

Membranes form a hydrophobic barrier between the cytosol and the extracellular space or between the compartments of the cells and the cytosol. They consist of various lipids like unsaturated and saturated phospholipids, sphingolipids, and cholesterol forming a bilayer, which incorporates 20% to 60% of proteins depending on the cell type (Voet and Voet 1998). To maintain the homeostasis of the cell, these membranes have to be highly selective as to which substances they permit to pass. Specialized pores and channel proteins allow the regulated uptake of water-soluble molecules and ions from the extracellular space, while hydrophobic molecules can cross the membrane by simple diffusion.

1.2.3 Passive transport by diffusion

Diffusion processes are directed by concentration gradients and potential differences that are summarized as the electrochemical gradient. The molecules can diffuse directly through the membrane or move through the channels formed by transmembrane proteins if they meet the selectivity criteria. In facilitated diffusion, the molecule binds to a carrier molecule on the outer leaflet of the membrane that enhances the solubility in the hydrophobic core of the membrane (Schmidt 1999).

The majority of drugs enters the cells by direct diffusion through the plasma membrane, so that the features of biological membranes need to be taken into consideration in the design

of small molecule drugs. The characteristics of molecules that are taken up by direct passive diffusion are described by a set of rules that have become known as “the rule of five” or “Lipinski-rules” (Lipinski and F. 1997). For efficient uptake, molecules should not be larger than 500 Da. The number of charged functional groups and of hydrogen-bond donors or acceptors should be adjusted to provide some solubility in the hydrophobic core of the lipid bilayer. At the same time, a certain degree of hydrophilicity is required to keep the molecule dissolved in the extracellular space and the cytosol. The proper balance of hydrophilicity and hydrophobicity is reflected by the oil-water or octanol/water partition coefficient of the molecule, which can be determined experimentally. In general, its value can be directly correlated with the membrane permeability of a molecule. To fit the criteria for uptake by diffusion, pharmaceutically active substances are often modified or substituted with non-polar groups. Novel drugs like antisense-oligonucleotides, DNA-vectors for genetic vaccination or ribozymes are too large and too hydrophilic as to permit uptake by passive diffusion.

1.2.4 Active transport by transmembrane transporters

For the uptake of nutrients, ions and signalling molecules against concentration gradients or electric potentials the cells have developed different forms of active transport ranging from ATP-dependent pumps to endocytosis. One has to distinguish primary active transport by so-called pumps, secondary active transport by carriers, and tertiary active transport that is driven by a gradient built up by secondary active transport processes (Hierholzer 1997).

Membrane transporters are specialized proteins or protein complexes that form hydrophilic membrane spanning passages by which only molecules of corresponding size, shape, and charge distribution can pass into the cytosol following the concentration gradient. To prevent ion exchange with the extracellular space and the subsequent loss of concentration gradients, some of these channels are gated, like the erythrocyte glucose transporter (Voet and Voet 1998). A common example for primary active transport is the ubiquitous $3\text{Na}^+-2\text{K}^+$ -ATPase pump. The hydrolysis of ATP drives the export Na^+ -ions and the simultaneous import of K^+ -ions. Two K^+ enter the cells with every three Na^+ that are pumped out of the cell. If a net charge is transported, the pumps are referred to as electrogenic. The Na^+ -gradient built up by this process is exploited by typical representatives of secondary transporters such as the glucose/ Na^+ carrier that simultaneously imports Na^+ and glucose acting as a symporter. Likewise, amino acids or Cl^- ions may be taken up. Antiporters, like the renal Na^+/H^+ carrier, utilize the influx of Na^+ to export protons or cationic molecules. Proton gradients established by these antiporters may drive tertiary transporters such as the intestinal dipeptide transporter acting as a symporter for protons and dipeptides (see Figure 1-13) (Hierholzer 1997).

Highly polar substrates like sugars and peptides are taken up by active transport. More than 200 different solute carrier transporters recognize different types of molecules that are permitted to cross the epithelium and enter into the bloodstream. Antibiotics mimicking the features of natural substrates can exploit these membrane transporters to enter the cells.

Other drug molecules can be chemically modified to be recognized by transporters. A prominent example is Valacyclovir, an anti-viral guanosine derivative coupled to L-lysine, which is recognized by a dipeptide transporter of the intestinal epithelium (Jacobson 1993).

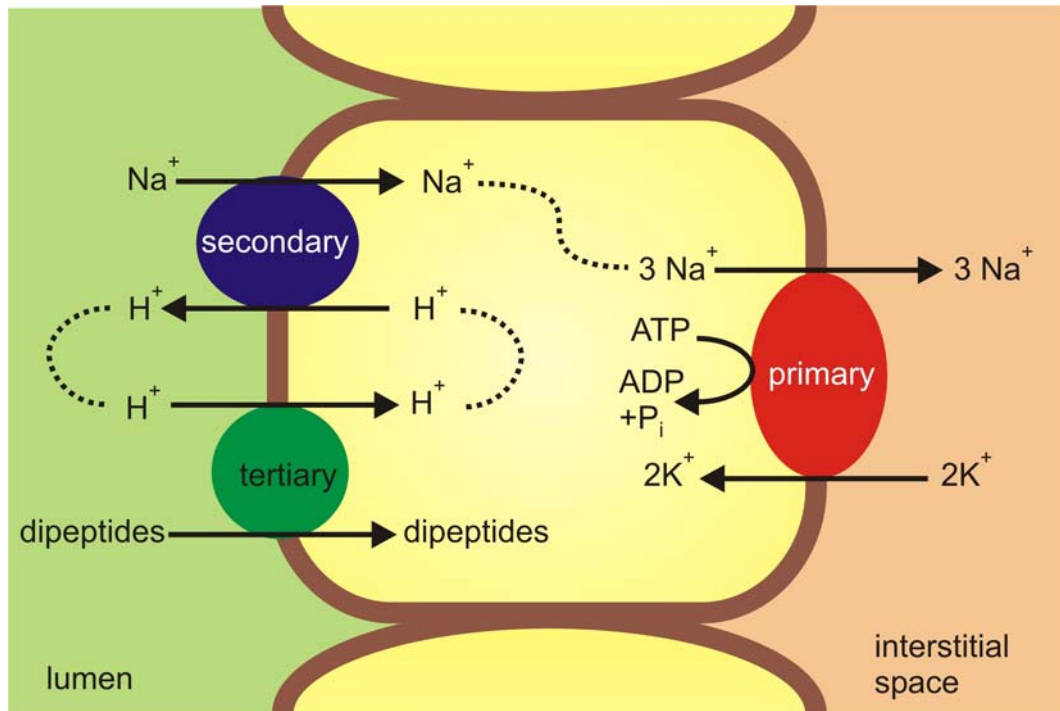


Figure 1-13 Active transport by the intestinal dipeptide transporter. The primary ATPase-pump imports K^+ and removes Na^+ from of the epithelial cell resulting in an Na^+ -gradient that drives the secondary Na^+/H^+ antiporter. Dipeptides are imported into the epithelial cells along with H^+ following the proton gradient (Schmidt 1999).

The same idea is exploited commercially by XenoPort (Santa Clara, CA, USA) who modify drugs with so-called XenoPorter molecules that enhance their uptake by solute carrier transporters in the gastrointestinal tract (Henry 2003). If the drug candidate possesses no recognizable features, it is conjugated to a known transporter substrate. If it bears some but not all of the required features it is only slightly modified to fit the targeted transporter. Xenoporter molecules are of great value if the uptake of the non-modified drug is limited by the transporter capacity as it was shown for the epilepsy drug gabapentin. Chemical modifications of the drug molecule to target different transporters greatly improved the absorption efficiency. Thus, lower doses of the drug are needed to reach the pharmaceutically required concentration, which leads to a reduction of costs and, more importantly, side effects.

1.2.5 Active transport by endocytosis

The most important mode of entry is endocytosis, which permits the internalization of larger hydrophilic substrates in a highly regulated and substrate specific process. The substrate adsorbs to small patches of the plasma membrane that invaginate in an energy-dependent process and pinch off to form intracellular vesicles in which the cargo is surrounded by a lipid bilayer.

Three modes of endocytosis are distinguished depending on the size of the internalized cargo and the mode of binding. In pinocytosis small volumes of fluid are taken up, while large

particles are incorporated by phagocytosis. Highly selective uptake is achieved by receptor-mediated endocytosis in which a substrate specifically binds to a receptor following endocytotic uptake of the receptor-ligand complex as it was originally demonstrated for the endocytosis of LDL (Brown and Goldstein 1986). Endocytic vesicles fuse with lysosomes in which the cargo molecules are often degraded or chemically modified before they are released into the cytosol (Fischer et al. 2002). Drugs that are taken up by endocytosis require features that permit a so-called “endosomal escape” of the functional molecule. The mechanism of this route is not defined so far, even though there are many speculations.

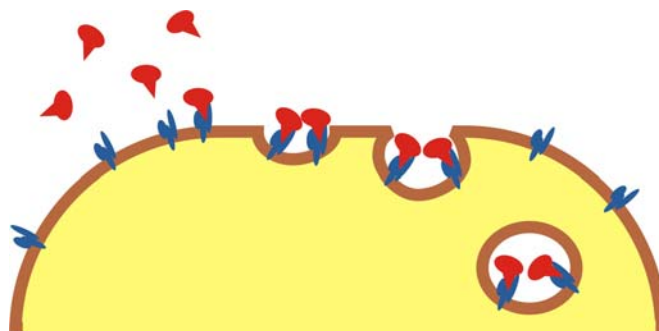


Figure 1-14 Receptor-mediated endocytosis. Binding of a ligand to the receptor molecule leads to energy-dependent invagination of the plasma membrane. The cargo is enclosed by a lipid bilayer that finally pinches off to form an endocytotic vesicle.

Receptor-mediated endocytosis is frequently exploited for targeted delivery. As shall be discussed in more detail later, the surface of transport vehicles to deliver drugs is loaded with ligand molecules that specifically bind to the receptors found on the targeted cell type. Thus, not only the efficiency but also the specificity of uptake is enhanced. This idea has been developed even further in synthetic receptor targeting. Here the plasma membranes of living cells are loaded with synthetic compounds that function as non-natural receptors, as it was shown for conjugates of protein-binding motifs with 3β -cholesteryl amines (Boonyarattanakalin et al. 2004). The macromolecular ligand comprising a recognition motif and the drug molecule binds to the receptor and triggers the formation of lipid rafts and the uptake of the receptor-ligand complex via endocytosis. These non-natural receptors capable of dissociating from the ligand are recycled to the cell surface. By this method the delivery of drugs can be enhanced by a factor of 300 compared to the free drug, and it is assumed that cell types with higher rates of endocytosis are more susceptible to delivery by this method than others.

1.2.6 Common methods of delivery

Many classes of bio-macromolecules are used in the study of cell function and in therapeutic approaches ranging from peptide inhibitors and antibodies to antisense nucleotides, siRNAs and ribozymes. However, the most important cargo is DNA. DNA plasmids may encode reporter proteins such as GFP or luciferase, or RNA transcripts that become active as ribozymes or trigger RNAi. In gene therapy, the DNA vectors encode recombinant proteins that substitute for defective or deficient endogenous proteins. Also, fragments from

pathogenic proteins may be recombinantly expressed to prime the immune system for viruses, bacteria or even cancer cells.

To introduce these bio-macromolecules into cells, a number of invasive methods have been developed under cell culture conditions. The plasma membrane can be disrupted by electroporation, particle bombardment, ultrasound or microinjection, or permeabilized by detergents, organic solvents, or hypotonic buffers. In most approaches the degree of membrane disruption cannot be controlled, so that very often the cell viability is low. Only two approaches, electroporation and particle bombardment, bear a high potential for clinical applications.

In electroporation experiments membranes are subjected to a high voltage electric field resulting in the temporary formation of pores that are large enough to allow almost all types of molecules to pass (Potter 1988). Although electroporation techniques have been refined to be able to treat almost all cell types and even tissues in fully-grown organisms, only few of them are suitable for clinical applications.

DNA vectors and other forms of nucleic acids can be delivered by ballistic particle-mediated delivery systems, also known as gene guns. The substrate molecules are attached to colloidal gold particles and accelerated by an inert gas to penetrate the target tissue, where a small fraction of the particles actually enters the nucleus and the DNA dissociates from its carrier. Although gene gun delivery is limited (Johnston and Tang 1993), it bears the advantages of high biocompatibility and ease of application, so that it may become the delivery method of choice for DNA-based vaccination (Chen et al. 2002a).

A widespread method to enable the cellular uptake of insoluble or highly charged compounds is liposome-based delivery, that was developed for the transfection of DNA vectors and has now become the major tool to introduce all kinds of nucleic acids and also proteins, peptides, and nanoparticles into cultured cells. Liposomes consist of cargo molecules enveloped by a lipid bilayer that is able to fuse with the plasma membrane and release its content directly into the cytosol. Depending on their composition, liposomes may as well be incorporated by endocytosis (Ulrich 2002). Liposomes mainly consist of amphipathic lipids, which may be cationic, anionic, or neutral. Sterols may be added to the lipid mixture to modify the liposome's behavior, and more new properties could be obtained by the incorporation of lipophilic or amphiphilic proteins, glycopeptides, and carbohydrates into the lipid bilayer.

In liposome-based drug delivery, the drug does not get into contact with the cell surface molecules, so that unspecific interactions are omitted and the intrinsic toxicity of the drug is reduced. Intensive research has led to liposomes with optimized pharmacological features such as long-term stability and serum compatibility, broad biodistribution, and slow plasma clearance rates. Moreover, selective tissue targeting and intracellular targeting is feasible by ligands or antibodies attached to the liposome mediating the recognition of specific cell types (Anwer et al. 2004; Kaneda 2000; Turk et al. 2004).

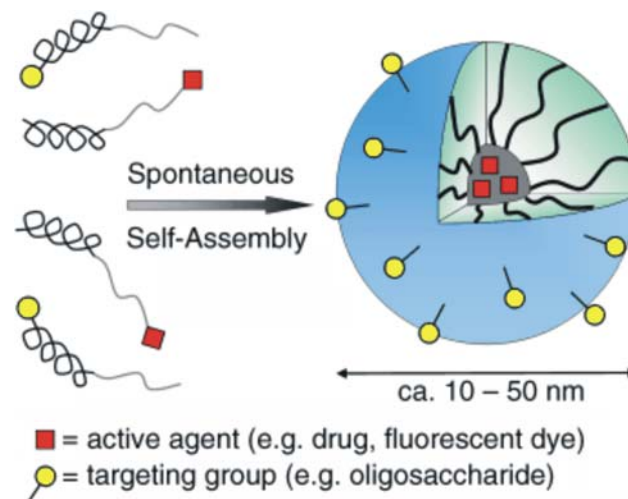


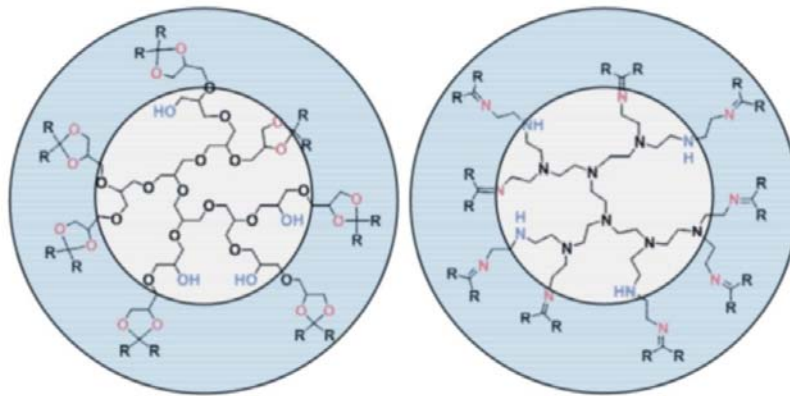
Figure 1-15 Self-assembly of target-specific liposomes. Both drug and target recognition motif are covalently linked to long hydrophobic chains so that a liposome can form by a self-assembly process that directs the drug to the interior and the target recognition motif to the exterior of the liposome (Haag 2004).

Different kinds of liposomes have already made their way to therapeutic applications (Cattel et al. 2003). In clinical studies antisense oligonucleotides against oncogens encapsulated in liposomes were applied as weekly intravenous infusions. This led to hypersensitivity reactions and dose-dependent thrombocytopenia, but resulted in the targeted growth inhibition of the tumor (Rudin et al. 2004).

Despite the large efforts to develop more efficient vectors for *in vivo* use, the behavior of a drug carrier system under *in vivo* conditions is still hard to predict (Tachibana et al. 2002). Liposomal transfection of nucleic acids, that has become the method of choice in cell culture, is not applicable *in vivo* as the required cationic lipids are toxic to fully-grown organisms.

As already discussed in context with RNAi, viral vectors have been successfully employed for the delivery of nucleic acids. They are also seen as a straightforward approach in gene therapy, where they are supposed to carry functional copies of a deficient gene into the tissue of interest. This technology makes use of viral cell-entry strategies to grant an efficient delivery of the nucleic acid drug into the cells. Even though the viral genome is depleted of sequences coding for pathogenic components, the risk of pathogenic mutations cannot be ruled out. Viral vectors can also randomly insert new sequences into the host genome leading to the disruption of genes and the formation of tumors or leukemias (Hacein-Bey-Abina et al. 2003a; Hacein-Bey-Abina et al. 2003b). Therefore, the use of viral vectors may remain limited to analytical application.

Dendrimers are successfully used for the *in vivo* application of several classes of molecules (Fischer 1999; Gittins and Twyman 2003; Haag 2001; Kono et al. 2002; Liu et al. 1999; Morgan 2002; Patri 2002). These highly branched, globular macromolecules are synthesized in a well-defined manner, that allows selective modifications in size, structure and physical properties, such as solubility (Twyman et al. 1999). Dendrimers with hydrophobic core and hydrophilic shell have been designed to encapsulate hydrophobic drugs in their interior and slowly release them to the surrounding tissue (Liu et al. 1999; Shultz 1999; Uhrich et al. 1999).



Scheme 1-2 Branched polymers like polyglycerol acetate (left) and polyethylenimine (right) are commonly used as transfection agents. Due to the highly branched core structure (white), the functional groups on the outer shell (light blue) adopt a spherical distribution. In this representation, the hydroxyl- and amino-functions of the outer shell are protected. After deprotection another generation of monomers could be attached to yield larger structures, or the spheres could be modified with other functional groups.

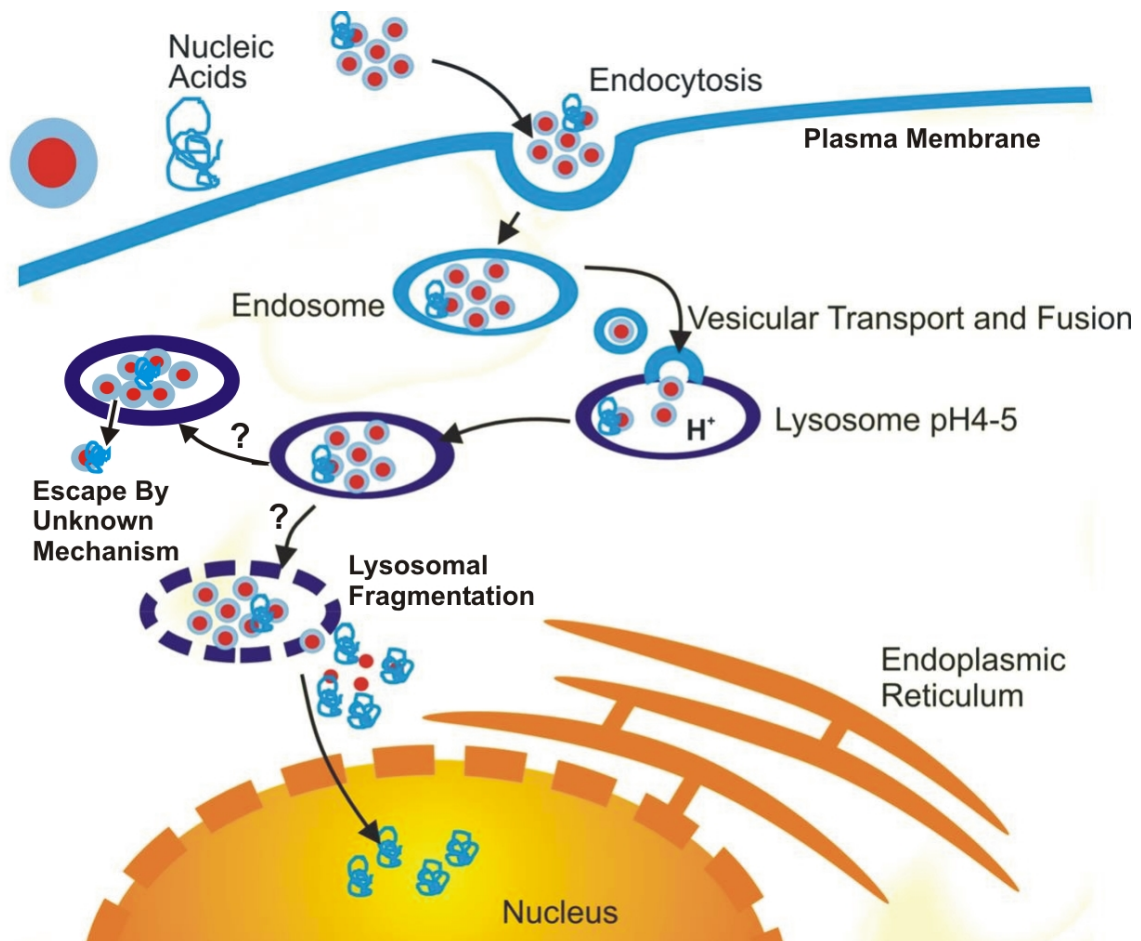


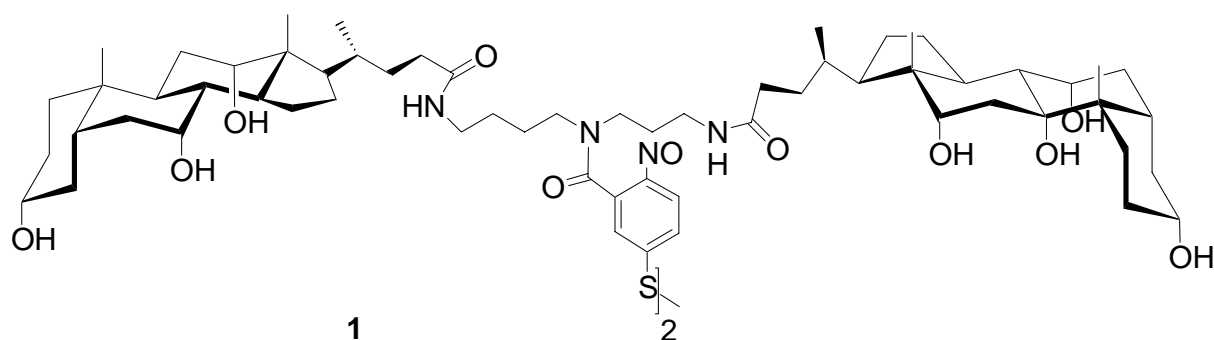
Figure 1-16 Transfection with polycationic dendrimers. The negatively charged cargo molecules form stable complexes with the transfection agent. Interacting with the plasma membrane, these transport vehicles are taken up by endocytosis. From the endosomes, the DNA-complexes are transferred to the lysosomes, from where they reach the cytosol and the nucleus by a so far unknown mechanism. One hypothesis is the intralysosomal accumulation resulting in the fragmentation of individual lysosomes, while the majority of lysosomes remains intact.

To circumvent toxic side effects of some of the widely used dendrimers, biodegradable and biocompatible dendrimers have been developed. Surface modification with polyethylene glycol (PEG) is a common method to obtain dendrimers with increased biocompatibility (Kobayashi et al. 2001). The pharmacological properties of dendrimers have been further improved by attaching various kinds of ligands, such as sugars, folate residues, receptor ligands and antibodies to the dendrimer surface. By these modifications the specificity of cellular targeting can be greatly enhanced. Rationally designed, dendrimer-based carriers help to accurately deliver drugs to their target site and increase the efficacy of drugs.

A related approach is the delivery of large molecules encapsulated in micro- and nanoparticles that are taken up by endocytosis upon interaction with the plasma membrane (Cui and Mumper 2003; Douglas et al. 1987; Kreuter et al. 2003; Simeonova et al. 2003). Nanoparticles consist of amphiphilic molecules that are degraded after uptake accounting for their low toxicity. They are easily prepared and help to stabilize sensitive drugs *in vivo* (Lockman et al. 2002). To enhance the exit from endosomes, endosomolytic agents like dioleoyl phosphatidyl ethanolamine, lipid A and cholera toxin have been incorporated into the nanoparticles (Cui et al. 2003; Cui and Mumper 2003).

Like dendrimers, nanoparticles can be designed to fit their purpose by variation of the polymer side chains and procedures of preparation. Coating with cell-specific ligands enhances the endocytotic uptake of nanoparticles by target-tissues (Bellocq et al. 2003; Cegnar et al. 2004; Cui and Mumper 2002; Farokhzad et al. 2004) and it was shown that internalization can be directed by coupling of specific antibodies to the nanoparticle (Muro et al. 2003). Until today nanoparticles have been very successfully used to deliver conventional drugs in the treatment of various diseases (Chawla and Amiji 2003; Mei et al. 2003; Zimmer et al. 1994). Recent applications with encapsulated proteins (Cegnar et al. 2004; Li et al.; Muro et al. 2003; Panyam 2003), gangliosides (Polato et al. 1994), nucleic acids (Chen et al. 2003; Kumar et al. 2003; Schiffelers et al. 2004), and RNA aptamers (Farokhzad et al. 2004) show that nanoparticles can indeed surpass the classical limitations of drug delivery. A broad field for nanoparticle application lies in genetic immunization. In this alternative vaccination process, a small quantity of the pathogenic protein is expressed from a recombinant vector to trigger an immune response leading to the formation of the appropriate antibodies and B-cells that recognize the pathogen (Kumar et al. 2003).

The interaction of cholesterol with the plasma membrane is exploited in a new class of transport molecules. These so-called umbrella transporters consist of a central spermidine moiety that is enclosed by two steroid molecules attached to its terminal amines. Cargo molecules like AMP or ATP can be attached to the thiol-functionalized central amine of the spermidine via a disulfide bond, that can be cleaved by millimolar concentrations of glutathione as it is found in the cytosol (Schafer and Buettner 2001). After successful tests of the prototype, this principle may be extended to the development of drugs, e.g. antisense oligonucleotides that can be delivered into cells (Janout et al. 2001). Plain lipids with one arginine headgroup and a cholesterol tail possess a significant capability for the delivery of DNA as discovered in library-screens for new transfection agents (Yingyongnarongkul et al. 2004).



Scheme 1-3 Umbrella transporter. The central spermidine moiety is flanked by two cholesterol molecules that are capable of inserting into the membrane. The cargo is coupled via a disulfide bond.

1.2.7 Membrane penetration by peptides and proteins

Principles to overcome membranes have evolved in viruses, microorganisms and parasites. Infective organisms such as viruses and bacteria possess proteins endowed with properties to penetrate living cells (Pugsley 1996). Pore-forming toxins such as tetanus toxin (Boquet and Dufloot 1982), anthrax toxin (Ballard et al. 1996), cytolysins (Rossjohn et al. 1997), and diphtheria toxin (Stenmark et al. 1991) facilitate the cellular entry for pathogens or help them to employ substrates from the host's cytosol for their own metabolism. The wasp venom peptide toxin mastoparan induces cell death by severely perforating the plasma membrane (Matsuzaki et al. 1996).

The principle of pore formation is also applied by higher organisms like insects and vertebrates. The insertion of a large number of pore forming peptides such as melittin, protegrins, or defensins into the plasma membrane leads to a leakage of the cytosol, which results in a breakdown of the gradients that fuel the metabolic processes. Finally, this leads to the decline of the affected cell or whole tissues (Ojcius and Young 1991). These toxic peptides are capable of forming amphiphilic structures that are responsible for their membrane activity (Fujii 1992). Some of these compounds are used to facilitate the exit from endosomes after endocytosis, such as cholera toxin in nanoparticles (Cui and Mumper 2002) and amphiphilic peptides for the cellular delivery of oligonucleotides.

1.2.8 The discovery of protein transduction

In virus studies in the late 80ies, it was found that HIV-1 *trans*-activator of transcription (Tat), a protein of 101 amino acids essential for HIV-1 replication, is rapidly taken up from the culture medium by cultured cells (Frankel and Pabo 1988; Green and Loewenstein 1988). It turned out that only a small proportion of the protein was responsible for the internalization of the whole protein. The relevant peptide comprises residues 49-57, eight of which are basic amino acids (Fawell et al. 1994; Pepinsky et al. 1994; Vives et al. 1997a; Vives et al. 1994). In the first examinations of the potential of the basic HIV-1 Tat domain (Tat peptide) to mediate the transport of other proteins into cells, large proteins like β -galactosidase,

horseradish peroxidase, RNase A and domain III of *Pseudomonas* exotoxin A were successfully incorporated when coupled to full-length HIV-1 Tat and Tat₄₉₋₅₇ peptide (Anderson et al. 1993). A fusion protein of Tat peptide with β -galactosidase was injected into mice to monitor the bioavailability of a Tat-coupled protein. The functional protein could be detected in various tissues like heart, liver, and spleen but also lung and skeletal muscle (Fawell et al. 1994; Schwarze et al. 1999). Later studies showed that Tat peptide exhibits toxic effects at concentrations above 5 μ M in the extracellular medium (Hallbrink et al. 2001; Vives et al. 1997b). Considering the good delivery properties, Tat peptide was soon discussed as a delivery vector for clinical applications.

Similar properties were found for short basic domains in the *Drosophila* Antennapedia homeobox protein (Derossi et al. 1994) and in the Herpes Simplex protein VP22 (Elliott and Ohare 1997). Thus, a rapid development was triggered in which more peptides with the capability to enter cells were discovered and broad variety of cargo molecules was delivered into cultured cells.

Initial assays suggested that these peptides could directly penetrate the plasma membrane by a novel mechanism that became known as protein transduction. Therefore, the new class of peptides was referred to as protein transduction domains (PTDs). After the development of synthetic delivery peptides the term cell-penetrating peptides (CPP) was coined to refer to naturally occurring PTDs and their functional homologs from organic synthesis. (Jeang et al. 1999; Lindgren et al. 2000b; Nagahara et al. 1998). As they help to deliver otherwise impermeable molecules into cells, they were also called Trojan peptides.

By the time of the discovery of the CPPs, fluorescence activated cell sorting (FACS) and fluorescence microscopy were the solely applied methods to estimate the amount of internalized fluorescently labeled CPPs, so that the absolute amount of compound and its distribution inside the cell was not quantitatively assessed. It was found that the fluorescent compounds were taken up by almost all of the treated cells within minutes, which was evaluated and reported as a "high uptake efficiency". Shuffling of the amino-acid sequence and the use of D-amino acids did not inhibit the internalization, so that a receptor-dependent mechanism was ruled out (Derossi et al. 1996). Since low temperatures and inhibitors of endocytosis, vesicular trafficking, and energy metabolism did not interfere with the observed rapid uptake, a non-endocytotic mechanism for protein transduction was proposed (Derossi et al. 1996; Polyakov et al. 2000). Reports from fluorescence microscopy indicated that fluorescently labeled CPPs reached the cytosol and accumulated in the nucleus (Vives et al. 1997a). Therefore, it was proposed that protein transduction acted by direct passage of the plasma-membrane, and the mechanistic explanations for this phenomenon ranged from penetration by passive diffusion through the membrane to pore formation and the generation of inverted micelles (Green et al. 2003; Schwarze et al. 1999).

1.2.8.1 Artifacts in early uptake studies

In 2003, two independent reports pointed out, that most of the previously obtained results in mechanistic studies had to be attributed to artifacts (Richard et al. 2003; Thoren et al. 2003). As the basic residues of the CPPs are positively charged under physiological conditions, CPPs interact strongly with negatively charged phospholipids and proteoglycans on the

surface of the plasma membrane. Thus, they cannot be removed by washing and are counted as internalized compounds in FACS experiments. Treated cells need to be incubated with trypsin prior to measurements to remove these artifactual CPPs from the exterior of the cell (Richard et al. 2003). Alternatively, the internalized CPPs can be distinguished from adhering ones by fluorescence quenching experiments, in which the fluorescently labeled peptide is quenched by externally added, non-permeant agents if it resides outside the cell (Drin et al. 2001; Hallbrink et al. 2001). In a novel method, extracellular peptides are chemically modified by a non-permeant reagent to be distinguishable from internalized peptides after cell lysis and HPLC analysis (Hallbrink et al. 2004).

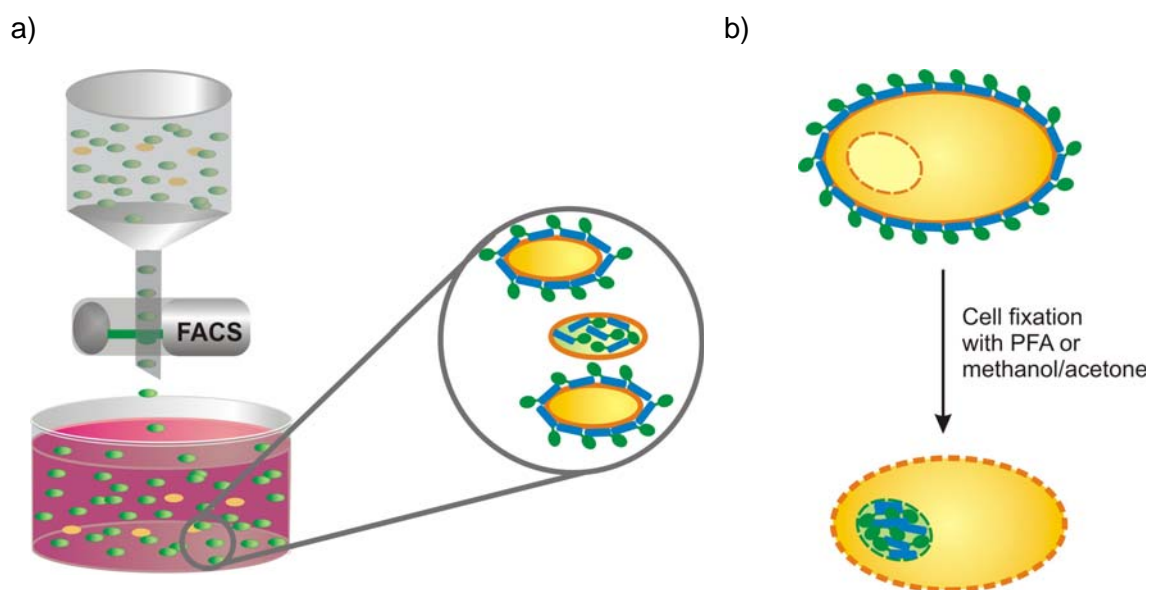


Figure 1-17 Artifacts in mechanistic studies on CPP uptake. a) Cells with CPPs attached to their surface are counted as cells with internalized CPPs. b) Fixation procedures allow an intracellular reorganization of CPPs.

Furthermore, the uptake of CPPs into the cytosol and their accumulation in the nucleus was put into doubt. Upon fixation, cellular membranes are ruptured and CPPs attached to the cell surface or residing in the cytosol are redistributed. Reaching the nucleus they interact with the negatively charged nucleic acids thus mimicking a nuclear accumulation (Leifert et al. 2002; Lundberg et al. 2003; Lundberg et al. 2002). To examine the real intracellular distribution, imaging has to be carried out in living cells (Drin 2003; Richard et al. 2003; Umezawa et al. 2002).

Studies using corrected procedures (i.e. imaging of living cells) to avoid artifacts revealed that fluorescently labeled CPPs were taken up on a much slower time scale. Inside the cells they were found localized in vesicular structures that suggested an endocytosis-like mechanism. However, a leaking of these compounds to the cytosol was also detectable after long incubation times. Fluorescently labeled CPPs were linked to a quencher via a disulfide bond, so that the fluorescence was quenched. Upon addition to cultured cells, fluorescence

was detected which was attributed to an entry of the compound into the cytosol, where the disulfide bond was cleaved and the fluorescent probe released from the quencher (Hallbrink et al. 2001). Furthermore, novel studies pointed out a nuclear localization of CPPs (Chiu et al. 2004a).

Moreover, up to 90% of fluorescent probe was found to be associated with degradation products of the peptides, which occur after cellular uptake. This was seen as a proof of lysosomal degradation by one group (Saalik et al. 2004), while others could show that the addition of chloroquine to inhibit lysosomal function did not interfere with the degradation (Hallbrink et al. 2004). These differing results have to be attributed to differing methods of preparation ranging from the study of single cells (Soughayer et al. 2004) to the preparation of lysates (Hallbrink et al. 2004), but also to the nature of the peptides themselves (Saalik et al. 2004). More publications dealing with the intracellular distribution of CPPs have been announced for the beginning of 2005.

Over the last months, novel attempts to quantify the intracellular concentration of CPPs and to determine their intracellular distribution have been reported (Chiu et al. 2004a; Hallbrink et al. 2004; Soughayer et al. 2004). Yet, the existing results are highly controversial: The reported overall intracellular concentrations of the CPPs range from an equilibrium with the extracellular medium to the 35fold of the external CPP concentration, which can be attributed to the peptide to cell ratio, the cell density, the cell-type, the used peptide and the attached cargo (Hallbrink et al.; Hallbrink et al. 2004; Lindsay). However and especially notable, none of the studies discriminates between the CPP content of cytosol or nucleus and the vesicular structures. As long as the decisive parameters have not been identified and standard protocols have been developed, the data from CPP uptake studies will be difficult to compare and evaluate. At present, the results obtained from mechanistic investigations do not fit into one consistent picture.

However, the literature confers to the uptake of CPPs as highly efficient. This means, that the peptide vector is taken up by all cells as opposed to some transfection methods in which only a small fraction of the treated cells incorporates the applied effector molecule. Internalized compounds are found in endosomes, lysosomes as well as in the cytosol and nucleus. The uptake efficiency as determined by FACS and fluorescence quenching experiments reflects the overall amount of labeled compound found in endosomes, lysosomes and the cytosol.

The first experiments to quantify the amount of internalized compound and to determine its distribution are expected in the upcoming months. It may turn out that the fraction of cargo-coupled-CPPs reaching in the cytosol or leaving the endosomal compartment is small. However, in numerous experiments it was sufficient to exhibit the desired biological function as shall be discussed in the following chapter. None of the current studies explains how the "endosomal escape" or endosomal exit might occur. Like the polycationic dendrimers, most of the CPPs are protonated within the acidic compartments and might aggregate with membranous structures leading to an accumulation in these compartments. Is a high concentration of these polycations responsible for the rupture of the lysosome/endosome or are there transporters or secretion processes responsible for the cytosolic release? These questions have to still be answered. For now, most of the studies refer to "endosomal escape" to describe the phenomenon.

1.2.9 Cell-penetrating peptides

Since the first reports about Tat peptide, a large number of naturally occurring CPPs have been discovered. They all contain a large proportion of basic amino acids that are positively charged under physiological conditions. Many of them can adopt an amphipathic α -helical structure. Isolated CPP sequences are able to introduce a variety of covalently bound cargo molecules with up to 100% efficiency into almost all cell types (Lindsay 2002; Schwarze and Dowdy 2000). To act as delivery vectors, CPPs can be attached to cargo-proteins as fusion tags in recombinant expression. They can be conjugated to proteins or non-protein cargo via amide bonds, thioethers or, reversibly, by disulfide bonds (Gil-Parrado et al. 2003). Until now, over a hundred of these peptides have been identified or generated synthetically based on structural similarities found in CPPs and on mechanistic assumptions.

It has to be remarked, that no common nomenclature has been established yet. The term CPP is used by many authors, but these membrane permeating peptides are also referred to as peptide delivery vectors, carriers, membrane permeating motifs (MPMs), cell permeable motifs, amphipathic model peptides for delivery, or delivery peptides, which makes it difficult to follow the proceedings in this field.

The first non-viral PTD was found in *Drosophila* Antennapedia homeobox protein (AntP), a 60 amino acid long carboxy-terminal DNA-binding domain that comprises three α -helices and one β -turn. A sequence of 16 amino acids from the third helix is responsible for the cellular internalization of the whole protein. Due to its ability to deliver active proteins of up to 100 amino acids, such as β -galactosidase, Antennapedia peptide (AntP) has been frequently used as a delivery vector, and a derivative of its sequence has been patented under the name Penetratin™ (Derossi et al. 1998; Derossi et al. 1994). None of the Penetratin™ variants tested so far was hemolytic or toxic (Christiaens et al. 2004), although toxic effects on cells were observed for systemic applications of Penetratin™ at concentrations exceeding 36 μ M (Derossi et al. 1998). When injected into rat brain *in vivo*, 10 μ g (~250 pmol) of fluorescently labeled Penetratin™ per animal led to neurotoxic cell death, whereas doses around 1 μ g were well tolerated (Bolton et al. 2000)

AntP/ Penetratin™ requires an essential tryptophan residue for efficient uptake, suggesting that this peptide may be taken up via a different mechanism than the other CPPs (Dom et al. 2003).

A remarkable feature was found for the CPP of Herpes Simplex Virus (HSV) structural protein VP22 (Elliott and Ohare 1997). If recombinantly expressed as a fusion protein in cultured cells, this fusion protein exits its cell of origin and is taken up by the surrounding cells (Stroh et al. 2003). This principle is exploited in a gene therapy approach in which cells from a patient are transfected with expression vectors for VP22 fusion protein *in vivo*. When reintroduced to the donor organism, these recombinant cells produce VP22 fusion proteins of an essential protein that is taken up by the surrounding tissue where it substitutes a deficient endogenous protein (Kretz et al. 2003). However, fusion proteins with VP22 can have a decreased solubility, which has to be considered when establishing new VP22-mediated delivery systems (Rutjes 2003).

Galparan is a synthetic peptide that combines the first 13 amino acids of the N-terminus of galanin with the 14 amino acid peptide toxin mastoparan (Pooga et al. 1998a). Galanin is a

galanin receptor ligand, whereas the wasp venom mastoparan acts by creating short living pores, which leads to lysis of the cells (Matsuzaki et al. 1996). To facilitate coupling to cargo molecules amino acid 13 of galparan was replaced by lysine to yield a derivative that has become known as transportan (Pooga et al. 1998a). In first studies, transportan was shown to deliver covalently coupled GFP into different cell types without losing the GFP fluorescence, indicating that the protein remains intact during the transport process (Pooga et al. 2001). Moreover, transportan has a considerably higher estimated half-life time than Penetratin™ (Lindgren et al. 2000a).

Many other proteins with transduction properties have been found, but are not yet used for cargo delivery. PTDs like the *Drosophila* Antennapedia peptide have been discovered in several homeoproteins and other proteins with gene regulating functions. Fushi-tarazu (254-313) and Engrailed (454-513), derived from homeodomains of the two equally named *Drosophila* homeoproteins, are able deliver GFP into cultured cells as efficiently as Tat and Penetratin™ (Han et al. 2000). The third helix of the homeodomain of rat insulin-1 gene enhancer protein comprises a peptide sequence pIsI that compares well to Penetratin™. Conveniently, it comprises one cysteine residue, which may be used couple cargo molecules (Kilk et al. 2001).

The pancreatic and duodenal homeobox factor-1 (PDX-1) is central to the regulation of pancreatic development and insulin gene transcription (Noguchi et al. 2003). Due to an AntP-like sequence, the PDX-1 homeodomain enters isolated pancreatic islets where it leads to stimulation of insulin gene expression. Therefore, it may be used to enhance insulin gene transcription and to facilitate differentiation of progenitor cells without gene transfer technology.

Homeobox (HOX) proteins are generally known to passively translocate through cell membranes. In stem-cell therapy, cultures of hematopoietic stem-cells could be expanded by co-culture with recombinant stromal cells secreting HOXB4 that entered into the surrounding cells (Amsellem et al. 2003).

The murine vascular endothelial cadherin (VEC) contains an 18 amino acid sequence that can enter into different endothelial cell lines. VEC peptide (pVEC) is able to transport both a hexameric peptide nucleic acid and a non-covalently attached 67-kDa protein, streptavidin-FITC (Elmqvist et al. 2001). Its transduction efficiency is lower than that of Tat peptide or transportan (Saalik et al. 2004). Another PTD was found in Kaposi fibroblast growth factor (FGF), albeit its import efficiency lies 3-4 times below that of penetratin (Lin et al. 1995; Peitz et al. 2002). SynB peptide vectors derived from protegrin have been shown to increase the transport of drugs across the blood brain barrier. They enter cultured mammalian cells by the same mechanism as penetratin (Drin 2003).

The capability to enter cells was even found in Cre recombinase. Its uptake can be greatly enhanced by the fusion with CPPs (Lin et al. 2004; Peitz et al. 2002).

A different class of CPPs was derived from human calcitonin (hCT). As opposed to most CPPs, it mainly consists of non-polar residues. In addition to cellular uptake, calcitonin derived CPPs are able to deliver cargo through epithelial barriers, albeit with a limited efficiency. Thus, hCT-derived CPPs may be used for localized epithelial delivery (Trehin et al. 2004). The ability to enter the interior of cells in a receptor-independent fashion appears

to be an intrinsic feature of many proteins involved in the regulation of development or the translocation to the nucleus.

| CPP | origin | sequence | reference |
|-----------------------|---|--|----------------|
| Tat (48-62) | HIV-1 transactivator of transcription (48-62) | G RKKRRQRRR PPQ | Vives 1997 |
| Tat (49-59) | HIV-1 transactivator of transcription (49-59) | Y GRKKRRQRRR | Nagahara 1998 |
| Antp, penetratin | Antennapedia homeodomain (43-58) | RQIKIWFQNRRMKWKK | Derossi 1994 |
| VP22 | Herpes simplex virus | NAATATRGRSAASRPTQRPRAPARSAS R RRRPVQ | Elliott 1997 |
| galparan, transportan | galanin + mastoparan | GWTLNSAGYLLGKINLKALAALAKKIL | Pooga 1998 |
| MPG | gp41 fusion sequence – SV40 NLS | GALFLGFLGAAGSTMGA WSQPKSKRKV | Morris 1997 |
| | <i>Caiman crocodylus</i> Ig(v) light chain – SV40 NLS | MGLGL HLLVLAALQGAWSQPKKKRKV | Chaloin 1998 |
| SynB1 | protegrin | RGGRLSYSRRRFSTSTGR | Rousselle 2000 |
| Fushi-tarazu | Fushi-tarazu (254-313) | SKRTRQTYTRYQTLELEKEFHFNRYITR RRRIDIANALSLSERQIKIWFQNRRMKSK KDR | Han 2000 |
| Engrailed | Engrailed (454-513) | EKRPR TAFSSEQLAR LKREFNENRYLTE RRRQQLSSELGLNEAQIKIWFQNKRAKI KKST | Han 2000 |
| pVEC | murine vascular endothelial cadherin (615-632) | TLLI LRRRIRKQ AHAHS | Elmqvist 2001 |
| plsl | Plsl (183-243) | RVRTVLNEKQLHTLRTC YAAN RPDAL M KEQLVEMTGLSPR VIRVWFQ NKRCKD KKRSIMM | Kilk 2001 |
| KALA | model amphipathic peptide | WEAKLAKALAKALAKHLAKALAKALKAC EA | Wyman 1997 |
| KLAL | model amphipathic peptide | KLALKLALKALKAALKLA | Oehlke 1998 |

Table 1-1 Prominent CPPs, their origin and their sequence

Potential for intracellular delivery was also found in nuclear localization sequences (NLS) and in the N-terminal signal sequences directing secreted proteins, membrane proteins, and organelle-specific proteins to their destination, mainly the nucleus and the ER. These signal

sequences resemble PTDs since they contain domains of positively charged amino acids and hydrophilic regions that give the overall sequence an amphiphilic character.

Possibly, the NLS not only acts as a signal sequence, but also participates in the process of translocation. Since localizations sequences for the same compartment do not necessarily share sequence homology, it is thought that characteristic patterns of charged and nonpolar residues may lead to characteristic amphipathic structures that are recognized by a less specific mechanism. NLS derived from several proteins, such as SV40 large T antigen, human T-cell leukemia virus type 1 (HTLV), or transcription factor NF- κ B, have been successfully used to transport large cargos, mainly DNA, into the interior of cells (Lin et al. 2004; Ragin and Chmielewski 2004; Ritter et al. 2003; Simeoni et al. 2003). Pep-1, a 21 amino acid CPP is likewise built up from a protein interacting domain and an NLS separated by a linker. It serves to deliver peptides and proteins (Morris et al. 2001).

The major application for NLS, however, is the intracellular direction of transfected DNA into the nucleus. NLS sequences are recognized by importins, protein transporters of the nuclear envelope (Aronsohn and Hughes 1998; Branden et al. 2001; Braun et al. 2002; Bremner et al. 2004; Ding et al. 2000; Schirmbeck et al. 2001; van der Aa et al. 2004; Zanta et al. 1999). Many parameters to grant efficient nuclear localization, from the choice of the NLS to DNA morphology and condensation of the DNA on the NLS peptide, still need to be refined (Bremner et al. 2004) as not all NLS-derived peptides show nuclear localization activity (van der Aa et al. 2004).

Viruses may also benefit from proteins comprising cell-penetrating domains that may facilitate anchoring on the host cell membrane. HIV-1 Vpr, a multifunctional 14 kDa protein, contains a CPP-like sequence at its carboxy terminus. Synthetic full-length Vpr and the Vpr- β -galactosidase fusion protein, but not the basic domain alone efficiently enter into cells (Sherman et al. 2002). The fusion peptide domain of HIV-1 gp41 in combination with the NLS of SV40 large T antigen was developed into a 27 amino acid gene delivery system MPG¹, that forms stable complexes with DNA (Morris et al. 1997). At nontoxic concentrations, peptides derived from dermaseptin S4, an antimicrobial peptide that destabilizes the membrane of bacteria, are found to enter HeLa cells and deliver different peptides. The attachment of commonly used NLS-derived peptides lead to an accumulation in the nuclei (Hariton-Gazal et al. 2002).

1.2.10 Modifications to optimize CPPs

No sequence homology has been found for CPPs, and their capability to deliver non-permeant cargo-molecules into cells seems to be linked solely to their composition of mainly basic amino acids and to their amphipathic character. Therefore, it was suggested, that the delivery properties are merely evolutionary side effects that had not undergone evolutionary refinement. Thus, it was assumed that the transduction potential could be still enhanced by *in vitro* evolution or by modifications based on mechanistic insights.

¹ The abbreviation is not explained by the authors.

The amphipathic KLAL (KLALKLALKALKAAKLA-NH₂) was one of the first synthetic peptides derived from characteristic features of NLSs. Its uptake rate and cargo delivery efficiency was indeed higher than that of Tat and transportan (Hallbrink et al. 2001).

Likewise, the exchange of some amino acid residues in Tat₄₉₋₅₉ enhanced its delivery efficiency up to 33fold rendering this peptide sequence to one of the best PTDs (Ho et al. 2001). Likewise, an oligopeptide of the sequence d(AAKK)₄, that mimics the alternating basic and non-polar residues found in NLSs (Kaihatsu et al. 2004; Lin et al. 2004), and (KFF)₃K, shown to permeate bacterial membranes (Geller et al. 2003; Petersen et al. 2004), have been used for the delivery of PNAs and antisense oligonucleotides.

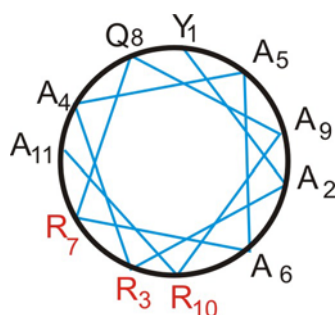
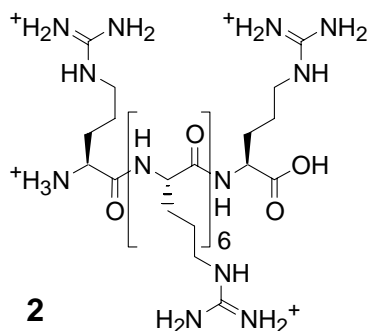


Figure 1-18 Helical wheel plot of an improved Tat-derivative (YARAAARQARA) with the 33x uptake efficiency of Tat. All arginine residues of the amphipathic helix point into the same direction (Ho et al. 2001).

In a combinatorial approach, a M13 phage library of 12-mer peptides was built up and putative CPPs were selected on the basis of their varying cationic charge content (Mi et al. 2000). These randomized peptides were able to deliver β -galactosidase to a variety of cell lines and primary cells including islet β -cells, synovial cells, polarized airway epithelial cells, dendritic cells, myoblasts, and tumor cells. Two of these peptides reached an efficiency comparable to that of Tat.

The high uptake rate of naturally occurring PTDs could be attributed to their high content of basic amino acids. Therefore, homo-oligomers of the basic amino acids lysine, ornithine, and arginine, were synthesized. Application to cultured cells showed that all compounds could be internalized (Emi et al. 1997; Jeang et al. 1999; Lindgren et al. 2000b; Mitchell et al. 2000; Ryser 1967; Vives et al. 1994). Even oligohistidine works as a pH-sensitive CPP that is almost as efficient as Tat (Robbins et al. 2002).



Scheme 1-4 Octaarginine 2 (Wender et al. 2001)

The highest uptake rates were observed for oligomers of arginine, the most basic of the tested amino acids (Rothbard et al. 2000), that surpassed the uptake rate of poly-L-lysine by a factor of 10 (Buschle et al. 1997). A factor of 20 was reported for the comparison of nonamers of L-arginine compared to lysine, histidine, ornithine and citrulline (Mitchell et al. 2000), and a factor of >100 for D-arginine nonamers (Wender et al. 2001). Apparently, the uptake rates correlated with the density of positive charges, as arginine ($pK_a = 12.0$) is more basic than lysine ($pK_a = 10.0$), and histidine ($pK_a = 6.0$) (Voet and Voet 1998). Molecular modeling of oligoarginines indicated that, due to the molecule's helical conformation, only a subset of the side chain guanidinium groups interacts with the negatively charged headgroups of the phospholipids of the plasma membrane (Rothbard et al. 2002). Correspondingly, decamers in which the three arginines facing away from the plasma membrane were replaced by non-polar residues exhibited the same uptake behavior as the decaarginine.

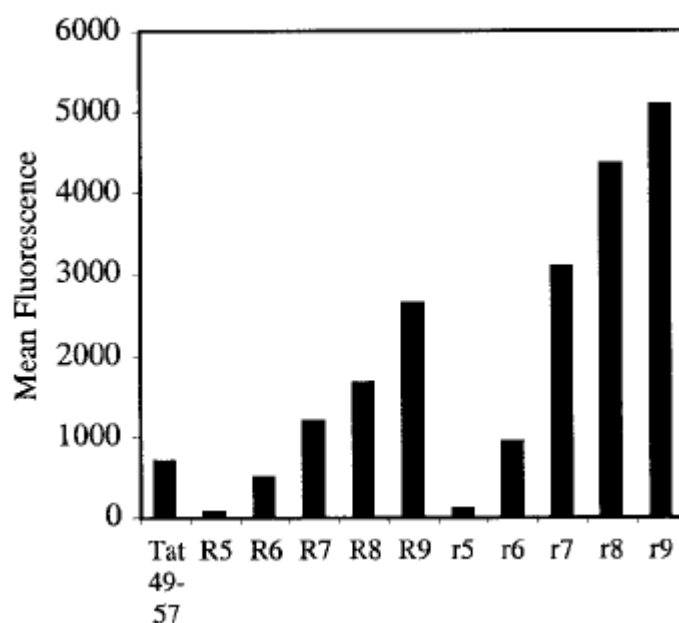


Figure 1-19 Cellular uptake of arginine-rich oligopeptides in Jurkat cells after 15 min of incubation with 12.5 mM at room temperature as estimated by FACS: The numbers indicate the number of arginine residues comprised by the peptide, R denotes the L-amino acids and r the D-enantiomers (Wender et al. 2001).

CPPs have been further developed to DNA condensing agents that exhibit a 50-60 times higher efficiency than conventional transfection agents. Due to electrostatic interactions, oligomers of lysine with N- and C-terminal cysteine residues aggregate with the negatively charged DNA strand, and the peptides can spontaneously oxidize to form interpeptide disulfide bonds. The cross-linked peptide DNA condensates can reach the cytosol of the cells, where the disulfide bonds are cleaved and the DNA cargo is released (McKenzie et al. 2000). Likewise, arginine-rich peptides with cysteine residues have been used for peptide-mediated DNA condensation. Interrupting the arginine sequences with glycines and histidine allowed reversible plasmid condensation, so that a plasmid could be more easily released inside the cell (Siprashvili et al. 2003).

Since their discovery, protein precipitation, toxicity issues and costs have retarded the entry of cationic peptides into clinical studies. Therefore, efforts were made to improve the stability, facilitate the synthesis, and reduce the costs. As a cost efficient alternative to solid phase synthesis, oligoarginine could be prepared in a scalable solution-phase synthesis in 13 steps with 28% overall yield (Wender et al. 2001).

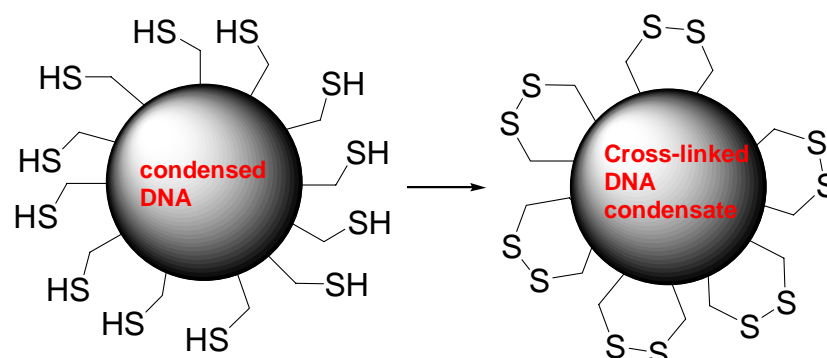


Figure 1-20 Condensation of DNA by cysteine-modified oligolysine (McKenzie et al. 2000). After aggregation of the positively charged peptides with the negatively charged DNA, the free thiol-groups spontaneously oxidize to form disulfide bonds.

1.2.11 Synthetic molecules to mimic CPPs

Peptides are sensitive to proteases, so that their plasma half-life time *in vivo* is rather short. To obtain stable transport vectors, peptide mimetics were synthesized that combine the functional groups of CPPs with a stabilized backbone.

In this context, three classes of peptide mimetics can be distinguished: Peptide analogs consist of oligomeric chains of isosters of naturally occurring amino acids and derivatives with modified non-natural side chains. In backbone mimetics, the functional side chains are attached to a different type of monomer that can be oligomerized in analogy to amino acids by amide bond formation as in the oligomerization of ω -amino acids. They may as well be oligomerized via ester or urethane bonds. In scaffold mimetics amino acid functionalities are attached to non-linear structures mostly dendrimers and cyclic or polycyclic structures.

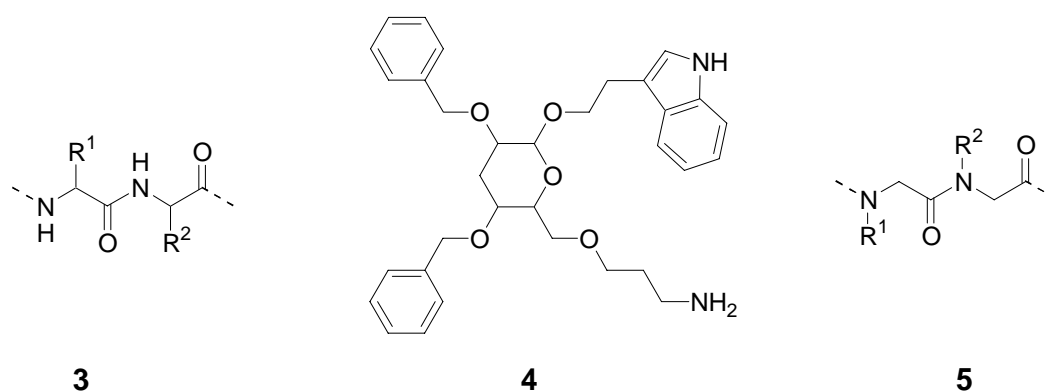


Figure 1-21 Examples of peptide mimetics: Peptide analog with alternative side chains (**3**), scaffold mimetic (**4**) backbone mimetic (here a peptoid **5**).

Peptide mimetics aim to imitate the spatial arrangement of functionalized side chains in order to fulfil the functions of their natural examples. For the function of CPPs, a high density of positively charged side chains, that can form an amphipathic secondary structure, appears to be crucial.

A prominent example for backbone mimetics are β -peptides, oligomers of β -amino acids, that have been studied extensively in recent years (Umezawa et al. 2002). They are not degraded by proteases (Schreiber et al. 2002) and adopt well-defined protein-like secondary structures (DeGrado 1999; Gademann 1999; Gellman 1998; Poenaru et al. 1999) which makes them attractive as mimetics of CPPs (Raguse et al. 2003; Raguse et al. 2002). Despite their different backbone, β -homoarginine (Rueping et al. 2002), β -homolysine (Garcia-Echeverria and Ruetz 2003), and β -Tat (Potocky et al. 2003) exhibit a remarkable membrane penetration activity. β -peptides adopt a 3_{14} -helical conformation with a helical pitch of exactly 3.0, so that all side chains are positioned in an angle of $\sim 120^\circ$ to one another and there are three discrete positions in a helical wheel plot, where the side chains reside. This facilitates the task of designing peptides in which side chains of similar properties are aligned at the same face as to form amphipathic helices (Rueping et al. 2004). Thus the effects of conformational constraints on translocation activity can be systematically tested.

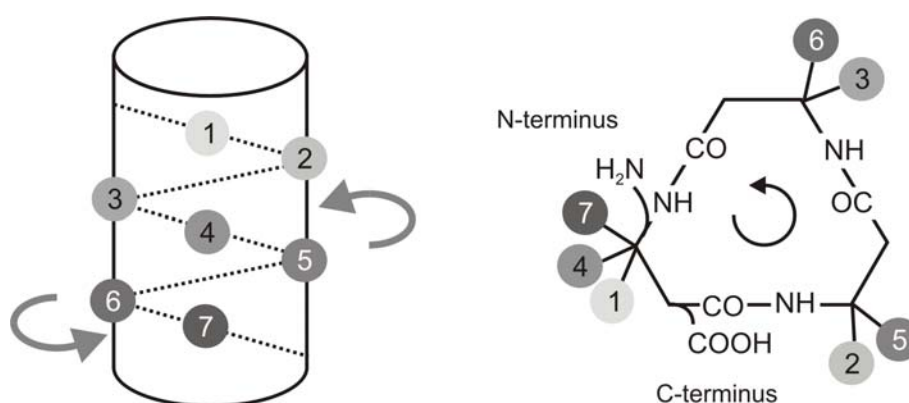
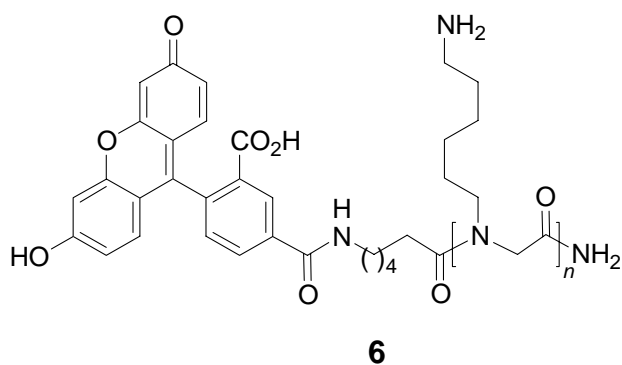


Figure 1-22 Schematic representation of the 3_{14} -helix and helical wheel plots β -peptides. The backbone of the β -peptide forces the residues into an eclipsed conformation leading to three predictable sites at which functional groups can reside (Rueping et al. 2004).

Another closely related class of backbone mimetics are poly-N-substituted glycines, known as peptoids, that have had an impact on combinatorial gene therapy, drug delivery, and biopolymer folding (Figliozzi et al. 1996; Wender et al. 2000; Zuckermann et al. 1994).

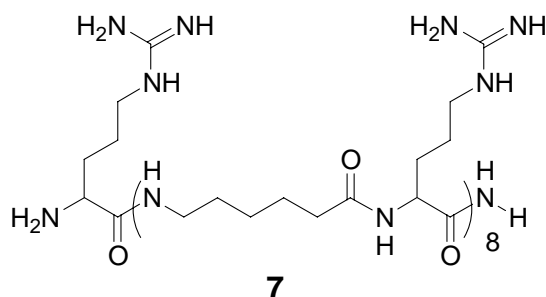
In the peptoid backbone, side chains are attached to the amine, so that the monomers can be easily prepared from functionalized diamines and bromoacetic acid. As opposed to α -peptides, these diverse non-natural, biomimetic oligomers are resistant towards proteases, which enhances their life-time in *in vivo* applications. Due to a lack of hydrogen-bond donors, the achiral peptoid backbone cannot form peptide helical structures. Yet, *N*-substituted glycines of only five residues with chiral, aromatic side chains form stable, polyproline-like helices, due to the steric influence of the bulky side chains (Sanborn et al. 2002).



Scheme 1-5 Fluorescein-coupled peptoid transporter, **6** ($n=5,7,9$), (Wender et al. 2000)

Like the highly efficient guanidine-rich α -peptides, guanidine-functionalized peptoids are taken up by mammalian cells in a concentration dependent manner (Wender et al. 2000). The highest uptake rate was observed for the hexamer. In tests of oligomers with side chains of varying lengths, it was found that cellular uptake efficiency could be enhanced to even exceed Tat peptide and oligoarginine if the guanidine functionalities were attached to the peptoid backbone on C6-side chains (Wender et al. 2000). None of the peptoids exhibits toxic effects in the lower micromolar concentration range in which the oligomers were applied to the cells, rising their potential for *in vivo* studies (Wender et al. 2000).

Apparently, the spacing between the individual residues is important for cellular uptake. In this context, guanidine-rich peptides and peptoids with 1,4-spaced side chains are more efficiently taken up than Tat peptide. Libraries of mixed arginine-rich oligomers were examined and a new series of molecular transporters was identified that is made up from alternating units of arginine and aminocaproic acid (aca) (Rothbard et al. 2002).



Scheme 1-6 Optimized oligoarginine-aminocaproic acid transporter **7** (Rothbard et al. 2002)

Replacing the amide backbone with carbamate results in increased spacing, higher flexibility and thus enhanced uptake (Wender et al. 2002). In agreement with studies on peptoids and CPPs, the rate of uptake increased with guanidine content ($8 > 7$) and concentration (Derossi et al. 1994; Dom et al. 2003; Vives et al. 1997a; Vives and Lebleu; Wender et al. 2000). The best internalization of fluorescein-coupled oligocarbamates into Jurkat cells as analyzed by FACS was found for the hepta- and nonamers. The latter belong to the best guanidine-based transporters studied to date entering cells 230 times faster than Tat peptide.

Finally, attempts have been made to use polyamines to increase the uptake of various substances. Polyamines are positively charged under physiological conditions, so that they interact with the plasma membrane and may use the same mechanism as CPPs to reach the interior of the cells. They might as well exploit the polyamine transporter (PAT) for internalization of covalently attached cargos. However, the capability of PAT to transport large cargos is limited by the size of a hydrophobic pocket adjacent to the polyamine binding site (Gardner et al. 2004).

In the further parts of this work, β -peptides, peptoids, oligocarbamates and other peptide mimetics that function like CPPs to deliver cargo molecules shall be referred to as synthetic transporters, while membrane-spanning proteins for the selective transport metabolites are denoted as cellular transporters.

1.2.12 The versatility of CPPs

CPPs and synthetic transporters have been shown to effectively deliver almost all kinds of cargoes ranging from peptides and proteins to nucleic acids and from insoluble small molecules to nanoparticles, liposomes and entire viruses. For some classes of substances peptide-mediated delivery may be the only form to reach the interior of the cells.

1.2.12.1 Peptides and proteins

PTDs were discovered as domains of larger proteins that could be internalized by cells due to the presence of the PTD (Derossi et al. 1998; Frankel et al. 1988; Green and Loewenstein 1988). Therefore, it was reasonable that the first studies of PTDs and later CPPs dealt with protein cargoes to replace the protein of origin. Today, fusions of CPPs with model peptides are introduced into cells as an important means to study the molecular mechanisms of signal transduction and other intracellular processes. Such fusion peptides can be easily prepared by solid phase synthesis or recombinant expression. Conjugation can also be performed via amide bonds or, reversibly, by disulfide bonds (Gil-Parrado et al. 2003). For non-peptidic cargos, chemical coupling constitutes the only way of conjugate formation (Fischer et al. 2001).

Coupled to CPPs, the cargo-peptides retain their original behavior with respect to potency and biological function. This method permits to study the function of individual domains derived from larger proteins. Thus, several signal sequences could be discovered, putative phosphorylation sites have been assessed and regions relevant to protein-protein interactions identified. From this, many new target sites for potential therapeutic intervention have been derived. (Chen et al. 2001; Gil-Parrado et al. 2003; Ruzza et al. 2001; Schaschke et al. 2002; Stolzenberger et al. 2001; Yakymovych et al. 2002). Like RNA aptamers, peptide aptamers can be refined to bind to specific targets by *in vitro* evolution. Coupled to CPPs these peptides could inhibit the epidermal growth factor receptor (Buerger and Groner 2003). The uptake efficiency has to be determined for each peptide-cargo construct individually, as pronounced differences in import efficiency were observed even for peptide cargos of very similar size (Fischer et al. 2002), and different CPPs could have varying effects on the

transport of the same cargo ranging from an increase of uptake efficiency to a decreased solubility (Lin et al. 2004).

The delivery of biologically active full-length proteins is a more challenging task. According to one of the proposed mechanisms, the process of internalization takes place under denaturing conditions and not all proteins are properly refolded upon reaching the cytosol (Schwarze et al. 2000). However, GFP coupled to transportan did not lose its fluorescence in the transport process (Pooga et al. 2001), and the activity of Tat-coupled β -galactosidase could be still detected in several tissues after in vivo application (Fawell et al. 1994; Schwarze et al. 1999). So depending on CPP and cell type, the cargo protein remains functional, which is of special interest for the treatment of pre-clinical disease models (Wadia and Dowdy 2002). Several clinically important proteins including antibodies have been delivered into cells with Tat₄₉₋₅₇, transportan, and NLS-derived peptides as fusion tags (Gius et al. 1999; Nagahara et al. 1998; Pepinsky et al. 1994; Pooga et al. 2001; Vocero-Akbani et al. 1999). The fusion protein of His₆-tagged Cre recombinase with an NLS is readily taken up. Its uptake, however, can be significantly improved by fusion with Tat peptide reaching over 95% of recombination efficiency in cultured fibroblasts, primary splenocytes and murine embryonic stem cells (Kasim et al. 2004; Peitz et al. 2002).

Another challenge is the delivery of artificial transcription factors to the nucleus. Exploiting naturally occurring gene-regulators that act on genomic DNA, the Tet-repressor was coupled to the full-length Antennapedia homeodomain from *Drosophila*. The conjugate entered the cells where it acted to repress a tetracycline regulated reporter unit that was either transiently transfected or inserted into the genome of HeLa cells (Mortlock et al. 2003).

It has to be kept in mind that the fusion with a CPP may also hinder the biological activity of its cargo, as it has occurred for kinase inhibitor peptides attached to Tat (Kelemen et al. 2002) and an anti-tetanus F_{ab}-fragment that was only active if the Tat peptide was conjugated by a cleavable disulfide bond (Stein et al. 1999).

1.2.12.2 Small molecules

For some drugs, topical application is desirable to avoid severe side effects that occur upon systemic application. To overcome the limitation posed by the low skin permeability of these drugs, they can be covalently coupled to CPPs. As an example, cyclosporin A attached to a heptamer of arginine was transported into cells of murine and human skin where it inhibited cutaneous inflammation (Rothbard et al. 2000). Similarly, arginine-based molecular transporters were conjugated to the anti-tumor agent taxol. Depending on the chosen linker structure, highly water-soluble substances were obtained that could release the drug in a pH-dependent manner (Kirschberg et al. 2003).

1.2.12.3 Inorganic particles

As proteins as large as 120 kDa (β -galactosidase) can be delivered by CPPs (Schwarze et al. 1999), further studies aimed to assess the size of particles that can be possibly internalized by CPPs. Biotin-coupled transportan was complexed with streptavidin-modified

gold particles. The largest conjugates taken up by commonly used cell-lines corresponded to proteins with a mass of more than 1 MDa (Pooga et al. 2001).

Superparamagnetic iron oxide nanoparticles (SPION) are used as contrast agents for magnetic resonance imaging (MRI) and as reagents for cell labeling. 9-10 Tat peptides per nanoparticle are required to improve the uptake efficiency of an MRI contrast agent by up to two orders of magnitude (Nitin et al. 2004; Zhao et al. 2002). Likewise, radioactive complexes for applications in molecular imaging and radiotherapy could be delivered by Tat peptide. For this purpose, oxotechnetium(V) and oxorhenium(V) were complexed by peptide based donors attached to Tat peptide. [⁹⁹Tc]-Tat peptide showed elevated accumulation and rapid uptake kinetics in Jurkat cells. Whole body distribution and rapid clearance were found in preliminary imaging studies in mice (Polyakov et al. 2000).

By conjugation with Tat, silica nanoparticles of 70 nm coupled with FITC (fluorescein isothiocyanate) could be introduced into cultured lung adenocarcinoma cells and into rat brain tissue *in vivo* for future applications in bioimaging applications (Santra et al. 2004)

To direct contrast agents specifically to tumor cells, activatable CPPs (ACPPs) have been designed, in which the capacity to enter cells is blocked by a linker consisting of negatively charged amino acids that interact with the basic residues of the CPP moiety leading to charge neutralization. Both domains are linked via a protease recognition site that is specific to matrix metalloprotease 2 and 9 that are secreted by tumor cells. Thus, approaching tumor cells, the CPP is cleaved from its inhibitor and its potential to associate with the plasma membrane is enhanced by one order of magnitude as opposed to the ACCP (Jiang et al. 2004).

1.2.12.4 Nucleic acids and PNAs

A special need for new delivery agents lies in nucleic acid-based approaches like gene therapy, antisense-mediated gene silencing and RNAi. Although many transfection methods have been developed and refined for most cell types, yields in primary and non-dividing cells are often low and the majority of cells is killed during the procedure. Moreover, the cationic lipids often used for transfection are toxic to fully-grown organisms. Therefore, many efforts have been undertaken to use CPPs for the delivery of nucleic acids.

As nucleic acids, especially RNA, are sensitive towards degradation by nucleases, chemical modifications have been introduced to increase their *in vivo* stability. The use of phosphorothioates is very common, even though the thiol-containing backbone exhibits toxic effects. Those can be minimized, if only small doses are applied. To obtain the desired effects with small doses of oligonucleotides the otherwise poor uptake efficiency of these molecules needs to be enhanced.

Peptoids could be used for the delivery of antisense oligonucleotides with a phosphorothioate backbone into cells, where they interfered with the transcription of homologous RNA. Due to their chemical structure, both, cell-penetrating molecule and antisense agent, were stabilized against nucleases and proteases (Innis 2001). Peptide nucleic acids (PNAs) are commonly used as antisense agents that are not recognized by proteases and nucleases. Coupling to transportan led to the internalization of a PNA designed against the transactivation response (TAR) element of HIV-1 to inhibit Tat-

mediated transactivation in HIV-1 infected H9 cells (Kaushik et al. 2002). Transportan (Pooga et al. 1998a), Penetratin™ (Braun et al. 2002; Villa et al. 2000), NLS, and an artificial peptide of the sequence D(AAKK)₄ (Kaihatsu et al. 2004) have also been used in antisense-PNA delivery, and (KFF)₃K was utilized for the internalization of artificial ribonucleases based on PNAs (Petersen et al. 2004).

PNAs attached to an NLS can be coupled to Penetratin™ via a disulfide bond. Thus, the cargo is taken up and the Penetratin™ moiety is cleaved in the cytosol so that it does not interfere with the nuclear import of the cargo (Braun et al. 2002). A similar strategy was employed to deliver an NFκB decoy that prevents the DNA binding of the transcription factor by binding it in the cytosol. A double-stranded consensus sequence mimicking the κB-site was synthesized with an overhanging single-strand corresponding to a PNA-sequence that would be linked to transportan (TP) or its shorter analog (TP10) via a disulfide bond. This complex was able to enter cultured rat insulinoma cells, where it successfully blocked an inflammatory response by inhibiting interleukin-6 expression (Fisher et al. 2004).

Comparison of peptide-mediated uptake with the lipid-mediated delivery of PNA/DNA hybrids led to the result that lipid transfection requires less PNA while peptide-mediated delivery was simpler and less toxic to primary endothelial cells (Kaihatsu et al. 2004).

In early experiments, single stranded oligonucleotides of up to 50 nt had been delivered by penetratin (Prochiantz 1996), which was not only of high interest for antisense-mediated silencing but also for attempts to regulate transcription. Triplex forming oligonucleotides (TFOs) are designed to bind to genomic DNA in order to modulate gene expression. Attached to penetratin, their efficiency *in vivo* was enhanced by a factor of 20, which implies that peptide-mediated delivery even reaches the chromosomal DNA located inside the nucleus (Rogers et al. 2004).

Genetic vaccination is another field where CPPs are on their way to become a valuable tool. In this new approach, the immune system is primed to new epitopes by applying the corresponding recombinant peptides or expression vectors coding for the respective epitopes. These epitopes are recognized by T-cells and induce the formation of specific T-cells from native lymphocytes. To improve intracellular delivery, an NLS was coupled to a minimalized expression vector of linearized DNA encoding a hepatitis B epitope. Thus, the formation of cytotoxic T-cells was triggered upon intramuscular injection into mice (Schirmbeck et al. 2001).

To deliver even larger nucleic acids, the cargo is encapsulated inside of recombinant viruses. The uptake of the virus could be greatly enhanced by modifying the surface of recombinant replication-deficient viruses with Penetratin™ (Gratton et al. 2003). Alternatively, λ-phages, can be used for gene delivery in mammals. As these viruses normally infect bacteria, they are less pathogenic in mammals. λ-phages displaying the SV40 NLS on their surface have a higher affinity for the nucleus, if delivered to the cytosol, and enhance the expression of the cargo DNA (Akuta et al. 2002). The drawbacks of viral therapies have been already discussed.

For the virus-free transfer of large nucleic acids, Tat and Penetratin™ were coupled to liposomes, which greatly enhanced the internalization efficiency if on average only five peptides per liposome were attached. For efficient delivery into a variety of cells, the liposome-attached peptides must be able to freely interact with the cell surface (Torchilin and

Levchenko 2003; Tseng et al. 2002). Fluorescent markers entrapped inside liposomes and incorporated into the liposomal membrane indicated that the Tat peptide-liposomes remain intact within first few hours before they migrate toward cell nuclei and completely disintegrate in the course of 9 h. Tat peptide-liposomes containing up to 10 mol % of a cationic lipid (DOTAP) are non-toxic toward cells and transfected a variety of cells (Torchilin 2002).

Unilamellar liposomes of ~100nm required at least 100 covalently linked Penetratin™ or Tat peptides for efficient cellular uptake (Marty et al. 2004).

In similar approaches, cell-penetrating peptoids were coupled to lipids (lipitoids) and sterol (cholesteroids) yielding a novel class of molecules for the transfection of cells with oligonucleotides. They exhibit low toxicity and are compatible with serum (Huang et al. 1998; Lobo et al. 2003).

The combination of an SV40 large T-antigen derived NLS peptide (NLSV40) with preformed polyethyleneimine or dendrimer-DNA complexes also resulted in a strong increase of transfection efficiency (Ritter et al. 2003).

Penetratin™ was also used to enhance the efficiency of Lipofectamine, a commonly used transfection agent. If a fusion peptide of penetratin and L-4F, an amphipathic lipid binding peptide, was pre-incubated with the transfection reagent, the transfection efficiency in coronary epithelial cell culture was increased by 64% without affecting the viability of the cells (Ou et al. 2003).

Nucleic acid delivery can be also achieved without the use of lipid transfection agents if the DNA is complexed with an excess of penetratin, VP22, Tat or NLS derived peptides (Dom et al. 2003; Kretz et al. 2003). Due to electrostatic interactions, the DNA is condensed by the peptides resembling the DNA condensation on the histone proteins. The use of NLS-derived sequences to complex antisense oligonucleotides leads to a nuclear localization of the cargo, as it was shown for fusion peptides from protamine DNA-binding domain with the SV40 NLS (Benimetskaya et al. 2002). However, it is assumed that these particles, also termed vectosomes, are taken up by a mechanism comparable to conventional transfection (Ignatovich et al. 2003; Zavaglia et al. 2003). Vectosomes based on VP22 have been used to deliver a variety of nucleic acids, including ribozymes, plasmid DNA and antisense RNA. VP22 vectosomes must be activated to release their cargo. Thus, they can be administered systemically but will act only locally upon radiation with the appropriate wavelength and intensity. As an example, antisense oligonucleotides directed against the c-Raf1 oncogene have been incorporated into vectosomes and successfully inhibited tumor growth in mice upon light activation (Brewis 2003; Zavaglia et al. 2003). Alternatively, different cleavage sites can be incorporated into the protein to use endogenous proteases for release. Very recently, the coupling of siRNAs to Tat peptide and penetratin has been reported by several groups (Chiu et al. 2004a; Davidson et al. 2004; Muratovska and Eccles 2004; Schmitz et al. submitted).

| Cargo | Transporters | Reference |
|--|--|--|
| Cyclosporin A | Heptaarginine | (Rothbard et al. 2000) |
| Methotrexate | Polylysine | (Ryser et al. 1988) |
| Doxyrubicin | SynB1 | (Rousselle et al. 2001) |
| Taxol | Oligoarginine | (Kirschberg et al. 2003) |
| Benzyl-Penicillin | SynB1 | (Rousselle et al. 2002) |
| GFP (238 aa) | Fushi-tarazu, Engrailed | (Han et al. 2000) |
| Cathepsin B inhibitors (5 aa) | Penetratin | (Schaschke et al. 2002) |
| Horseradish peroxidase | poly-L-lysine (6.7 kDa) | (Shen and Ryser 1978) |
| β -galactosidase | Tat peptide | (Fawell et al. 1994; Schwarze et al. 1999) |
| Biotin | Oligocarbamate transporters | (Wender et al. 2002) |
| GFP | Transportan | (Pooga et al. 2001) |
| Cre-recombinase | Tat peptide, NLS | (Kasim et al. 2004; Peitz et al. 2002) |
| Fab-fragment | Tat peptide | (Stein et al. 1999) |
| Tet-repressor | Antennapedia full-length | (Mortlock et al. 2003) |
| silica nanoparticles + FITC | Tat peptide | (Santra et al. 2004) |
| Superparamagnetic iron oxide nanoparticles | Tat peptide | (Nitin et al.; Zhao et al. 2002) |
| Radioactive isotopes, | Tat peptide | (Polyakov et al. 2000) |
| Fluorescein | Oligoarginine | (Vives et al. 1997b) |
| Fluorescein | Peptoids | (Wender et al. 2000) |
| Fluorescein | β -peptides | (Umezawa et al. 2002) |
| Fluorescein | Oligocarbamates | (Dom et al. 2003) |
| NF- κ -B decoy | Transportan | (Fischer et al. 2001) |
| DNA | Penetratin (non-covalent) | (Dom et al. 2003) |
| DNA | Penetratin, VP22, Tat or NLS | (Kretz et al. 2003) |
| DNA | MPG | (Morris et al. 1997) |
| Linearized DNA vector | NLS | (Schirmbeck et al. 2001) |
| Antisense-PNA | Transportan | (Kaushik et al. 2002; Pooga et al. 1998c) |
| Antisense-PNA | D(AAKK) ₄ | (Kaihatsu et al. 2004) |
| Triplex-forming oligonucleotides | Penetratin | (Rogers et al. 2004) |
| Antisense RNA | Penetratin | (Astriab-Fisher et al. 2002) |
| Antisense oligonucleotides | Tat peptide, penetratin, VP22 (non-covalent) | (Brewis 2003; Zavaglia et al. 2003) |
| Antisense nucleotides | Peptoids | (Zuckermann et al. 1994) |
| siRNAs | Penetratin | (Davidson et al. 2004; Muratovska and Eccles 2004; Schmitz et al. submitted) |
| siRNAs | Tat peptide, oligocarbamates | (Chiu et al. 2004a) |
| λ phages | SV40-NLS | (Akuta et al. 2002) |
| Recombinant viruses | Penetratin | (Gratton et al. 2003) |
| Adenovirus | Polylysine | (Mulders et al. 1998) |
| Dendrimer-DNA complexes | NLS-SV40 | (Ritter et al. 2003) |
| 200-nm liposomes | | (Torchilin et al. 2001) |
| Stabilized liposomes | Tat peptide, penetratin | (Tseng et al. 2002) |
| 100 nm liposomes | Tat peptide | (Marty et al. 2004) |
| Lipofectamin/DNA | Penetratin | (Ou et al. 2003) |

Table 1-2 Conjugates of various cargos with different transporter molecules.

Even oligocarbamates could be used to internalize siRNAs (Chiu et al. 2004a). The so-called V-siRNAs or pepsiRNAs were internalized by a variety of cells, even primary neurons and

fibroblasts, were they triggered the degradation and translational inhibition of the targeted mRNAs.

1.2.13 The mechanism of peptide-based delivery

Despite the wide use of CPPs and synthetic transporters to deliver bioactive molecules into all kinds of cells, the mechanism of their internalization is still poorly understood, and the results obtained in numerous studies lead to controversial hypotheses.

All proposed mechanisms need to explain the localization of labeled CPPs in vesicular structures and their exit from these compartments to the cytosol. They also have to account for the fact that no receptors are required and that no leakiness of the cells has been observed implying that the plasma membrane is neither ruptured nor perforated in the process as measured by 2-[³H]-deoxyglucose-6-phosphate leakiness (Hallbrink et al. 2001; Terrone et al. 2003).

It is commonly assumed that CPPs and synthetic transporters enter the cells in a two-step mechanism that is now referred to as peptide-mediated delivery or uptake. First, the positively charged transporter interacts with negatively charged residues on the plasma membrane where it adopts an active conformation. This induces a membrane reorganization process in which the affected region of the membrane is internalized by endocytosis (Console et al. 2003; Drin 2003; Vives 2003). Most CPPs accumulate in the endosomal/lysosomal compartment, but at least a small portion of the CPPs leaves the endosome to reach the cytosol by an as yet unknown mechanism. The mode of uptake may depend on cell-type, cargo, and the CPP or synthetic transporter itself, and it is even possible that several mechanisms are involved simultaneously (Letoha et al. 2003).

1.2.13.1 Non-endocytotic concepts

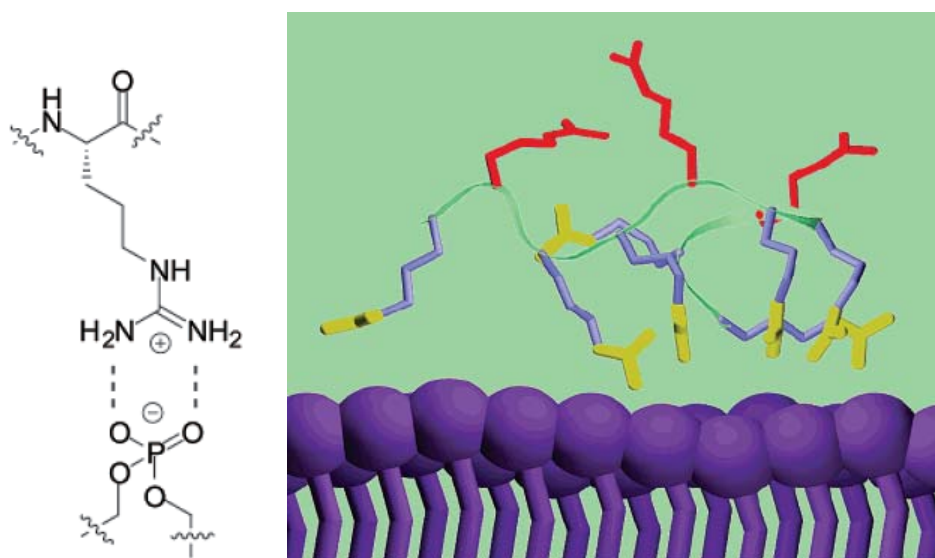
Other models are based on non-endocytotic pathways. One early hypothesis was the formation of inverse micelles. The CPP attached to the membrane was thought to disturb the membrane structure due to surface charge neutralization and thus induce the formation of a hydrophilic cavity that encloses the peptide and its cargo (Berlose et al. 1996; Derossi et al. 1998). However the dimension of cargo molecules like β -galactosidase (120 kDa) (Schwarze et al. 1999) and nanoparticles of 45 nm in diameter (Lewin et al. 2000), that have been delivered by CPPs, forbids the formation of corresponding micelles within the hydrophobic core of the plasma membrane that measures less than 5 nm.

Pore formation was proposed, when the hydrophobic helix domain of KLAL was detected on the inner monolayer of phospholipid vesicles at high peptide concentrations (Dathe et al. 1996). In an electroporation-like mechanism the asymmetrical distribution of the peptide was proposed to cause a transmembrane electrical field that leads to lateral and curvature stress resulting in the disruption of the membrane (Binder and Lindblom 2003). However, entrapped carboxyfluorescein does not leak from phospholipid vesicles upon action of Penetratin™ (Persson et al. 2003) and cellular membranes remain intact during Tat internalization (Potocky et al. 2003; Ziegler et al. 2003). However, spontaneous pore formation has not been abandoned from discussion until today.

1.2.13.2 CPP-membrane interactions

The interaction of the positively charged CPPs with the negatively charged surface of the plasma membrane is essential to peptide-mediated uptake. This was confirmed by alanine exchange studies with penetratin and Tat peptide (Christiaens et al. 2004; Dom et al. 2003; Thoren et al. 2003) and by the fact, that oligomers of basic amino acids are functional as CPPs (Jeang et al. 1999; Lindgren et al. 2000a; McKenzie et al. 2000; Mitchell et al. 2000; Vives et al. 1994).

Peptide interactions with lipid model membranes have been subject to intense studies. Small unilamellar vesicles (SUVs) can be made up from phospholipids with hydrophobic tails of differing chain length and differently charged polar head groups. Measurements of circular dichroism (CD) detect changes in the secondary structure of the peptide upon its interaction with the membrane. The behavior of Penetratin is monitored by the fluorescence of its two tryptophan residues that is indicative of the hydrophobicity of its environment and therefore of its insertion into the membrane. Similarly, the insertion of aromatic residues changes their contribution to CD spectra (Persson et al. 2004). Shifts of individual signals of $^1\text{H-NMR}$ spectra can be also taken as a measure of peptide-membrane interaction



Scheme 1-7 Peptide membrane interactions a) Interaction of guanidinium headgroups with phospholipids. The formation of two hydrogen bonds and the electrostatic interaction result in a tight binding. b) Upon membrane interaction decaarginine adopts a conformation in which 7 arginine residues face the membrane, while three are oriented in the opposite direction (Rothbard et al. 2002).

In most cases, the peptide adopts an amphipathic structure that can interact with the model membrane via hydrophobic interactions, that have been calculated to be independent from the surface charge density (Persson et al. 2003). As determined by isothermal titration calorimetry, the nonclassical hydrophobic effect and a lipid-induced change of the secondary structure make up for an exothermic partial molar enthalpy of -20 to -30 kJ mol^{-1} that drives membrane binding of penetratin (Binder and Lindblom 2003). For neutral vesicles or those

with a low surface charge these hydrophobic interactions are decisive. If the model vesicles bear a highly negative surface charge, electrostatic interactions prevail (Magzoub et al. 2002). This is confirmed by the finding that most CPPs interact much stronger with negatively charged vesicles than with neutral ones (Bellet-Amalric et al. 2000; Christiaens et al. 2002; Dathe et al. 1996; Drin et al. 2001; Magzoub et al. 2001). The amount of internalized peptide correlates with the quantity of peptide initially associated with the cell surface (Drin et al. 2001).

Although the presence of tryptophan residue 48 is essential for the uptake of Penetratin™, it appears to be not involved in the initial interaction of the peptide with the membrane (Christiaens et al. 2004). For the cationic peptide derived from NF-κB, the replacement of individual basic residues by alanine had a weaker effect on uptake efficiency than substitution of a glutamine and a leucine residue (Ragin and Chmielewski 2004). Both findings indicate that there are more factors determining the driving force for membrane translocation.

1.2.13.3 Structural requirements for CPPs

Studies of the relationship between CPP conformation and its membrane translocation ability have led to contradicting results.

Tat peptide and Penetratin™ can both form an amphipathic helix in which all positively charged residues point into one direction and the non-polar residues to the opposite direction (Drin et al. 2001; Rothbard et al. 2002). Therefore, it was proposed that helical amphipathy is a prerequisite for membrane interaction. Indeed, the interaction with phospholipid vesicles grows stronger if the helical amphipathy is increased (Drin et al. 2001). The magnitude of hydrophobic moment and helical wheel plots for fusion peptides with Penetratin™ and Tat peptide are a direct measure for their ability to deliver the attached cargo-peptide (Li et al. 2002). Correspondingly, the most efficient arginine-rich oligopeptides are able to form this kind of amphipathic helices (Ho et al. 2001). Studies on amphiphilic peptides designed to prefer an α -helical or a β -sheet conformation showed that conformational properties can influence the interactions with phospholipids (Deshayes et al. 2004).

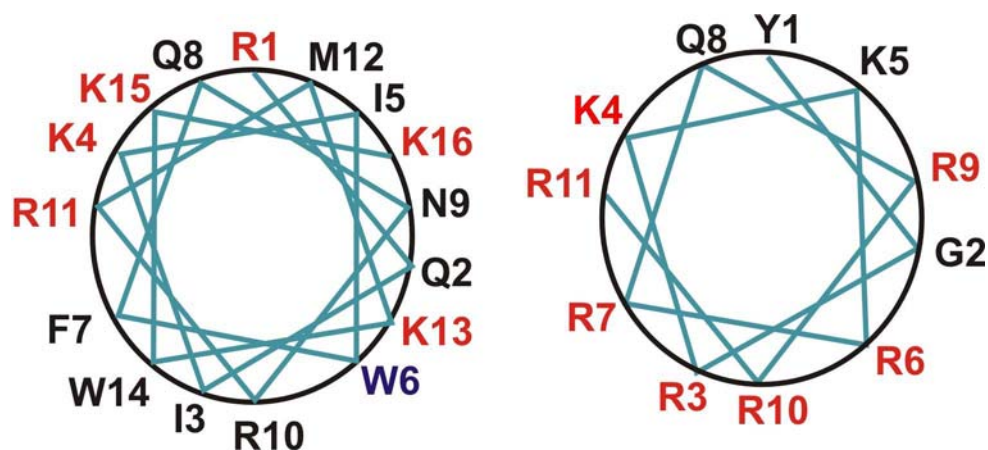


Figure 1-23 Helical wheel plots of Penetratin™ (left) and Tat peptide (right). Positively charged residues (red) are located toward one face of the helix.

However, no correlation between helical conformation and membrane translocation could be found for Penetratin™ and its homologs (Drin et al. 2001). Moreover, the introduction of the “helix-breaker” proline into the Penetratin™ sequence does not alter its cellular uptake (Derossi et al. 1996). Amphipilic proline-rich peptides from the antimicrobial peptide bactenecin7 have recently been discovered as a novel class of CPPs (Fernandez-Carneado et al. 2004; Sadler et al. 2002). Possibly, a non-helical conformation can mediate uptake as long as the majority of positive residues can interact with the membrane.

Apparently, the membrane composition itself determines the secondary structure of the CPPs, many of which show no ordered conformation in free solution. The α -helical state is adopted at low concentrations of peptide and at low surface charges (Christiaens et al. 2002; Magzoub et al. 2002; Magzoub et al. 2001) and has little effect on the membrane as the peptides lie parallel to surface. β -sheet-like structures are induced by vesicles with high negative surface charges or high peptide concentrations and lead to membrane perturbation (Magzoub et al. 2002). The artificial MPG generally adopts a β -sheet upon interaction with phospholipids, while Pep-1 is found in a helical conformation (Deshayes et al. 2004). The α -helical conformation of Penetratin™ and its homologs is increased when associating with model membranes. The peptide resides at the water-lipid interface with the tryptophan residue partially buried in the membrane. The membrane insertion is increased if individual arginines and lysines are replaced by alanine (Christiaens et al. 2004). Using PEGylated lipids, it was shown that vesicle aggregation induces an α -helix to β -sheet conformational transition in Penetratin™ and homologous peptides (Persson et al. 2004). It has been proposed that the lipid-induced secondary structure determines the hydrophobicity of the CPPs and thereby the insertion mode that precedes internalization (Binder and Lindblom 2003).

1.2.13.4 Other components involved in CPP-membrane interaction

In none of these studies the peptide was found inside the vesicle indicating that uptake by spontaneous membrane penetration is less likely and that some other features of living cells are required for internalization (Drin et al. 2001; Kramer and Bentley 2003; Ziegler et al. 2003). As already mentioned, receptor interactions had been ruled out by the first reports about protein transduction. Non-lipid negatively charged structures such as extracellular glycosaminoglycans appeared to be a suitable target for CPP binding (Console et al. 2003). Indeed, the internalization of Tat and Penetratin™ was significantly reduced in mutant cells defective for glycosaminoglycan synthesis. Free heparan sulfate proteoglycans (HSGs) diminished the uptake of penetratin, while heparin and dextran sulfate inhibited Tat-mediated uptake indicating that the specific interaction with distinct glycosaminoglycan species is preferred over the interaction with the lipids of the plasma membrane (Console et al. 2003). Heparin also inhibited the uptake of Tat and Penetratin™ modified liposomes, and these cargos could not be taken up by glycosaminoglycan-deficient CHO cells, confirming the role of glycosaminoglycans for CPP uptake (Marty et al. 2004).

These results were contradicted by studies in which Tat peptide entered readily into HeLa and KB 3-1 cells, but not into renal epithelial and colonic carcinoma cells, although all cell

lines express HSGs (Violini et al. 2002), and in which the uptake of Tat peptide did not involve HSGs (Silhol et al. 2002).

1.2.13.5 Energy requirements and Endocytosis

After correcting the procedures to avoid artifacts it was found that CPPs are taken up over a time-course of several hours (Richard et al. 2003; Umezawa et al. 2002) rather than minutes as had been previously reported (Vives et al. 1997a). Up to 10 hours were required to fully internalize a Tat-GFP fusion protein (Fittipaldi et al. 2003). However, due to the high membrane interaction of the cationic peptides, pulsed incubation times of only 5 min are sufficient to attach a significant amount of peptide-coupled cargo to the membrane to be taken up in the course of the following hours (Soughayer et al. 2004).

Fluorescently labeled CPPs reside in vesicular structures (Drin 2003; Fischer et al. 2004; Kaihatsu et al. 2004; Richard et al. 2003; Thoren et al. 2003; Trehin et al. 2004; Umezawa et al. 2002; Vives and Lebleu 2003). Tat and nonaarginine conjugates with fluorescein were not only found distributed in dots, but also colocalized with endocytotic markers (Diaz-Griffero et al. 2002). And also fusion proteins of VP22, Tat, oligoarginine, and oligolysine are confined to the endosomes (Lundberg et al. 2003; Richard et al. 2003).

The uptake of CPPs is markedly reduced at 4°C pointing at an energy-dependent mechanism. Correspondingly, the accumulation of CPPs in endosomes could be inhibited by the addition of sodium azide and 2-deoxyglucose that interfere with oxidative phosphorylation leading to ATP depletion (Console et al. 2003; Drin 2003; Lin et al. 2004; Saalik et al. 2004; Thoren et al. 2003; Vives et al. 2003). All these findings propose an endocytosis-based mechanism.

This is confirmed by a series of studies using inhibitors of endocytosis to inhibit the uptake of SynB (Drin 2003), Penetratin™ (Drin 2003; Fischer et al. 2004), Tat peptide and Arg₉ (Fischer et al. 2004). Likewise, inhibition of endocytosis by hyperosmolar medium containing 0.4 M sucrose decreased the uptake of penetratin, Tat peptide, transportan and pVEC (Saalik et al. 2004). Treatment of the cells with β-cyclodextrin leads to a cholesterol depletion that goes along with a disappearance of rafts and caveolae and the inhibition of their re-formation (Thyberg 2002). Under cholesterol depletion none of the tested CPPs was taken up, which indicates an involvement of rafts or caveolae in peptide-mediated uptake (Saalik et al. 2004). Recently, it was found that fusion peptides of Tat with Cre recombinase are taken up by macropinocytosis of lipid rafts (Wadia et al. 2004).

The fact that only a fraction of the CPP-related fluorescence co-localized with the transferrin receptor, confirmed the original reports about a receptor-independent process (Potocky et al. 2003). Strong evidence exists that lipid rafts and caveolae are involved in the uptake of Tat (Fittipaldi et al. 2003).

Interestingly, Penetratin™ and Tat are not taken up by isolated mitochondria even when conjugated to lipophilic triphenylphosphonium (TPP) cations, that are known to trigger the uptake of attached molecules into the mitochondria driven by the membrane potential. In cell culture, Tat and Tat-TPP accumulate in endosomes but do not enter into mitochondria. Obviously, neither CPP can overcome the mitochondrial phospholipid bilayer. As

mitochondria do not possess a vesicular transport system, this result strongly supports the view of an endocytosis-mediated uptake of CPPs (Ross and Murphy 2004).

One could imagine, that CPPs simply stick to the surface of the plasma membrane from where they are internalized along with their cargo in the process of membrane recycling. Considering that half of the fibroblast cell surface is recycled within a few minutes (Thilo et al. 1995) the CPP-coupled cargo molecules are likely to be rapidly internalized once they associate with the plasma membrane.

In microorganisms like *Staphylococcus aureus*, *Candida albicans* and *Mycobacterium smegmatis*, pVEC and TP10, a transportan derivative, act very much like antimicrobial peptides. Within minutes, the peptides accumulate on the microbial surface and enter into the cells leading to a lethal permeabilization of the membrane. At low micromolar doses, microbes are seriously damaged, while HeLa cells remain unharmed, so that mammalian cell cultures can be cleared from microbial infections (Nekhotiaeva et al. 2004). Endocytosis may actually help to protect mammalian cells from membrane damage caused by CPPs. Alterations of membrane thickness and structure upon interaction with CPPs have been shown for phospholipid vesicles (Binder and Lindblom 2003; Deshayes et al. 2004; Salamon et al. 2003), and transportan alters the resistance of an epithelial barrier model (Lindgren et al. 2004). Such changes in membrane constitution may trigger a series of events that result in the removal of the destabilized patch of membrane by endocytosis. Yet, as opposed to microinjection or pinocytic loading, neither membrane repair pathways, nor stress induced or proteolytic pathways were triggered by Tat-fusion peptides (Soughayer et al. 2004).

1.2.13.6 The way to the cytosol

The endocytotic model accounts well for the overall integrity of the plasma membrane observed throughout the internalization process. However, CPPs have been found leaking to the cytosol and entering the nucleus in the course of few hours (Fischer et al. 2004; Thoren et al. 2003; Zaro and Shen 2003). CPP-delivered substrates for cytosolic kinases were even shown to be accessible after 30 min with the majority being available after 1h (Soughayer et al. 2004). Many more biological responses obtained from otherwise non-permeant molecules (see 1.2.12) can only be explained by a cytosolic localization of the cargo molecules. The leaking of fluorescently labeled CPPs to the cytosol is not observed if ammonium chloride, an inhibitor of endosomal acidification, is added to the culture medium (Potocky et al. 2003; Thoren et al. 2003) suggesting that a pH-shift is required for “endosomal escape” or release.

In recent studies, it was found that intact fluorescein-labeled Penetratin™ and Arg₉ escaped into the cytosol, while Tat peptide had obviously been degraded by endosomal proteases so that its fragments were found in the supernatant of the cultured cells (Fischer et al. 2004). Here, the incubation of the cells with bafilomycin A1 and chloroquine, inhibitors of endosomal acidification, led to an increase of the Tat related fluorescence in the endosomes, confirming that acidification is required for release from the endosomes. Although a direct pH-dependent membrane penetration has been observed for botulinum C2 toxin (Barth et al. 2000), acidification of the cell culture medium could not trigger a direct cytosolic localization of either

peptide (Fischer et al. 2004). None of the tested peptides colocalized with lysosomal trackers, indicating that endosomal escape takes place at an early stage of maturation. Co-incubation of the cells with CPPs and fluorescently labeled dextran led to the same distribution as found for dextran alone, so that the endosomes must stay intact while the CPPs exit to the cytosol (Fischer et al. 2004).

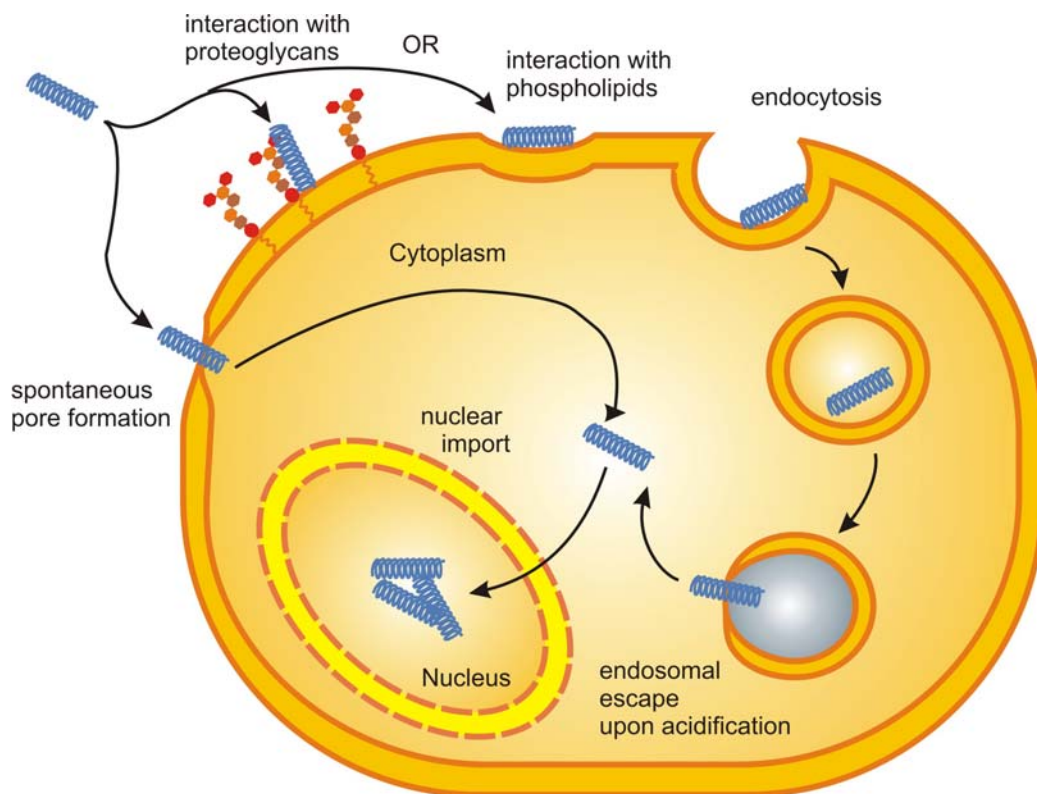


Figure 1-24 Suggestions for the mechanism of peptide mediated delivery. The peptide interacts with negatively charged phospholipids or glycosaminoglycans on the cell surface. Thereby the membrane composition is disturbed and the peptide is taken up by endocytosis. Acidification is required for endosomal escape that releases the peptide into the cytosol. Alternatively, interaction with the plasma membrane could lead to spontaneous pore formation followed by internalization of the peptide.

Brefeldin A, an inhibitor of retrograde trafficking, could interfere with the uptake and cytosolic activity of Tat-GFP conjugates (Fittipaldi et al. 2003). For fluorescein-labeled Tat, the exit to the cytosol was also inhibited by Brefeldin A. Apparently, the CPPs are taken up into a compartment distinct from endosomes, that is functionally coupled to the cytosol (Fischer et al. 2004). Correspondingly, NDGA, that induces the rapid retrograde movement of Golgi stack and TGN membranes, led to an increase of cytosolic fluorescence, when cells were pre-incubated with peptides and then chased with the lipoxygenase inhibitor NDGA. If Golgi stack and TGN are disrupted by the addition of NDGA prior to CPP incubation, much less cellular fluorescence was observed. Co-incubation with Bodipy-ceramide, a cell permeant Golgi tracer, led to only a partial colocalization with the labeled Penetratin™ and Tat peptide, which may be due to a rapid passage through the Golgi (Fischer et al. 2004). It was concluded that cationic CPPs act similar to some plant and bacterial toxins such as ricin and

Shiga toxin that after endocytosis pass the Golgi and the ER to enter the cytosol (Sandvig and van Deurs 2000). Interestingly, all of these toxins contain an arginine-rich motif. Moreover, gentamycin and other cationic aminoglycosides reach the cytosol by retrograde transport (Sandoval and Molitoris 2004), that may constitute a general pathway for cationic low molecular weight compounds (Fischer et al. 2004).

1.2.13.7 Recent indications for direct transduction

In most experiments, CPP uptake was never fully inhibited at low temperatures or when endocytosis was inhibited, giving room for speculations about non-endocytotic side-mechanisms of CPP uptake (Drin et al. 2001; Letoha et al. 2003; Soughayer et al. 2004; Thoren et al. 2003; Zaro and Shen 2003) that have not been settled, yet. Many recent reports still hold to the idea of pore formation, as in the process of MPG-mediated delivery of oligonucleotides (Deshayes et al. 2004; Letoha et al. 2003). These ideas are supported by the finding that Penetratin™ and its homologs, in which individual arginine and lysine residues are replaced with alanine, lead to the leakage of calcitonin-filled vesicles (Christiaens et al. 2004). Of the well-studied CPPs, Penetratin™ is most likely to act by a different mechanism, as its cellular uptake strongly depends on the presence of tryptophan residue 48 (Christiaens et al. 2004; Dom et al. 2003). On the contrary, the Norden group reported that substitution of the tryptophan residues did not alter the uptake characteristics. However, they found that a heptaarginine peptide with a tryptophan residue at its C-terminus is internalized via an energy-independent non-endocytotic pathway (Thoren et al. 2003).

Penetratin™ (Binder and Lindblom 2003; Thoren et al. 2003), but also hexamers of arginine and lysine, were found to enter into artificial systems (Terrone et al. 2003). In the presence of a transmembrane potential, they were detected on the inner leaflet of large unilamellar vesicles (LUVs) bearing negative charge inside. The uptake efficiency strongly depends on the lipid composition. Remarkably, leakiness assay detected only minor disturbances of overall barrier function of the lipid bilayer upon peptide uptake (Terrone et al. 2003). These findings were confirmed by a study in which penetratin and its homologs readily entered giant unilamellar vesicles (GUVs, >1µm), but not LUVs (100nm), and accumulated at the inner leaflet of the vesicles (Persson et al. 2004).

According to Binder and Lindblom, a transmembrane potential can be generated in vesicles with a high concentration (>50%) of negatively charged phospholipids. At a critical peptide-to-lipid ratio of ~1/20 the membrane becomes permeable and the peptide can enter in a kind of electroporation mechanism that involves inversely curved transient membrane structures. However, this is only possible if the negative charges on the membrane are high enough to recruit a sufficient amount of peptide accounting for the required field strength (Binder and Lindblom 2003). Domains of sufficiently high negative charge density may occur in the plasma membrane (Murray et al. 1999), and more negatively charged lipids are recruited to the vicinity of membrane associated cationic peptides (Binder and Lindblom 2003; May and Ben-Shaul 2000). The central question remains whether the peptides can directly penetrate the plasma membrane or whether direct penetration plays a role in the exit from the endosomes, where a comparable potential is built up upon acidification and accumulation of positively charged peptides.

1.2.13.8 The specificity of peptide-mediated delivery

According to the latest results, CPPs act nonspecifically by attaching to negatively charged residues on the cell surface. The stronger the interaction with the plasma membrane, the more efficient is the cellular uptake. It was shown as early as 1993 (Anderson et al. 1993) that Tat-coupled F_{ab}-fragments targeting a cell surface antigen enter the cells more readily with more peptide moieties attached at the cost of a reduced specificity. This non-specificity of CPP-membrane interactions sets a limit to attempts to target specific cell types or tissues. To restrict peptide mediated delivery to a certain tissue, the peptide-coupled compound needs to be applied locally, as for example cutaneously to treat skin disease, orally or intranasally to reach the respective mucosa, or by injection into the tissue of interest.

A way towards more specificity lies in activatable CPPs (ACPPs), in which the capacity to interact with the cell surface is blocked by a linker consisting of negatively charged amino acids that neutralize the basic residues of the CPP. If both domains are linked via a protease recognition site that is specific to a protease secreted by a specific cell type, the CPP is cleaved from its inhibitor once it approaches the targeted cells. This concept was first applied to direct contrast agents specifically to tumor cells secreting matrix metalloprotease 2 and 9. Cleavage of the inhibiting domain enhanced the CPP's potential to associate with the plasma membrane by one order of magnitude as opposed to the ACCP (Jiang et al. 2004).

2 Aims of this work

As it has been shown in the introduction, RNA interference bears an enormous potential for medical application that will only become fully exploitable if methods are found to transport dsRNAs or siRNAs into human tissues with the highest efficiencies and with as few side effects as possible.

The aim of this work is the establishment of a new concept to introduce siRNAs into mammalian cells for the transient generation of RNAi phenotypes as an alternative to transfection, electroporation and direct injection.

To enhance their cellular uptake, siRNAs are to be covalently linked to cell-penetrating peptides modified with a C-terminal cysteine. The coupling shall be performed via disulfide bridges that are susceptible to the reducing environment of the cytosol, so that the siRNAs are released once they enter this compartment.

These so-called peptide-coupled siRNAs (pepsiRNAs) are to be tested upon their uptake in mammalian cell culture in comparison to chemical transfection of siRNAs as the standard procedure of transient RNAi today.

This requires efficient strategies to generate the pepsRNA building blocks in large quantities. Cell-penetrating peptides have to be synthesized and modified with a cysteine moiety that needs further activation to permit the formation of peptide-RNA heterodimers. Likewise, siRNAs with a thiol-modification are required. Due to the sensitivity of RNAi toward antisense-strand modifications and alteration of 3'-overhangs, this functionality has to be specifically attached to the 5'-end of the sense strand.

Moreover, new cell-penetrating molecules are to be synthesized and tested upon their capability to transport reporter molecules into mammalian cells, and linked to siRNAs as a first step toward the larger class of cepsRNAs, cell permeating siRNAs.

3 The concept of pepsRNAs

The first and still broadly used transient RNAi-method introduced by Tuschl and coworkers (Elbashir et al. 2001a) is based on the transfection of siRNAs by liposomal transfection. With the technologies at hand, transient RNAi experiments can be performed in a straightforward fashion: With the help of computer programs and databases, it is possible to design a set of highly efficient siRNA-sequences. Of the currently available methods to generate siRNAs of a specific sequence, *in vitro* transcription by T7 RNA polymerase and solid phase synthesis are the most important ones. These siRNAs are then transfected into cultured cells with liposomal transfection reagents and cell-type specific protocols readily available.

If pepsRNAs are to be developed as an alternative system to expand the possibilities of transient RNAi for applications in tissue culture and fully-grown organisms, a system consisting of individual building blocks would be most convenient for the potential user.

To achieve this, different ways have been developed to provide siRNAs of any given sequence with a functionality that can form disulfide bonds with a set of thiol-modified cell-penetrating peptides or synthetic cell permeable molecules. Thus, the membrane permeability of the siRNAs would be greatly enhanced. As opposed to transfection reagents,

cell-penetrating peptides have as yet exhibited a low cytotoxicity up to concentrations of 10-30 μM which is about three orders of magnitude above the concentration range needed for RNAi experiments. Thus, the use of pepsRNA *in vivo* appears feasible.



- synthetic peptides
- recombinantly expressed peptides
- cell permeable small molecules
- synthetic siRNAs
- in vitro* transcribed siRNAs
- (•siRNAs processed by Dicer)

Figure 3-1 Schematic representation of pepsRNAs consisting of three essential building blocks: The CPP (light blue) can be coupled to the siRNA (red) via a variety of linkers that require specific functionalities upon the peptide (blue) and siRNA (orange) moieties.

Both peptide and siRNA can be synthesized on solid phase yielding compounds with high purity in the order of milligrams or micromoles at comparatively high costs (Table 3-1). As this approach permits specific modification of the oligomers at specific sites by the use of modified monomers or the attachment of functional residues prior to cleavage from the solid phase, it is of great use for proof-of-principle experiments in which the cellular localization of the compounds shall be determined or the effects of sequence variations on uptake and knock-out efficiency are to be examined.

| Substance | Quantity | Price | Provider |
|-------------|---|----------------------|-----------|
| Penetratin™ | 500 μg | € 370.60 | Qbiogene |
| siRNAs | 5 nmol (purified) 10 nmol (unpurified) | € 330.00 € 220.00 | Proligo |
| RiboMAX™ | 10 reactions | € 224.62 | Promega |
| DNA-Oligos | 2x 38nt + 1x 17 nt | ~ €50.00 | Sigma-ARK |

Table 3-1 Comparing prices of commercial compounds obtained from solid phase synthesis

If larger quantities are required, molecular biological methods become more interesting. siRNAs can be generated by *in vitro* transcription from DNA-oligonucleotides that can be obtained from customized solid phase synthesis offered at comparatively low prizes considering that one set of template-DNAs is sufficient for several hundred *in vitro* transcription reactions. If the transcription of sense and antisense strand is carried out separately, one strand can be selectively functionalized by the addition of functionalized nucleotides to the reaction mixture or subsequent enzymatic ligation of modified nucleotides to the RNA strands. An alternative route is the generation of long stretches of dsRNA from the cDNA covering 800-1000bp of the target gene that are subsequently cleaved into native siRNAs by recombinant Dicer or appropriate RNase III mutants. These siRNAs are then modified for coupling by enzymatic ligation of modified nucleotides.

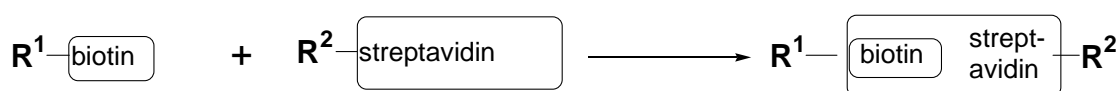
Apart from solid phase synthesis, cell-penetrating peptides can be obtained in large quantities from expression in *E. coli*. For this purpose, recombinant plasmids are generated by cloning an artificial gene that encodes the CPP. This approach also permits the functionalization of the peptide by adding a cysteine codon for a later disulfide-bond formation to the 3'-end of the synthetic nucleic acid sequence. The expression as fusion proteins greatly facilitates the purification of the peptides. Moreover, cell permeable small molecules can replace the CPPs. If their structures are sufficiently simple their synthesis on solid phase may be straightforward and less costly than the synthesis of peptides and maintain the opportunity to incorporate reporter groups and other useful modifications.

Over the last decades, a set of coupling groups has been used to attach biomolecules to reporter molecules and drugs or to immobilize them on solid phase. Functional groups for coupling are easily introduced into the respective molecules under physiological conditions. These functional groups can form covalent or non-covalent bonds. Some of these bonds are stable *in vivo*, others are cleaved under reducing conditions or at low pH (see Figure 3-2). For *in vivo* applications, disulfide bonds appear to be particularly useful. CPPs accelerate the uptake of attached cargo molecules, but also increase the rate of cellular escape until an equilibrium is reached (Lindgren et al. 2004). The escape of the cargo molecules can be prevented, if the conjugates break apart upon reaching the cytosol. Thus, the tissue distribution of pepsRNAs would be restricted allowing for locally focused applications. Moreover, if the conjugates are cleaved, the siRNA is released and the CPP can no longer interfere with the RNAi machinery.

In this work, the disulfide coupling strategy is followed exclusively. However, thiol-modified compounds can also form stable thioether linkages that are more interesting for systemic applications.

CPPs obtained by recombinant expression (AntP from *Drosophila* Antennapedia protein and TAT from HIV-TAT protein) and from solid phase synthesis (Penetratin™) as well as synthetic peptide mimetic were used. siRNAs were either custom-made or generated by a modified *in vitro* transcription that permits a selective functionalization of the siRNA:

Non-covalent



Covalent

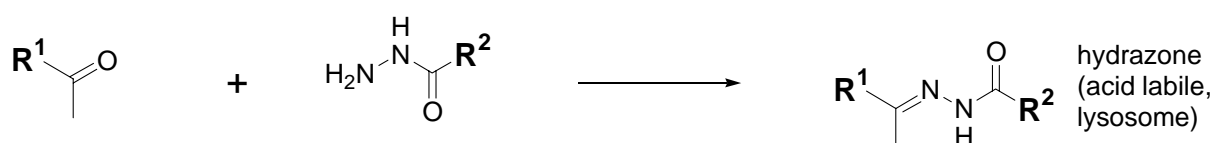
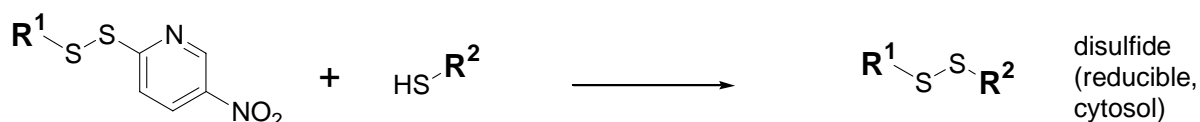
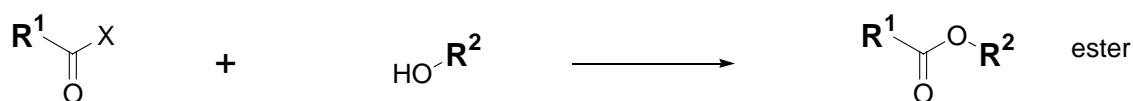
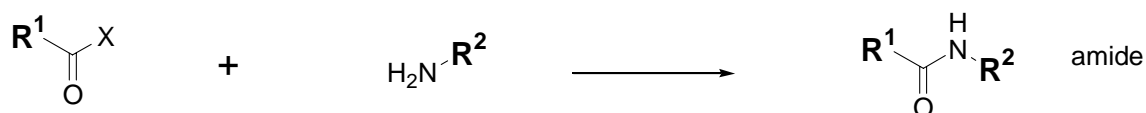
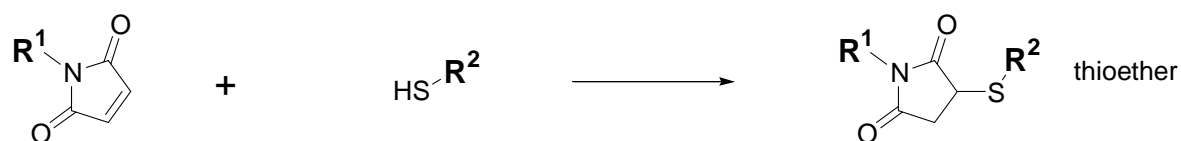
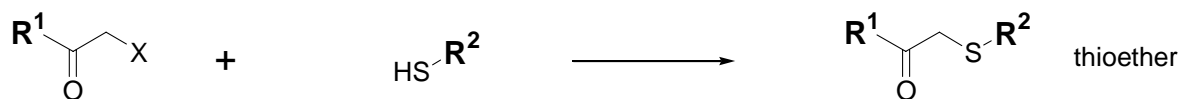


Figure 3-2 Common strategies for the formation of bioconjugates. Linkers after coupling and the complementary functionalities on the peptide (R^1) and the reporter or cargo-molecule (R^2) required for linker formation are shown. Depending on the available functional groups, R^1 and R^2 may be exchanged.

1. The first part describes the development of a strategy for the thiol-modification of *in vitro* transcribed siRNAs and their subsequent coupling to activated Penetratin™ from solid phase synthesis.

2. The hence obtained pepsRNA are tested in cell culture and compared with traditional transfection strategies. This is described in part 2.

3. The third part deals with the expression and purification of the CPPs Antp-Cys and Tat-Cys as GST-fusion proteins from *E. coli*. Also, the generation of a GST- or His₆-labeled TEV-protease and its utilization for the cleavage of GST-CPP-fusion proteins is described.

4. The final part reports the development of novel small molecules with cell permeating properties, that were coupled to fluorescein and porphyrin to assess their capability to enter cultured cells and to deliver large, otherwise non-permeant cargo-molecules.

3.1 Design and synthesis of thiol-modified siRNAs

For an efficient *in vivo* RNAi it is absolutely essential to choose the most efficient siRNA. For its design, many factors have to be considered. Thus, 2nt 3'-overhangs are important for recognition (Zamore et al. 2000). 5'-phosphorylation of the antisense strand increases the efficiency, but can be provided by kinases in the cytosol if the 5'-termini are non-phosphorylated (Chiu and Rana 2002; Nykänen et al. 2001), whereas 5'-triphosphates are discussed as a trigger for interferon response and non-specific effects (Kim et al. 2004). 5'-modifications on the sense strand are well tolerated, while modification of the 5'-terminus of the antisense strand lead to a dramatic loss of efficiency (Czauderna et al. 2003). However, 3'-modifications on both strands are generally tolerated (Chiu and Rana 2002; Czauderna et al. 2003). The introduction of larger residues like fluorescent probes to the central region of both strands is less tolerated, especially modifications of the antisense strand abolish its activity (Elbashir et al. 2001c). Finally, 3'-deoxy overhangs have been found to stabilize synthetic siRNAs *in vivo* (Elbashir et al. 2001c). The tolerated modifications are summarized in Figure 3-3.

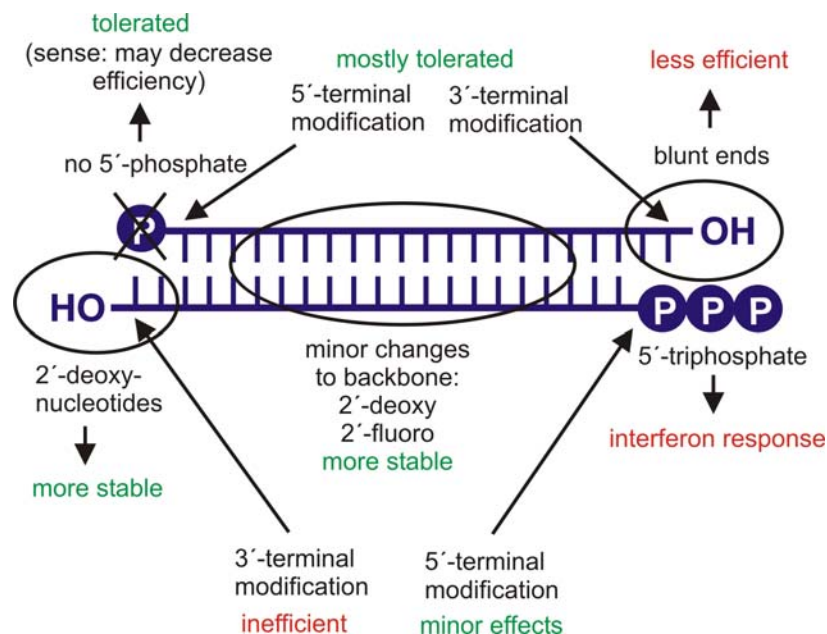
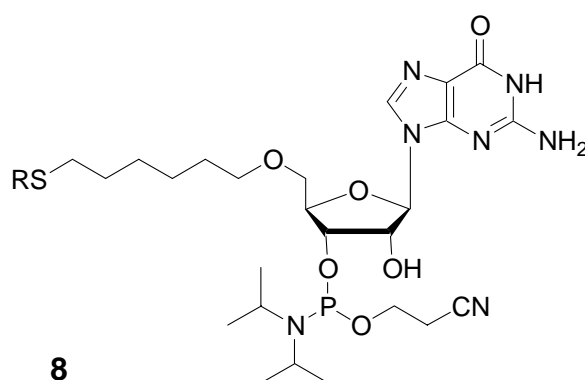


Figure 3-3 Effects of various modifications on the efficiency of siRNAs.

These issues determine the site of siRNA functionalization for coupling experiments. It was decided to attach the thiol-group to the 5'-terminus of the sense-strand to maintain the 3'-hydroxyl groups and to leave the antisense-strand unchanged.

Additional functionalities can be easily introduced by solid phase synthesis. The modified sense strand and the antisense strand are synthesized separately and hybridized after cleavage from the solid phase. Here, a C6-SH-function was introduced to the 5'-end of the sense strand of a commercially synthesized siRNA (Dharmacon, Promega). As already discussed, solid phase synthesis yields pure substances in good yields but still at comparatively high prices (Dharmacon, 749,- US-\$ for 80 nmol). However, synthetic siRNAs were used in preliminary experiments to test the functionality of pepsRNAs.



Scheme 3-1 Guanosine with a ω -thiol-C6-modification at its 5'-position **8**. It can be coupled to the 5'-end of oligonucleotides under standard solid phase conditions.

To establish the pepsRNA technique in a variety of cell lines, larger amounts of siRNAs are required, so that enzymatic generation of siRNA by *in vitro* transcription becomes an interesting issue. With the increasing use of siRNA transfection for reverse genomic experiments in mammals and the growing demand for larger quantities of siRNAs, *in vitro* transcription methods have been refined for the generation of siRNAs and are readily available. As first reported by Milligan (Milligan et al. 1987), T7 RNA polymerase recognizes a double stranded DNA T7 recognition sequence and synthesizes RNA in 5'→3'-direction from a single stranded DNA-template attached to the 3'-end of the recognition sequence (see Figure 3-4).

Adenosine and guanosine have been found to enhance the initiation rate of the T7 *in vitro* transcription, in which guanosine is superior to adenosine. The optimal sequence for a transcription start is GGG followed by GG or GC. GGG should be followed by 17–22 gene-specific nucleotides. Avoiding A and T in the first three base pairs would greatly enhance the yield but decreases the silencing efficacy (Reynolds et al. 2004).

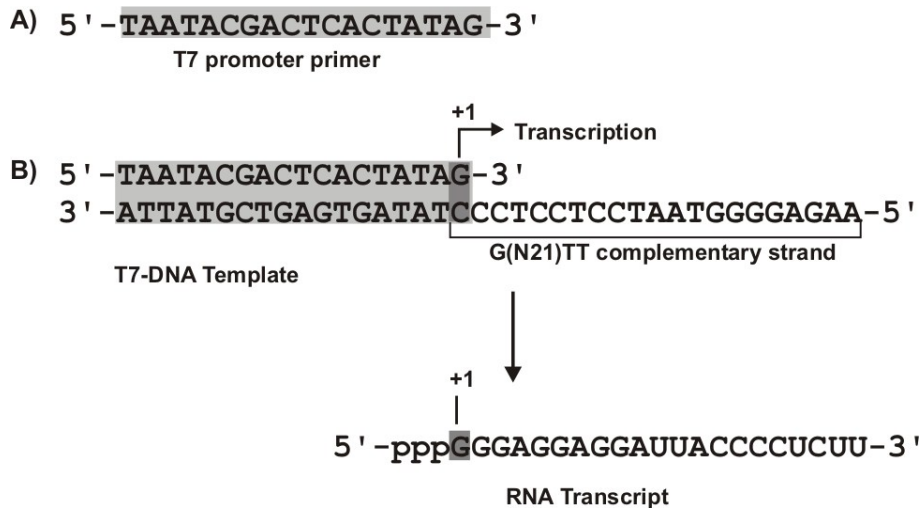


Figure 3-4 Schematic representation of the function of T7 RNA polymerase. Starting at the 3'-end of the double-stranded T7-recognition sequence, the antisense strand is transcribed in 3'-5'-direction with respect to the template strand yielding a single stranded RNA transcript. Two cytosine residues at the 3'-end of the DNA-template are required for the optimal function of the T7-RNA-polymerase (Milligan et al. 1987). All DNA-templates end with a 5'-terminal AA that is transcribed into a 3'-terminal UU, which in turn yields the most efficient 2 nt 3'-overhang upon hybridization of the single strands to form siRNAs (Elbashir et al. 2001a).

The oligonucleotides consist of the target sequence plus a minimal or elongated T7 RNA polymerase promoter sequence. Moreover, the elongated version of the T7 promoter may increase yield by allowing more efficient polymerase binding and initiation (see Figure 3-5), but is more expensive.

- A) 5' - **TAATACGACTCACTATAG** - 3' Minimal T7 sequence
B) 5' - **GGATCCTAATACGACTCACTATAG** - 3' Elongated T7 sequence

Figure 3-5 T7 recognition sequences. Additional bases at the minimal T7 promoter (A) may increase the yield as they allow more efficient T7 polymerase binding and initiation (B).

siRNA sequences can be designed according to the latest design rules aided by freely available computer software offered by siRNA providers (Dharmacon, Qiagen, Invitrogen) (Schepers 2004). The selected target mRNA sequence needs a guanosine at its 5'-terminus and three cytidines at its 3'-terminus.

DNA-templates with the T7 recognition sequence (Milligan et al. 1987) are easily obtained from commercial synthesis. After degradation of the DNA templates, the RNA transcripts for sense and antisense-strand are purified and hybridized to yield siRNAs with the appropriate 3'-2nt overhangs.

In the fast growing field of RNA research comprising RNA aptamer and ribozyme techniques, RNA libraries, and *in vitro* evolution, the search for convenient methods to functionalize enzymatically generated RNAs has been going on for several years, and two major approaches have been established:

- modification of the 3'-terminus by attaching synthetically modified nucleotides or oligonucleotides with T4-RNA-ligase (Hausch 1997; Igloi 1996; Romaniuk and Uhlenbeck 1983)
- modification of the 5'-terminus by selective incorporation of GMP derivatives as initiator nucleotides during transcription reaction with T7 RNA polymerase (Pitulle 1992; Seelig 1997, 1999).

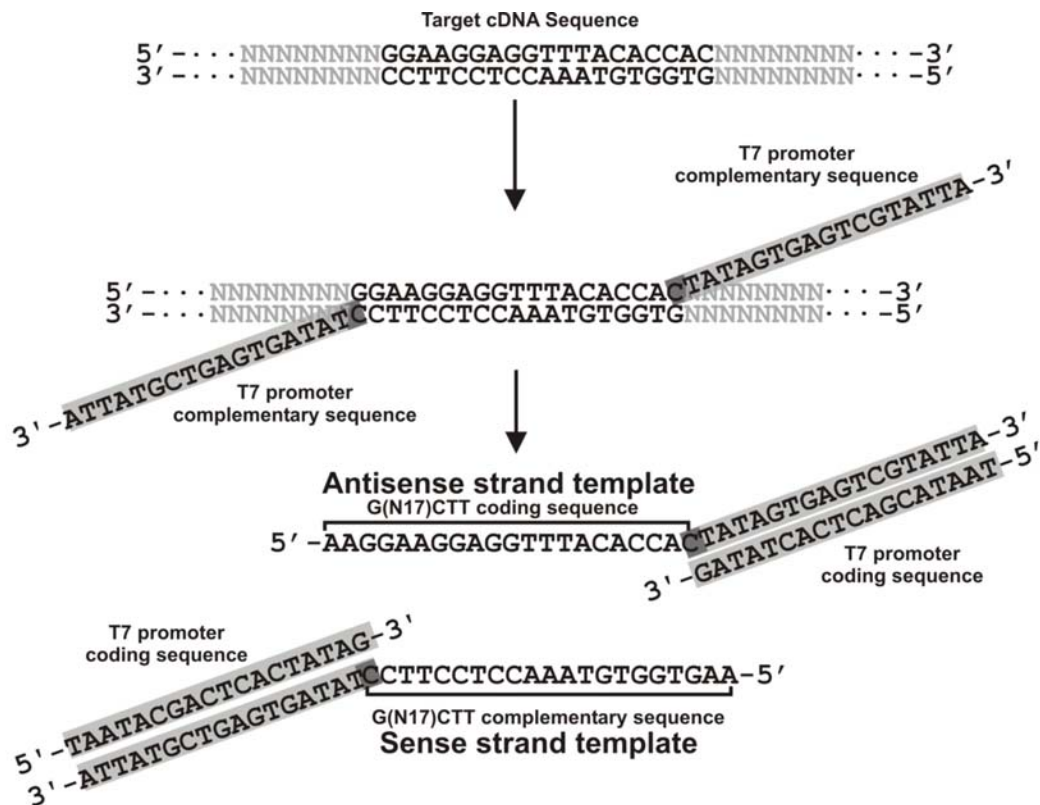


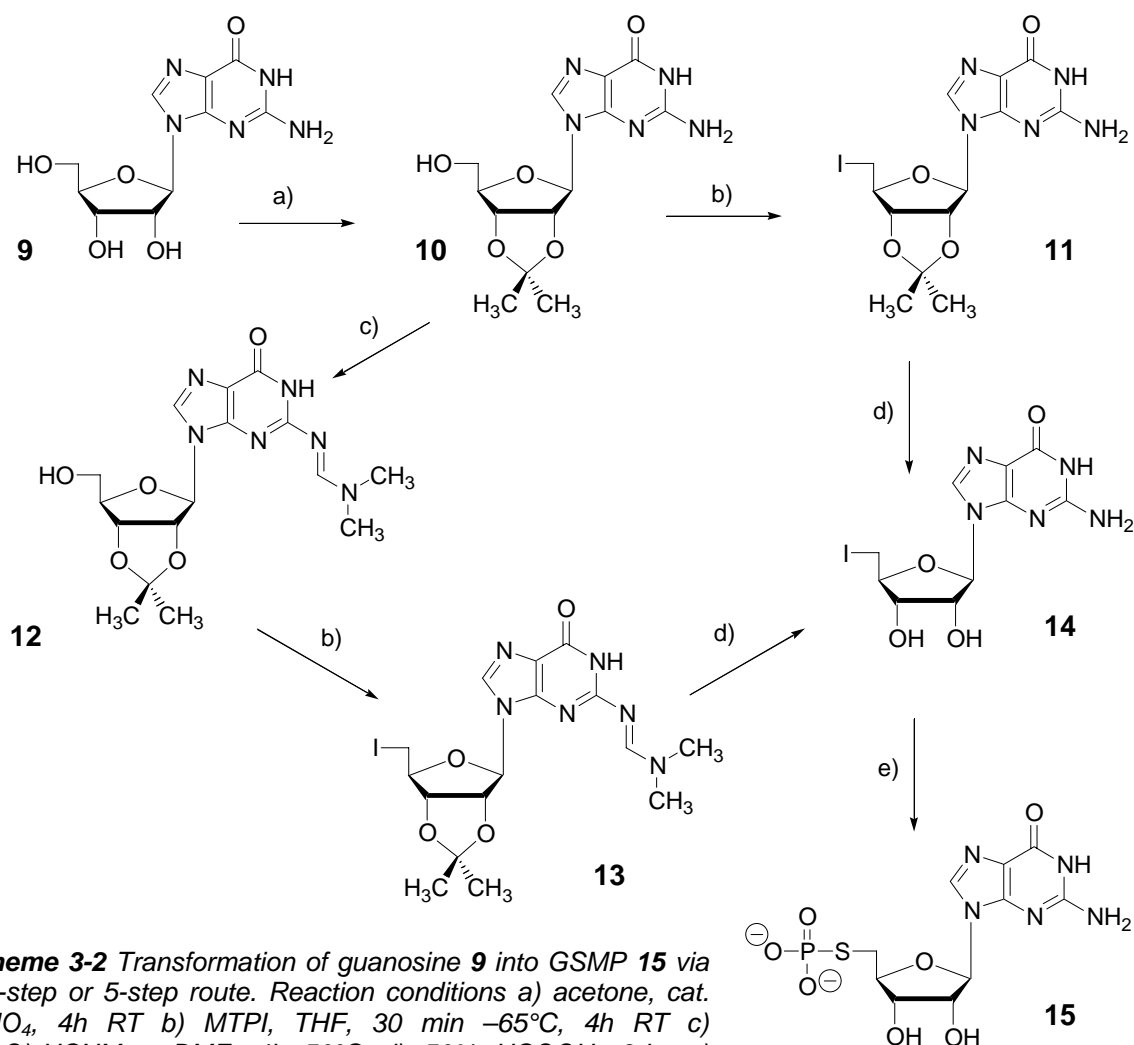
Figure 3-6 Design of primers for enzymatic generation of siRNA by in vitro transcription. The minimal T7 promoter sequence is attached to the 5'-termini of both strands of the target sequence 5'-G(N)₁₇CTT-3'. A deoxyoligonucleotide complementary to the T7-promoter sequence is needed to form the double-stranded recognition sequence. Note that both templates require a 3'-terminal CC to allow the incorporation of the initiator nucleotide, a GMP derivative, and a 5'-GAA to yield transcripts with a UU at their 3'-terminus that increases the efficiency of the hybridized siRNAs. Only the N17 sequence is complementary in sense and antisense-strand template (Schepers 2004).

The latter bears the advantage that the modified RNA can be generated in one step. Once the modified guanosine monophosphate (GMP) is available, it is added to the reaction mixture and no further changes of the procedure are necessary to achieve 5'-modified RNA. Moreover, nucleoside monophosphates can only act to start the reaction but not to elongate the RNA transcript like triphosphates. So the modification carried out by a GMP derivative will be restricted to the 5'-terminus. This method has been successfully established by the groups of Jäschke (Seelig 1997, 1999) and Zhang (Zhang et al. 2001a).

The use of 5'-thioguanosine monophosphorothioate (Zhang et al. 2001b) is of special interest to the pepsRNA approach. Once incorporated at the 5'-terminus of the RNA the phosphate ester can be cleaved by alkaline phosphatase and a sulfhydryl group is liberated at the 5'-terminus. Thus, the interference of the modification with the RNAi enzymes can be minimized. Moreover, as opposed to a long flexible linker, a minimal linker should diminish the probability of an intramolecular aggregation of the positively charged peptide with the negatively charged siRNA.

3.1.1 Synthesis of GSMP

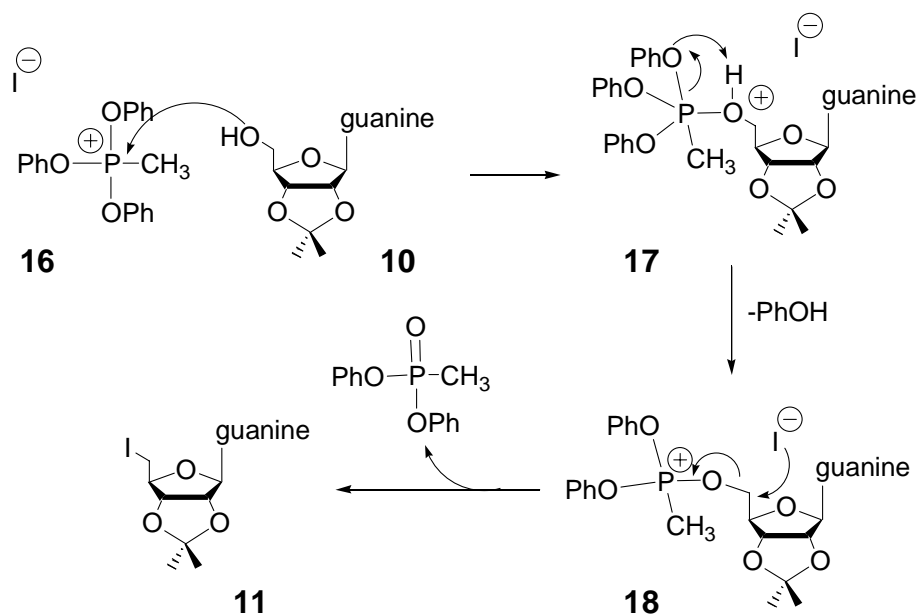
5'-Deoxy-5'-thioguanosine monophosphorothioate (GSMP, in reference to GMP) was synthesized according to Zhang (Zhang et al. 2001b) with some modification as shown in Scheme 3-2.



Scheme 3-2 Transformation of guanosine **9** into GSMP **15** via a 4-step or 5-step route. Reaction conditions a) acetone, cat. HClO_4 , 4h RT b) MTPI, THF, 30 min -65°C , 4h RT c) $(\text{MeO})_2\text{HCNMe}_2$, DMF, 4h 50°C d) 50% HCOOH , 3d e) $\text{Na}_3\text{PO}_3\text{S}$, water, 3d, RT.

To selectively modify the 5'-hydroxyl group, the 2'- and 3'-hydroxyl groups were protected by an acetal. Reaction of guanosine with acetone in the presence of catalytic amounts of perchloric acid led to 2',3'-O,O-isopropylidene guanosine (**10**) in 94% yield in a straightforward reaction.

To substitute the 5'-hydroxyl group with iodine, **10** was reacted with methyltriphenoxyphosphonium iodide (MTPI, **16**) in a Moffat reaction. The 5'-hydroxyl group substitutes one of the phenoxy-substituents at the phosphonium center. Then the nucleophilic iodide anion attacks the 5'-carbon, and the methyl phosphate acts as a leaving group, which is favored by the oxophilic nature of the phosphorous center (see Scheme 3-3).



Scheme 3-3 Mechanism of the Moffat reaction to transform alcohols into iodides (Brückner 2000).

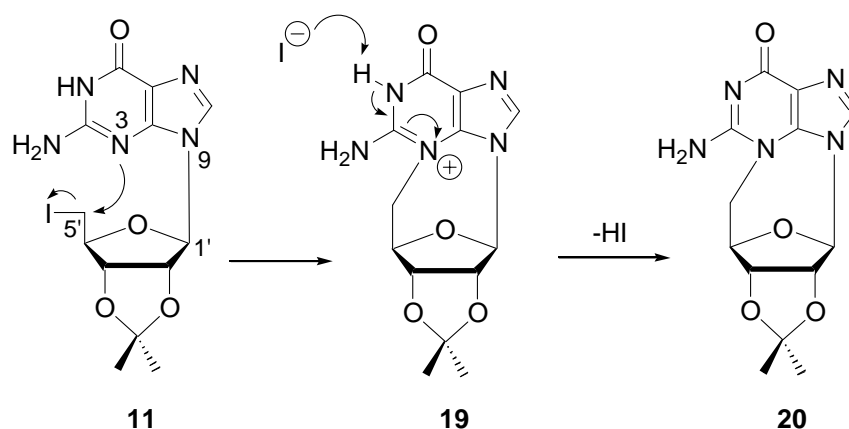
The reaction had to be carried out at -65°C to avoid the cyclization of the iodoguanosine derivative (Verheyden and Moffat 1970). The crude product was a sticky paste that obstructed chromatography columns even when mounted on silica gel/sodium sulphate. The light-sensitivity of the product and its poor solubility in most organic solvents complicated the purification procedure. Pure 5'-deoxy-5'-iodo-2',3'-O,O-isopropylidene-guanosine **11** was obtained in 39% yield as a white powder.

A side product was observed in all NMR spectra of **11**. The $^1\text{H-NMR}$ shifts in $\text{d}_6\text{-DMSO}$ correspond to 2',3'-O,O-isopropylidene-N3,5'-C-cycloguanosine **20** that is formed by the nucleophilic attack of the purin-N3 on the ribose-C5' and substitution of the iodide ion as first described by Verheyden and Moffat (Verheyden and Moffat 1970). The $^1\text{H-NMR}$ of **20** is characterized by the two 5'-H signals at 3.98 ppm and 4.74 ppm, respectively, that split into doublets of doublets with a large geminal coupling constant of 14.0 Hz (see Figure 3-7 and Figure 3-9).

$^1\text{H-NMR}$ Spectra of pure **11** in $\text{d}_6\text{-DMSO}$ could be only obtained if the dried compound was dissolved in the deuterated solvent immediately prior to measurement.

A strong tendency towards cyclization was even found in the dried iodide **11**. After 4 weeks of storage at -20°C under argon, only $\sim 31\%$ of the purified compound could be recovered in a new round of column chromatography on silicagel, while the larger proportion had reacted

to the less soluble cyclized compound as verified by TLC. The cyclized side-product was also found as a contamination in the following reaction step, so that efforts had to be undertaken to stabilize the iodide and to increase the yield of pure **11**.



Scheme 3-4 Cyclization of **11** to yielding 2',3'-O,O-isopropylidene-3,5'-C-cycloguanosine **20** according to Verheyden and Moffat (Verheyden and Moffat 1970). The purine base can rotate freely along the C1'-N9-axis. In the *syn*-form with the purine base residing above the ribose ring, the N3-nitrogen is in close proximity to the C5'-carbon. In an intramolecular nucleophilic substitution, the nucleophilic purin-N3 attacks the electrophilic ribose-C5' releasing the iodide that in turn abstracts the H1-proton.

As the cyclization requires a freely accessible purin-N3 center (see Figure 3-6), it was assumed that the reaction rate could be decreased by incorporating a bulky group at the purin-N3 or in its proximity. Thus, the free energy of the *syn*-form of the nucleoside, in which the purin-N3 is in close proximity the 5'-C, would be increased. Moreover, a bulky group would sterically hinder the nucleophilic attack of N3 on C-5'

The free amino group was protected to reduce the rate of cyclization and thereby stabilize the iodination product. After testing different protection groups, the formation of a Schiff base with dimethylformamide-dimethylacetal appeared to be most convenient (Zhang et al. 2001b). **10** was reacted with the acetal in DMF and the pure 2-*N,N*-dimethylaminomethylene-2',3'-O,O-isopropylidene-guanosine **12** was obtained by precipitation in 80% yield. Preliminary experiments showed that both protecting groups, the acetal and the imine, can be removed by stirring in 50% formic acid for 3 days at room temperature.

Iodination of **12** was performed under the same conditions as the iodination of **10**. The increased solubility of 2-*N,N*-dimethylaminomethylene-2',3'-O,O-isopropylidene-5'-deoxy-5'-iodoguanosine **13** in methanol facilitated its purification by column chromatography on silicagel leading to a yield of up to 99%. For **13**, cyclization in d_6 -DMSO to the protected cycloguanosine **21** was also observed, but at a much slower rate. After the dried compound had been stored for 4 weeks at 4°C, no contamination of the cyclization product could be identified in a sample of compound **13**.

To compare the rates of cyclization, two long-term ^1H NMR experiments were performed, in which spectra of the same sample were recorded in intervals of 30 min over 24h for the

iodide **11** (see Figure 3-7 and Figure 3-9) and the protected iodide **13** (see Figure 3-8 and Figure 3-11). For iodide **11**, integration of the individual signals with reference to the solvent signal and plotting of the average from 5 significant signal integrals against time revealed first order kinetic with $k = 0.181 \pm 0.008 \text{ h}^{-1}$ corresponding to a half life of 3h 50min ($\pm 10 \text{ min}$) (Equation 1-1 and Figure 3-10). These values were confirmed by the plot of the average integrals of the product signals that could be fitted with the same rate constant according to Equation 1-2.

| | |
|-----|------------------------------------|
| (1) | $C_{\text{iodide}} = C_0 e^{-kt}$ |
| (2) | $C_{\text{cyc}} = 1 - C_0 e^{-kt}$ |

Equation 1 The transformation of **11** follows a first order kinetic with C_0 as the initial concentration of **11**, C_{iodide} the concentration of **11** at time t , C_{cyc} the concentration of A3 at t , and the rate constant $k = 0.181 \pm 0.008 \text{ h}^{-1}$.

The long-term ^1H NMR experiment for **13** showed that the protected iodide was also subject to cyclization, but at a much slower rate (see Figure 3-8 and Figure 3-11). Integration of the relevant signals and plotting of the average integrals against time yielded another first order kinetic which could be fitted to $k = 0.0145 \pm 0.0008 \text{ h}^{-1}$ corresponding to a half life of 47h 48min ($\pm 2\text{h } 40\text{min}$) (Figure 3-12).

Thus, it could be shown, that the introduction of the protection group prior to iodination increased the stability of the iodide in solution by a factor of 12.

The ease of preparation and the higher overall yield (79% in two steps versus 39% in one step) justified the introduction of the additional protection step.

The protection groups in **11** and **13** were removed with 50% formic acid for 3 days. All side products (acetone, DMF, formic acid) could be removed under reduced pressure and the ^1H -NMR shows a sufficiently pure substance, so that no further purification is required. 5'-Deoxy-5'-iodoguanosine **A7** is obtained in quantitative yield from **11** and **13**. About 5% of the cyclized product are observed after deprotection of **11**. Remarkably, 5'-deoxy-5'-iodoguanosine yields no defined degradation product after 48h in d_6 -DMSO. Apparently, the conformation forced upon the ribose ring by the five-membered acetal ring plays a crucial role in the cyclization reaction.

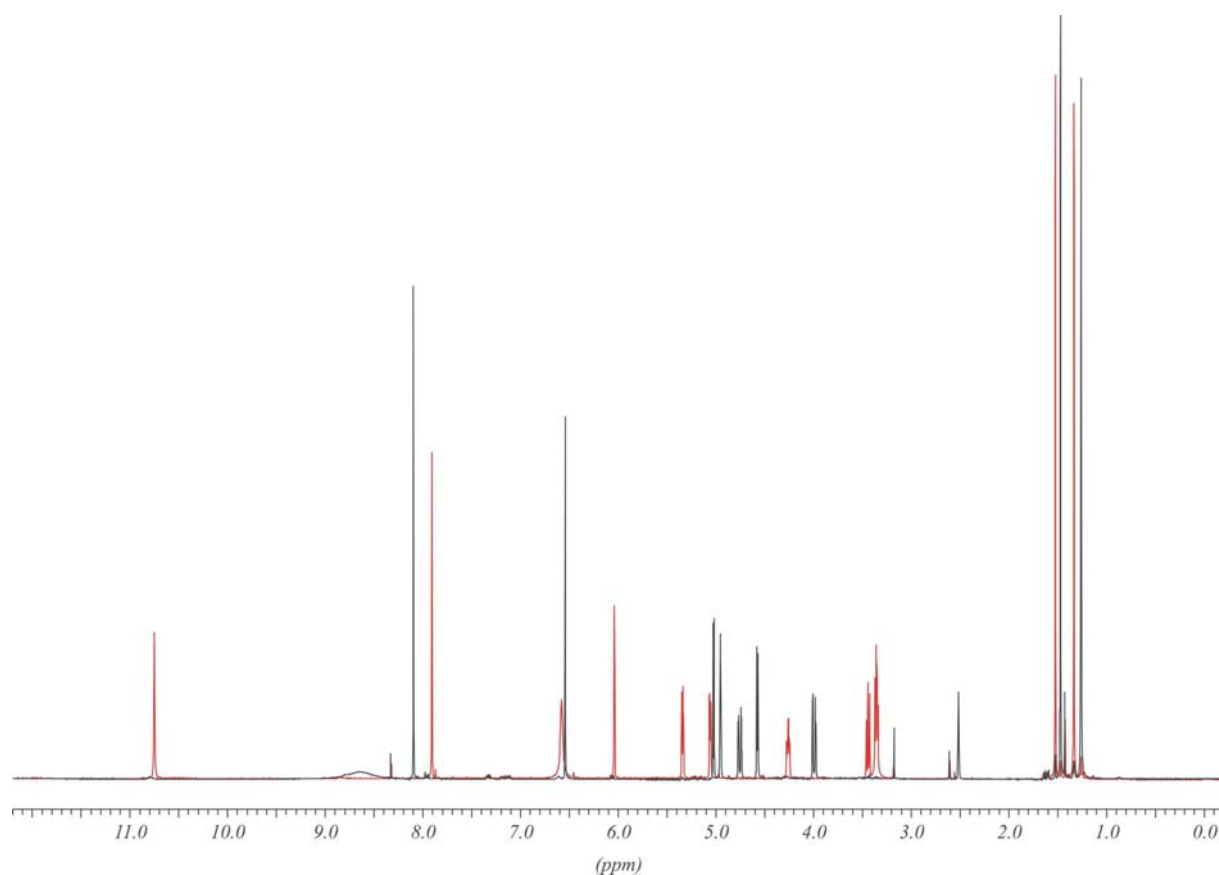
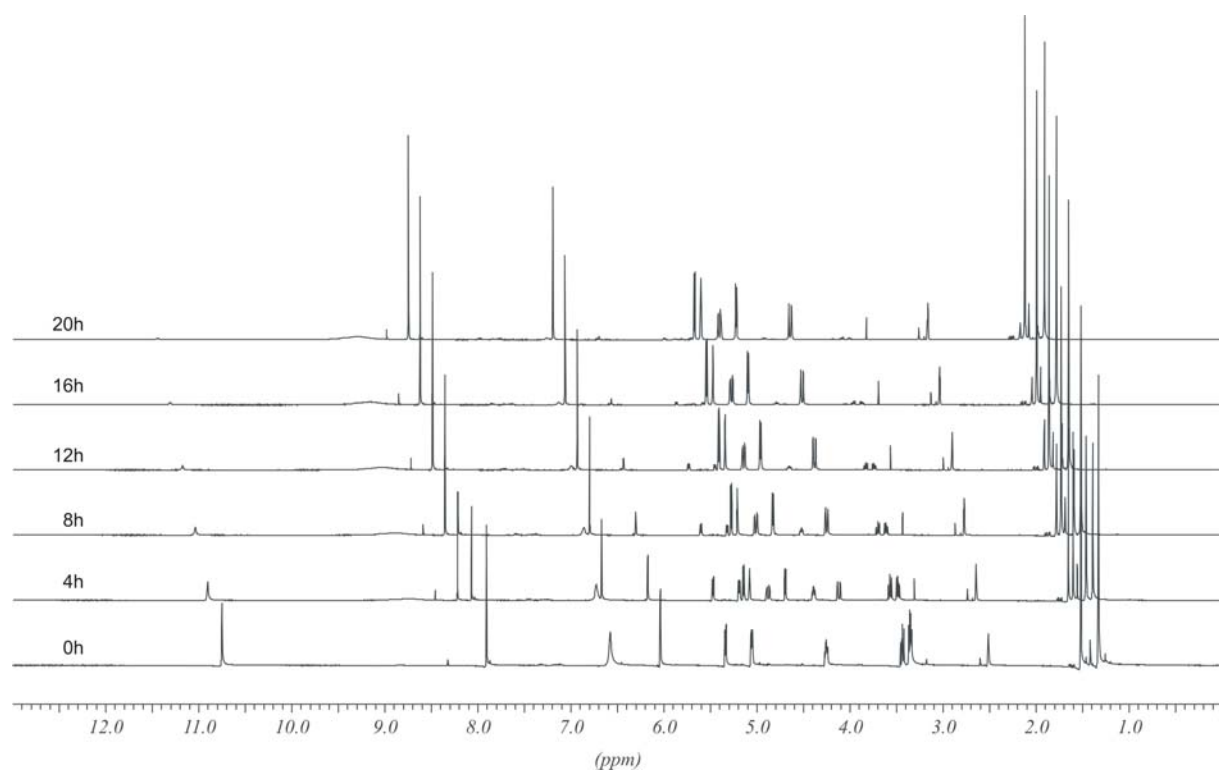


Figure 3-7 Cyclization of **11** yielding **20**. Stacked plot of ^1H NMR spectra taken in 4 h intervals at RT (top). Overlay of the ^1H NMR spectra of 2',3'-isopropylidene 5'-deoxy-5'-iodoguanosine (**11**, red) and its cyclization product (**20** black) (bottom). Note the two 5'-H signals at 3.98 and 4.74 ppm, that split into doublets of doublets with a large geminal coupling constant of 14.0 Hz.

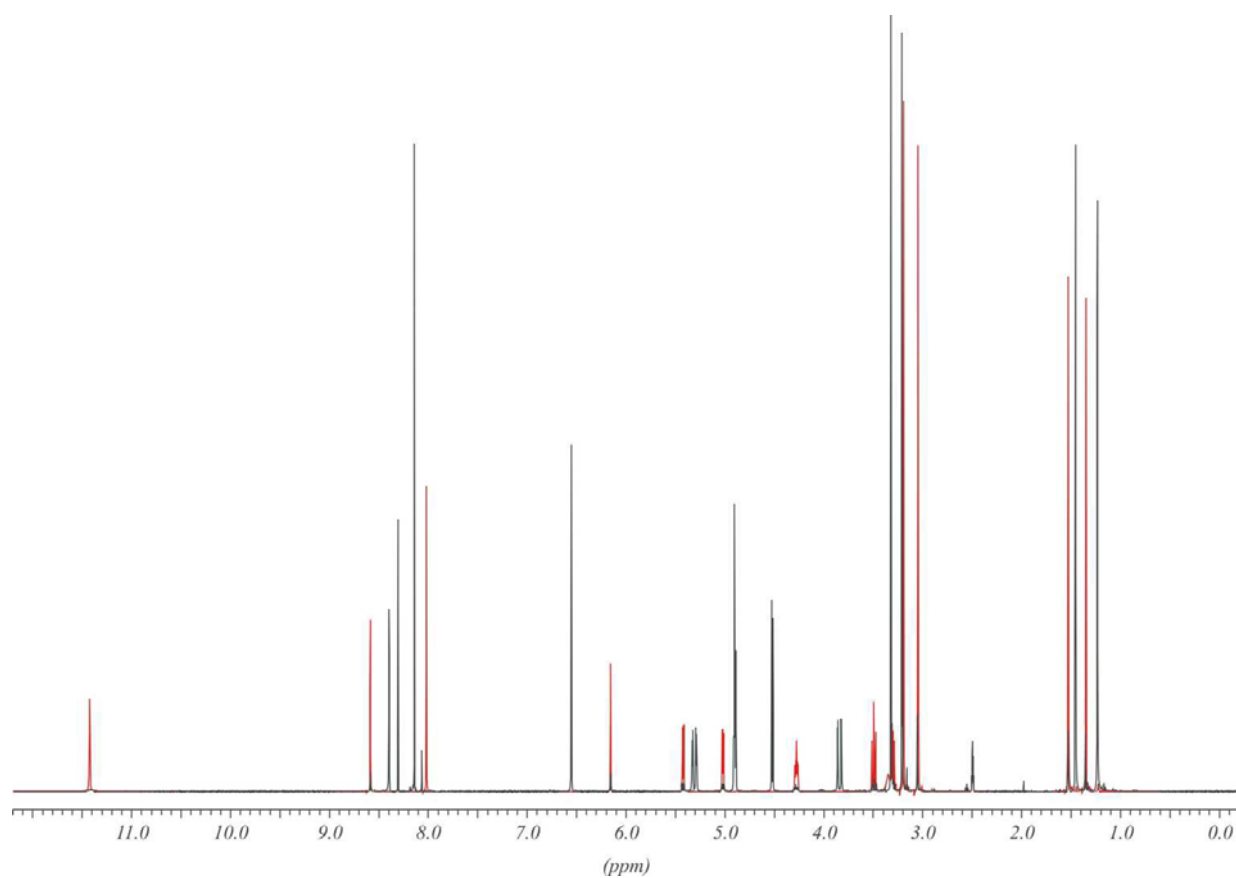
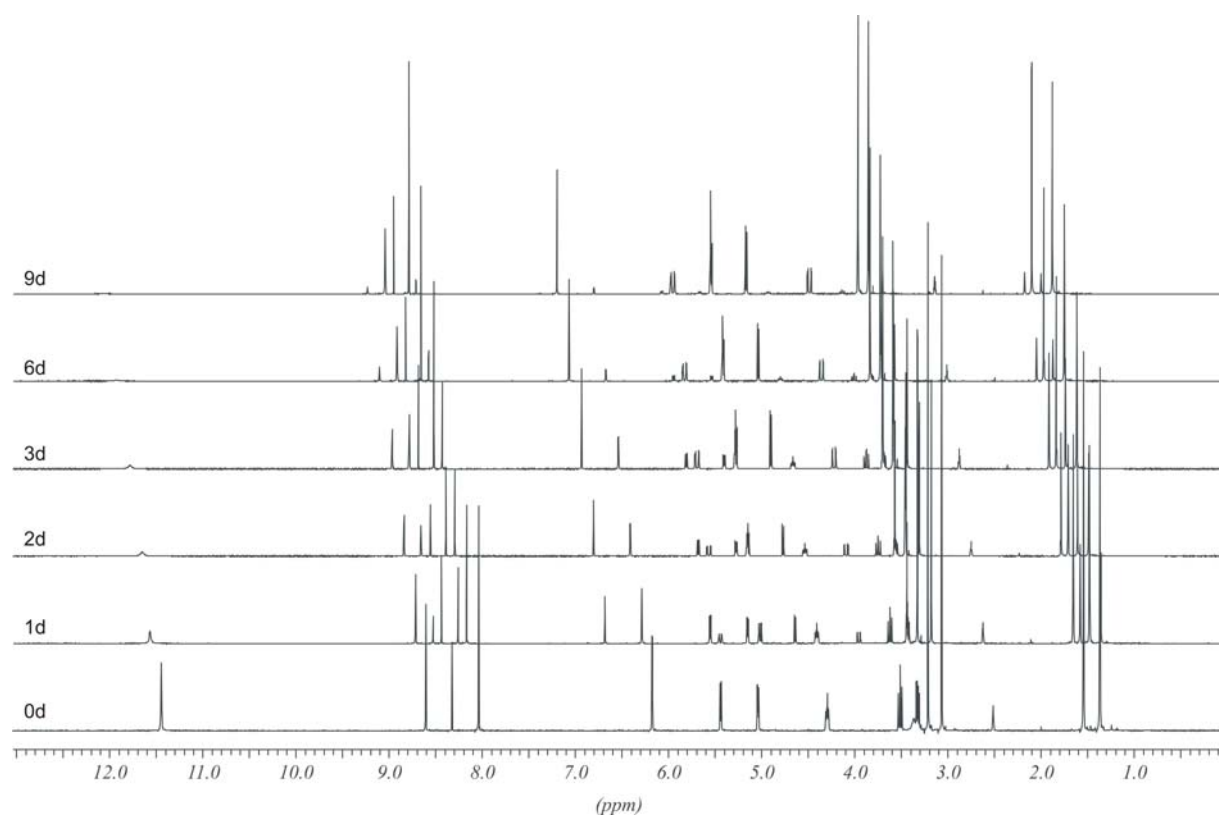


Figure 3-8 Cyclization of iodide **13** yielding **21**. Stacked plot of ¹H NMR spectra taken after 0, 1, 2, 3, 6, and 9 days at RT (top). Overlay of the ¹H NMR spectra of 2-N,N-dimethylaminomethylene-2',3'-isopropylidene-5'-deoxy-5'-iodoguanosine (**11**, red) and its cyclization product (**21** black) (bottom). Note the two 5'-H signals at 3.83 and 5.30 ppm, that split into doublets of doublets with a large geminal coupling constant of 15.0 Hz.

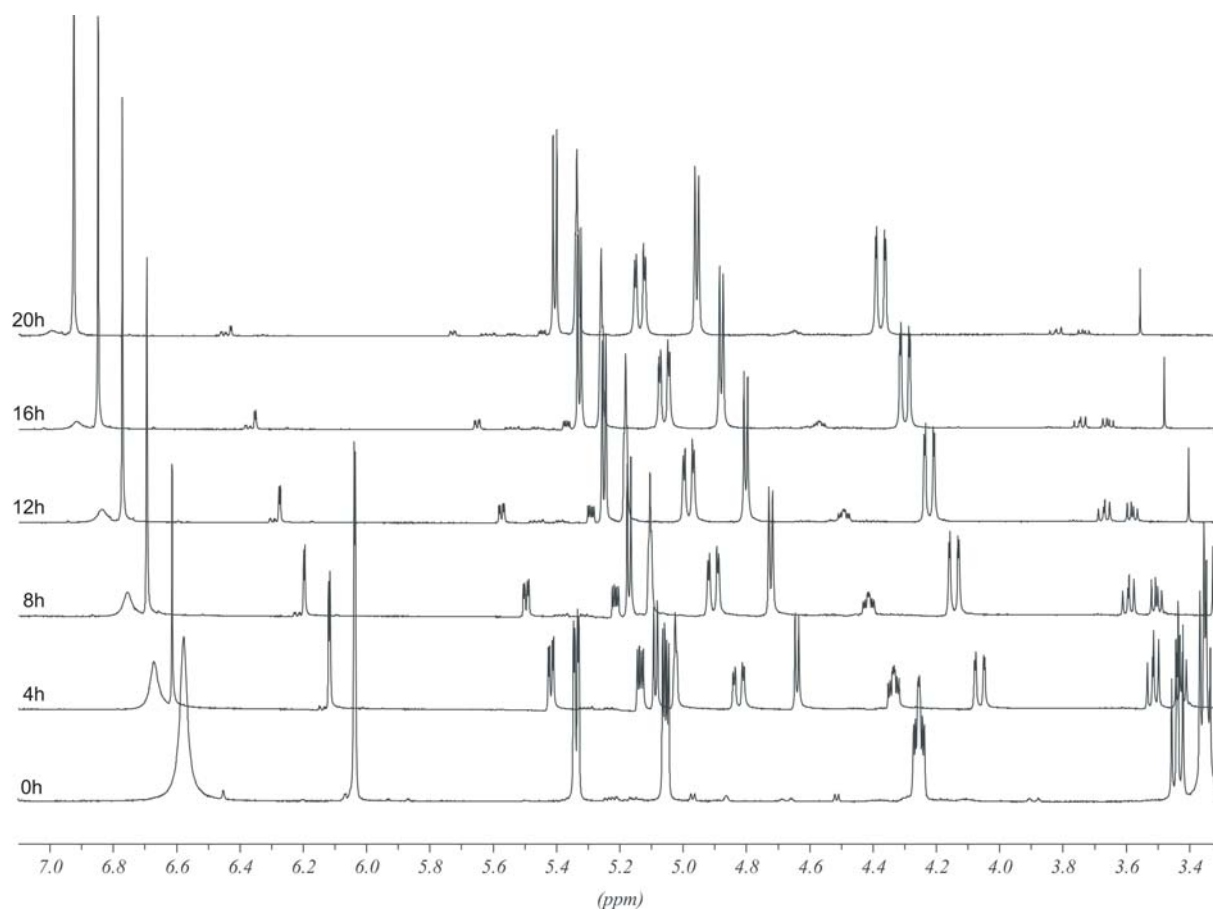


Figure 3-9 Cyclization of iodide **11** yielding **20**. Stacked plot of ¹H NMR spectra taken in 4 h intervals at RT. The region representing the ribose protons is enlarged.

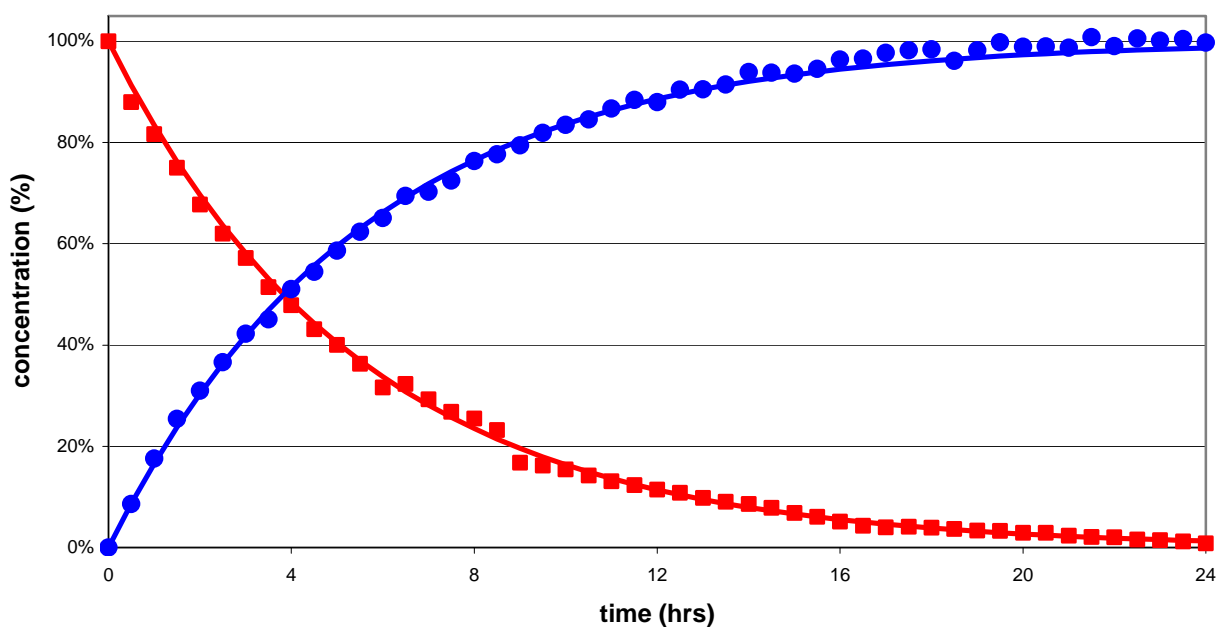


Figure 3-10 Cyclization of **11**. Averages of significant integrals for **11** (red solid squares) and the cyclized product **20** (blue open circles) plotted against time. The continuous lines correspond to the fitted first order kinetics with $k = 0.181 \text{ h}^{-1}$.

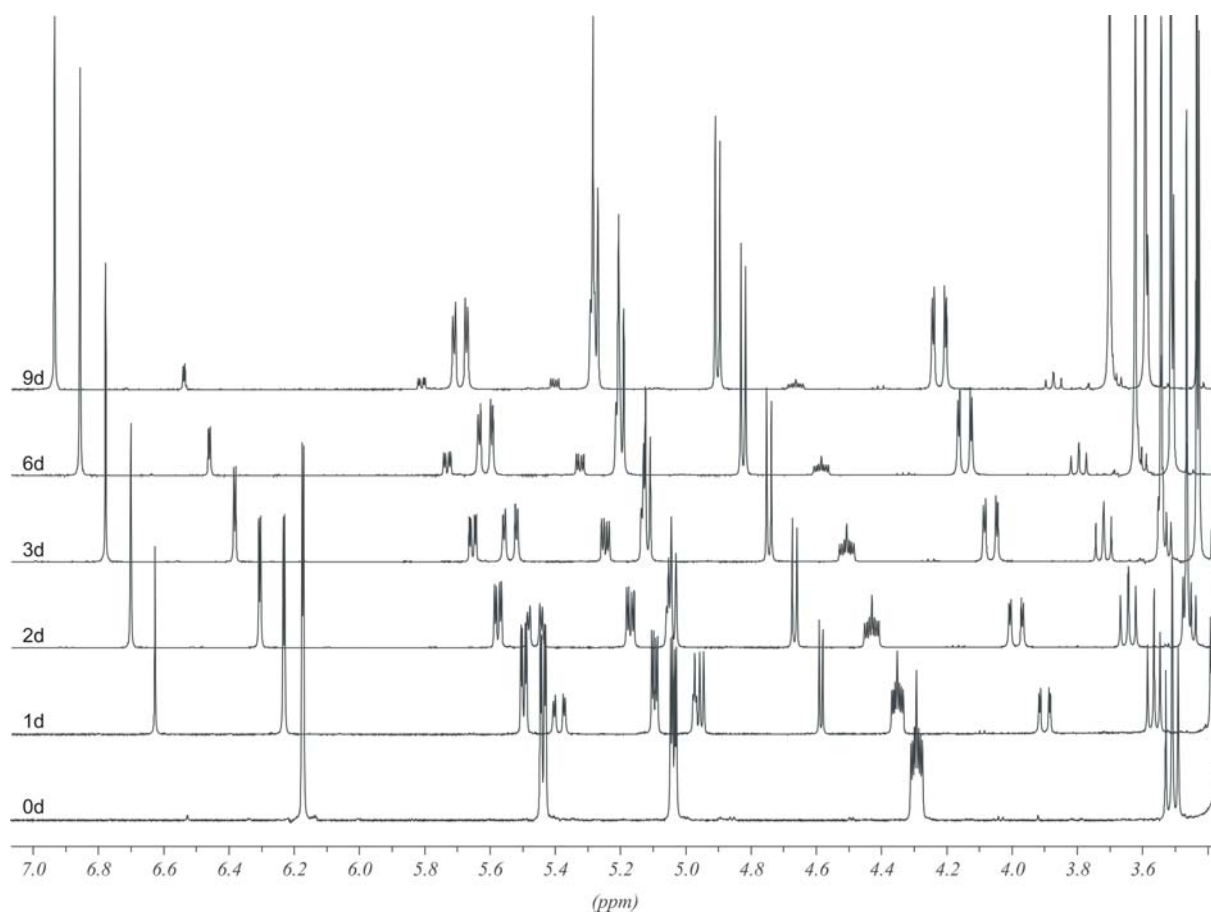


Figure 3-11 Cyclization of iodide **13** yielding **21**. Stacked plot of ¹H NMR spectra taken after 0, 1, 2, 3, 6, and 9 days at RT. The region representing the ribose protons is enlarged.

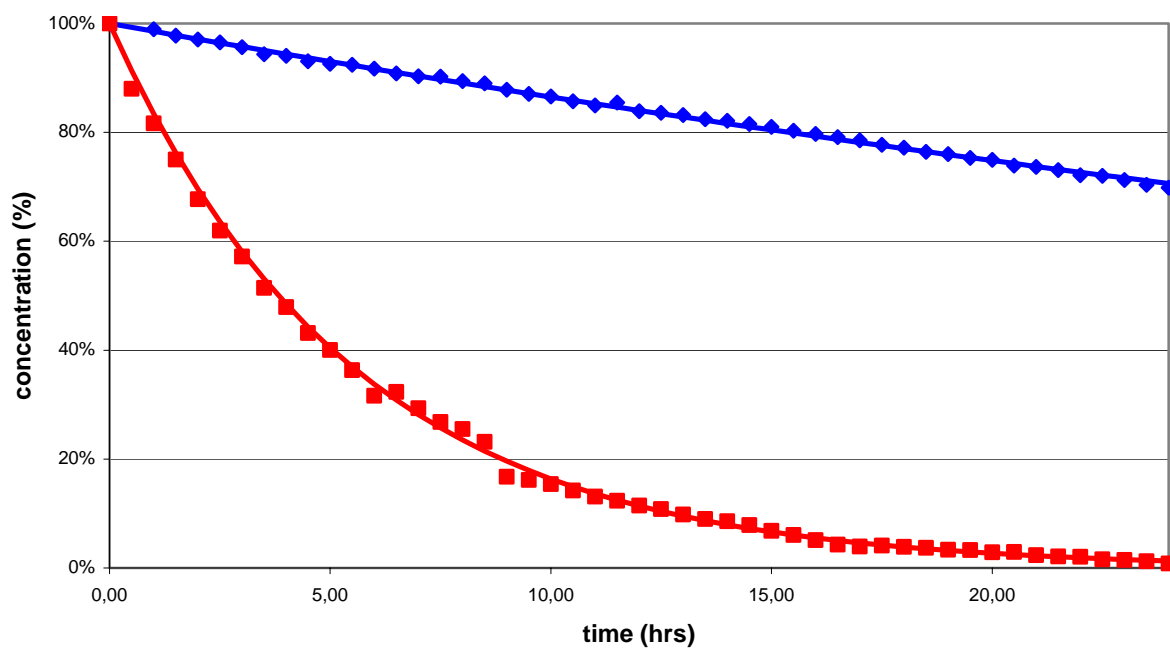


Figure 3-12 Introduction of an *N,N*-dimethylaminomethylene protection group increases the half life time of **11** by a factor of 12. Averages of significant integrals for **13** (blue diamonds) and unprotected **11** (red squares) plotted against time. Both sets of data are fitted with a 1st order kinetic with $k=0.0145h^{-1}$ and $k=0.181h^{-1}$, respectively.

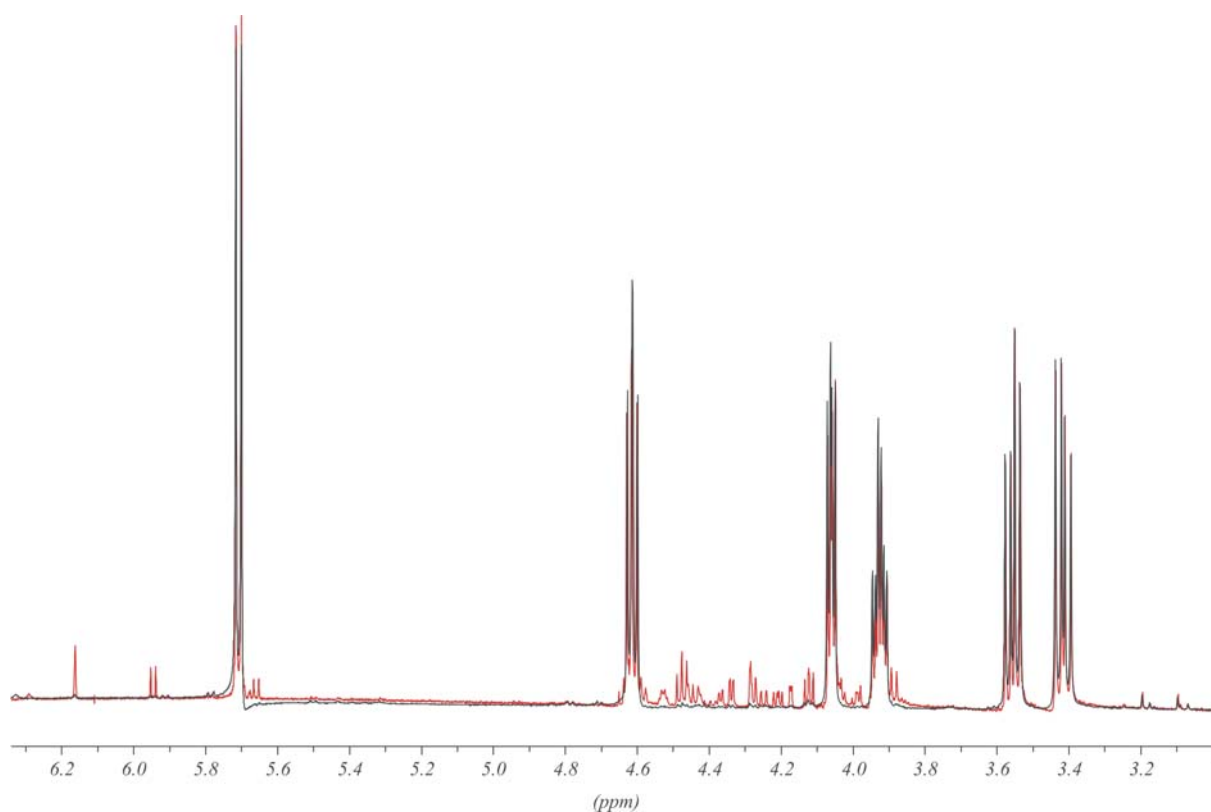


Figure 3-13 Deprotected 5'-deoxy-5'-iodoguanosine is stable towards cyclization. After 4 days in d_6 -DMSO at room temperature only small amounts of degradation products are found in the region of the ribose protons.

14 was reacted with a 2-3fold molar excess of sodium thiophosphate in degassed water under argon to yield 5'-deoxy-5'-thioguanosine monophosphorothioate **15** (GSMP). Yields can be improved if the thiophosphate is dissolved in degassed water and the precipitate is removed prior to the addition to the degassed suspension of **14**. After three days, a clear solution has formed and $^1\text{H-NMR}$ indicated a complete transformation of **14**. $^{31}\text{P-NMR}$ spectroscopy indicated quantitative formation of the 5'-thio-monophosphorothioate **15** (GSMP, $\delta = 19$ ppm) rather than the 5'-oxo-monophosphorothioate (GMPS, $\delta = 43$ ppm).

| compound | C5'-X | $\delta(^{13}\text{C-NMR})$ in ppm |
|-------------|------------|------------------------------------|
| 10 | C-O | 62.0 |
| 12 | C-O | 61.9 |
| 20 | C-N | 55.3 |
| 21 | C-N | 54.1 |
| 11 | C-I | 7.7 |
| 13 | C-I | 6.9 |
| 14 | C-I | 8.5 |
| GSMP | C-S | 34.5 |
| Ref | C-S | 26.4 |

Table 3-2 ^{13}C NMR shifts of the 5'-C-carbon depending on the neighbor-atom X (Ref = reference substance, 5'-deoxy-5'-thioguanosine (Mariott 1990)).

Moreover, the ^{13}C NMR shift could be taken as an evidence for a carbon-sulfur bond as illustrated by

Table 3-2. As it constitutes the only methylene-carbon in the molecule, the C5' can be easily identified as the only negative signal in the DEPT-135 NMR-spectrum.

3.1.2 Purification of GSMP

The purification of GSMP from sodium thiophosphate turned out to be difficult due to the similar solubility of the two substances and the sensitivity of GSMP to temperatures above 30°C.

The water was removed from the reaction mixture under reduced pressure without avoiding temperatures above 25°C. To remove a proportion of the excessive thiophosphate, the residue was resuspended in water and the thiophosphate was precipitated with methanol. Different purification strategies were assessed.

1) The crude product was subjected to anionic exchange chromatography on 2-(diethylamino)ethyl (DEAE) Sephadex A-25 sepharose. It was eluted with a gradient of triethylamine bicarbonate buffer (TEAB, 0.01 (pH 6.9) to 1.00 M, (pH 7.5)). The HPLC run was monitored by UV absorption at 260 nm. A typical chromatography profile is shown in Figure 3-14. Fractions 32-39 were pooled and lyophilized. To remove triethylamine, the product fraction was repeatedly lyophilized from water and GSMP was obtained as a brown oil in poor yields (2-5%).

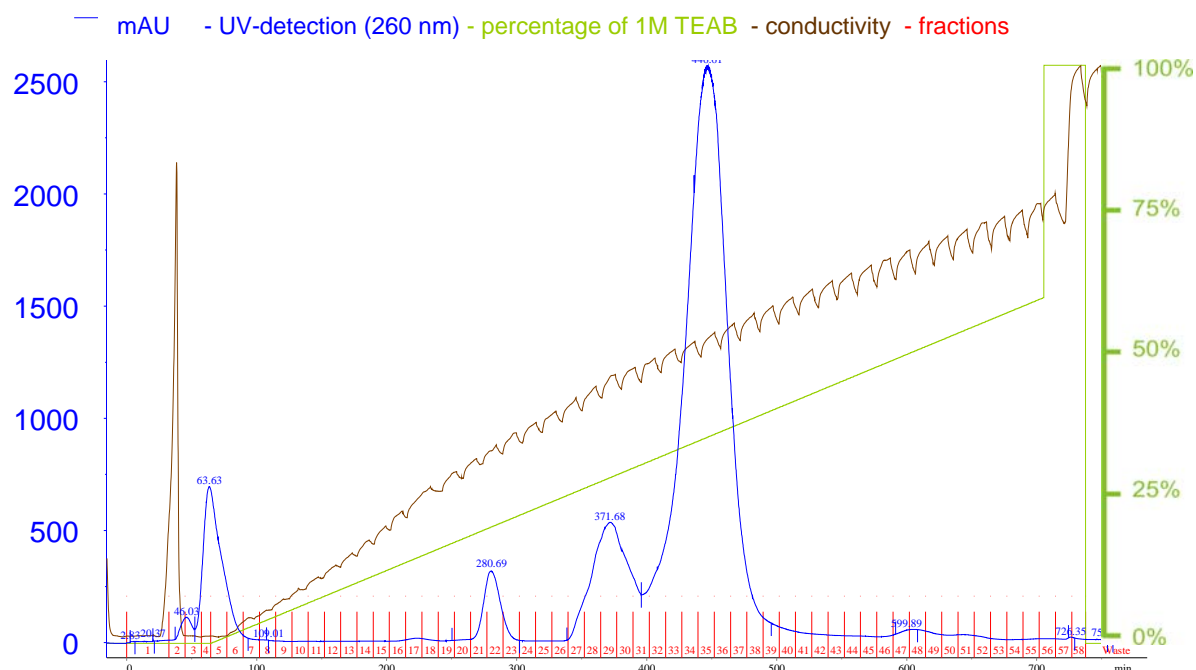


Figure 3-14 Purification of GSMP by FPLC using a DEAE Sephadex A-25 anionic exchange column. Thiophosphate salts are eluted before the beginning of the gradient (fractions 1-2) while GSMP **15** is eluted at ~0.31 M TEAB (fractions 31-39), so that the compounds are well separated. The peaks ranging from fractions 21-23 and 27-31 are small if fresh product is purified and become larger, if the crude product is stored for prolonged times before purification.

2) As the formation of GSMP can be monitored by thin layer chromatography on silicagel plates with a mixture of isopropanol, water and 25% ammonia (6:1:3 (v/v/v)), the same solvent was used for column chromatography on silicagel. GSMP was obtained as a pale yellow solid in 35% overall yield. $^1\text{H-NMR}$ indicated a contamination with about 13% of a hydrolysis product.

3) The crude product was subjected to reverse phase chromatography on an analytical RP-18 column and GSMP **15** was eluted with water. Due to the similar solubility of GSMP and sodium thiophosphate the two fractions overlap if the capacity of the column is exceeded. The HPLC run was monitored photometrically at 260 nm. Figure 3-15 shows a typical chromatogram.

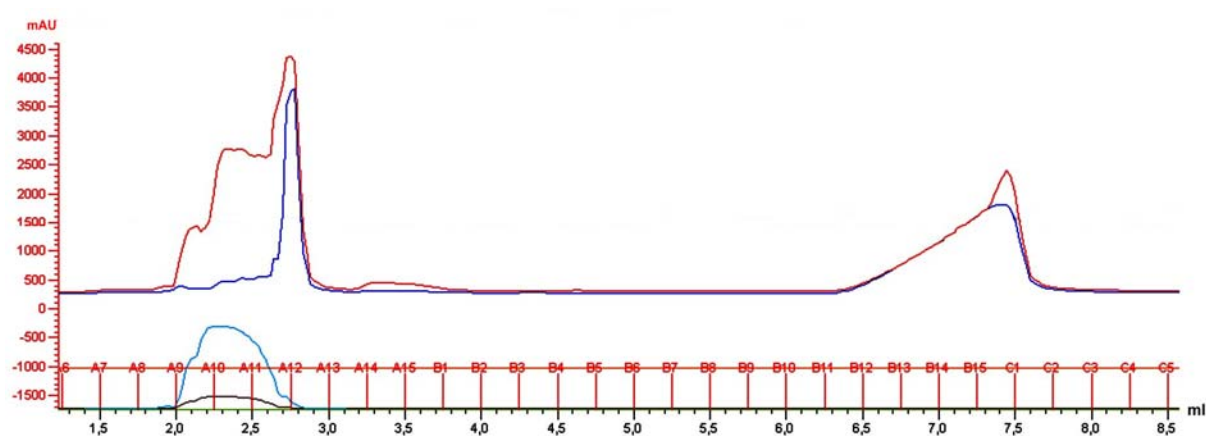


Figure 3-15 Purification of GSMP by FPLC with an analytic RP-18 column (\varnothing 2mm; h = 25 mm, resin $3\mu\text{M}$). The elution with water is monitored at 260 nm (red), 280 nm (blue) and by its conductivity (light blue) and fractions of $200\ \mu\text{l}$ are collected. GSMP **15**, absorbing at 260 and 280 nm, is eluted at 2.7-2.9 ml immediately after the thiophosphate (2.0-2.8 ml) that can be identified by the increase in conductivity. Both peaks overlap, so that the purification capacity is reduced if larger amounts of crude product are applied to the column. The peak at 6.5-7.6 ml has the retention time and pattern of guanosine.

Fractions A11, that contain a mixture of thiophosphate and GSMP **15**, and A12 containing the pure product were collected separately. Mixtures of GSMP **15** and thiophosphate were lyophilized and purified again. Product fractions from subsequent runs were pooled and the concentration was determined photometrically at 260 nm against GTP standards. The aqueous GSMP solution could be readily used for *in vitro* transcription without further purification. It was split into aliquots sufficient for an *in vitro* transcription reaction in a total volume of $100\ \mu\text{l}$ and stored at -80°C . 16% of pure GSMP could be obtained in this procedure.

4) Flash chromatography on RP-18 (LiChroprep 40-63 μm , Merck) was found to be the most efficient purification method. The product was eluted with water by gravity flow, and the fractions were monitored by TLC. Pure GSMP **15** was obtained as a white solid in 68% yield.

Thiophosphate contaminations lead to a yellow stain as the compound decomposes. Product fractions were pooled, lyophilized and stored under argon at -20°C .

An overall yield of 53% was obtained for the synthesis of GSMP **15** in 5 steps as opposed to the reported 35% in 4 steps (Zhang et al. 2001b).

3.1.3 *in vitro* transcription of siRNAs from T7-DNA-oligonucleotides

Short DNA-oligonucleotides coding for 19 nt of the sense or antisense strand of the siRNA were designed as templates for the *in vitro* transcription experiments. The sequences were chosen from the ORF of the target gene that was obtained from the NCBI database according to the rules for the design of highly efficient siRNAs and of efficient templates for *in vitro* transcription (Schepers 2004):

- 5'-GG or 5'-GGG for enhanced initiation rates and 5'-incorporation of GSMP
- exclusion of homologies to other mRNAs (controlled by a BLAST search)
- low secondary structure to facilitate access to the mRNA-*target*-sequence
- sequences >200 nt downstream of the start-codon to avoid interference with promoters
- modification of the 3'-terminus by AA

Target sequences for siRNAs targeting GFP, Lamin A/C, and glucosyl ceramide synthase (see Table 3-3) were selected from database sequences of the corresponding genes, and sense and antisense-templates were designed, so that hybridization of the transcripts would yield duplexes with the characteristic 2nt 3'-overhangs. The 17 nt T7 recognition sequence was added at the 5'-terminus of the template sequence. Recognition required hybridization of the T7 sequence with a 17 nt complementary strand. Figure 3-16 illustrates a ready-to-use T7-DNA-template.

in vitro transcription reactions were carried out with the T7 RiboMAX-Kit (Promega) according to the manufacturers instructions. To allow the modification of the sense strand without affecting the antisense strand, the two templates were transcribed in separate reactions. An eightfold excess of GSMP over rNTPs was added to the reaction mixture of the sense strand. This leads to an incorporation of GSMP into ~80% of all strands (Zhang et al. 2001a).

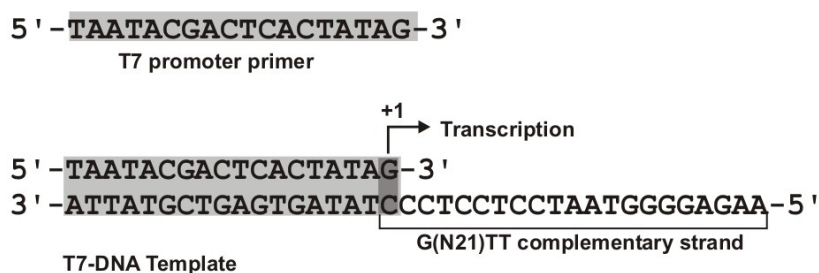


Figure 3-16 Double stranded DNA recognition sequence for T7 polymerase (Milligan et al. 1987). Note that all DNA templates require a C or CC at the 5'-end of the double-stranded T7-recognition

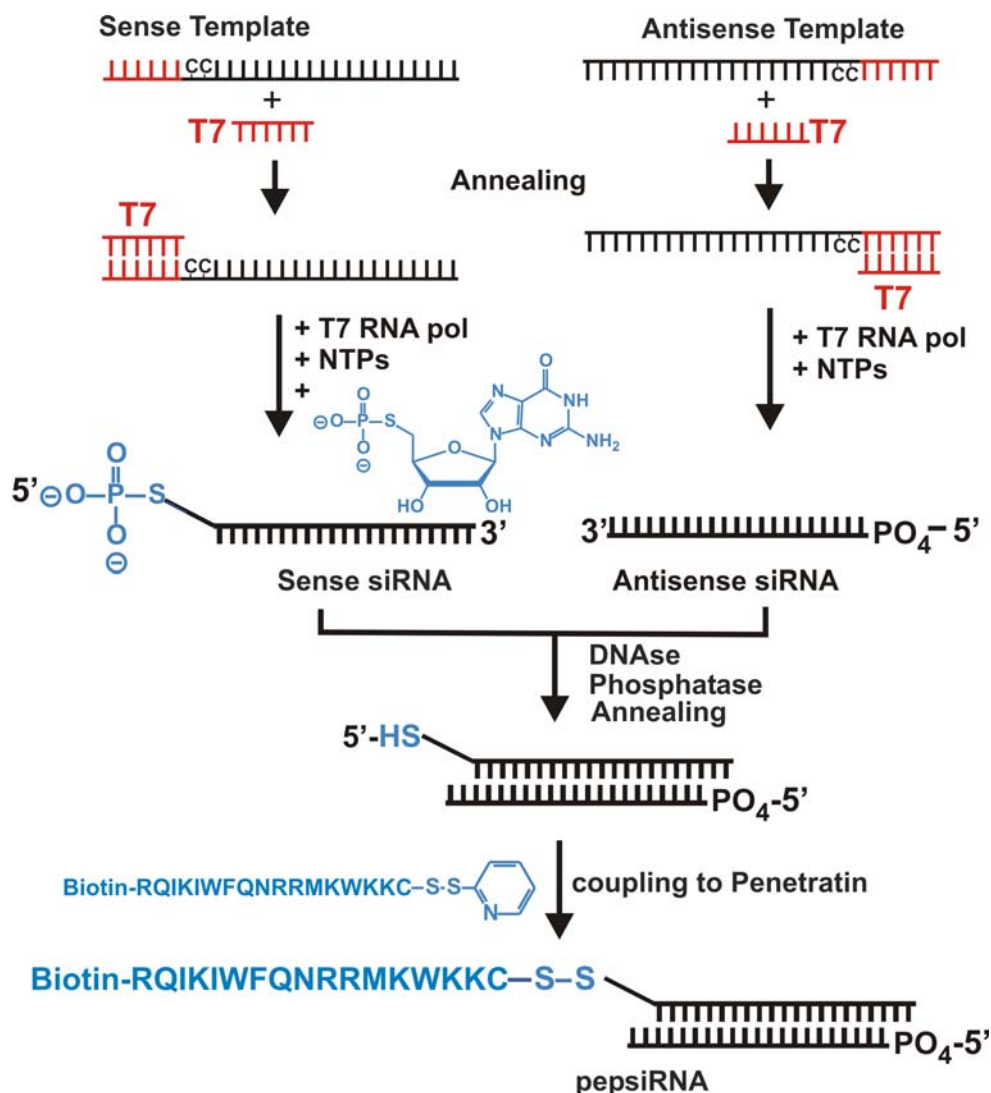
sequence to enable the incorporation of guanosine-derived initiator nucleotides. GAA at the 5'-terminus leads to 21 nt transcripts with CUU ends that have been shown to render siRNAs more efficient (Elbashir et al.).

| Oligo | template | sequence |
|-------|-----------|---|
| 273 | T7 | 5' -TAATACGACTCACTATAG-3' |
| 331 | Lamin as1 | 5' -AAGGGCGCAGGCCAGCTCCACTATAGTGAGTCGTATTA-3' |
| 332 | Lamin s1 | 5' -AAGTGGAGCTGGCCTGCGCCCTATAGTGAGTCGTATTA-3' |
| 333 | Lamin as2 | 5' -AAGCAGGAGCTCAATGATCGCTATAGTGAGTCGTATTA-3' |
| 334 | Lamin s2 | 5' -AAGCGATCATTGAGCTCCTGCTATAGTGAGTCGTATTA-3' |
| 335 | Lamin as3 | 5' -AAGGTCAGCCGCGAGGTGTCCTATAGTGAGTCGTATTA-3' |
| 336 | Lamin s3 | 5' -AAGGACACCTCGCGGCTGACCTATAGTGAGTCGTATTA-3' |
| 337 | Lamin as4 | 5' -AAGCCCGCCTGCAGCTGGAGCTATAGTGAGTCGTATTA-3' |
| 338 | Lamin s4 | 5' -AAGCTCCAGCTGCAGGCGGGCTATAGTGAGTCGTATTA-3' |
| 339 | Lamin as5 | 5' -AAGGTGACCTGATAGCTGCTCTATAGTGAGTCGTATTA-3' |
| 340 | Lamin s5 | 5' -AAGAGCAGCTATCAGGTCACCTATAGTGAGTCGTATTA-3' |
| 430 | GCS s1 | 5' -AAGGAGGACAGGGTGGGCGCCTATAGTGAGTCGTATTA-3' |
| 431 | GCS as1 | 5' -AAGGCGCCACCCTGTCCTCCTATAGTGAGTCGTATTA-3' |
| 432 | GCS s2 | 5' -AAGGCAGCCCGTGAACCAAGCTATAGTGAGTCGTATTA-3' |
| 433 | GCS as2 | 5' -AAGCTTGGTTCACGGGCTGCCTATAGTGAGTCGTATTA-3' |
| 434 | GCS s3 | 5' -AAGGATTCCTCTGCTGTACCTATAGTGAGTCGTATTA-3' |
| 435 | GCS as3 | 5' -AAGGTACAGCAGAGGAAATCCTATGTGAGTCGTATTA-3' |

| siRNA | sequence |
|-------|---|
| GFP | 5' -GCUGACCCUGAAGUUCAUCdTdT-3' 3' -dTdTTCGACUGGGACUUCAAGUAG-5' |
| HexA | 5' -UGAUGACCAGUGUUUACUCdTdT-3' 3' -dTdTACUACUGGUCACAAAUGAG-5' |

Table 3-3 DNA-primers used for the generation of siRNAs against various targets.

Lyophilized GSMP **15** aliquots were dissolved in water or 10 mM Tris-HCl pH 7.5 prior to use and the insoluble residue was removed by centrifugation. The concentration was determined at 260 nm with reference to a commercial rGTP (Promega). According to the protocol for *in vitro* transcription in 100 µl (RiboMAX), a defined volume of rNTPs (30 µl, 25 mM) is added and the reaction mixture has to be filled up to 100 µl with water. In the modified experiment, this volume is filled up by a solution of rNTPs and GSMP with a molar ratio of 1:8 for GTP to GSMP. Usually, 50-300 nmoles of rNTPs would be used in a 100 µl reaction mixture. An equal amount of rNTPs was used in the antisense reaction mixture and the remaining volume filled up with water.



Scheme 3-5 Generation of 5'-thiol-modified siRNAs by in vitro transcription. GSMP is added in excess to the reaction mixture of the sense strand to be incorporated at the 5'-terminus. Phosphatase is added to both transcripts to liberate the 5'-thiol-group or remove triphosphate groups that may trigger an interferon response.

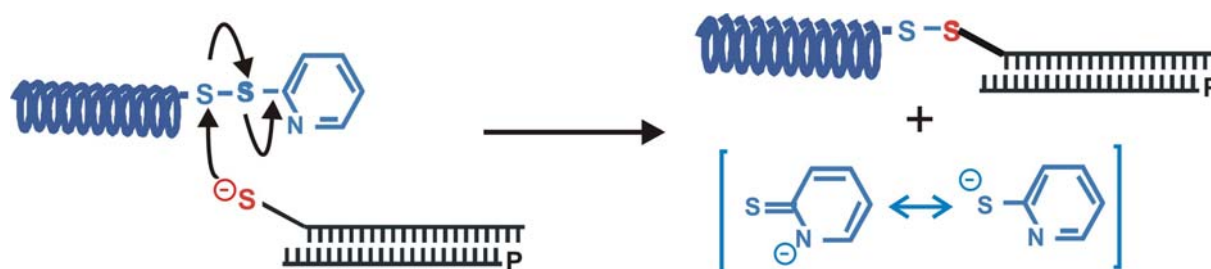
Transcription was carried out at 37°C overnight (18-24 h). The DNA-templates were digested with DNase. Eventually, calf intestine phosphatase (CIP) was added to both reaction mixtures to liberate the 5'-thiol group and to remove 5'-triphosphates that might lead to non-specific effects in cell culture experiments.

The RNA transcripts were precipitated and dissolved in 100 mM DTT-solution to avoid the formation of homodimers. Concentrations were determined photometrically and equimolar amounts of RNA were mixed together and hybridized to siRNAs. *In vitro* transcriptions with 250-750 pmoles of template yielded 65-130 µg RNA in a total volume of 100 µl.

3.1.4 Coupling of 5'-thiol modified siRNAs to Penetratin™

Cell-penetrating peptides are used in several fields of research and a modified form of the protein transduction domain of Antennapedia has been patented and is commercially available as Penetratin™ (Q-biogene). The product is synthesized on solid phase and can be modified according to the customer's needs. In this work, a Penetratin™ derivative with a C-terminal thiol-modification and an N-terminal biotin-tag was used. The latter was needed to localize the Penetratin™ moiety in the interior of treated cells as a proof of successful uptake.

To favor the formation of peptide-siRNA heterodimers over the formation of homodimers, the peptide moiety needs to be activated. Thiopyridine is a convenient activating group as it yields mesomery-stabilized thiopyridone upon disulfide exchange reaction for which the back reaction is unfavorable. The mechanism of the disulfide exchange reaction is shown in Scheme 3-6. The reaction can be monitored by the characteristic absorption of thiopyridone ($\lambda_{\text{max}} = 345 \text{ nm}$).



Scheme 3-6 Disulfide exchange reaction with activation by thiopyridine. Nucleophilic attack of the free thiol-group on the disulfide bond leads to the formation of heterodimers $R_1\text{-S-S-R}_2$ and a thiopyridone ion that is stabilized by mesomery.

siRNAs were incubated with DTT to reduce putative homodimers. Prior to coupling, DTT was removed by gel filtration on MicroSpin G-25 columns (AP-Biotech). Upon the first elution only 30-40% of the siRNA is obtained. The full amount of siRNA can only be recovered after 3 further elutions with 10 mM Tris-HCl pH 7.5. However, DTT co-eluted with these fractions rendering them useless for coupling experiments.

The concentration of the siRNA-eluate was determined photometrically at 260 nm. Considering that only 80% of the siRNAs are thiol-modified (Zhang et al. 2001b), 0.8 equivalents (eq) of aqueous Penetratin™ solution were diluted to the same volume and added dropwise to the reaction mixture supplying an inert atmosphere with argon. An appropriate amount of 10x PBS was added to both components to avoid the dissociation of the siRNA and the aggregation of free peptides with siRNAs. At high concentrations a yellow ring of thiopyridone ($\lambda_{\text{abs}} = 345 \text{ nm}$) could be observed at the interface of the two components. One hour of incubation at 37°C is sufficient to drive the coupling reaction to completion (Antopolsky et al. 1999). In some cases, a white precipitate formed due to

aggregation. It could be partially dissolved by adding 3M sodium chloride solution up to a total concentration of 400 mM as suggested by Vives and Lebleu for the coupling of DNA-oligonucleotides to Tat peptide (Vives and Lebleu 1997)

3.1.5 Gel electrophoresis with pepsirNAs

The success of the coupling reactions was tested by reducing and non-reducing 15% SDS-PAGE. Samples of peptide-coupled siRNA (pepsiRNAs) and free peptide were prepared with the corresponding amounts of reducing and non-reducing 5x Laemmli buffer. 50µg of Penetratin™ and pepsirNAs with a peptide content of 17.6µg were separated in a 20% SDS-PAGE and stained with Coomassie blue. The results are shown in Figure 3-17.

The band of the non-reduced pepsirRNA lane was shifted to a higher mass of about 8 kDa and could be clearly distinguished from the free peptide bands at ~4kDa and the reduced pepsirRNA. This also shows that the thiol-linker is indeed cleaved under reducing conditions. It has to be noted, that the gel shift observed for the conjugate does not correspond to the mass of ~10 kDa expected for the denatured conjugate (peptide+ssRNA), which may be due to the coupling of the siRNA and its separation properties. The control with Penetratin™ under non-reducing conditions shows that no peptide-homodimers were formed that may be mistaken for the conjugate.

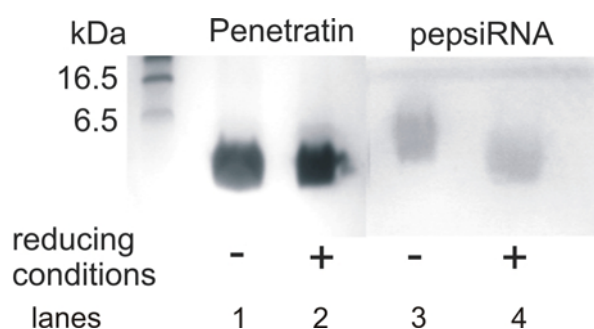


Figure 3-17 Control of the coupling of Penetratin™ with siRNA by 20% SDS-PAGE (Coomassie Stain). Samples of penetratin (lanes 1 and 2) and pepsirRNA (lanes 3 and 4) were prepared under reducing (lanes 2 and 4) and non-reducing conditions (lanes 1 and 3). Under non-reducing conditions, pepsirNAs show a higher mass due to the coupled siRNA moiety. The siRNAs is cleaved under reducing conditions, so that only the peptide band can be seen. No peptide-homodimers can be seen under non-reducing conditions for the peptide control.

As the silver stain is more sensitive than Coomassie stain (0.1-1.0 ng versus 0.1 µg (Sambrook 1989)) control gels could be routinely run as coupling controls without losing too much of the compounds. 20% SDS-PAGE was repeated with smaller amounts of peptide (2-20 µg) and pepsirRNA (1-6 µg peptide content). However, the silver stain failed for both standard SDS-polyacrylamide and SDS-urea-acrylamide gels.

3.1.6 MALDI-TOF mass spectrometry of pepsRNAs

Matrix assisted laser desorption ionization (MALDI) provides sufficiently mild conditions to transfer entire pepsRNAs into the gas phase. Commercially obtained thiol-labeled siRNAs were reacted with biotin-labeled activated Penetratin™ in an equimolar ratio for one hour. After gel filtration, the reaction mixture was prepared for MALDI-MS. Trihydroxyacetophenone (THAP) has favorable properties as a matrix for the measurement of oligonucleotides (Jensen et al. 1996). First measurements were carried out in the negative mode with an DNA-oligonucleotide of known size as a reference.

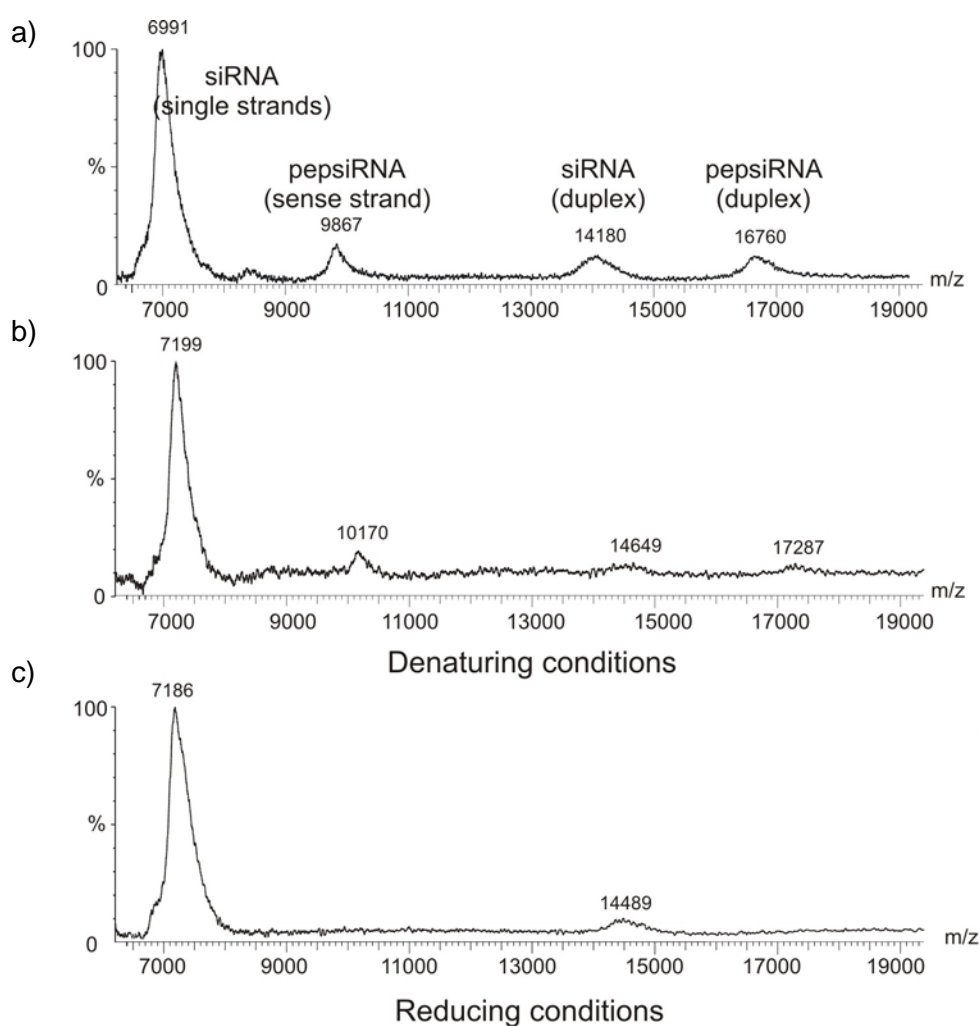


Figure 3-18 MALDI analysis of pepsRNAs a) The MALDI spectrum of the unmodified substance (negative mode, matrix: THAP, NH_4Ac added) shows five peaks corresponding to ssRNA (~7kDa), ssRNA coupled to Penetratin™ (~9.8 kDa), siRNA (~14kDa) and siRNA coupled to Penetratin™ [$\text{M}]^-$ ~16.8 kD, [$\text{M}]^{2-}$ ~8.4 kDa).

b) Denaturation of the sample by heating to 80°C and immediate cooling to 0°C before preparation leads to a significant reduction of the peaks representing dsRNA.

c) Peaks corresponding to disulfide-coupled compounds are diminished if the compound is treated with DTT to reduce disulfide bonds prior to sample preparation. (calculated masses: sense-RNA 6.804 kDa, asRNA 6.757kDa, ssRNA-Penetratin™-biotin 9.379, siRNA 13.561 kD, siRNA-Penetratin™-biotin 16.137kD).

Both pepsRNA and standard oligonucleotide were detected as broadened peaks. Due to the high acidity of the backbone phosphates, these residues are deprotonated at neutral pH. The siRNAs bear 42 negatively charged residues and are thereby found as mixtures of sodium and potassium salts, so that broadened peaks are found. As described by Jensen (Jensen et al. 1996), the pepsRNA and reference samples were treated with ammonium acetate to exchange sodium and potassium ions for ammonium ions that dissociate to volatile NH_3 and H^+ in the gas phase leaving behind protonated phosphate residues. The thus obtained peaks were much more focused, but could still not be assigned to one distinct mass. In three measurements of aliquots of the same sample, the value for the dsRNA peak varied between 14180 and 14649 Da corresponding to a maximum deviation of 1.8% from the average of the three measured values. This was much higher than the deviations of 0.08% reported for short model conjugates of peptides with oligodeoxynucleotides of an overall mass of 1942 to 4381 Da as determined by MALDI-MS (Jensen et al. 1996). One reason for this was the low signal to noise ratio obtained for the pepsRNAs, which led to ambiguous results in the determination of the peak maximum. Additionally, the incomplete removal of associated Na^+ ions resulted in a mass distribution of the oligoribonucleotides, and finally, the siRNAs might have been subject to nuclease degradation during sample preparation leading to fragments of different size. Evidence for this comes from 12% TBE-PAGE (7 M urea) by which fragments could be detected in a sample of radioactively labeled, denatured siRNAs (see Figure 3-19). This could be also due to strand termination during solid phase synthesis.

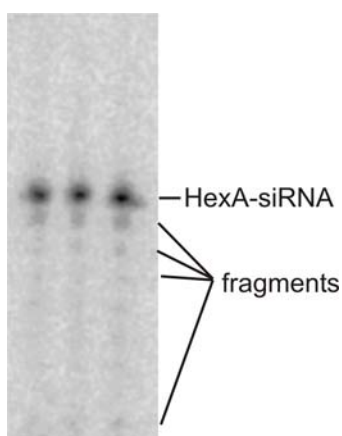


Figure 3-19 12% TBE-PAGE (7 M urea) with three different aliquots of a commercially obtained siRNAs to target HexA. siRNAs were labeled at their 5'-ends with [^{32}P]- γ -ATP by T-4 kinase, dissolved in loading buffer and denatured prior to loading to the gel. Radioactivity was detected with a phosphoimager screen (Bas III, Fuji). The siRNAs do not exhibit a uniform size distribution. Shorter nucleotides may result from degradation by nucleases during sample preparation or from strand termination during solid phase synthesis.

In the mass spectrum obtained for the pepsRNA sample, all expected species are present: pepsRNAs at ~16.8 kDa and ~8.5 kDa (for the doubly charged species), free siRNAs at ~14kDa, Penetratin coupled to the siRNA sense strand at ~9,8 kDa and 21nt single stranded RNAs that form the largest peak at ~7 kDa. The chemical identity of these peaks was confirmed by two experiments as shown in Figure 3-18.

Denaturation of the sample by heating to 80°C and rapid cooling on ice greatly reduced the amount of double stranded RNA (14 kDa) and pepsRNAs (16.8 kDa). Reduction of the sample with DTT prior to measurements led to the elimination of the peaks representing the disulfide-bridged compounds (double stranded (16.8 kDa) and single stranded RNA-penetratin conjugates (9.8 kDa).

The peak corresponding to single stranded RNAs is large compared to dsRNA peptide coupled RNAs. It has been reported, that conjugates of peptides and nucleotides pose special problems, since the two polymeric components have conflicting requirements for ionization (Jensen, 1996). This may be more pronounced for the larger conjugates as 21 bp siRNA coupled to the 16 residues of PenetratinTM, than for the reported conjugates of an 11-amino-acid peptide with thymidine decamers and hexamers. It is also likely that a proportion of the dsRNAs dissociated during the ionization process or that the double strands partially separate in the desalted solution after gel filtration. The signal at 7.2 or 7.0 kDa originated from dissociated dsRNAs as well as from antisense-strands dissociated from the pepsRNA. However, the existence of a dsRNA signal indicated, that not all of the siRNAs in the reaction mixture had reacted with the peptide.

Thus, the result from the MALDI-TOF-MS analysis has to be evaluated as proof of the existence of peptide-coupled siRNAs. It cannot be taken as a quantitative measure of the coupling efficiency, but indicates qualitatively that not all of the siRNAs were coupled to the peptide, which could not be detected by SDS-PAGE. Therefore, for the following cell culture studies one must consider that the concentration estimated for the experiments might be much lower than depicted, even though the pepsRNAs were subjected to gel-filtration. The final concentration was determined by photometrical measurements at 260 nm.

3.2 Test of pepsRNAs for their potential to trigger RNAi *in vivo*

After the successful generation of pepsRNAs, this new tool was to be tested in cell culture. To provide a comparison to conventional methods, model systems were chosen, for which siRNA-induced RNAi experiments had been reported. To probe the versatility of the pepsRNAs, different cell lines were to be tested with an emphasis on cells that were known to be difficult to address by liposomal transfection, like primary cells and non-dividing cells and especially neurons.

3.2.1 Targeting recombinant genes with pepsRNAs

For proof-of-principle the pepsRNAs were tested in cells of transgenic mice ubiquitously expressing the green-fluorescent protein (GFP) (Schmitz 2002). This system is especially convenient as a successful GFP knockout can be readily observed as a loss of fluorescence without further detection methods. With a turnover of about 24 h, GFP levels should be visibly reduced 2-3 days after its biosynthesis is knocked out.

In cooperation with the Wernig group (Institute of physiology II, Bonn), it was possible to test anti-GFP pepsirNAs in dividing myocytes and non-dividing myotubes of GFP-expressing mice.

Cultured myocytes were treated with 10, 25, 50, 100, 200, and 400 nM of pepsirNA built up from solid phase-synthesized peptides and siRNAs. The cells were washed several times and the treatment was carried out in serum free medium (SFM) to avoid undesired interactions of the CPP with free DNA from the serum. As negative controls, the cells were treated with uncoupled Penetratin™ to assess non-specific or toxic effects of the CPP, and with pepsirNAs directed against HexA (Sandhoff et al. 1977) (data not shown). Additionally, the cells were treated with SFM alone.

Due to the strong interactions of CPPs with the plasma membrane, it is likely that pepsirNAs adhere to cells adjacent to the site of application rather than distributing evenly over the culture dish. Therefore, pepsirNAs are added dropwise to the adherent cells covered with half the total volume of SFM to ensure an even distribution of the compound.

After 30-60 min of incubation at 37°C, the serum free medium was exchanged for culture medium supplemented with 10% serum (fetal calf serum (FCS)) and the cells were incubated for 24-72 h before the GFP-knock-down yield was assessed by fluorescence microscopy. A significant loss of fluorescence was already observed in myocytes at concentrations of 10-25 nM. Fluorescence levels found in control cells treated with free Penetratin™, anti-HexA-siRNAs and SFM alone resembled those of the non-treated controls. Figure 3-20 showed that pepsirNAs are well capable of triggering RNAi in myocytes in the 25 nM range and that the downregulation of GFP levels cannot be attributed to non-specific effects of pepsirNA, CPPs or the depletion of serum (see Figure 3-20). To monitor the effect of biotinylated pepsirNAs on over-expressed mRNA such as GFP, treated primary myogenic cell cultures from a transgenic GFP mouse were analyzed using immunofluorescence staining. Using a concentration of 25 nM pepsirNA(GFP) completely decreases the GFP expression, while the biotinylated Penetratin can be detected in the nuclei of the cells (see Figure 3-20).

,n of the pepsirNAs that was estimated photometrically. The concentration for the experiments might be much lower than depicted, even though the pepsirNAs were subjected to gel filtration due to incomplete coupling and degradation of the compounds.

3.2.2 pepsirNAs to knock out Lamin A/C in HeLa cells

In the first report of RNAi to knock out endogeneous genes in mammalian cells, Lamin A/C was downregulated in HeLa cells (Elbashir et al. 2001a). Therefore, the next experiments were carried out with anti-Lamin A/C pepsirNAs of equal sequence in HeLa cells.

The downregulation of the protein was monitored by immunofluorescence microscopy. The cells were plated on 6well plates and incubated 24h prior to treatment. To synchronize the cell cycles of HeLa cells and obtain comparable levels of lamin A/C in all cells, the cells were incubated at 4°C for 1h to force the cells into cell cycle arrest and allowed to recover for 30 min at 37°C. As described in 3.2.1, the cells were washed with serum free medium and the pepsirNAs were also diluted in serum free medium for treatment. PepsirNAs were applied in concentrations of 10, 25, 50, 100, 200, and 400 nM. As a control, 200 nM of non-specific pepsirNA and 200 nM of uncoupled peptide were applied to control cells. After 30 min of

incubation at 37°C, the application medium was removed and the cells were incubated in culture medium supplemented with 10% FCS.

After 6 days, the cells were plated on FCS-coated cover slips in 24well dish and allowed to attach over night. The cells were fixed with 4% paraformaldehyde (PFA) and incubated with anti-Lamin A/C IgG (mouse, kindly provided by M. Osborn, Göttingen) as primary antibody and anti-mouse IgG coupled to Cy3 as secondary antibody. The cells were attached to microscopy slides suspending in a drop of anti-bleach. Fluorescence microscopy revealed equal levels of Lamin A/C in untreated and Penetratin™ treated control cells. Protein levels were significantly reduced in cells treated with 100 nM anti-Lamin A/C pepsirRNAs. Co-staining of the same cells with anti-hexosaminidase A antibody showed no reduction in the levels of the non-targeted protein (see Figure 3-20).

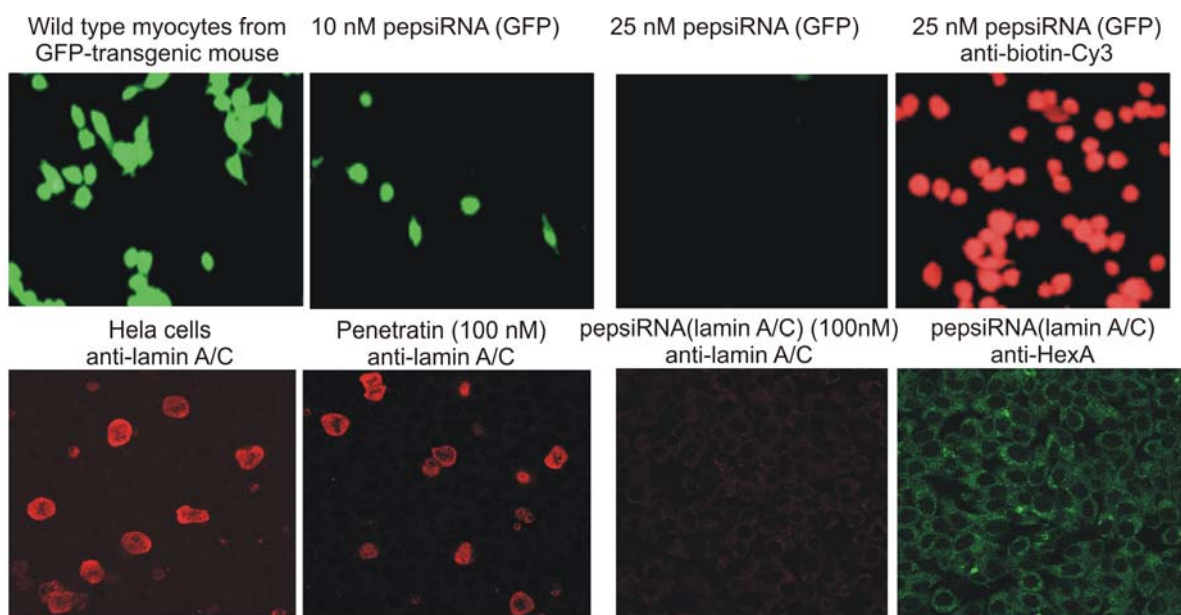


Figure 3-20 Gene silencing with pepsirRNAs. Upper row: Downregulation of GFP by treatment with anti-GFP pepsirRNAs. Fluorescence microscopy shows the basic fluorescence level of untreated myocytes, cells treated with 10 nM, and with 25 nM anti-GFP pepsirRNA. The slide on the right shows treated cells after staining the CPP-biotin-tag with streptavidin-coupled dye. Lower row: Downregulation of Lamin A/C levels in HeLa cells after the treatment with anti-Lamin A/C pepsirRNAs. Immunofluorescence detection of Lamin A/C (red) in untreated HeLa cells, cells treated with 100 nM uncoupled peptide, and cells treated with 100 nM anti-Lamin A/C pepsirRNAs. Staining with anti-hexosaminidase A IgG (green) shows that overall protein expression is not impaired (Zeiss Axiovert 35, filter set 15: $\lambda_{excit.} = 546nm$, $\lambda_{em} >590nm$, filter set 17: $\lambda_{excit.} = 485nm$, $\lambda_{em} = 515-565nm$).

3.2.3 PepsirRNAs to knock out proteins of the sphingolipid metabolism in fibroblasts

In further experiments, proteins of the sphingolipid metabolism were targeted with hexosaminidase A (anti-HexA) (Sandhoff et al. 1977) and glucosylceramide synthase (anti-GCS) pepsirRNAs. These proteins play a significant role in the metabolism of the skin and the brain (Schuette et al. 2001), where large effector molecules are generally difficult to apply.

Therefore, it was of great interest whether pepsirNAs could be taken up by the corresponding cell types and silence their target-genes. mRNA levels were to be estimated by RT-PCR and protein levels by Western blotting. The corresponding pepsirNAs were tested in primary fibroblasts and melanocytes as a model for primary cells that are more difficult to transfect. As opposed to HeLa cells, the cell cycle is arrested for fibroblasts once the bottom of the culture dish is covered with a confluent monolayer of cells. Thus, the cells did not have to be diluted in the course of the experiment and the RNAi phenotypes were expected to last longer as no siRNAs were lost due to dilution by cell division.

The cells were treated as described in 3.2.2 for HeLa cells. pepsirNAs were applied in concentrations of 5, 10, 25, 50, 100, 200, and 400 nM, and 200 nM of uncoupled peptide were applied to control cells. After 30 min of incubation, the cells were incubated in culture medium for varying times.

After 2 days the cells were harvested and the total RNA was isolated. To assess the residual amounts of Lamin A/C mRNA an RT-PCR with Lamin A/C specific primers was carried out. Lamin A/C levels were normalized against the levels of sphingolipid activator precursor protein (SAP) as a negative control. At high concentrations of 100-400 nM no residual mRNA of HexA and GCS, respectively, could be detected. At 50 nM mRNA levels were decreased to ~2 % compared to the untreated control, at 25nM ~2% were detected for HexA but 8% for GCS. At 10 mM 70% of the GCS mRNA in myoblasts and 80% of the HexA mRNA in fibroblasts was degraded. At 5nM of pepsirNA still 25% of HexA mRNA and 75% of GCS mRNA could be found. No down-regulation was observed for non-specific pepsirNA and Penetratin controls. The results are summarized in Figure 3-21.

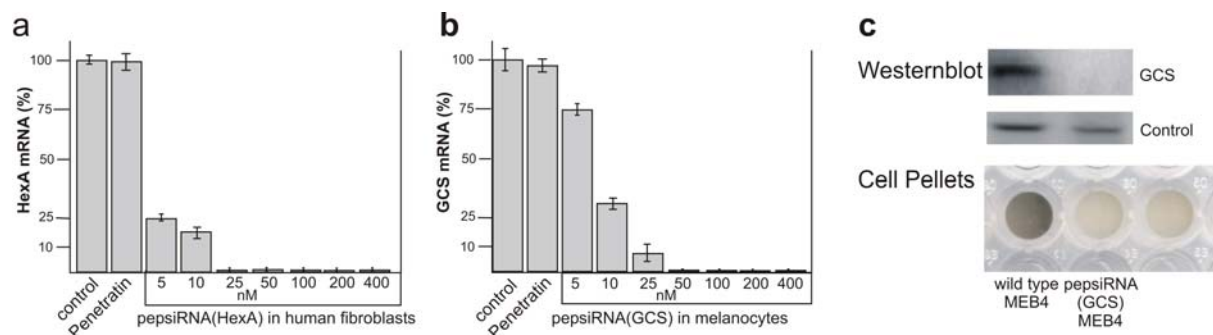


Figure 3-21 Treatment of primary fibroblasts with HexA-pepsiRNAs (a) and melanocytes with GCS-pepsiRNAs (b). The totalRNA levels were corrected with respect to a SAP control (sphingolipid activator protein (Schuette et al. 2001), residual mRNA levels are normalized to the untreated control. Concentrations of 50-400 nM lead to an almost complete degradation of target-mRNA. Residual levels are observed at 5-25 nM, where a stronger effect is observed for HexA in primary fibroblasts. (c) Degradation of GCS leads to a loss of black pigment in melanocytes. The degradation of GCS protein is confirmed by the Western blot.

Further, the protein levels were assessed after 7 days by preparing the harvested cells for 12% SDS-PAGE, blotting the protein samples to a PVDF membrane and immunostaining for HexA, GCS and Lamin A/C (control) as primary antibodies and anti-mouse and rabbit IgG coupled to horse raddish peroxidase (HRP) as the secondary antibody, which was detected by the chemiluminescence induced by the HRP in reaction with the LumiGlo reagent.

The results matched those found for the mRNA levels.

Remarkably, the melanocytes had lost their pigmentation 7 days after treatment with anti-GCS pepsRNA (see Figure 3-21 c). In wildtype melanocytes, tyrosinase is transported within specialized vesicles to the melanosomes, where it converts tyrosine to L-DOPA in the first rate-limiting step of melanine synthesis and pigmentation. It was suggested that tyrosinase is transported within vesicles enriched in glucosylceramide (GlcCer), which is generated by the addition of a glucosyl residue to ceramide catalyzed by GCS. Wildtype melanoma cells stain almost black due to pigmentation, while in GCS knock-out mice, tyrosinase is mislocated, so that the cells do not show any pigmentation (Sprong et al. 2001). The same was found for melanoma cells expressing lhrRNA targeted against GCS (Diallo et al. 2003b). Thus, the findings from the pepsRNAs experiment are in good agreement with these results. The degradation of GSC could be shown by Western blotting as depicted in Figure 3-21c.

3.2.4 Test of pepsRNAs in various mammalian cell lines

To assess the versatility of this new technique, pepsRNAs directed against HexA were applied to various mammalian cell lines. The same treatment protocol as in 3.2.2 was applied. The cells were treated with 100 nM of anti-HexA pepsRNA for 30 min and after 2 days of incubation the knockdown efficiency was assessed by RT-PCR. The normalized results are shown in Figure 3-22. In HeLa cells, human primary fibroblasts, human epithelial kidney cells and even primary murine neurons the target-mRNA was completely degraded. A knock-down up to ~98% was found for melanocytes, while mRNA levels of 7% and 20% were found in myotubes and myocytes, respectively. The residual activity might be explained by the setup of the experiment. Due to serum reduction the myocytes begin to differentiate very quickly to myotubes that are much more difficult to address. However, it can be concluded that treatment with pepsRNAs in the upper nanomolar range leads to a significant reduction of target mRNA in a variety of cell lines and primary cells. To ensure a complete knockout, the appropriate amounts of pepsRNA need to be estimated for every given cell line.

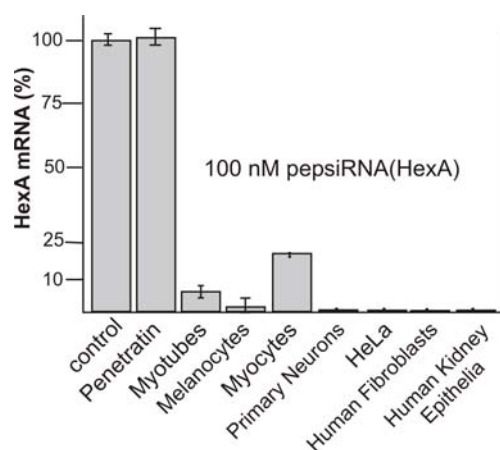


Figure 3-22 Versatility of pepsRNAs. 100nM of pepsRNAs directed against Lamin A/C were tested in various human cell lines and primary cells and the RNAi efficiency was estimated by RT-PCR with isolated total RNA.

3.3 Recombinant expression of CPPs in *E. coli*

As an alternative to solid phase synthesis, recombinant expression allows the generation of large amounts of the desired CPP once an appropriate expression and purification system has been established.

In this work, the protein transduction domains of the antennapedia protein (Antp) from *D. melanogaster* and the HIV-1 transactivator of transcription (Tat) were chosen as CPPs, since they have been successfully used to transport various cargo molecules. The sequences of interest comprise only 15 amino acids for Antp and 11 for Tat, respectively. Thus, the coding DNA sequences could be generated as synthetic genes by hybridizing overlapping DNA-oligonucleotides comprising the appropriate sequences. To allow coupling of the expressed peptide with the modified siRNAs, a cysteine codon was added to the 3'-terminus of either gene sequence prior to the stop-codon.

| CPP | Sequence |
|------|--|
| Tat | Tyr-Gly-Arg-Lys-Lys-Arg-Arg-Gln-Arg-Arg-Arg-Cys-SH |
| Antp | Arg-Gln-Iso-Lys-Iso-Trp-Phe-Gln-Asn-Arg-Arg-Met-Lys-Trp-Lys-Lys-Cys-SH |

Table 3-4 Amino acid sequences of Tat and AntP modified with a C-terminal cysteine residue.

Due to their highly positive overall charge, cell-penetrating peptides are likely to aggregate with negatively charged macromolecules like mRNAs or the bacterial genome. Therefore, the CPPs are to be expressed with a large fusion tag to compensate the overall charge and prevent diffusion to the extracellular space. In addition to this the purification of the target protein from the bacterial lysate can be greatly enhanced if the fusion protein functions as an affinity tag. Here, glutathione-S-transferase (GST) was chosen as a fusion partner to allow purification by affinity chromatography on glutathione-sepharose. The pGEX-expression system (AP Biotech) provides a cloning vector with a multiple cloning site adjacent to a GST fusion cassette. To subsequently release the CPPs from the N-terminal GST-tag, an additional sequence was introduced at the 5'-terminus of the synthetic CPP-genes coding for the recognition site of tobacco etch virus (TEV) protease. Figure 3-23 shows the fusion protein and the corresponding full-length synthetic gene.

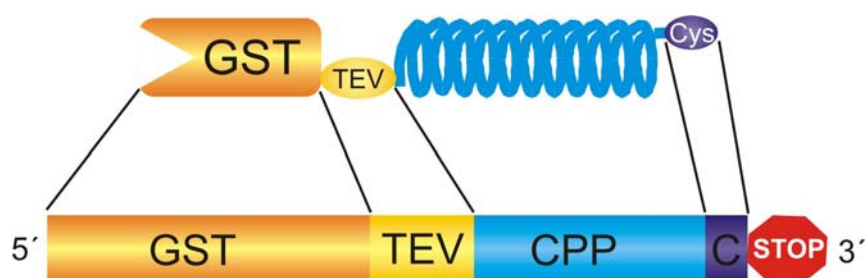


Figure 3-23 Schematic representation of the GST-CPP-Cys fusion protein and the corresponding synthetic gene and GST-expression cassette.

3.3.1 Generation of a recombinant expression vector for modified CPPs

The full ORF-sequences of Antennapedia and HIV-1 Tat were obtained from NCBI database genebank Locuslink and the stretches encoding the CPPs selected according to Derossi (Derossi et al. 1994). The full-length synthetic genes comprising the codons for TEV recognition site, the CPP and the cysteine residue as well as the stop-codon were designed to bear cohesive 5'-ends corresponding to the restriction sites of the *Bam*HI and *Eco*RI in the multiple cloning site (MCS) of the pGEX-vector. This double stranded sequence was synthesized as five (four) different overlapping oligonucleotides as shown below.

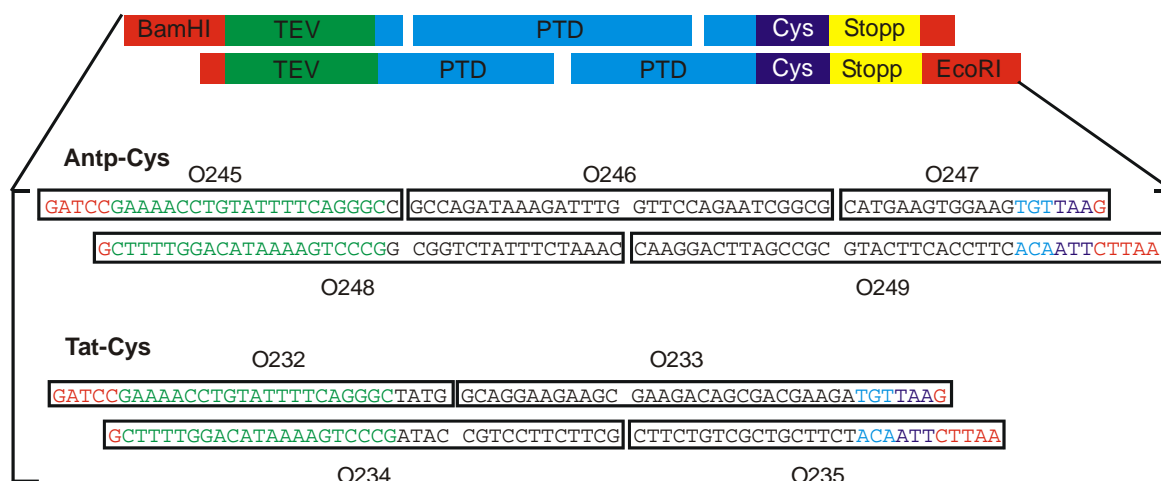


Figure 3-24 Sequences of synthetic genes and their distribution into overlapping oligonucleotides for hybridization.

Equal amounts of corresponding oligonucleotides are hybridized to yield the full double-stranded peptide-coding sequence. The best results were obtained with denaturation temperatures of 80°C and the use of an appropriate amount of 10x annealing buffer II. The double-stranded constructs were ligated into the *Bam*HI and *Eco*RI site of the pGEX-4T2 vector (AP Biotech).

The ligated vectors were amplified in *E. coli* DH5 α . Vectors purified from monoclonal overnight cultures were tested for successful ligation by restriction analysis and PCR.

Digestion with *Bam*HI and *Eco*RI yielded 78 bp for the Antp insert or 66bp for the Tat insert. The linearized vector was observed as a 4900 bp band.

In PCR control-experiments the vector was used as a template for the amplification of the insert. A GST-specific forward oligonucleotide (GST uni 5', see appendix) and one of the reverse oligonucleotides corresponding to the CPP were used as primers, so that a 140 or 128bp PCR product was expected for positive clones.

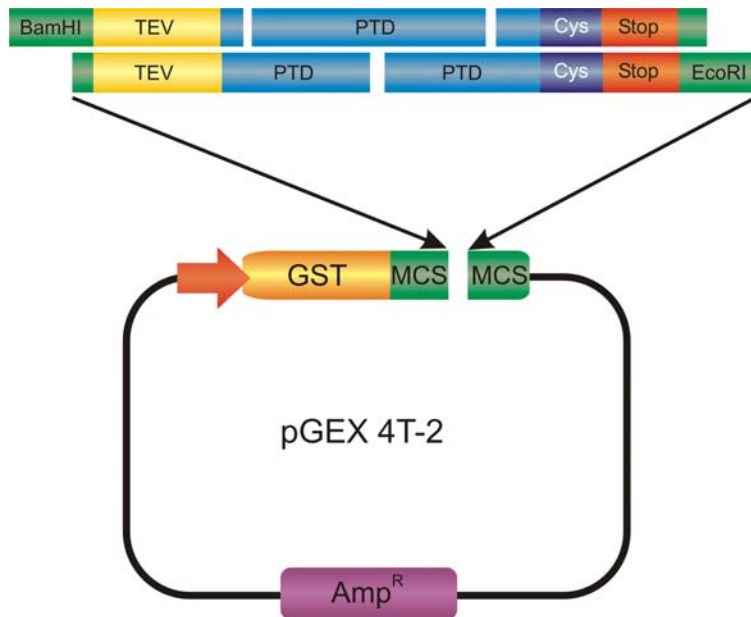


Figure 3-25 Cloning of synthetic genes into the MCS of pGEX-4T2.

Results for Tat and AntP vectors are shown in Figure 3-26. The exact size of the restriction fragments and PCR products could not be determined by gel electrophoresis. Thus, the positive vectors were sequenced to ensure that the full-length peptide-encoding sequence had been inserted and that it contained neither mutations nor single nucleotide insertions that would shift the reading frame.

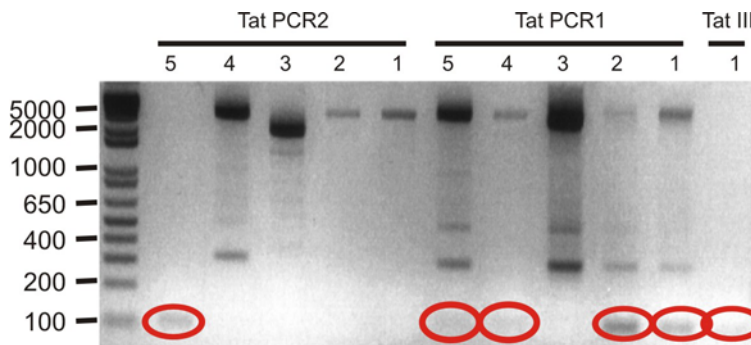


Figure 3-26 Results from control-PCR with putative Tat and AntP-vectors as templates (1.5% agarose gel electrophoresis, ethidium bromide stain). The amplified inserts can be seen as 120-140 bp bands. Re-ligated vectors yield bands of ~5 kbp representing the plain vector.

Sequencing revealed that successful clones with full-length inserts were comparatively rare, point mutations were corrected by site directed mutagenesis-PCR with the corresponding full-length oligonucleotide-primers. Only one primer per reaction mixture was used. Thus, the number of corrected copies would increase linearly with the number of PCR-cycles and the yield would be significantly lower than in reaction with forward and reverse primers, for which the number of copies grows exponentially.

After PCR reaction mixtures were digested with *Dpn I* to specifically remove the methylated DNA templates. Thus, only the non-methylated products of the mutagenesis reaction were

obtained. A small fraction of the PCR-product was analyzed by agarose-gel electrophoresis and the larger fraction was transformed into *E. coli* DH5 α and incubated on ampicillin selection plates.

The sequence of antennapedia peptide was easily corrected from an A→T mutation and the insertion of a guanosine residue with the standard site directed mutagenesis and a clear band for the mutagenesis product could be detected after 1% agarose gel-electrophoresis.

For Tat peptide the annealing temperature had to be adjusted from 55°C to 58°C in order to obtain the desired vector. Although the band for the mutagenesis product could be hardly seen on the agarose-gel, transformation and selection from ampicillin-LB-agar yielded recombinant colonies. The plasmids from all successful clones were amplified and analyzed by sequencing.

3.3.2 Expression of GST-CPPs in *E.coli*

Amplified vectors containing the correct CPP insert were transformed into *E. coli* BL21 cells for expression. During the mutagenesis experiments, one Tat vector had been obtained, in which one of the arginine codons (R6, CGG) was mutated to glutamine (CGG → CAG, Tat-R6Q). This vector was included in the expression experiment to compare the uptake properties in differently charged CPPs.

In a preliminary experiment, 20 ml of LB or S.O.C. medium were inoculated with a clone from an overnight culture. Expression was induced with 100 μ M IPTG (isopropyl-thiogalactopyranoside) during the exponential growth phase ($OD_{600} = 0.6-0.7$). By the addition of this structure mimetic of galactose, the suppression by the lac-repressor upstream of the recombinant sequence in the expression vector is released and the cells start to overexpress the recombinant gene.

Control expression was carried out in recombinant bacteria containing the plain pGEX-4T2 vector. Protein samples were taken 18h after inoculation and analyzed by 12% SDS-PAGE to assess the expression efficiency of the individual clones. A clear shift in size was observed between the GST-CPP fusion proteins (28-29 kDa) and the pure GST (26 kDa) expressed in control cultures as shown in Figure 3-27. Double protein bands were obtained from clones expressing both GST-CPP fusion protein and plain GST.

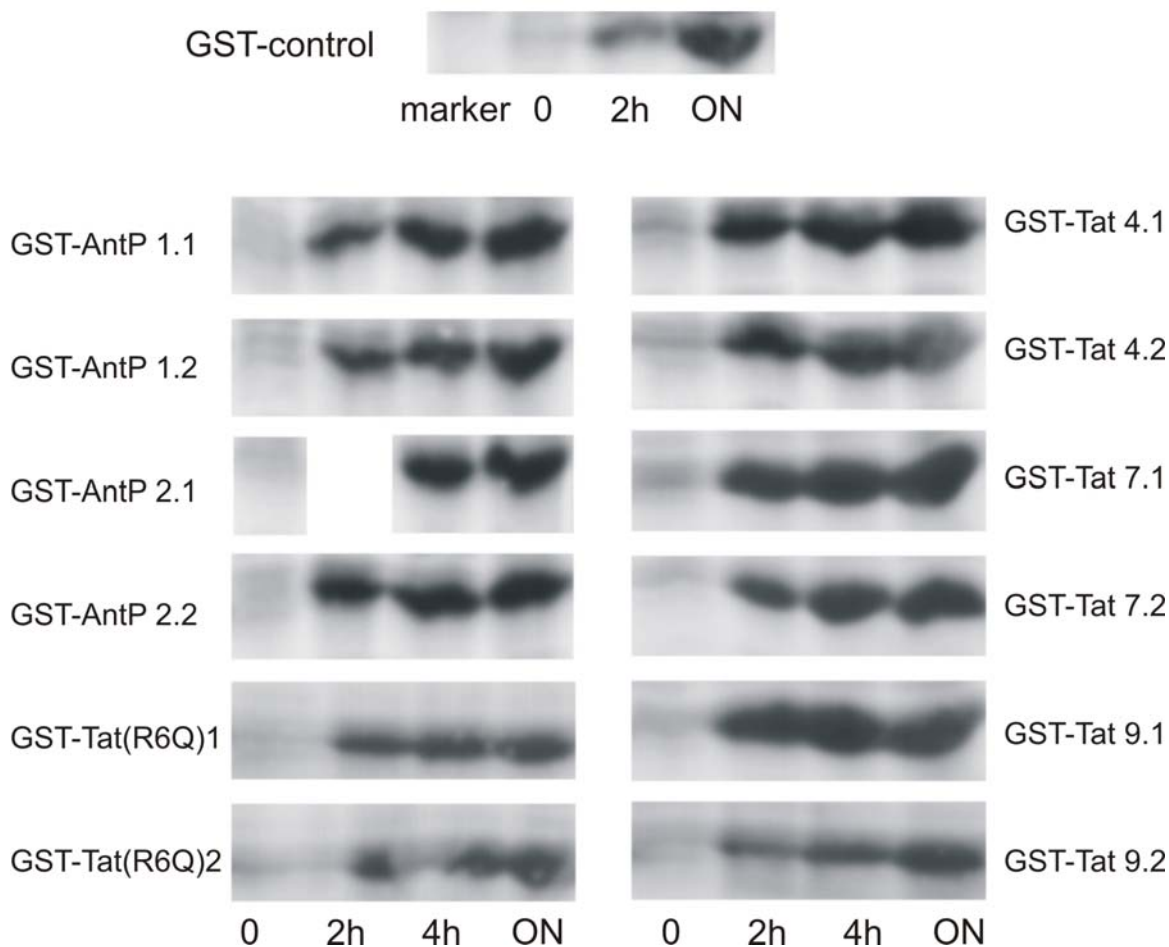


Figure 3-27 15% SDS-PAGE of expression of GST and GST-fusion proteins in *E. coli* stained with Coomassie Stain. Expression bands can be seen at 26 kDa for pure GST and at 28-29 kDa for the GST-fusion proteins with AntP and Tat. GST was used as a size marker in all gels. The numbers are derived from the number of the plasmid and the number of the clone.

3.3.3 Purification of GST-CPP fusion proteins by affinity chromatography

The pellets from expression cultures with high expression rates were chosen for further purification. Plain GST was purified as a control.

Pellets from 20 ml expression culture were resuspended in pGEX-Lysis buffer supplemented with DTT, lysozyme and DNase. After 30 min incubation on ice, the cells were homogenized and the insoluble components pelleted by centrifugation. Samples were taken from pellets and supernatants to be analyzed by SDS-PAGE. The lysates were incubated with glutathione-sepharose-beads that bind the GST-tagged proteins with high affinity. The supernatant was removed by filtration and the sepharose beads were washed with several volumes of lysis buffer and pre elution buffer to remove non-specifically bound protein. The GST-fusion proteins were eluted with reduced glutathione solution (10 mM in 50 mM Tris-HCl pH 8.0) and collected in several fractions. The protein content was determined photometrically against BSA-standards. As shown in Table 3-5, only very small amounts of GST-Tat and GST-Antp could be eluted from the glutathione sepharose, although the large

yields of plain GST indicated that the utilized glutathione resin was functional. Remarkably, slightly higher amounts of GST-Tat(R6Q) were obtained in comparison to GST-Tat.

| protein | yield from 20 ml expression culture | yield per liter of expression culture |
|---------------|-------------------------------------|---------------------------------------|
| GST (control) | 190 μ g | 9.5 mg |
| GST-AntP | 2 μ g | 0.1 mg |
| GST-Tat | 11 μ g | 0.7 mg |
| GST-Tat(R6Q) | 57 μ g | 2.9 mg |

Table 3-5 Protein yields obtained from affinity purification on glutathione sepharose. Protein amounts were estimated photometrically against a BSA standard after incubation of protein samples with Bradford reagent.

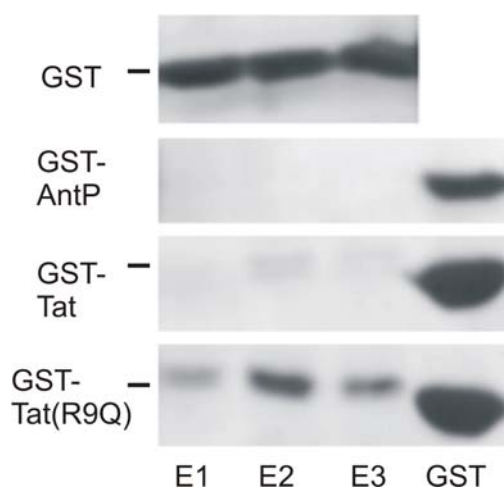


Figure 3-28 12% SDS-PAGE of eluates (E1-E3) from purification experiments (Coomassie Stain). GST eluate 2 was used as a size marker for the GST-CPP eluates. Double bands in GST-Tat can be discerned consisting of GST-CPP and plain GST.

The values obtained by comparison with BSA standards have to be taken as relative values. It is known that the extinction of the BSA-Coomassie complex that forms in the reaction with Bradford reagent differs from that of most other proteins, so that a correction factor has to be estimated for every individual protein to obtain absolute values (BioRad, User manual). However, the obtained values reflect the order of magnitude of the purified proteins.

As confirmed by 12% SDS-PAGE, only plain GST was dissolved in the supernatant, while GST-Tat, GST-Tat (R6Q) and GST-Antp resided in the pellet (data not shown). Apparently, the potential of CPPs to strongly interact with membranes leads to an association with lipids and membrane fragments in the bacterial pellets (see Figure 3-28). It has to be noted, that substitution of a single arginine residue in GST-Tat-R6Q leads to an increased solubility and a weaker membrane association.

3.3.4 Refining of the purification protocol for GST-fusion proteins for GST-CPPs

To solubilize the GST-CPPs the pellets were resuspended in pGEX-lysis buffer supplemented with 5 mM DTT and 1% of Triton X-100 (Lysis + Buffer, see Table 3-6). After centrifugation, samples of supernatants and pellets were analyzed by 12% SDS-PAGE in comparison to pellets and supernatants from cell lysis in pGEX lysis buffer see Table 3-6. An improved solubility could be observed for all GST-CPPs. The amount of soluble GST-AntP is markedly smaller than the amount of soluble GST-Tat.

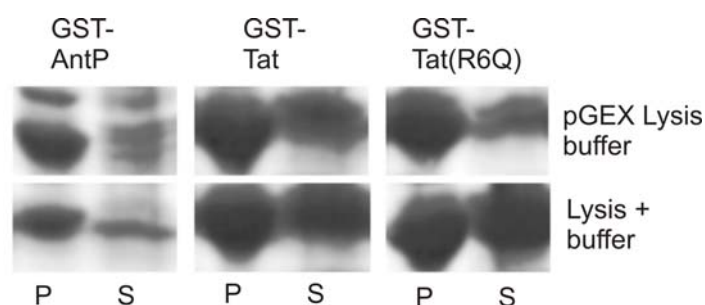


Figure 3-29 Resuspension of pellets with Lysis + buffer increases the amount of soluble protein in the supernatant. Equal volumes of supernatant were used for all samples. The product bands were identified in comparison with GST-eluate as a size marker. (15% SDS-PAGE, Coomassie Stain, S = supernatant, P = pellet)

Apparently the amount of soluble protein depends on the composition of the lysis buffer. Since the basic CPPs bear less positive charges at high pH, their interaction with membrane fragments in the pellet may be reduced by a more basic buffer. Therefore, the pH of the pGEX lysis buffer was adjusted from 7.4 to 8.0, which corresponds to the maximum pH at which GST efficiently binds to glutathione. According to the pGEX user manual, urea concentrations of up to 2M may be used to increase the yield of soluble GST-fusion proteins. Thus, four buffers with different concentrations of urea, DTT, and Triton X-100 based on pGEX lysis buffer were used for the preparation of fresh 20ml GST-Tat expression cultures:

| buffer | DTT | Triton X-100 | urea | pH |
|---------|-------|--------------|------|-----|
| pGEX | 1 mM | 1% | - | 7.4 |
| Lysis + | 5 mM | 2% | - | 7.4 |
| A | 10 mM | 3% | - | 7.4 |
| B | 5 mM | 2% | - | 8.0 |
| C | 5 mM | 2% | 1M | 7.4 |
| D | 5 mM | 2% | 2M | 7.4 |

Table 3-6 Supplements to pGEX-lysis buffer yielding buffers A, B, C, and D.

For evaluation, equal amounts of the four supernatants were analyzed by 12% SDS-PAGE in comparison with the supernatants obtained from the pGEX-lysates and the pellets resuspended in Lysis + buffer as shown in Figure 3-30. No significant difference was observed for the 4 buffers and only a small increase to GST-Tat lysed with plain pGEX lysis

buffer could be discerned. Remarkably, resuspending the pellet in Lysis + Buffer yielded an additional amount of soluble protein.

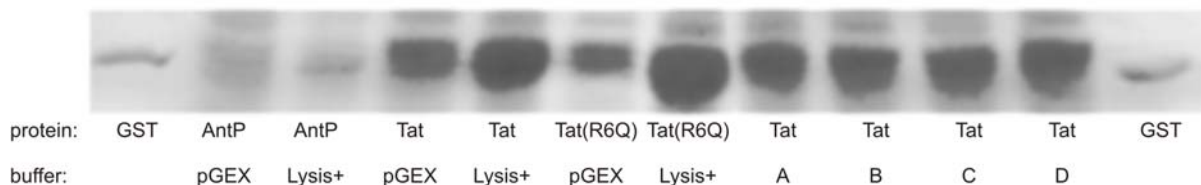


Figure 3-30 Influence of lysis buffer composition on soluble GST-CPP. Equal amounts of the corresponding supernatants were applied to the gel and GST eluate was used as a size marker. Lysis+ buffer was used to resuspend the pellets obtained from lysis with pGEX lysis buffer. Buffers A-D were used for lysis. The names of the fusion proteins are abbreviated to the name of the fusion peptide (15% SDS-PAGE, Coomassie Stain).

Therefore, the four GST-Tat pellets were resuspended in buffer B and left at room temperature (~22°C) for 1 h before centrifugation. The supernatants obtained after centrifugation contained a markedly increased amount of protein. Apparently, incubation at elevated temperature helps with the solubilization of the GST-CPPs.

GST-Antp was treated similarly as GST-Tat. Although the amount of recombinant protein in the overnight cultures was comparable to that of GST-Tat, the amount of soluble GST-Antp protein obtained after lysis with buffers A and C was markedly smaller than that of GST-Tat, and resuspension of the pellets in buffer B did not increase the yield, either. With the notion that solubilization may be temperature-dependent, the pellets were dissolved again in buffer B and incubated for 90 min at room temperature and at 37°C, as well as at 37°C on a thermo mixer at 400 rpm. Indeed, a considerable amount of GST-Antp was found in the supernatants after centrifugation. Incubation at 37°C yielded higher amounts than incubation at ambient temperature, while shaking of the sample at 37°C did not increase the yield of soluble GST-Antp.

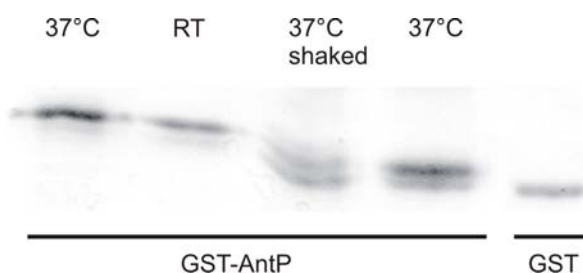


Figure 3-31 Incubation of insoluble pellets from GST-Antp expression in buffer B under at elevated temperatures. Equal volumes of supernatant were loaded onto the gel. Incubation at RT (23°C) and incubation at 37°C under constant rocking lead to lower yields of soluble protein than incubation at 37°C. GST was used as a size marker (15% SDS-PAGE, Coomassie Stain).

From these findings, a new purification protocol was established in which the bacterial pellets were worked up at room temperature and the homogenates were allowed to incubate at 37°C before centrifugation. Using the modified protocol, large amounts of soluble protein were obtained from new GST-Tat and GST-Antp over night expression cultures. The yield of

GST-Tat could be further improved by sonication of the homogenate prior to incubation at 37°C, while sonication reduced the yield of soluble AntP.

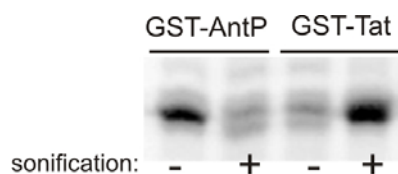


Figure 3-32 Preparation of homogenates from GST-CPP expression cultures with the modified purification protocol. Equal volumes of supernatant were loaded onto the gel. The homogenized suspensions were split and one fraction incubated at 37°C for 1h while the other was sonicated in a cup horn (3x 10s-blasts, 200W, 20 MHz, 15s intervals). Remarkably, the yield of soluble Tat was increased by sonication, while less soluble GST-Antp was obtained from the sonicated homogenate. This finding was confirmed by repetitive experiments (15% SDS-PAGE, Coomassie Stain).

The supernatants obtained in the last step were incubated with GST-sepharose beads as described in 3.3.3. The eluates were tested upon their protein content with Bradford reagent and the protein content of the pooled eluates was estimated by photometric evaluation against a BSA standard. For GST-Tat a total amount of 1,2 mg was obtained from 60 ml of expression culture corresponding to ~20 mg/l, while the total amount of GST-Antp was 0,6 mg corresponding to ~10 mg/l. This corresponds to the amount of GST purified from the control expression after preparation with the pGEX protocol.

3.4 Expression of TEV protease in *E. coli*

The GST-tag needs to be cleaved to liberate the cysteine-modified CPPs. Purification of the CPPs from tobacco etch virus (TEV) NIa protease and the cleaved fusion tag can be greatly facilitated if the protease itself is attached to a fusion-tag. If GST is used as a fusion tag, both protease and cleaved tag can be removed by a single step affinity chromatography as illustrated in Figure 3-33.

The GST-tag is almost as big as TEV-protease (26 kDa versus 28.6 kDa, respectively). Its pH for optimum folding lies at 7.0-7.5, whereas TEV-protease requires a pH of 8.5 for refolding. Thus, it is uncertain whether conditions exist under which both moieties fold to their functional conformation. Moreover, it cannot be ruled out that affinity binding to glutathione or cleavage activity of the protease renders the opposed domain dysfunctional so that the purification strategy cannot be carried out to its end.

Therefore, it was not only attempted to generate a GST-TEV fusion protein but also TEV protease with the much smaller His₆-tag. Six N-terminal histidine residues do not interfere with TEV function (Kapust et al. 2001). However, His₆-TEV cannot be removed from reaction mixtures along with the cleaved GST-tag, but needs to be bound by Ni-NTA in a distinct step.

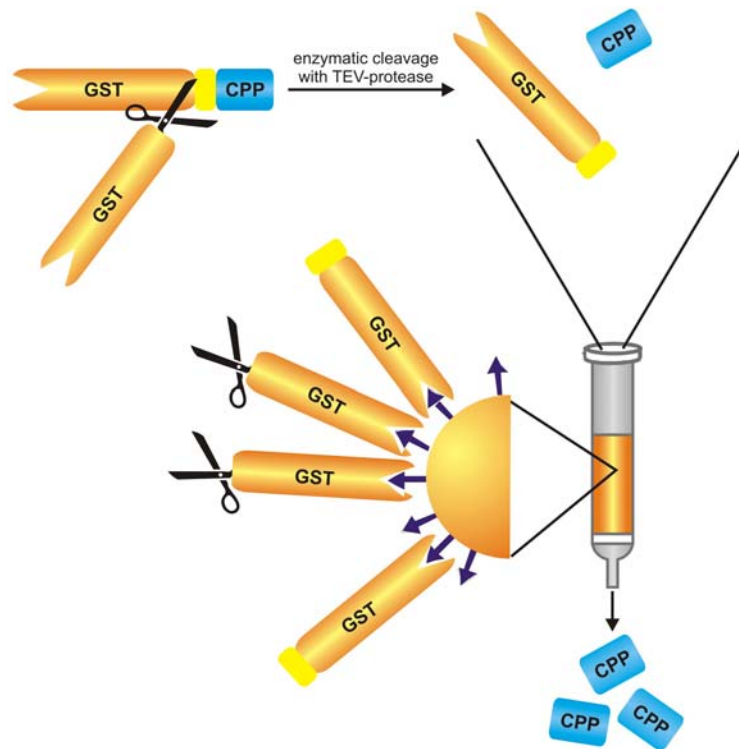


Figure 3-33 Schematic representation of GST-CPP cleavage and purification of the CPP. GST-tagged TEV-protease cleaves the fusion protein at the C-terminus of the TEV recognition site. Both GST-tag and GST-TEV protease are then removed by affinity binding to glutathione-sepharose.

3.4.1 Expression of GST-TEV-protease in *E.coli*

The ORF of TEV-protease was amplified from a cDNA clone and ligated into the *Bam*HI and *Eco*RI restriction sites of the pGEX-4T2 expression vector. The vector for the expression of GST-tagged TEV protease (GST-TEV) was amplified in *E. coli* DH5 α and after restriction tests transformed into *E.coli* BL21. Positive colonies were selected on ampicillin-LB-agar plates and grown as overnight cultures. As a test-expression, 20 ml LB were inoculated with GST-TEV overnight-cultures. The plain pGEX vector expressing GST was used as a control. Expression was induced with 100 μ M IPTG at an optical density of OD₆₀₀=0.6-0.7 and protein samples were taken after 90 min and over night incubation at 37°C and analyzed by 12% SDS-PAGE. The 55 kDa band of overexpressed GST-TEV and the 26 kDa band of the GST-control could be easily detected (see Figure 3-34).

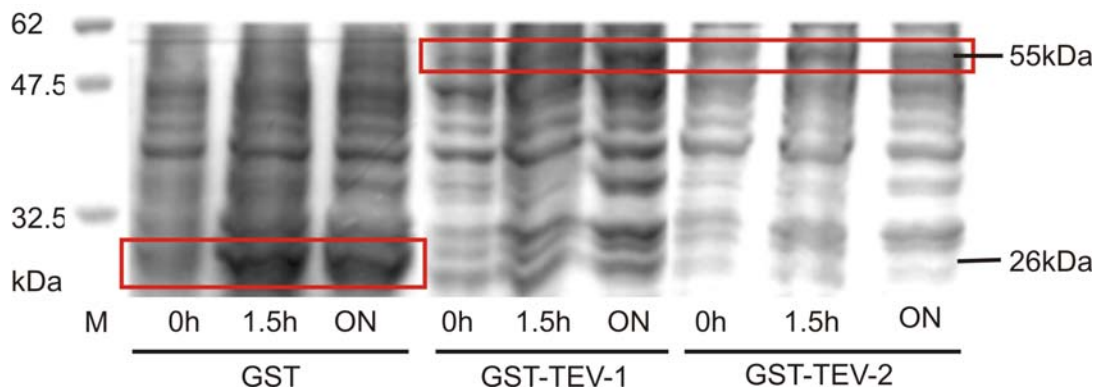


Figure 3-34 10% SDS-PAGE (Coomassie stain) of GST-TEV test expression. After over night (ON) expression the 55 kDa band of GST-TEV can be seen for both clones. Plain GST was expressed as a control.

As the expression in BL21 cells was rather weak, the GST-TEV expression vector was transformed into *E. coli* BL21 DE3 pLysS. The expression experiment was repeated with two clones of each strain in 20 ml LB as described above. After expression over night, the cells were harvested by centrifugation and purified according to the pGEX-protocol (Amersham Bioscience). SDS-PAGE of the pellets and supernatants obtained by centrifugation of the homogenized lysates revealed that the protein exclusively resided in the pellet. No difference could be determined between the expression levels in *E. coli* BL21 and BL21 DE3 pLysS.

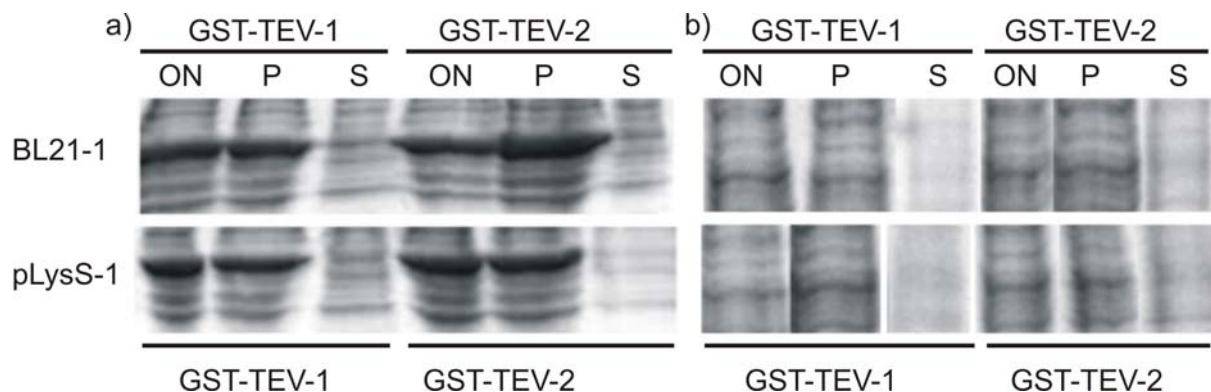


Figure 3-35 10% SDS-PAGE of GST-TEV lysates. After cell lysis according to the pGEX-protocol the recombinant protein resides in the pellet (P). Expression in BL21 or BL21 DE3 pLysS and at 37°C (a) leads to no significant changes in the amount of soluble protein. Only poor yields of recombinant protein are obtained by overnight expression at 17°C (b). (ON = overnight culture, P = pellet, S = supernatant, the numbers refer to the clone).

As the amount of soluble protein may depend on the expression temperature, the experiment was repeated with an incubation temperature of 17°C. However, overnight expression at these temperatures yielded very low levels of recombinant protein, so that no detectable amounts of soluble GST-TEV were obtained after cell lysis.

Apparently, GST-TEV forms inclusion bodies. The two equally sized protein domains might interfere with each others folding process leading to the precipitation of the misfolded protein. To obtain soluble GST-TEV protease from inclusion bodies, a protocol for the purification of His₆-TEV protease is applied with some modifications (Lucast et al. 2001).

The cell pellets were resuspended in lysis buffer supplemented with lysozyme and DNase. After 1h of incubation on ice, the cells were homogenized and the insoluble components pelleted by centrifugation. SDS-PAGE from pellets and lysates revealed that the major proportion of the overexpressed protein still resided in the pellet (data not shown).

Therefore, the pellet containing the insoluble protein was purified under denaturing conditions as described previously (Lucast et al. 2001). For affinity binding to glutathione-sepharose, the protein needs to be refolded. Therefore, the denatured protein solution was dialyzed against TEV-refolding buffer and pGEX-Lysis buffer, respectively. In both buffers a large fraction of the protein precipitated. The precipitate was removed by centrifugation and the supernatant was incubated with glutathione sepharose for 2h at room temperature to recover any fusion protein with a properly refolded GST-fusion tag. SDS-PAGE of the supernatants and eluates indicated that the recombinant protein was dissolved in the denaturing supernatant and in the dialysis sample albeit a major proportion of protein was lost due to precipitation. However, only very small amounts of the protein could be eluted from the resin (see Figure 3-36). GST-TEV bands in the eluates from the BL21 DE3 pLysS strain originate from a protein precipitate that occurred during the incubation with glutathione sepharose, that could not be fully removed from the resin by repeated washing.

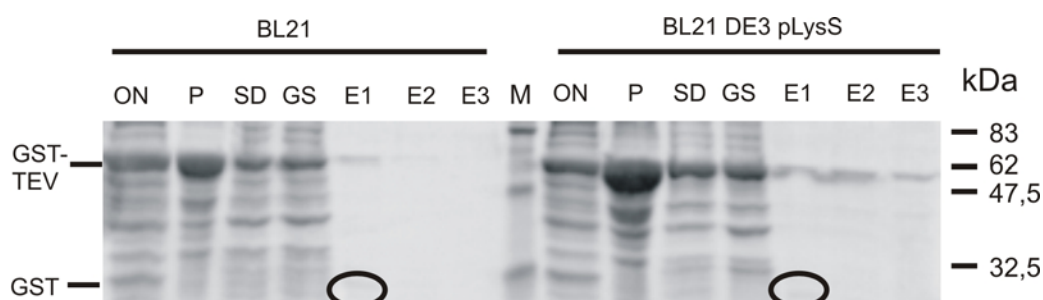


Figure 3-36 Inclusion body preparation of GST-TEV expressed in BL21 and BL21 DE3 pLysS. The recombinant protein from the overnight culture (ON) forms inclusion bodies that are found in the insoluble pellet (P). Treatment of the pellet with denaturing buffer redissolves GST-TEV that is found in the dialyzed supernatant but does not bind to glutathione sepharose as shown by the eluates (E1-3) and the supernatant decanted from the resin (GS). Note the thin GST band that is copurified at ~26 kDa (12% SDS-PAGE, Coomassie Stain).

As the pH optimum for refolding is 7.0 for GST (Amersham Bioscience) and 8.5 for TEV-protease, the pH of the refolding buffer was adjusted to values between 7.5 and 8.5. The dialyzed protein solutions were incubated for 2h with glutathione-sepharose beads. During the incubation the protein precipitated, and no significant amounts of protein could be detected in the eluates with Bradford reagent or by 10% SDS-PAGE (see Figure 3-37). Photometric quantitation of the eluates against a BSA standard indicated that the protein yield was below 1 mg/l for both samples.

Incubation of the supernatant for 3h on ice did not improve the results (data not shown).

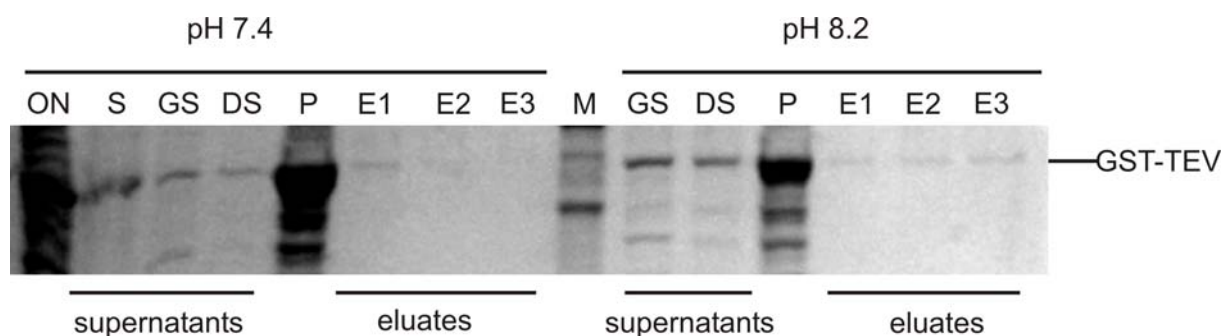


Figure 3-37 10% SDS-PAGE of GST-TEV refolding and purification experiments at different pH (Coomassie Stain). Dialysis to refolding buffer at pH 7.4 and 8.2 does not yield properly refolded protein, so that no GST-TEV can be bound by glutathione-sepharose and no protein can be seen in the eluates. (ON = overnight expression culture, S = supernatant from cell lysis, DS = denaturing supernatant, GS = supernatant after incubation with glutathione sepharose, P = pellet from cells lysis, E = eluates).

The precipitated protein could neither be redissolved in larger volumes of refolding or pGEX buffer nor by the addition of DTT to a concentration of 2 mM. Also, sonification with a cup horn could not redissolve the protein.

3.4.2 Expression of His₆-TEV-protease from E.coli

To avoid interactions of the GST-tag with TEV protease and the formation of inclusion bodies, TEV protease was expressed with 6 histidine residues attached to its N-terminus (His₆-tag), which permits affinity purification on Ni-NTA sepharose. The addition of 6 amino acids is less likely to interfere with the folding of TEV protease.

The ORF of TEV-Protease was amplified from a cDNA clone and ligated into the *EcoRI* and *Sall* restriction sites of the pQE-30 expression vector. The vector for the expression of His₆-tagged TEV protease (His-TEV) was amplified in *E. coli* DH5 α , tested by restriction experiments, and transformed into *E.coli* BL21. First expression experiments were carried out in 20ml LB inoculated with GST-TEV and plain GST overnight-cultures. Expression was induced with 100 μ M IPTG at an optical density of OD₆₀₀=0.6-0.7, and protein samples were taken after 4h incubation at 37°C and analyzed by SDS-PAGE. The 28 kDa band of overexpressed His-TEV was clearly visible (see Figure 3-34).

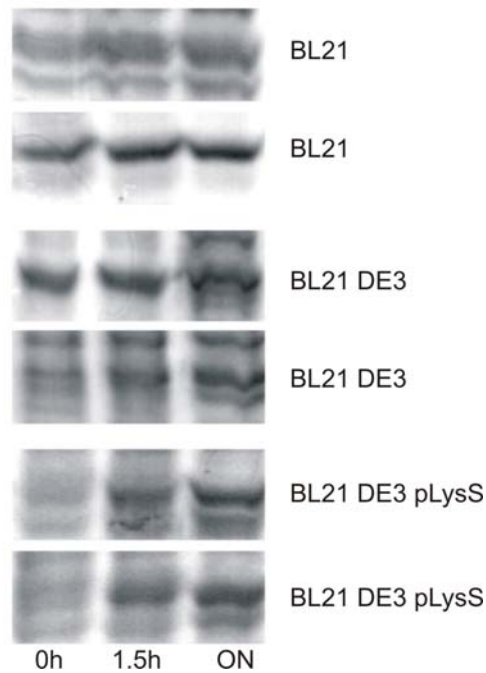


Figure 3-38 15% SDS-PAGE of test expression of His-TEV. The 28 kDa band of His-TEV can be detected in all samples. Three different E. coli BL21 strains were used (Coomassie Stain, ON = overnight expression culture).

The expression was continued overnight (18 h) and the cells were harvested by centrifugation at 100,000 x g. The cells were lysed under native conditions with lysozyme in lysis buffer supplemented with DNase according to the Qiagen Ni-NTA protocol. After homogenization and centrifugation, samples were taken from pellets and supernatants. The supernatants were applied to Ni-NTA mini-spin columns according to the provider's manual. After washing with pre elution buffer to remove non-specifically bound protein, elution was carried out with imidazole elution buffer. SDS-PAGE of the obtained eluates revealed that hardly any protein had been bound by the Ni-NTA columns, and a large amount of protein appeared to be residing in the pellet.

The experiment was repeated under denaturing conditions. Cells were lysed in 6M urea buffer. After centrifugation, the supernatants were applied to the Ni-NTA mini-spin columns. The columns were washed with pre-elution buffer at pH 6.3 and eluted with elution buffer at pH 4.3. However, no binding to the columns was observed in SDS-PAGE samples. It was found that most of the recombinant protein was again residing in the pellet. Expression at 20°C and reduction of the amount of IPTG for induction to 40 μM failed to increase the amount of soluble protein.

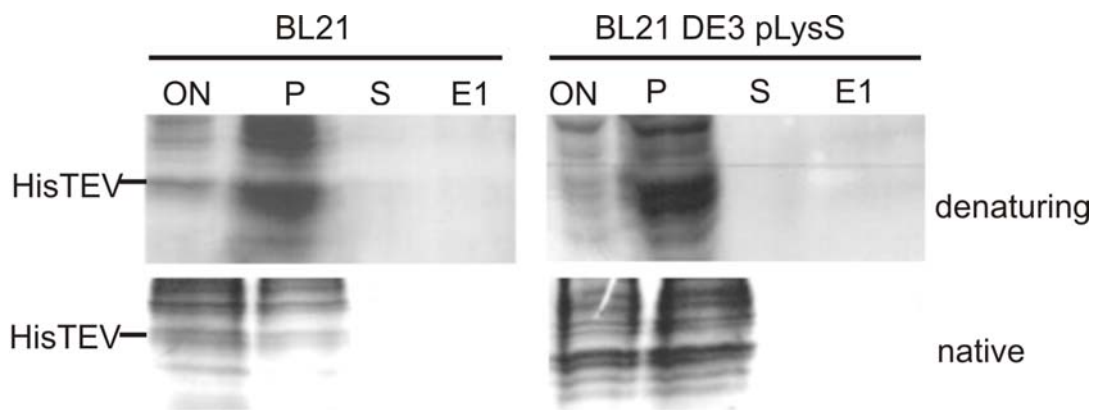


Figure 3-39 15% SDS-PAGE of HisTEV purification under denaturing and native condition using the Qiagen NiNTA MiniSpin Kit (Coomassie Stain, ON = overnight expression culture, P = pellet, S = supernatant from lysis, E1 = eluate1).

Apparently, even the shorter His-TEV fusion protein is not properly refolded in *E. coli* and accumulates in inclusion bodies. Preparation of the lysates as described in 3.4.1, did not increase the amount of soluble protein. The pellets containing the insoluble His-TEV were dissolved in denaturing guanidinium chloride buffer. After centrifugation, the supernatant was incubated with loose Ni-NTA beads (Amersham Bioscience) for several hours. However, after washing with denaturing pre-elution buffer, no protein could be eluted from the Ni-NTA beads with elution buffer (see Figure 3-40).

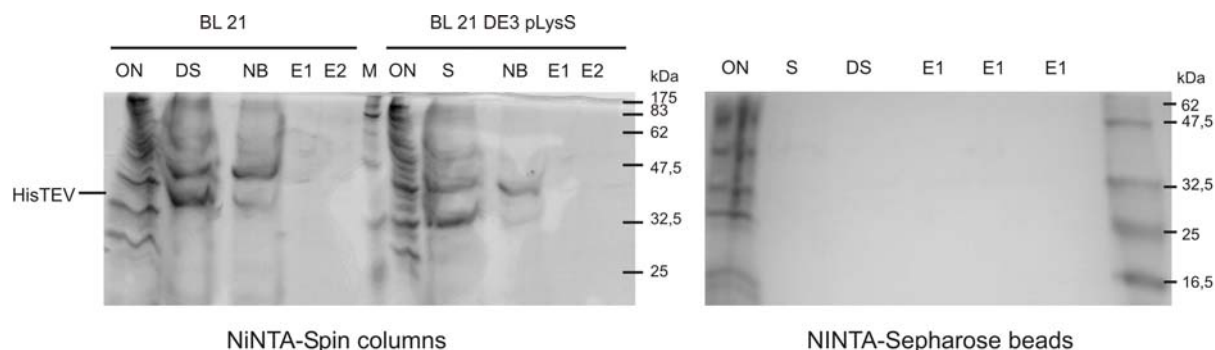


Figure 3-40 Purification of HisTEV after inclusion body preparation. No binding of the protein to the NiNTA columns or loose NiNTA resin was observed. (15% SDS-PAGE, Coomassie-Stain; ON = overnight expression culture, S = supernatant from Lysis, NB = supernatant decanted from NiNTA beads, E1-3 = eluates)

It appeared that the His₆-tag is not freely accessible in the denatured form of His-TEV. Dialysis in the refolding buffer described by Lucast led to precipitation of the protein, so that no His-tagged protein could be recovered from the filtrates with loose Ni-NTA beads (data not shown).

As reported by others, exchange of serin at position 219 against valin (S219V) markedly increases the solubility of recombinant TEV (Kapust et al. 2001), albeit it is reported that eluates of the mutant His-TEV are contaminated by significant amounts of other proteins (Lucast et al. 2001). The vector for the expression of soluble mutant form HisTEV (HisTEV (S219V)) transformed in *E. coli* BL21 (DE3) RIL was kindly provided by Anne Ulrich,

University of Karlsruhe (TH). Expression experiments were carried out in 20 ml TB medium inoculated with overnight cultures of the mutant strain. Expression was induced at an $OD_{600} = 0,6$ after 30 min of cooling the cells on ice by addition of IPTG to a final concentration of 100 μM . Control experiments showed that a considerable amount of recombinant protein was overexpressed during the first 4 h but no significant increase was observed if the expression is continued over night. Preparation of the pellets obtained by centrifugation led to good yields of soluble protein. The supernatant was incubated with Ni-NTA beads (Amersham Bioscience) for 90 min at RT, and the beads were thoroughly washed with native pre-elution buffer and eluted with elution buffer containing 250 mM imidazol. As shown by 12% SDS-PAGE large amounts of HisTEV (S219V) could be eluted from the Ni-NTA resin. Quantification of the eluates with Bradford reagent against a BSA standard showed that 230 μg of protein were obtained from the 20 ml expression culture corresponding to a yield of 11,5 mg of protein per liter expression culture.

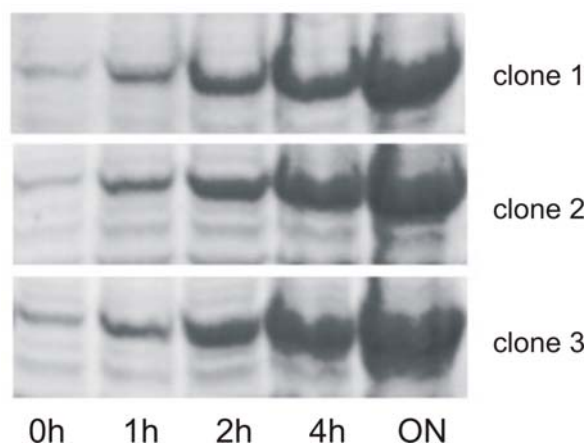


Figure 3-41 Expression of TEV-protease. Expression bands are found at $\sim 28\text{kDa}$ in comparison to a prestained protein marker (NEB, not shown). Protein levels increase over time. Clone 3 exhibits the strongest expression (15% SDS-PAGE, Coomassie Stain).

3.4.3 Cleavage of GST-CPP fusion proteins with TEV protease

The recombinantly expressed HisTEV (S219V) protease was tested upon its activity to cleave GST-CPP fusion proteins in comparison of commercially available TEV protease (AcTEV, Invitrogen). According to the manufacturers protocol, 20 μg of GST-Tat eluate were incubated with 10 u of AcTEV, the amount required to cleave 85% of 30 μg control substrate in 1h at 30°C in 1h according to the manufacturer in TEV-buffer supplemented with DTT in an overall volume of 150 μl at 30°C. Correspondingly, 20 μg of GST-Tat eluate were incubated with 5 and 10 μg of purified HisTEV (S219V).

Samples of 20 μl were taken after 1, 2, 4, and 16 h and analyzed by 15% SDS-PAGE. Unmodified samples of GST-Tat and HisTEV were used as controls. No peptide bands were observed due to the low peptide concentrations (0.1 μg per sample if all peptide was cleaved from GST). However, GST-Tat bands of $\sim 28\text{kDa}$ were clearly visible in close proximity of the HisTEV bands. (As HisTEV (S219V) and AcTEV have approximately the same molecular

weight, 26 kDa, they are both referred to as HisTEV in the discussion of the SDS-PAGE results). In the course of the experiment, the GST-Tat bands become weaker as the fusion protein is degraded to GST and Tat peptide.

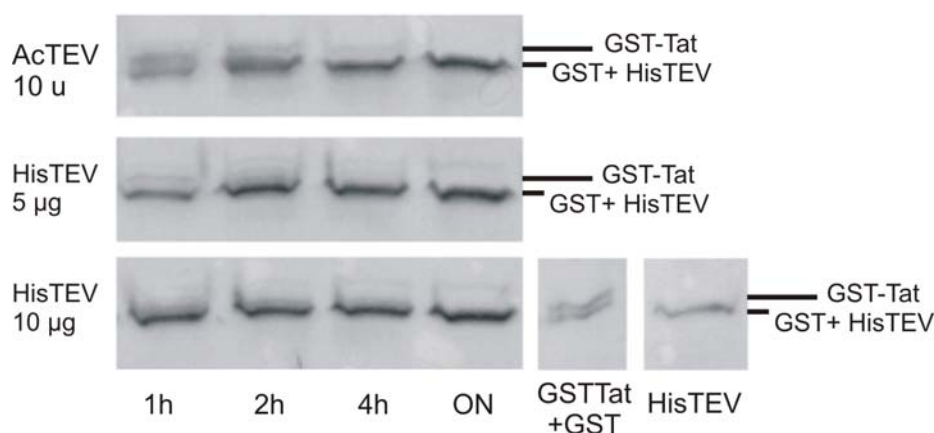


Figure 3-42 15% SDS-PAGE of cleavage of GST-Tat with commercially obtained TEV protease (AcTEV, invitrogen) and recombinantly expressed HisTEV (S219V) protease (HisTEV) (Coomassie Stain).

As AntP and Tat peptide make up for only 6% and respectively 4% of the mass of the fusion protein, the cleavage experiments were repeated with 300 µg and 400 µg of GST-AntP and GST-Tat, respectively, to provide peptide amounts visible in SDS-PAGE. If all fusion protein was cleaved, 18 µg of either peptide were to be obtained. As before, the cleavage experiment was carried out with 10 u of AcTEV or 10 µg of HisTEV (S219V) in TEV buffer supplemented with DTT 150 µl. According to the manufacturer's information, 1 u of AcTEV cleaves 3 µg of protein in 1h at 30°C, so that incubation over night should lead to a complete cleavage of the applied fusionprotein. No peptide could be seen when 20µl samples were analyzed by 15% SDS-PAGE (data not shown).

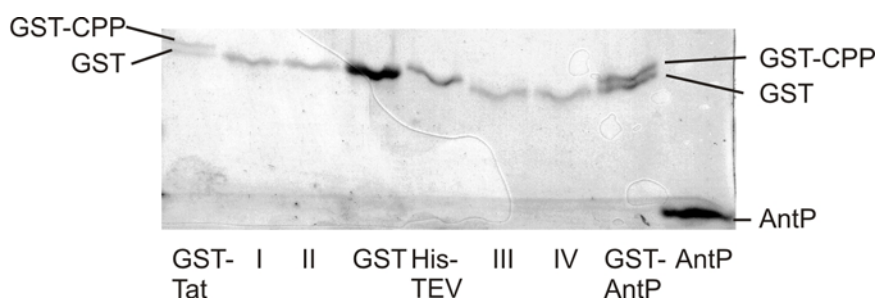


Figure 3-43 15% SDS-PAGE of over night cleavage reaction with GST-Tat and GST-AntP. The non-incubated GST-CPPs, GST, HisTEV (S219V) and Penetratin™ (AntP) are used as standards. Reaction mixtures: I = 400 µg GST-Tat + 10 u AcTEV, II = 400 µg GST-Tat + 10 µg HisTEV (S219V), III = 300 µg GST-AntP + 10u AcTEV, IV = 300 µg GST-Tat + 10 µg HisTEV (S219V). Equal amounts of the four reaction mixtures were loaded onto the gel. No GST-CPP bands can be discerned in any of the samples after incubation at 30°C overnight (Coomassie Stain).

However, analysis of 1 µl with references of untreated GST-CPPs, GST and HisTEV revealed that the band corresponding to the GST-CPPs could not be detected for any of the

over night reactions. This shows that 1 u of commercially obtained AcTEV and 1 µg of recombinantly generated HisTEV (S219V) are able to cleave up to 400 µg of GST-CPP at 30°C over night.

The obtained amounts of peptide may be too small to be detected by the Coomassie stain. They may be detected photometrically when purified from the reaction mixture by FPLC reversed phase chromatography. This would separate the peptides from GST, HisTEV, and, more importantly, from DTT, that is required in the reaction buffer, but would prevent the formation of disulfide bonds.

3.5 Novel cell-penetrating molecules for the delivery of siRNAs

It could be shown that cell-penetrating peptides bear a high potential to deliver siRNAs *in vivo*. However, as already described, many protein transduction domains used as CPPs do not fulfil any known function *in vivo* and it is thought, that they have not been optimized by evolutionary processes. This opens up the possibility of improving the cell-penetrating function of these molecules by varying the amino acid sequence. Synthetic peptides with enhanced cell-delivery properties have already been synthesized (Emi et al. 1997; Hallbrink et al. 2001; Ho et al. 2001; Mi et al. 2000; Rothbard et al. 2000; Vives et al. 1994) and also the synthesis of peptide analogs that mimic CPP function has been described (Potocky et al. 2003; Raguse et al. 2002; Rueping et al. 2002; Rueping et al. 2004; Wender et al. 2000; Wender et al. 2002).

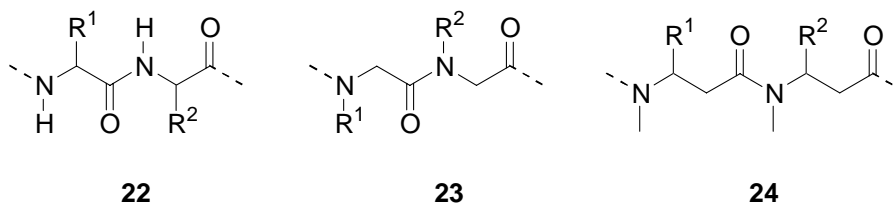
Peptide mimetics bear several advantages over CPPs. They are not degraded by proteases *in vivo*, so that they stay intact in the gastrointestinal tract or in the bloodstream, which improves the range of possible applications *in vivo*. Their toxicity and pharmacokinetic properties may be optimized by alterations of the molecular structure of potent candidates. Once the synthesis of effective structures has been established, it may be optimized toward ease of preparation and cost efficiency.

As many reports have pointed out a role for amphipathy and secondary structure in the cellular uptake process, synthetic CPP analogs ought to be designed as backbone mimetics that provide enhanced stability *in vivo* and a straightforward synthesis. A high density of positively charged side chains appears to be even more important for uptake efficiency. Therefore, backbone mimetics need to be functionalized with basic functionalities such as amine or guanidinium groups in order to exhibit cell-penetrating behavior.

β-peptides have been intensively studied (Rueping et al. 2004). With one methylene group inserted between the carboxyl group and the former α-carbon, these backbone analogs constitute the higher homologs of the α-peptides. They form stable helices that are structurally more confined than those formed by α-amino acids. They are also stable toward degradation by proteases, and their structures can be more readily predicted. It could be shown that β-peptides functionalized with guanidinium groups (in comparison to arginine) are able to translocate into the interior of cultured mammalian cells (Wender et al. 2000).

Likewise, oligo-N-alkylglycines, more commonly known as peptoids, have been subject to intensive studies (Figliozzi et al. 1996; Goff and Zuckermann 1992; Wender et al. 2000). As opposed to α-peptides, the side chains are attached to the amine, so that the monomers can be readily synthesized from functionalized diamines by reaction with 2-bromo-acetic acid.

Peptoids with guanidinium-headgroups attached to alkyl chains of varying lengths are taken up by mammalian cells (Wender et al. 2000). They have been successfully used to mimic peptide-hormones, antibiotics and receptor ligands (Uno et al. 1999).



Scheme 3-7 Representatives of peptides (**22**) and peptoids (**23**) and β -peptides (**24**).

In this work, two approaches toward small cell-penetrating molecules were followed up in collaboration with Tina Schröder and Yvonne Schmidt (Schmidt; Schroeder 2004)

- the use of unbranched oligoamines of varying length to transport reporter molecules into cells and
- the development of peptoids of varying chain length and side chain composition to mimic CPP function.

3.5.1 Preliminary tests of polyamines

It is well known that high densities of positive charges are essential for delivery molecules. Aliphatic polyamines appear to be suitable as backbones for polycationic structures, since they are positively charged at physiological conditions. As players in several biochemical pathways, such as signaling and protein biosynthesis (Igarashi and Kashiwagi 2000), they naturally occur in cells at millimolar concentrations, so that they are not expected to exhibit toxic side effects at the micromolar range that is reached in uptake experiments.

In preliminary experiments, the cell-uptake or delivery properties of naturally occurring oligoamines and long synthetic polyamines was assessed. Propylamine, ethylenediamine, spermine and a mixture of synthetic polyamines (Lupasol) were coupled with rhodamine 100 isothiocyanate to yield N-terminally labeled compounds (see Figure 3-44a). HeLa cells and primary fibroblasts were treated with the crude products at different concentrations (0.5, 1, 3, and 6 μ M) for different times (5, 10, 15, 30, and 60 min). The cells were washed, fixed with methanol/acetone, and immediately examined by fluorescence microscopy. Ethylenediamine and propylamine did not enter into the cells. Spermine and polyamine were found to attach to the plasma membrane and enter the cytosol after 5-15 min of incubation. Incubation times of 30 min and one hour lead to an accumulation of the fluorescent compound in the nucleus of the cells. This demonstrates the potential of the utilized backbones to enter into mammalian cells when attached to a cargo.

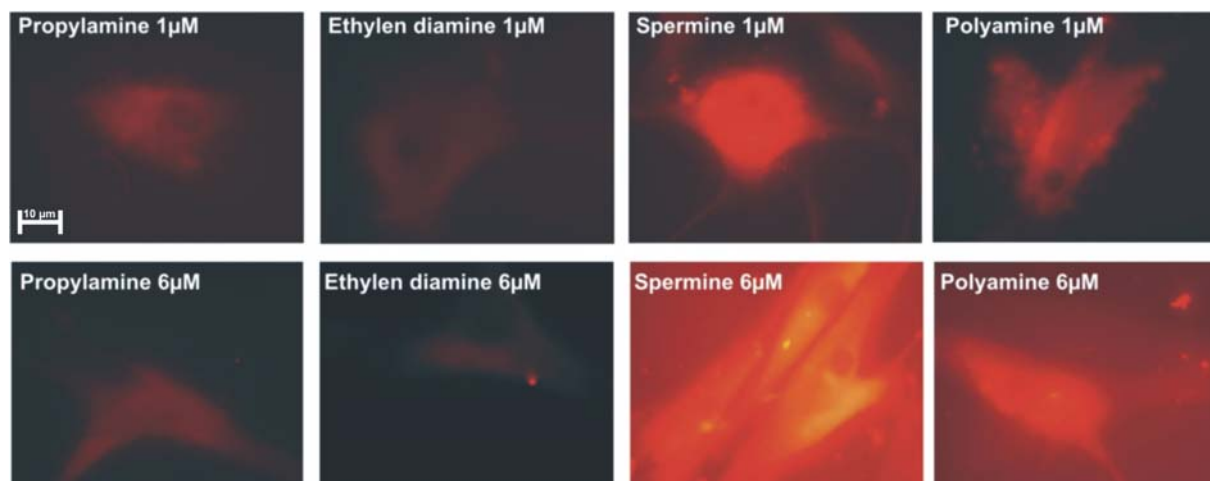


Figure 3-44 Fluorescence micrographs of preliminary tests of rhodamine-labeled oligoamines for their uptake by HeLa cells. After one hour of incubation with the labeled propylamine and ethylenediamine, the cells are only weakly stained, while cells treated with labeled spermine and polyamine exhibit a much stronger staining. Interestingly, the rhodamine-spermine conjugate accumulates in the nuclei, while the nucleus seems to be precluded to propylamine and ethylenediamine conjugates. (All pictures were taken with an exposure time of 16 seconds to obtain a sufficiently strong and comparable signal; Zeiss Axiovert 35, filter set 15: $\lambda_{excit.} = 546\text{nm}$, $\lambda_{em} > 590\text{nm}$, exposure time 16s).

3.5.2 Spermine-coupled porphyrin for photodynamic therapy

Based on these experiments, spermine appeared to be a promising candidate for the development of a new transporter. Over the last decade, the tetra-amine spermine has gained considerable importance for the delivery of DNA (Boletta et al. 1997; Kichler et al. 1997; Mack et al. 1994), RNA (Lu et al. 1994) and antisense oligonucleotides (Aoki et al. 1998; Guy-Caffey et al. 1995; Wong et al. 2002). Due to its four positive charges at neutral pH it forms non-covalent complexes with the negatively charged DNA (Symons 1995). Conjugates of spermine or spermidine with lipids as in dioctadecylaminoglycyl-spermine (DOGS, transfectam) are commonly used as a transfection agent (Boletta et al. 1997; Kichler et al. 1997; Mack et al. 1994) and likewise, spermine conjugates with cholesterol enhance the cellular uptake of oligonucleotides (Guy-Caffey et al. 1995; Lee et al. 1996; Lee et al. 2004a). The relative non-toxicity of the polyamines toward mammalian cells is a great advantage over other cationic headgroups (Guy-Caffey et al. 1995).

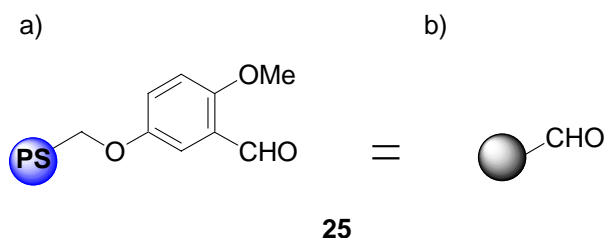
By covalent attachment of spermine, DNA cleaving agents such as acridine and iron chelators have been targeted to the DNA (Bergeron et al. 2003; Delcros et al. 2002). Finally, covalently coupled spermine was shown to enhance the activity of an RNA cleaving DNA enzyme and its affinity to the target RNA (Kubo et al. 2003).

For these reasons, novel transporters based on spermine were synthesized and coupled to a variety of cargo molecules such as the fluorescent dyes fluorescein and porphyrin. Porphyrin is of specific interest for the treatment of tumors. In photodynamic therapy (PDT), porphyrins are transferred into their excited triplet state upon irradiation with light. Upon relaxation to the ground state, the absorbed energy is transferred to oxygen, which is in turn excited to its singlet state. Singlet-oxygen is highly reactive leading to the oxidation of unsaturated lipids,

nucleobases, and aromatic amino acids. As porphyrin undergoes many rounds of excitation and relaxation, a large number of radical species is generated inducing severe damage in the affected cell that is killed in the process. To avoid damage to the entire organism, porphyrins need to be locally taken up by the tumor and kept from diffusing to healthy tissue. This can be achieved by enhancing the cellular uptake of porphyrins by covalent coupling to transport molecules such as spermine.

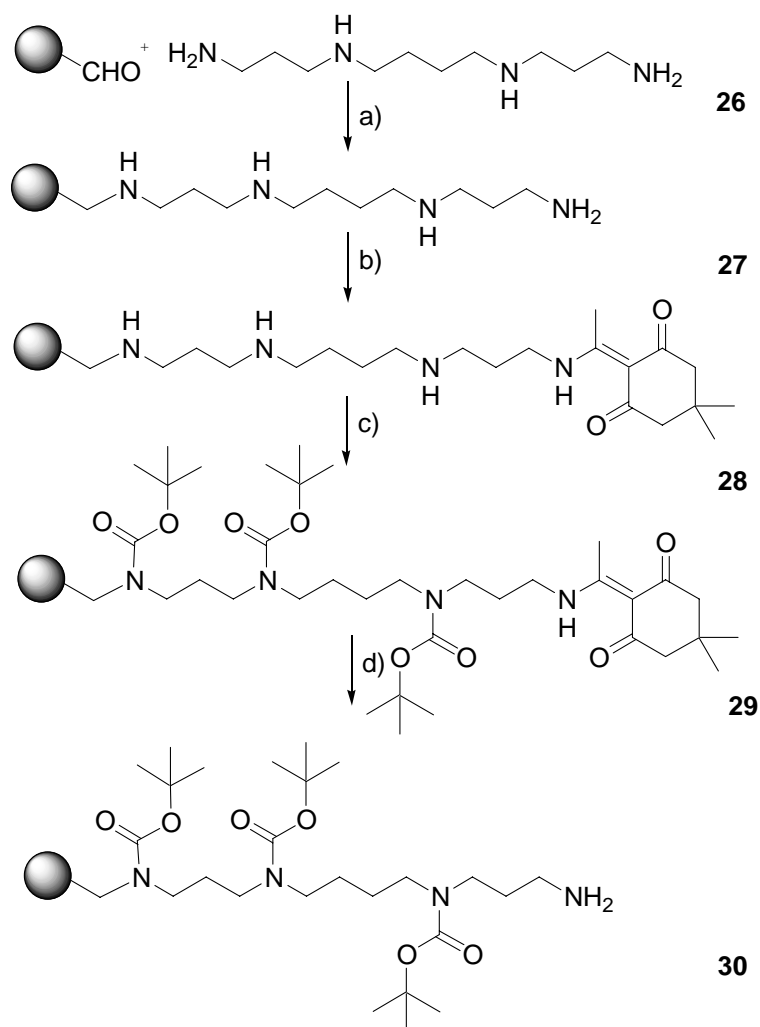
To this means, spermine was coupled to the solid phase and functionalized with either fluorescein as a probe to assess cellular uptake or with a hydrophobic porphyrin derivative with long aliphatic side chains upon its methylene groups. The syntheses as carried out by Y. Schmidt (Schmidt 2004) and F. Hahn (Hahn 2005) are briefly outlined in the following:

Spermine **26** was attached to 4-formyl-3-methoxy-phenoxyethyl-polystyrol (FMOP)-resin **25** by reductive amination, in which the resin's aldehyde function and the spermine's primary amines form an imine in the presence of trimethylorthoformate (TMOF). The Schiff base is in turn reduced with tetrabutylammoniumborohydride (TBAB) to yield a secondary amine.



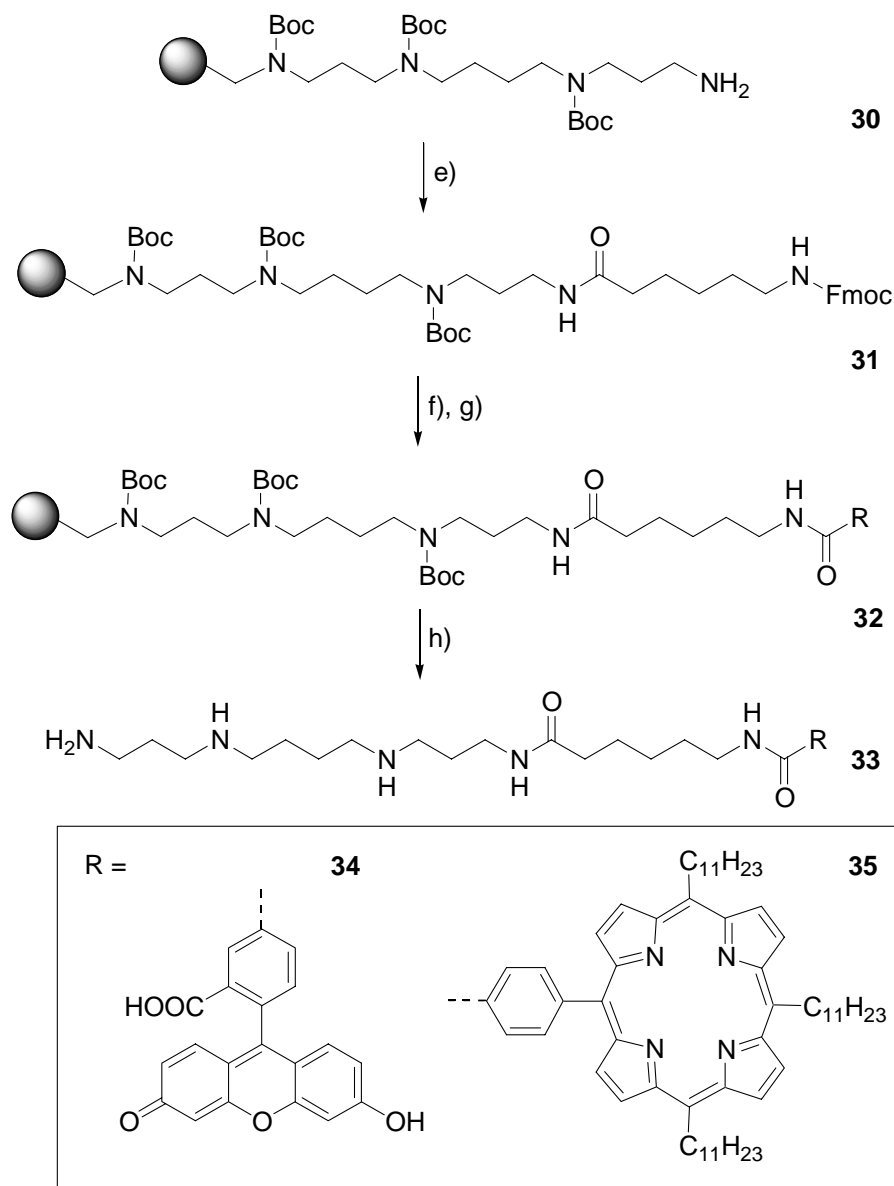
Scheme 3-8 a) FMOP resin consists of polystyrene (PS) beads functionalized with an aldehyde group that permits coupling of amines by reductive amination. Upon treatment with trifluoroacetic acid (TFA) the amine is released. The graphic representation of the resin is facilitated as shown in b).

To distinguish the free primary amine from the secondary amines the functionalization step the primary amine is protected with acetyldimedone (Dde-OH). The secondary amines are then protected with tert-butoxycarbonyl (Boc)-groups, that are not affected by the subsequent deprotection of the primary amine with 2% hydrazine hydrate. N-Fmoc-protected aminohexanoic acid was activated with PyBrOP and coupled to the free amino-terminus via a peptide bond as in solid phase peptide synthesis. This C6-spacer was meant to diminish interactions of spermine with the cargo molecule.



Scheme 3-9 Immobilization and protection of spermine. Spermine **26** is coupled to FMOP-resin by reductive amination (a). After selective protection of the primary amine with Dde (b), the secondary amines are protected with Boc-groups (c) and the orthogonal Dde-group is removed (d). Reaction conditions: (a) 1.) 5 eq spermine, DMF/TMOF (4:1) 17 h, RT 2.) 4 eq TBAB, 15 min, RT, 3.) glacial acetic acid, RT, 5h (b) 10 eq Dde-OH in DMF, 17h, RT (c) 10 eq di-tert-butyl-dicarboxylate in 1,4-dioxane, 20h, RT, argon (d) 2% hydrazine hydrate in DMF, 2x5 min, RT.

After removal of the Fmoc-protection group with piperidine, the cargo molecule, carboxyfluorescein **34** or carboxy-porphyrin **35** (Balaban et al. 2003), was attached to the free amine via an amide bond. Finally the conjugates were deprotected and cleaved of the solid phase by reaction with 50% trifluoroacetic acid (TFA) in one step.



Scheme 3-10 Synthesis of fluorescein **34** and porphyrin **35** conjugated to spermine. *N*-Fmoc-aminohexanoic acid is attached as a linker (e), deprotected (f) and in turn linked to the carboxyfluorescein or carboxyporphyrin (g). Deprotection of the secondary amines and cleavage from the solid phase occur simultaneously to yield functionalized spermine **33** (h). Reaction conditions: (e) 3 eq *N*-Fmoc-aminohexanoic acid, 2 eq PyBrOP, 5 eq DIPEA in CHCl_3 , 20h, RT (f) 20% piperidine in DMF, 3x2 min, RT (g) 3 eq carboxyfluorescein, 3 eq HOBt, 3 eq DIC, $\text{CH}_2\text{Cl}_2/\text{DMP}$ (1:1, (v/v)), 5d, RT (h) 50% TFA in CH_2Cl_2 2 min, RT.

The uptake behavior of porphyrin-labeled spermine (PorSp) was examined in HeLa cells, primary fibroblasts and COS cells. For preliminary uptake experiments the compounds were thoroughly dried, characterized by mass spectrometry and used without further purification. The preparation of stock solution with PorSp and free carboxy-porphyrin revealed that the spermine modification greatly enhances the compound's solubility. The precursor-porphyrin is insoluble in water and only poorly soluble in methanol. Upon sonication in methanol a saturated solution of 840 μM could be obtained. The spermine-porphyrin conjugate exhibited

a markedly higher solubility in both water and methanol. A 20 mM stock solution in methanol could be easily prepared.

Preliminary uptake experiments were performed in HeLa cells, human primary fibroblasts and COS7 cells at 0.1, 1, 10, 50 and 100 μM . After 4 hours the cells were thoroughly washed as described in the CPP section and evaluated by transmission and fluorescence microscopy without any fixation to avoid artifacts due to membrane perforation and diffusion or simple adsorption to the membrane.

At the highest concentration, severe toxic effects were observed for all cell types (Figure 3-45). In comparison with the untreated controls, about 5-15% of the cells remained attached to the culture dish exhibiting signs of necrosis. However, a large portion of these cells was fluorescent with the internalized compound.

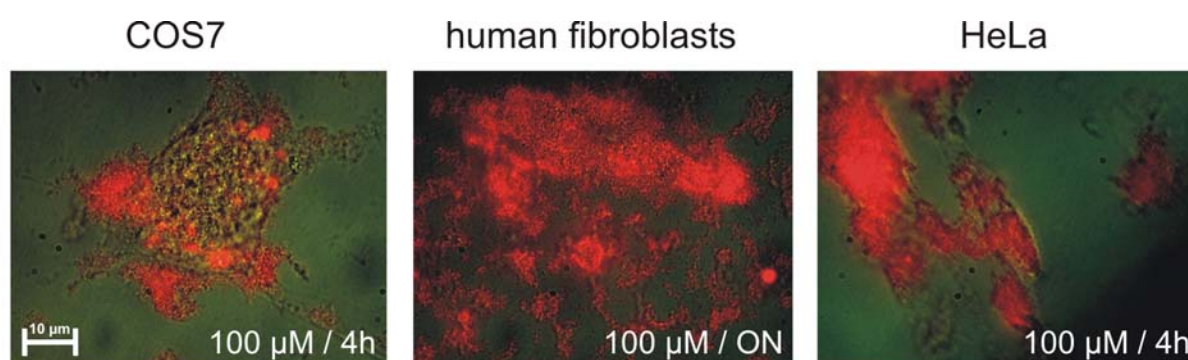


Figure 3-45 Phototoxicity of porphyrins. If cells are illuminated after treatment with high doses of spermine-coupled porphyrin, the majority of cells is killed. Fragments of cells treated with 100 μM of the compounds show intense red fluorescence from the associated porphyrin. (Zeiss Axiovert 35, filter set 15: $\lambda_{\text{excit.}} = 546\text{nm}$, $\lambda_{\text{em}} >590\text{nm}$; exposure time: 7s)

To test whether the toxicity at high concentrations could be attributed to photochemical reactions induced by the porphyrin moiety, the experiment was repeated in the dark, which led to an increase of the cell viability to 70-80%.

As opposed to the unmodified compound that could not be detected inside the cells the PorSp exhibited a cellular uptake to a certain extent. A further confocal fluorescent microscopic analysis is underway to clearly localize the compound to the cell's interior. At a concentration of 10 μM all cells were stained after 4h. The porphyrin fluorescence was restricted to vesicular structures, endosomes or lysosomes that appeared to accumulate in the perinuclear region. Remarkably, fluorescent staining could also be observed on the cell surface resembling PorSp molecules clustered in highly restricted regions of the cellular membrane or attached to surface molecules.

After incubation over night, fluorescence could also be seen in the cytosol. After long incubation times, cellular uptake could even be observed for concentrations as low as 100nM in almost all cells which would imply a slow uptake of the material from the loosely attached compound on the plasma membrane. No reliable signs for uptake could be detected at lower concentrations. However, punctuated fluorescent staining could be detected on the surface

of fibroblasts incubated with as little as 10 nM. Possibly, the fluorescence intensity of the porphyrin is not sufficient to be detected in low concentrations.

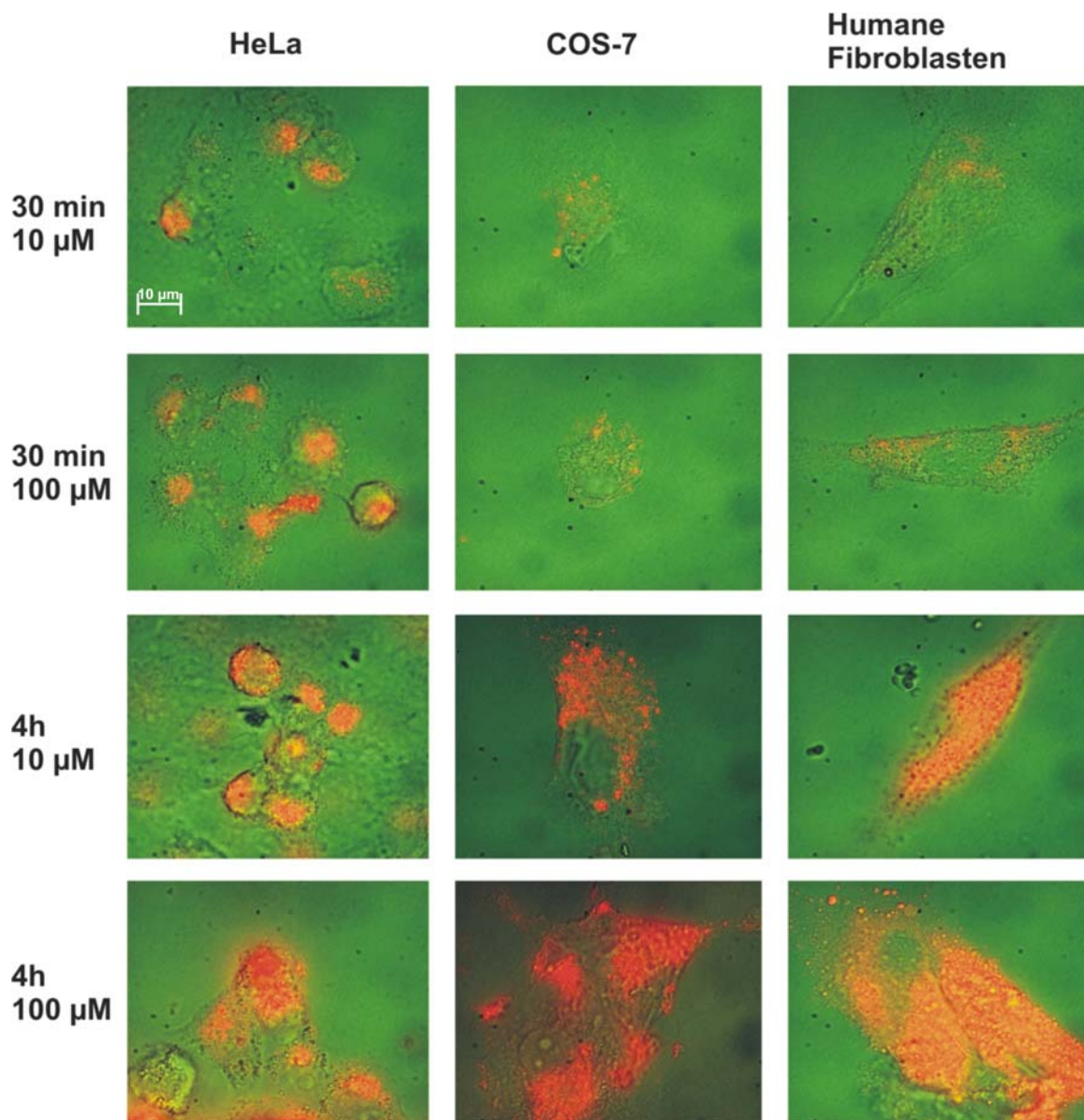


Figure 3-46 Treatment of COS-7, HeLa cells and human fibroblasts with spermine-coupled porphyrin. After 30 min incubation with 10µM, the compound is taken up into vesicular structures that accumulate in the perinuclear region. After incubation for 30 min with 100µM, more fluorescence is detected in a similar pattern. After 4h the intensity of fluorescence inside the cells increases and diffuse fluorescence is observed throughout the cells, while the nuclei are precluded (Zeiss Axiovert 35, filter set 15: $\lambda_{excit.} = 546nm$, $\lambda_{em} >590nm$; exposure time: 7s).

For the control experiments with unmodified porphyrin the highest concentration tested was 42 µM implying a methanol concentration of 5% in the medium. After 4 hours weak fluorescence could be detected inside all tested cells. Almost no Porphyrin was detected in the cells.

This demonstrates that a simple spermine modification on an otherwise poorly soluble porphyrin greatly enhances its solubility in both water and methanol and increases its cellular uptake.

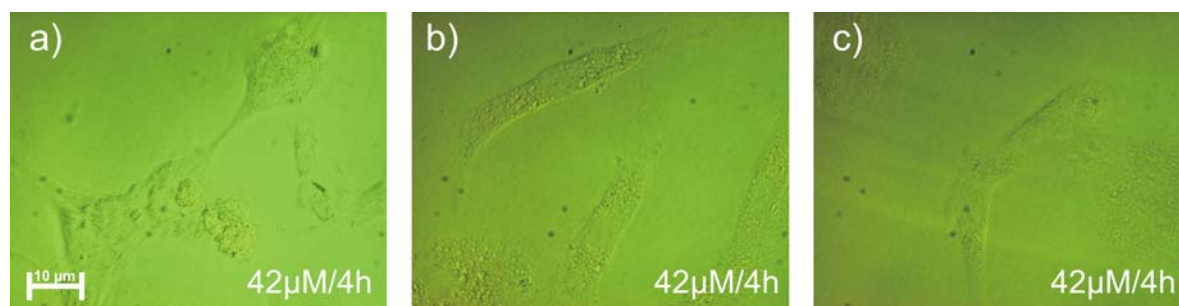


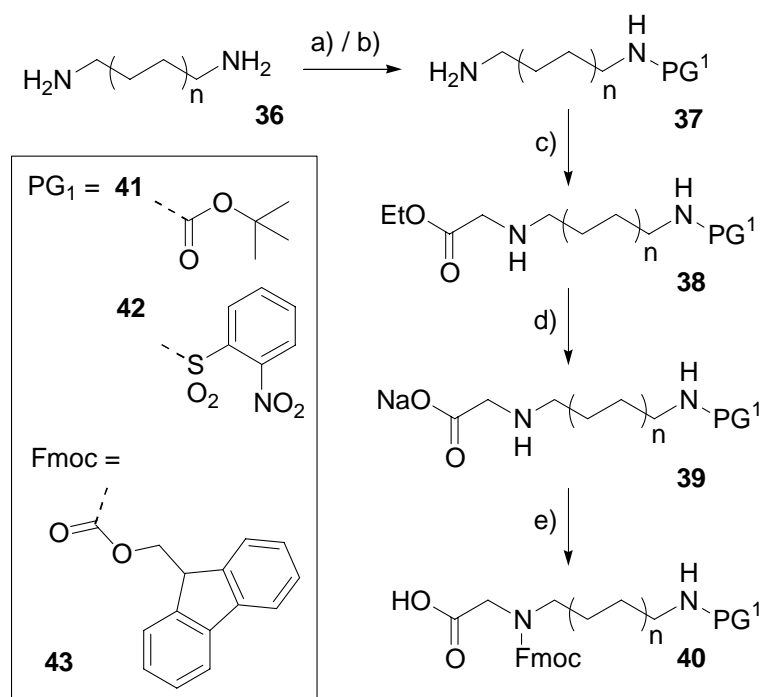
Figure 3-47 Control experiment. Unmodified porphyrin in a concentration of 42 μM is taken up by COS-7 (a), HeLa cells (b), and fibroblasts (c), but with a much lower efficiency than the spermine modified compound (Zeiss Axiovert 35, filter set 15: $\lambda_{\text{excit.}} = 546\text{nm}$, $\lambda_{\text{em}} > 590\text{nm}$; exposure time: 7s).

The observed fluorescence patterns and the long times required for uptake suggest that PorSp is taken up by an endocytosis-like mechanism followed by endosomal escape, which is indicated by an increased cytosolic staining after long incubation times. Once taken up into the cells, the porphyrin exhibits its phototoxic effects. During the treatment with high concentrations (50, 100 μM), daylight is sufficient to kill the majority of the cells within 30 min. However the concentration of the compounds to kill the cells is still in the μM range. The spermine-porphyrin solution used in these preliminary experiments was used from solid phase synthesis and was not further purified and contained a mixture of conjugates with and without aminohexanoic acid. The dosage experiments have to be refined by using a single species of the conjugates since one of the conjugates might be more active than the other.

3.5.3 Solid phase synthesis of peptoid transporters

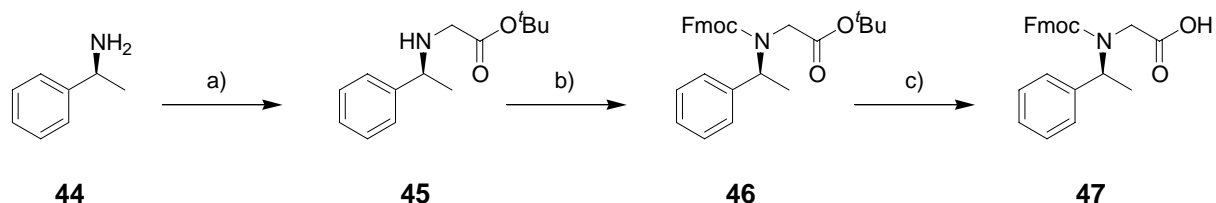
In the peptoid approach, a polyamide backbone with amino-functionalized side chains was synthesized. Different side chain lengths and peptoids built from varying numbers of monomers have been tested in cell culture. The patterns of alternating side chain lengths had to be assayed on their effect on uptake efficiency. The syntheses that were carried out in collaboration with the Bräse group by T. Schröder (Schroeder 2004), are briefly outlined:

Monomeric building blocks were built up from diamines **36** ($n = 1,2,3$) of varying lengths (C4, C6 and C8, respectively). After protecting one amino group with the *tert*-butyloxycarbonyl (Boc, **41**) group or 2-nitrophenylsulfonyl (*o*-Nosyl, **42**), respectively, to permit orthogonal deprotection of the side chains, the mono-protected diamines **37** were reacted with bromoacetic acid ethylester and the resulting amino acetic acid esters **38** were hydrolyzed with sodium hydroxide. The secondary amines were finally protected with 9-fluorenylmethoxycarbonyl to yield ready-to-use **39** as building blocks for solid phase synthesis.



Scheme 3-11 Synthesis of monomeric building blocks **40** ($n=1,2,3$) for peptoid synthesis. Diamines of varying lengths **36** ($n = 1-3$) are protected with Boc (a) or *o*-Nosyl at one side (b), reacted with bromoacetic acid ethylester (c), hydrolyzed (d) and protected with Fmoc **43** (e). Reaction conditions: (a) 0.13 eq Boc_2O , dioxan, RT, under argon, 22.5 h, (b) 0.13 eq *o*-nosyl-chloride, dioxane, RT, under argon, 22.5 h, (c) 1 eq bromoacetic acid ethylester, THF, RT, 16 h, (d) 4N NaOH, MeOH, MeCN, RT, 30 min, (e) 1 eq 9-fluorenylmethylsuccinidylcarbonate, $\text{H}_2\text{O}/\text{MeCN}$ (1:1), RT, 30 min.

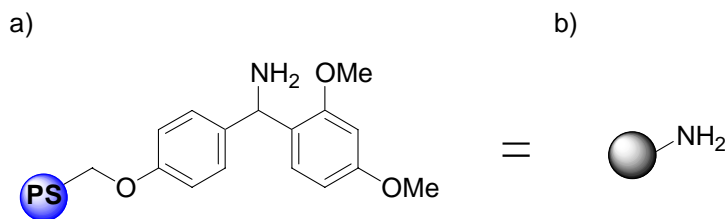
An additional chiral building block **47** was provided by F. Lauterwasser, University of Karlsruhe (TH) (Lauterwasser 2004). Instead of a protected amino side chain it contains an aromatic ring derived from *S*-1-phenylethylamine that is reacted with bromoacetic acid ester, hydrolyzed and protected with Fmoc to yield a chiral monomer to impose steric restrictions upon the conformation of the assembled peptoid.



Scheme 3-12 Chiral building block **47** derived from *S*-1-phenylethylamine **44** in a 3-step synthesis as kindly provided by S. Bräse, F. Lauterwasser, Karlsruhe. Reaction conditions: (a) bromoacetic acid butylester, KI, K_2CO_3 , DMF, (b) 9-fluorenylmethylsuccinidylcarbonate, THF, $0^\circ\text{C} - \text{RT}$, 12h, (c) HCl/ H_2O , reflux, 2h.

Peptoid transporters were synthesized on solid phase using Fmoc-chemistry. Solid phase synthesis greatly facilitates the synthesis as the growing oligomer attached to a solid support can be easily purified from excess reactants by washing the resin with the appropriate solvents and filtration. The protection of free amino groups with Fmoc as a temporary protection group has been well established as it can be quantitatively removed under mild

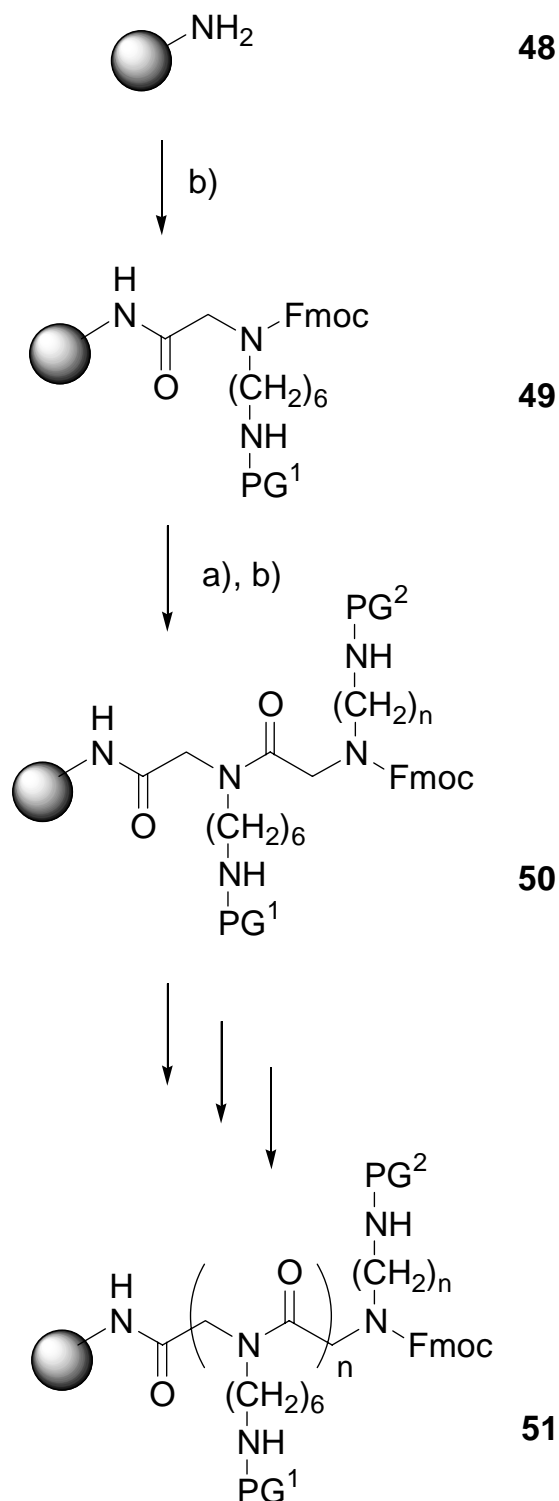
conditions in a short time. Rink resin (see Scheme 3-13) was chosen as a solid support due to its stability at ambient conditions, ease of the first coupling step, and mild cleavage conditions.



48

Scheme 3-13 a) Rink amide resin **48** consists of polystyrene (PS) beads functionalized with an amide group that permits coupling of activated carbon acids by the formation of peptide bonds. The chemical environment further facilitates cleavage by trifluoroacetic acid (TFA). The graphic representation of the resin is shown in b)

After removal of the Fmoc group that protects the amino-functionalized resin, an activated, Fmoc-protected monomer was coupled to the solid support via a peptide bond. In this reaction, bromo-tris(pyrrolidino)phosphonium-hexafluoro-phosphate (PyBrOP) was used to generate an activated ester, and *N,N*-diisopropylethylamine (DIPEA) to enhance the rate of ester formation. The Fmoc-group is removed with piperidine to prepare the coupled monomer for the attachment of the next building block. Coupling of the monomers to the growing peptoid chain proceeds under the same conditions as the attachment of the first building block to the solid support. All reaction steps are followed by repetitive washing steps ending with a solvent, in which the resin is expanded to expose the reactive sites to the next reagents. The cycles of coupling and deprotection were repeated until a peptoid of desired length had been obtained. The procedure is outlined in Scheme 3-14.

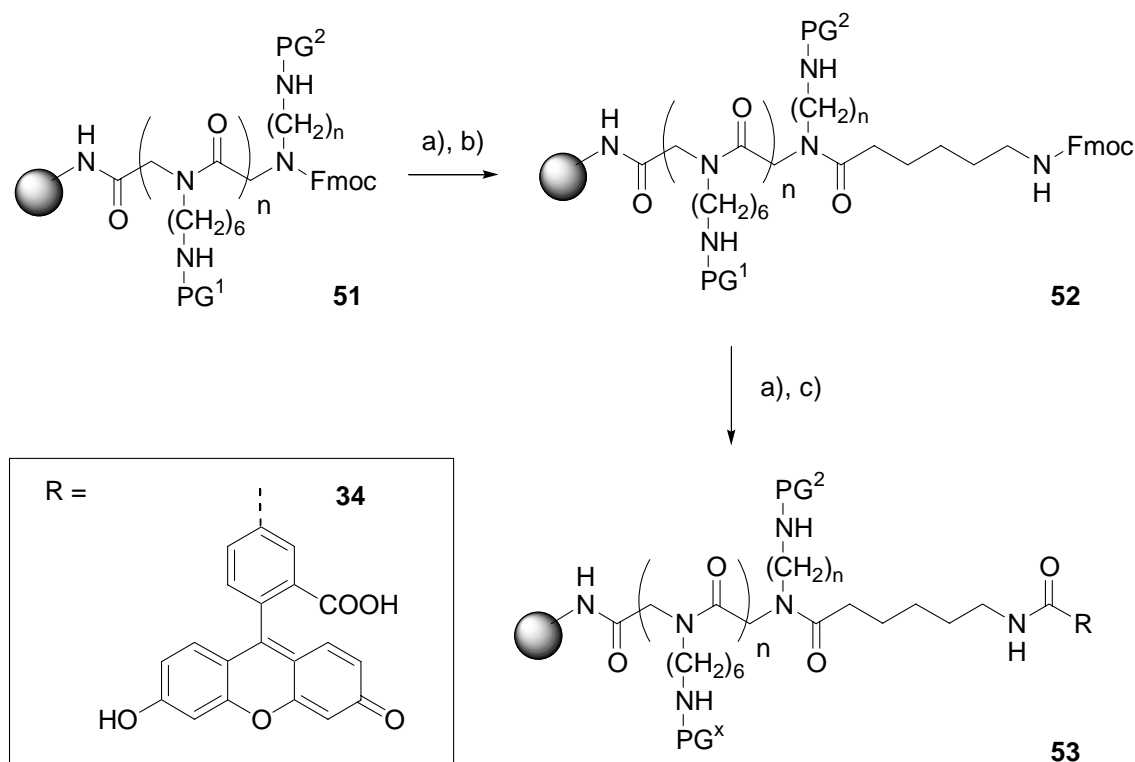


Scheme 3-14 Solid phase synthesis of peptoids: After deprotection of the resin, the first monomer is coupled via a peptide bond. The Fmoc-group protecting the amino terminus is removed and the following building blocks attached under the same conditions. Reaction conditions a) 20% pyridine in DMF, 3x 2min; b) 2 eq monomer, 2 eq PyBrOP, 4 eq DIPEA in CH_2Cl_2 , RT, 24h.

A reporter group was required to monitor the cellular uptake of the different peptoids under the microscope. 5(6)-Carboxyfluorescein **34** ($\lambda_{\text{abs}} = 492 \text{ nm}$, $\lambda_{\text{em}} = 517 \text{ nm}$) was coupled to the transport molecules prior to cleavage from the solid phase. 6-Aminohexanoic acid was used as a linker to prevent interactions of the reporter molecule with the peptoid moiety. As outlined in Scheme 3-15, the Fmoc-protected linker molecule was attached to the amino termini of the peptoids under standard coupling conditions **52** and the protection group was removed with piperidine to yield **53**. 5(6)-Carboxyfluorescein could form a peptide bond via its carboxy group under mild coupling conditions with no detectable side reactions. In this reaction step 1-hydroxybenzotriazole (HOBt) and diisopropylcarbodiimide (DIC) were used to activate the carboxyl function.

In the final step, the labeled peptoids **53** were cleaved from the solid phase and the Boc-protection groups were simultaneously removed by treatment with trifluoroacetic acid (TFA) supplemented with 5% triisopropyl silane (TIS). Peptoids

containing the *o*-Nosyl-protection group had to be deprotected by treatment with 2-mercaptoethanol and DBU prior to cleavage from the solid supports. The free peptoids were precipitated with diethylether and characterized by mass spectroscopy.



Scheme 3-15 Attachment of fluorescein **34** as a reporter molecule. Fmoc-6-aminohexanoic acid was coupled to the peptoids **51** under standard conditions and 5(6)-carboxyfluorescein was attached via a peptide bond **53**. Reaction conditions: a) 20% pyridine in DMF, 3x 2min; b) 2 eq Fmoc-aminohexanoic acid, 2 eq PyBrOP, 4 eq DIPEA in CH_2Cl_2 , RT, 24h, c) 3 eq 5(6)-carboxyfluorescein, 3 eq HOBt, 3 eq DIC in DMF/ CH_2Cl_2 (1:1), RT, 5h.

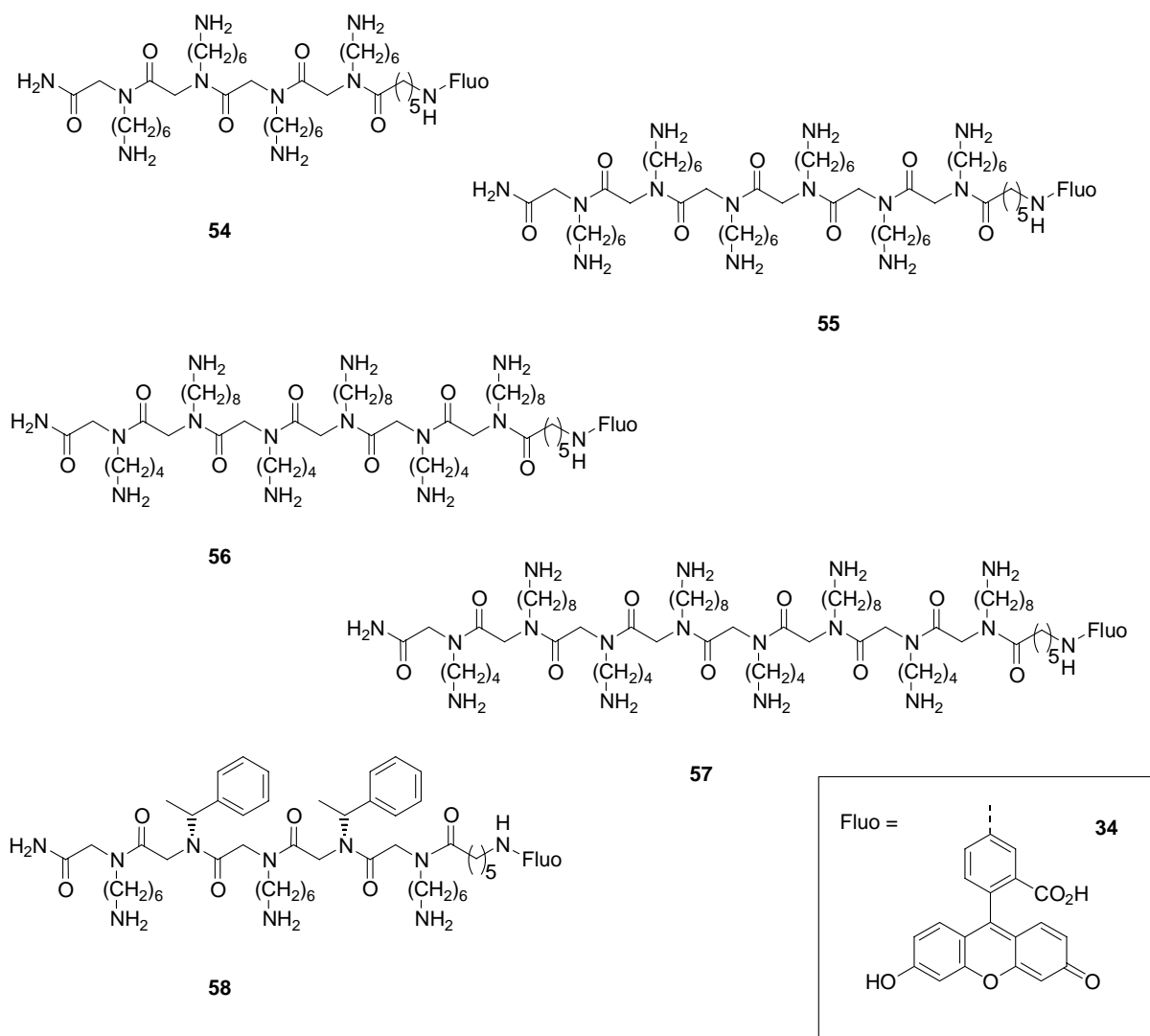
Five different peptoid transporters of varying lengths and side chain compositions were synthesized as depicted in Scheme 3-16. Peptoid **54** comprised four monomers with C6 side chains (**40** ($n=2$)) of which the carboxy-terminal pair was protected with o-Nosyl and the amino-terminal pair with Boc. Peptoid **55** was assembled likewise with two additional Boc-protected C6-building blocks attached to its amino terminus. Peptoids **56** and **57** consisted of 6, respectively 8 building blocks with alternating Boc-protected C4- (**40** ($n=1$)) and C8-side (**40** ($n=3$)) chains starting with a C4-side chain at the N-terminus.

Peptoid **58** was synthesized as a pentamer starting from the N-terminus with an o-Nosyl-protected C6-monomer **40** ($n=2$) followed by an alternating sequence of two chiral building blocks **47** and two Boc-protected C6-monomers **40** ($n=2$) (see Scheme 3-16).

3.5.4 Cellular uptake of fluorescein-labeled peptoids

The fluorescein-labeled peptoids obtained by solid phase synthesis (as provided by T. Schröder) were tested in cultured mammalian cells upon their potential to act as molecular transporters. The minimal concentrations required for visible uptake and the maximum non-toxic concentrations were to be estimated. Fluorescence microscopy (Zeiss, Axiovert 200, $\lambda_{\text{excit}} = 490\text{-}520$ nm, $\lambda_{\text{em}} = 517$ nm) provided a means to assess the mode of uptake and to recognize the intracellular localization of the internalized compounds.

The peptoids were tested on human and simian cancer cell lines (HeLa and COS7, respectively), as well as on human primary fibroblasts (91/21). At the beginning of the cell experiments, the appropriate treatment conditions had to be estimated. Serum free medium was tested versus serum containing medium as many transfection reagents had been shown to be sensitive to serum due to interaction with proteins or nucleic acids and other compounds contained in the serum. On the other hand, the cells might suffer from lack of serum for prolonged times.



Scheme 3-16 Fluorescein-labeled peptoids **54-58** after deprotection and cleavage from the solid phase. Cleavage from the Rink-resin leads to a C-terminal amide functionality.

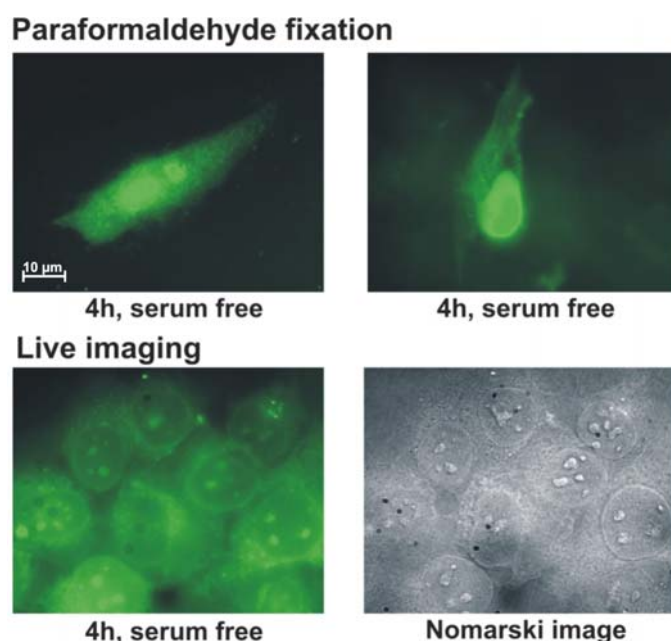
With reference to the recent findings that fixation procedures lead to an artifactual uptake (Lundberg et al. 2002; Potocky et al. 2003; Richard et al. 2003), cells were prepared for microscopy either with the standard paraformaldehyde fixation protocol or without fixation by simple washing and attaching the cover slips to the microscopy slides in isotonic solution. The cell morphology under both conditions was compared.

For preliminary tests, the peptoids were thoroughly dried, assessed by mass spectroscopy and applied without further purification. All experiments with the fluorescein-labeled compound were carried out in the dark to avoid photo-bleaching of the light-sensitive probe molecule.

Tetrapeptoid **54** was dissolved in PBS to yield a 10 mM stock solution, which was further diluted with serum-containing (+FCS) or serum free (-FCS) culture medium to final concentrations of 5, 10, 50, 100, 500 nM and 1 μ M, respectively. Uncoupled carboxyfluorescein was used as a control.

The cells were grown on 24-well plates on cover slips (\varnothing 13 mm) coated with fetal calf serum (FCS) to 10-20% confluency. After removal of the culture medium, the individual 24-wells were filled with half of the final volume of medium +FCS or -FCS and a doubly concentrated peptoid solution was added dropwise while constantly rocking of the culture dish to ensure a homogenous distribution of the compound. After 5, 20, 60 or 120 min of incubation at 37°C, the peptoid-containing medium was removed and the cells prepared for fluorescence microscopy.

No signal could be detected at concentrations below 1 μ M, which could be attributed to the weak intensity of fluorescein fluorescence or to the small amounts taken up by the cells. Therefore, subsequent experiments were carried out at 20, 50 and 100 μ M as described for the related peptoid in a similar study (Peretto et al. 2003). These dosages appear to be very high especially since it is known that cationic amphiphiles are mainly stored in the lysosomes eventually leading to the disruption of the latter.



Scheme 3-17 PFA fixation leads to an artifactual redistribution of peptoids in the interior of the cells. While in PFA-treated cells fluorescence is localized to vesicular structures and the nucleus, which corresponds to an artifactual distribution, aggregation in proximity to the unstained nucleus, cytosolic staining and nuclear uptake with accumulation in the nucleoli are observed for fixed cells (Zeiss Axiovert 35, filter set 17: $\lambda_{excit.} = 485\text{nm}$, $\lambda_{em} = 515\text{-}565\text{nm}$; exposure time: 10s).

It can be assumed that in agreement with other cationic amphiphiles the peptoids as well as the polyamines or the CPPs tested in the previous sections are protonated when they reach the acid lysosom (pH 4.5). There they will interact with any kind of negatively charged lipids and might aggregate while slowly getting released into the cytosol. Since the compounds tested in these experiment are still crude after the cleavage from the resin and comprise a mixture of labeled and unlabeled peptoids the dosages have to be refined with further purified peptoids. A new synthesis of peptoids is still ongoing and the experiments will be repeated with purified peptoids and analyzed by confocal microscopy to determine the uptake kinetics.

Cells fixed with paraformaldehyde (PFA) actually showed a different intracellular distribution than the living cells. The latter show a characteristic pattern of vesicular structures that appear to aggregate around the nucleus, which is devoid of fluorescence. Fixed cells, on the contrary, exhibit cytosolic and nuclear staining with remarkably less vesicular structures, which confirms the reports of artifacts caused by fixation procedures that rupture membranes and permit diffusion of charged molecules to oppositely charged cellular components. Living cells prepared on ice exhibit a clear morphology for about 2h even at room temperature. After longer intervals, the morphological changes have to be attributed to the effects of the anti-bleach and starvation of the cells.

In control experiments with hexameric **55**, prolonged incubation in –FCS medium led to significant changes in cell morphology and cell death as depicted by Figure 3-48. Compared to the +FCS group, absence of serum did not result in an increase of uptake for any of the tested concentrations or incubation times. Therefore, subsequent tests were carried out in serum-containing medium.

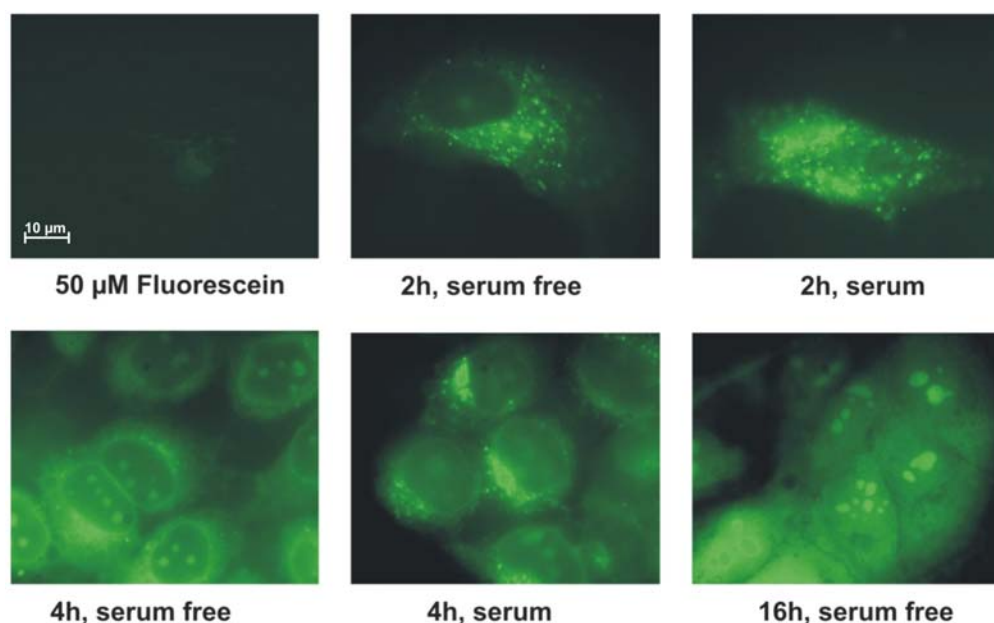


Figure 3-48 Depletion of serum leads to changes in cell morphology after 2 h of incubation. COS7 cells incubated for 2h and 4h in –FCS (a) and +FCS (b) treated with 50 μ M of tetrapeptoid **54** are shown. (Zeiss Axiovert 35, filter set 17: $\lambda_{excit.} = 485nm$, $\lambda_{em} = 515-565nm$; exposure time: 10s).

The vesicular structures observed in the preliminary experiment indicate an endocytosis-like mechanism for the uptake of the peptoids. Therefore, the experiment was repeated with incubation times of 4 and 16h, respectively to monitor the fate of the vesicular structures and whether the fluorescent peptoids are able to escape to the cytosol. The cell treatment with peptoid medium could be facilitated toward direct application of the medium without rocking of the culture plate. To avoid the strong background fluorescence observed at high peptoid concentrations, additional washing steps with 0.2% BSA solution in PBS+ were included into the preparation protocol as described for the CPPs and the spermine-coupled porphyrin. Under the given conditions, uncoupled carboxyfluorescein is not taken up by the cells even if incubated over night (16h, Figure 3-49).

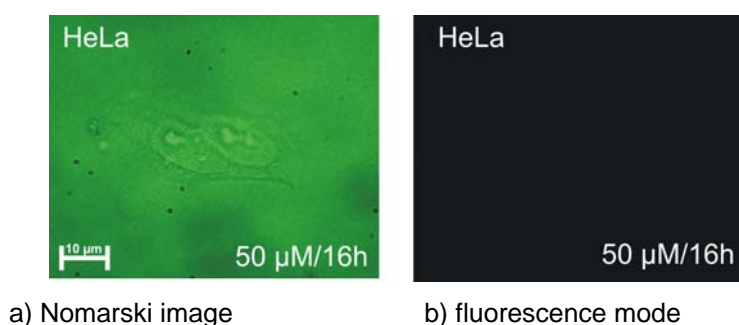


Figure 3-49 Uncoupled carboxyfluorescein is not taken up by mammalian cells after 16h of incubation at 37°C. The picture was taken in transmission (a) and fluorescence mode (b) to illustrate the outline of the cell. (Zeiss Axiovert 35, filter set 17: $\lambda_{excit.} = 485nm$, $\lambda_{em} = 515-565nm$; exposure time: 10s).

In further experiments, it was shown that the other fluorescein-labeled peptoids **56**, **57**, and **58** were taken up by all cell types. Comparison of images taken in the fluorescence mode with the same pictures taken in the transmission mode revealed that the compounds had entered the interior of all cells.

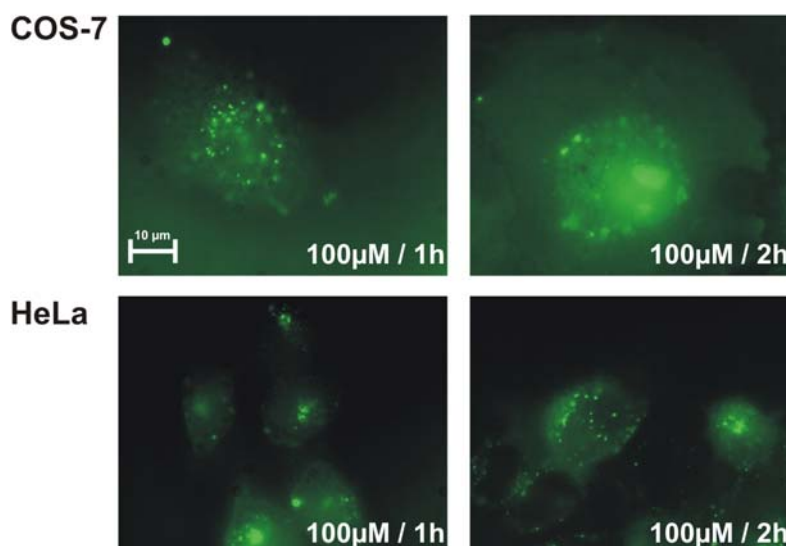


Figure 3-50 Treatment of COS-7 and HeLa cells with 100 μM of the tetrameric peptoid **54** coupled to fluorescein. Vesicular structures accumulated in the perinuclear region and a diffuse fluorescence in the cytosol can be seen after one hour. Two hours after treatment, the fluorescence-labeled compound starts to enter the nucleoli of both cell types and is found in the nucleus of COS-7 cells. (Zeiss Axiovert 35, filter set 17: $\lambda_{excit.} = 485nm$, $\lambda_{em} = 515-565nm$; exposure time: 10s).

At the applied concentrations of 20 to 100 μM , intracellular fluorescence was clearly discernible. At 20 μM the signal was weaker and at lower concentrations the fluorescein labels could be only recognized at longer exposure times. For HeLa and COS7 cells internalization at 100 μM was detectable after 1-2h. At these shorter times, punctate fluorescence could be seen on the plasma membrane, while the center of the cells exhibited diffuse fluorescence.

Vesicular structures throughout the cell and accumulated in the perinuclear region were observed in all experiments. After incubation over night, staining of the nucleoli was visible and the fluorescence of the interior of the cells was markedly increased. Thus it was assumed that the labeled molecules had escaped from the vesicles into the cytosol. Whether this is due to the active or vesicle mediated transport mechanisms or to rupture of the lysosomal compartment remains to be analyzed. This assumption was supported by different forms of nuclear staining observed for different compounds in different cell lines. Experiments using confocal microscopy are required to decide how much of the compounds enters the cytosol or whether the diffuse staining originates from compounds evenly distributed on the plasma membrane. The use of lysosomal markers, would help to decide whether the components are entrapped in lysosomes or another species of transport vesicle.

Those studies have been performed on other peptoids by Wender and Bradley using confocal microscopy (Peretto et al. 2003; Wender et al. 2002). They could show an internalization of the peptoids rather than a loose attachment of the peptoids on the cell membrane. Those studies would support our experiments and give rise to further experiments on this field.

While the uptake of all tested peptoids shares some common features, pronounced differences could be observed among the individual compounds and in different cell types.

The tetramer **54** showed a perinuclear localization of the vesicular structures and a distinct homogenous fluorescence throughout the cells even after one and 2 hours at 100 μM . Weak staining of the nuclei was also observed (Figure 3-50).

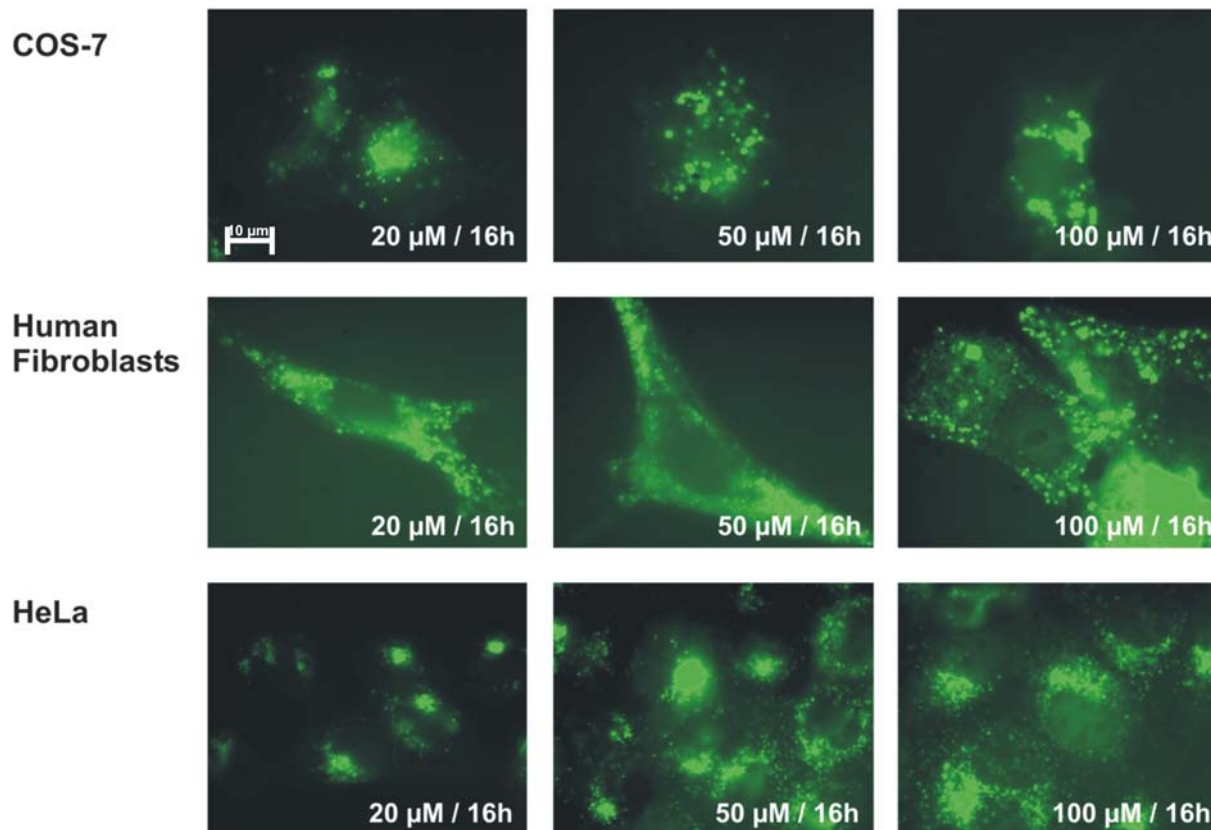


Figure 3-51 Treatment of COS-7, HeLa-cells, and human fibroblasts with the chiral pentameric peptoid **58** coupled to fluorescein. At concentrations of 20, 50, and 100 μM , the fluorescence is found localized to vesicular structures after incubation over night. Diffuse fluorescence is observed from the interior of all cells. In HeLa cells, the vesicular structures tend to aggregate in the perinuclear region and some fluorescence can be seen from the nucleus at 100 μM . At this concentration some fluorescence is also found in the nuclei of COS-7, while at lower concentrations the fluorescent compound is precluded from the nuclei. In fibroblasts, no nuclear uptake is observed. (Zeiss Axiovert 35, filter set 17: $\lambda_{\text{excit.}} = 485\text{nm}$, $\lambda_{\text{em}} = 515\text{-}565\text{nm}$; exposure time: 10s).

The chiral pentameric peptoid **58** was entrapped in vesicular structures. A tendency to accumulate in the perinuclear region was only observed in HeLa cells and much less pronounced in COS-7 cells. Staining of the nuclei was only visible after incubation over night at 100 μM (Figure 3-51)

The hexameric peptoid **55** was visible in vesicular structures even after one hour of incubation at 50 and 100 μM . Remarkably, after two hours a clear distinction could be made between vesicles associated with the plasma membrane and those localized in the perinuclear region. Also, a patchy background fluorescence and a staining of the nucleoli was observed (Figure 3-52).

After treatment with the hexameric peptoid with alternating C4- and C8-side chains **56**, an increased amount of diffuse fluorescence was observed throughout the interior of the cells in addition to the vesicular structures of bright fluorescence.

In COS-7 cells and HeLa-cells, these structures accumulate in the perinuclear region, which is less obvious for the fibroblasts even after incubation over night. In all cells, the nuclei are stained, with bright fluorescence in the nuclei of COS-7 cells and the weakest staining in the nuclei of the fibroblasts.

Finally, the octameric compound **57** exhibited the highest amounts of putative cytosolic staining, while the vesicular fluorescence was decreased in cells with a high degree of diffuse staining. Fluorescence was precluded from the nuclei but resided in the nucleoli. After incubation over night, vesicular structures were found to aggregate in the perinuclear region (Figure 3-54).

In summary, the putative cytosolic stain was stronger for peptoids with longer chain-lengths and went along with uptake into the nucleoli. The chimeric compound appeared to be entrapped in vesicular structures with markedly less diffuse fluorescence. With an increase of incubation time, vesicular structures redistributed from the proximity of the plasma membrane to the proximity of the nucleus. This tendency was markedly less pronounced for the hexamer with alternating side chain lengths than for the homohexamer. The results are summarized in Table 3-7. Nevertheless, the uptake kinetics have to be further analyzed with purified peptoids and the mechanism of uptake refined by biochemical and further cell biological experiments as mentioned above.

| Compound | vesicular structures | perinuclear localization | “cytosolic” fluorescence | nuclear staining | nucleolar staining |
|--------------------|----------------------|--------------------------|--------------------------|------------------|--------------------|
| tetramer 54 | H, C | H,C | H,C | - | C |
| pentamer 58 | H,F,C | H(+), C(-) | F (-) | H, F, C (100) | - |
| hexamers 55 | H, C | H (+), C (+) | H, C (-) | - | H, C(-) |
| hexamers 56 | H,F,C | F (-) | C>H>F | C>H>F | - |
| octamer 57 | H,F,C | H,F,C | H(+),F(+),C(+) | - | H,F,C |

Table 3-7 Comparison of cellular uptake of different peptoids. (+) and (-) indicate pronounced or weak effects. Note that the tetramer and the hexamers **55** were not tested in fibroblasts (C = COS-7; F = human fibroblast; H = HeLa).

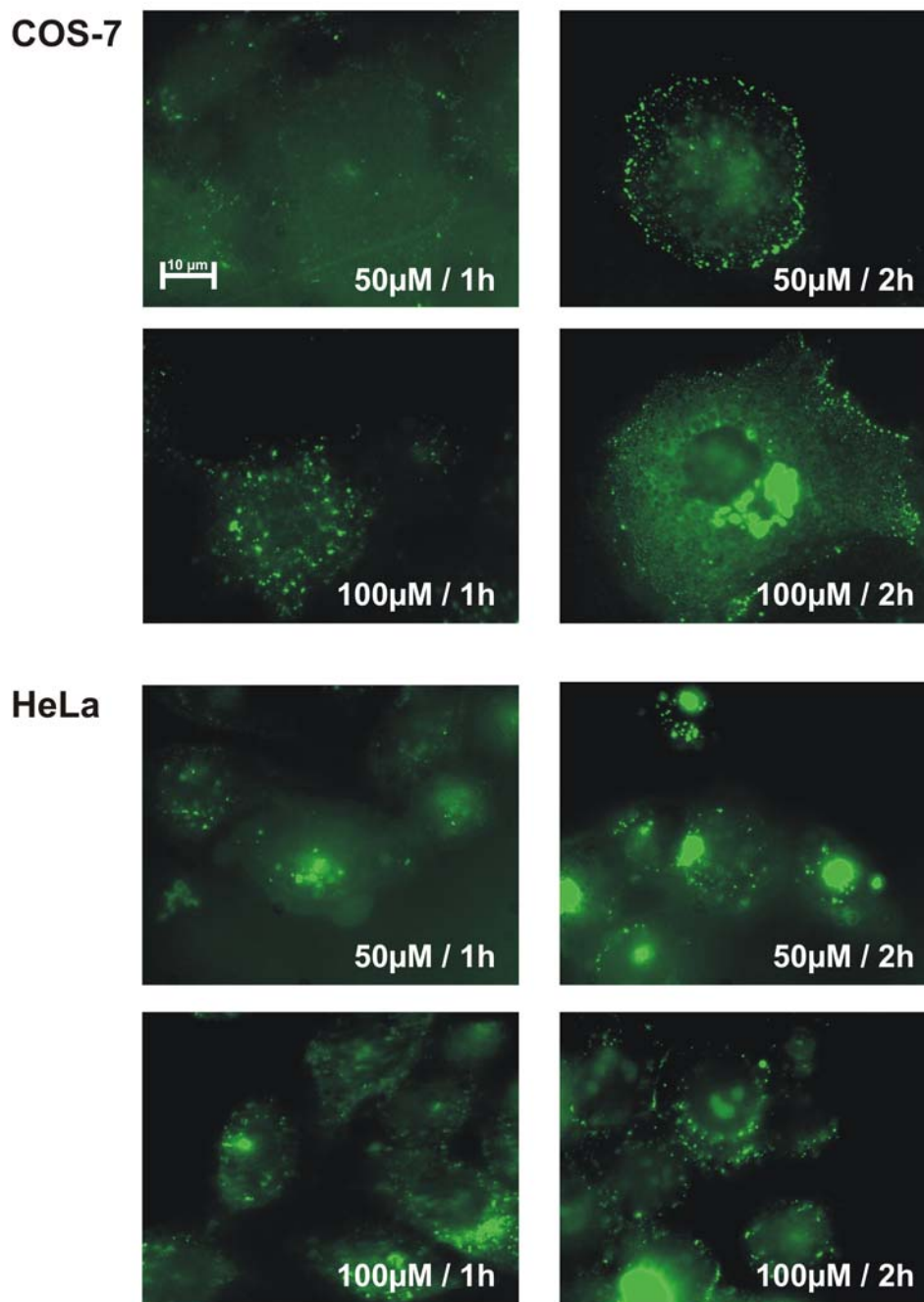


Figure 3-52 Treatment of COS-7 and HeLa cells with 100 μM of the hexameric fluorescein-labeled peptoid **55**. Fluorescence is found concentrated in vesicular structures and more dilute in the interior of the cells. After two hours, the vesicular structures start to accumulate in the perinuclear region and staining of the nucleoli is already visible, pointing out that the compound must have reached the interior of the cells. Note the assembly of vesicular structures along the plasma membrane of the COS-7 cells. (Zeiss Axiovert 35, filter set 17: $\lambda_{\text{excit.}}$ = 485nm, λ_{em} = 515-565nm; exposure time: 10s).

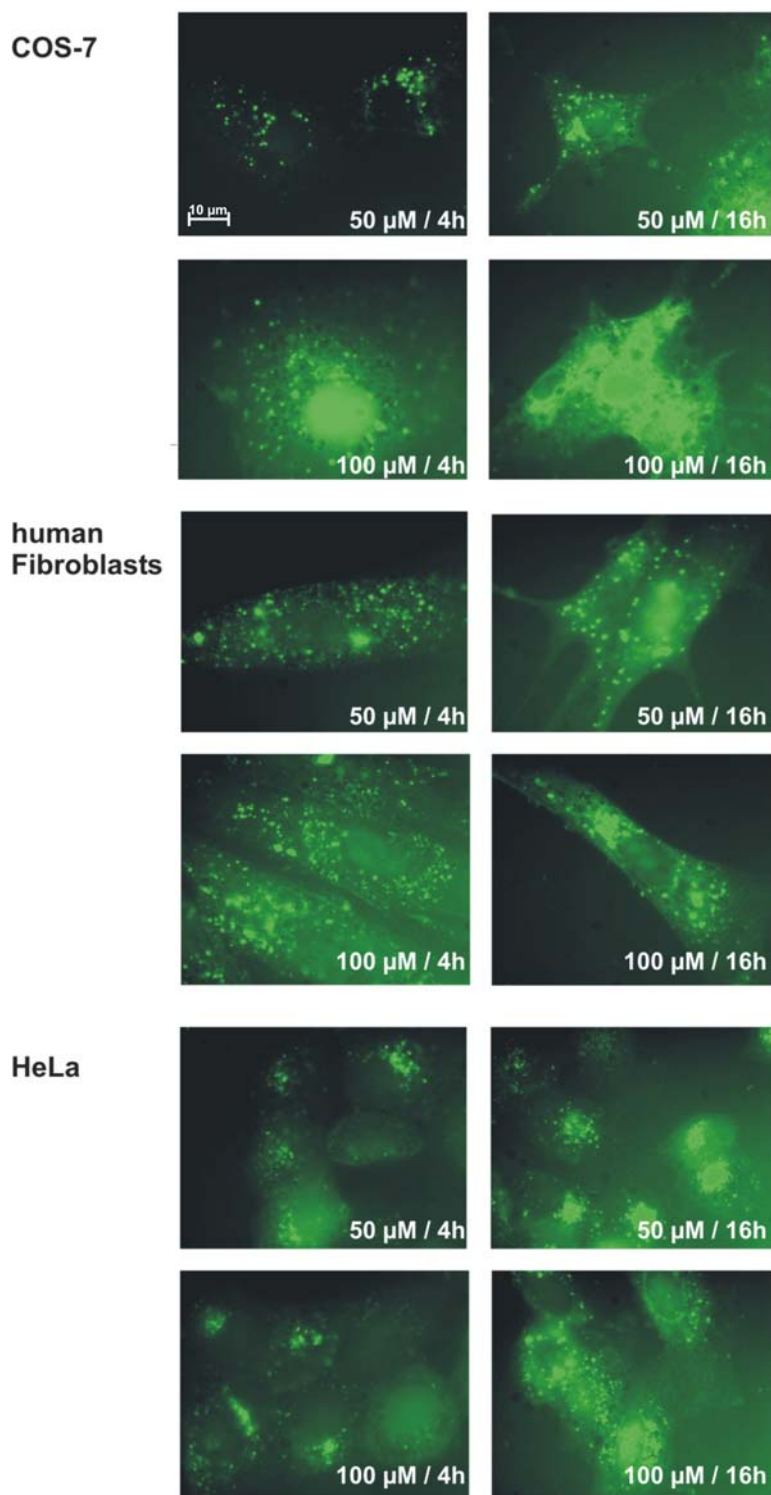


Figure 3-53 Treatment of COS-7, HeLa-cells, and human fibroblasts with the fluorescein-labeled hexameric peptoid with alternating of C4- and C8-side chains **56**. In all cells fluorescence is concentrated in vesicular structures, but a diffuse staining of the interior of the cells is also observed. In COS-7 cells the vesicular structures tend to accumulate in the perinuclear region. After 4h at 100 μM the nuclei are intensely stained. A less pronounced nuclear staining is also observed for the 50 μM after incubation over night. In fibroblasts, no accumulation of the vesicular structures in the perinuclear region can be seen, but for the 100 μM overnight sample. Nuclear staining is observed at 100 μM , albeit less pronounced than for the COS-7 cells. In HeLa cells, the fluorescent vesicular structures accumulate in the perinuclear region and the staining of the nuclei is stronger than in the fibroblasts but much weaker than in COS-7 cells. (Zeiss Axiovert 35, filter set 17 $\lambda_{\text{excit.}} = 485\text{nm}$, $\lambda_{\text{em}} = 515\text{-}565\text{nm}$; exposure time: 10s).

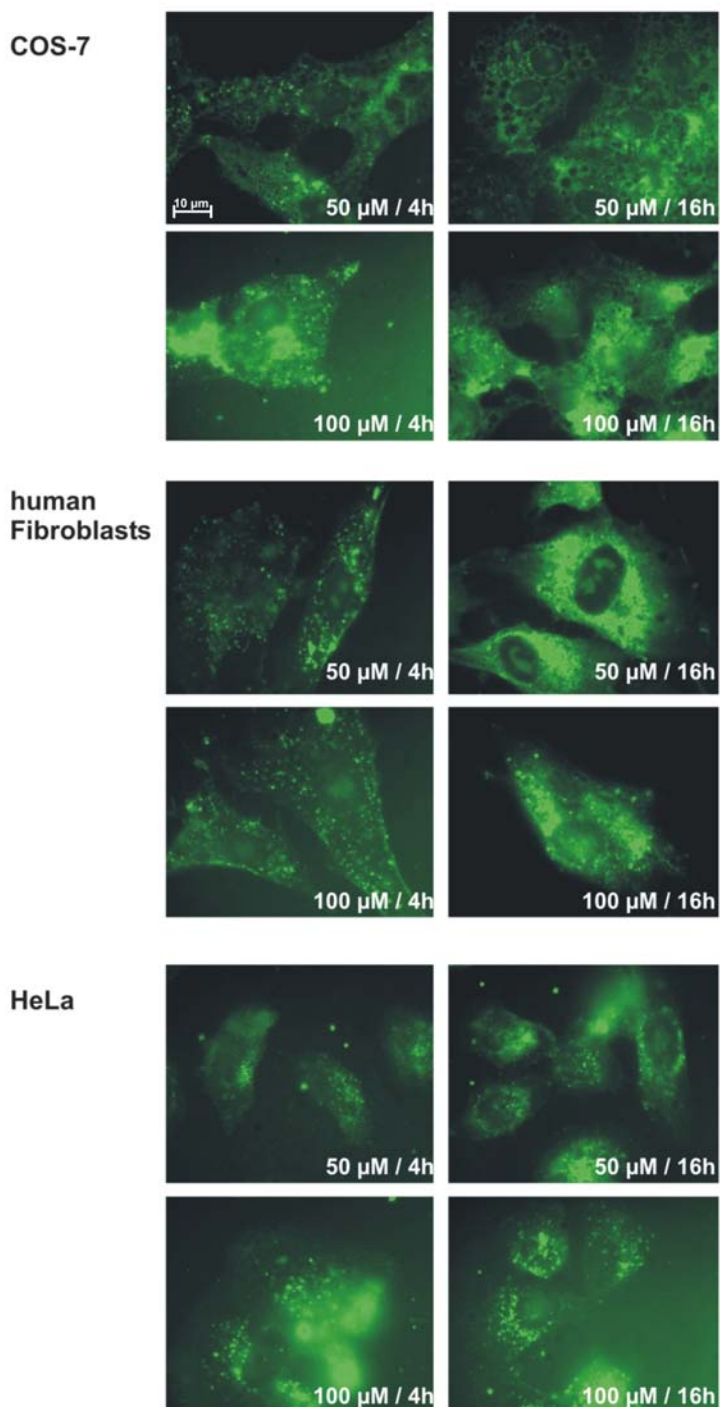


Figure 3-54 Treatment of COS-7 and HeLa-cells with the fluorescein-labeled octameric peptide **57**. Fluorescence is localized to vesicular structures and staining of the nucleoli can be observed, while the main region of the nucleus is precluded from staining. In COS-7 cells, the vesicular structures are less pronounced in favor of more diffuse fluorescence spread over the interior of the cells indicating a cytosolic localization of the compound. In fibroblasts, the intracellular fluorescence is much less pronounced after 4h but increases after incubation over night. At these long incubation times, brightly fluorescent vesicular structures accumulate in the perinuclear region. Diffuse fluorescence throughout the cells is also observed in HeLa cells. A concentration of vesicular structures around the nuclei is also visible (Zeiss Axiovert 35, filter set 17: $\lambda_{excit.} = 485nm$, $\lambda_{em} = 515-565nm$; exposure time: 10s).

4 Discussion

Since the discovery of RNAi as an efficient tool for gene silencing, it has been discussed to cure diseases related to genetic defects like cancer or inherited genetic disorders, or to combat infections of viruses and parasitic organisms. In recent years, great advances have been made into this direction and experiments showed that RNAi was indeed able to reduce viral titers of HIV in cell culture (Novina et al. 2002) or to inhibit hepatitis B in mice (McCaffrey et al. 2002). However, it turned out that one major obstacle was the delivery of siRNAs *in vivo*.

Viral vectors were introduced to transfer siRNAs or shRNA expressing plasmids into mammalian cells (Brummelkamp et al. 2002a; Hemann et al. 2003; Paddison et al. 2002b). The adenoviral approach, that was appreciated for its versatility (Tomar et al. 2003) was soon abandoned, since it was shown to lead to random insertion into the host genome with the risk of causing leukemias (Hacein-Bey-Abina et al. 2003a). Lentiviral vectors appeared to be a more convenient solution. However, it turned out that the delivery of shRNA expressing plasmids by lentiviral vectors triggered significant immunogenic responses, so that it is likely to exhibit adversary effects on fully-grown organisms (Fish and Kruithof 2004).

Tail vein injection of naked siRNAs turned out to be efficient for gene silencing in the liver, where siRNAs accumulate upon high-pressure injection (Lewis et al. 2002; McCaffrey et al. 2002). However, this mode of application is not transferable to clinical studies, since it requires large volumes to be injected in short times and leads to severe changes in blood pressure and liver enzyme levels (Heidel et al. 2004).

Cell-penetrating peptides offer a new possibility to solve the delivery issue. They have been shown to efficiently deliver a broad variety of cargos into almost all types of cells, even beyond the blood brain barrier (Schwarze et al. 1999). Moreover, the rapid uptake reported for CPPs conjugated to cargo molecules (Lindsay 2002; Schwarze et al. 2000), and the accumulation of CPPs from the culture medium in the interior of the cells (Hallbrink et al. 2001; Lindsay 2002) were favorable features for a versatile delivery tool. Finally, they appeared to exhibit no toxic effect in the concentration range required for RNAi (Hallbrink et al. 2001; Vives et al. 1997b). At the beginning of this work, the delivery of CPP-coupled antisense-oligonucleotides (Innis 2001; Prochiantz 1996) and PNAs (Derossi et al. 1998; Pooga et al. 1998b) had already been reported. Later, NLS sequences, PenetratinTM, VP22 and Tat peptide were used to deliver siRNAs into cells by formation of non-covalent complexes (Benimetskaya et al. 2002; Dom et al. 2003; Kretz et al. 2003).

Very recently, comparison of peptide-mediated uptake with the lipid-mediated delivery of PNA/DNA hybrids has led to the result that lipid transfection requires less PNA while peptide-mediated delivery was simpler and less toxic to primary endothelial cells (Kaihatsu et al. 2004).

The coupling of siRNAs with CPPs to yield pepsRNAs appeared to provide a promising tool for RNAi applications *in vivo* that allowed the specific silencing of endogenous or parasitic genes even in non-dividing cells and primary cells that had been found difficult to transfect with siRNAs by conventional methods. It even held a promise for applications in fully-grown

mammalian organisms. It was decided to use disulfide bonds for coupling so that the siRNA would be released from the delivery peptide once it reached the reducing milieu of the cytosol (Fischer et al. 2001; Schafer and Buettner 2001). Thus interactions of components of the RNAi machinery with the delivery peptide could be avoided.

In the course of this work, proof of principle experiments with commercially obtained, thiol-modified siRNAs coupled to PenetratinTM showed that these pepsRNAs enter primary myocytes and silence recombinantly expressed GFP when applied in concentrations of 25-100 nM. With reference to the first siRNA experiments in mammals (Elbashir et al. 2001a), pepsRNAs targeting lamin A/C were applied to HeLa cells and primary fibroblasts and it was found that the endogenous gene was silenced as proven by immunostaining experiments. However, it should be noted that the immunostaining is restricted to the quality of the antibody and the detection efficiency.

To assess the versatility of this new technique, pepsRNAs directed against HexA were applied to various mammalian cell lines. The same treatment protocol was applied. The cells were treated with 100 nM of anti-HexA pepsRNA for 30 min and after 2 days of incubation the knockdown efficiency was assessed. In HeLa cells, human primary fibroblasts, human epithelial kidney cells, and even primary murine neurons the target-mRNA was completely degraded.

A knock-down up to ~98% was found for melanocytes, and greater than 99% for neurons, HeLa cells, kidney epithelial cells, and fibroblasts, while mRNA levels of 7% and 20% were found in myotubes and myocytes, respectively. The residual activity might be explained by the setup of the experiment. Due to serum reduction, the myocytes begin to differentiate very quickly to myotubes that are much more difficult to address. However, it can be concluded that treatment with pepsRNAs in the upper nanomolar range leads to a significant reduction of target mRNA in a variety of cell lines and primary cells.

Thus, pepsRNAs are functional as triggers of RNAi in the intermediate nanomolar range for endogenous and recombinant target genes. They are evenly distributed, taken up by all cells in the culture dish, and efficiently trigger RNAi even in primary cells.

When the first steps were taken into the generation of pepsRNAs, the combination of RNAi and CPPs seemed to offer unlimited possibilities. However, later findings indicated that the RNAi efficiency in mammals is lower than in *C. elegans*, where it was first described. Unlike worms, mammals do not possess an RNA dependent RNA polymerase (Stein et al. 2003) so that the efficiency of RNA solely depends on the number of catalytic cycles undergone by RISC (Haley and Zamore 2004). However, human RISC can perform up to 50 cycles of mRNA degradation so that RNAi keeps its advantage of catalytic activity over stoichiometric antisense techniques.

Furthermore, siRNAs can be bound by the dsRBD of ADARs, which decreases their intracellular concentration (Yang 2004). As the RNAi machinery in mammals mainly serves regulatory processes, and the processing of siRNAs may share components with the miRNA pathway, side effects are to be expected if all available RISC complexes are saturated with exogenous siRNAs (Zeng and Cullen 2003).

However, these effects can be circumvented by keeping the concentration of siRNAs as low as possible by designing highly efficient siRNAs. If the design of an siRNA leads to a preferred incorporation of the antisense-strand into RISC, less siRNAs are lost by incorporation of the sense-strand (Schwarz et al. 2003) and putative off-target effects caused by RISC loaded with the sense-strand are avoided (Jackson et al. 2003). Today, the design of highly efficient siRNAs has been greatly facilitated by novel design rules and corresponding computer tools (Khvorovova et al. 2003; Reynolds et al. 2004; Schwarz et al. 2003; Yamada and Morishita 2004).

Additionally, the stability of siRNAs towards nucleases can be enhanced by modifications of the ribose-phosphate backbone such as the incorporation of phosphorothioates (Harborth et al. 2003), locked ribonucleotides (Braasch et al. 2003; Grunweller et al. 2003), boranophosphates (Hall et al. 2004), 2'-methylated or 2'-fluorinated ribonucleotides or deoxyribonucleotides at selected sites (Amazguioui et al.; Askjaer et al. 2002; Chiu and Rana 2003). Thus, a prolonged effect can be achieved with an equal dose of stabilized siRNAs.

The broad field of CPP based research suffered a drawback, when it was reported that many of the early mechanistic findings were due to artifacts. Due to their high membrane affinity, these highly basic peptides adhere to the negatively charged compounds of the plasma membrane thereby mimicking high uptake rates in cell counting assays (Richard et al. 2003; Thoren et al. 2003). They also reorganize during cell fixation procedures and accumulate in the nucleus (Leifert et al. 2002; Lundberg et al. 2002). After correcting the procedures to avoid artifacts, it turned out that CPP-coupled reporter molecules were taken up within 2-4 h rather than in 10-30 min. No uptake was observed at 4°C and the molecules were localized in vesicular structures all pointing out an endocytosis-like mechanism (Drin 2003; Fischer et al. 2004; Richard et al. 2003; Thoren et al. 2003; Umezawa et al. 2002; Vives 2003).

However, it was the high uptake rate that had to be revised, while the high membrane association of CPPs was confirmed by these reports. Many publications about CPP-coupled cargos that exhibited their desired effects in the cytosol, suggested that these bioconjugates must have reached the cytosol (Braun et al. 2002; Derossi et al. 1998; Kasim et al. 2004; Peitz et al. 2002; Pooga et al. 1998c; Soughayer et al. 2004). In fact, novel mechanistic studies confirmed that CPP-coupled reporter molecules were taken up by endocytosis, but were able to escape the endocytic vesicles (Thoren et al. 2003; Zaro and Shen 2003). It is assumed that they reach the cytosol via retrograde transport across the trans-Golgi network similar to cholera-toxin (Fischer et al. 2004). Since no quantitation has been made this is still an assumption.

Although the rate of uptake is much slower than previously reported, short incubation times are still sufficient to achieve a good cellular uptake even though it is not clear in which compartments the CPPs are present. As described before most of the studies do not report the quantitation of the CPPs that are taken up and the CPPs that remain in the medium after thorough washing. Those studies are still ongoing. Although those numbers are still not known, it can be assumed that the amount of the CPPs that actually enter the cells is much

lower than the applied concentrations reflect so far. CPPs strongly interact with the plasma membrane, they attach to cellular surfaces within the first minutes after their applications. The binding is strong enough to withstand repeated washing steps and can only be released by treatment with proteases (Richard et al. 2003). Thus the CPP-conjugates remain associated with the cells when the medium is exchanged after 15-30 min of incubation. They can then enter the cells by endocytosis, wherein the prolonged time of uptake can be exploited as a depot effect for prolonged availability of the compounds inside the cells.

Thus, peptide mediated delivery, like the pepsRNA approach, bears the advantage, that incubation times and thereby the exposure to serum free medium can be kept short which is less stressing for sensitive cell types.

The high membrane affinity of CPPs also conveys some degree of specificity to this approach. The cationic peptides quickly associate with negatively charged structures in the close proximity. Therefore, when applied to a fully-grown organism, a large proportion of a CPP conjugate would be taken up at the site of application while a smaller amount would circulate in the bloodstream. Thus, the pepsRNA approach provides a local restriction of the siRNA-mediated gene silencing. At the same time, the strong membrane interactions prevent the delivery to specific cell types by targeting specific surface structures.

Early studies using a CPP-coupled FAB fragment have shown that proteins coupled to few CPPs are taken up more specifically but less efficiently and vice versa (Anderson et al. 1993).

An elegant approach to circumvent the specificity issue is the development of activatable CPPs (ACPPs), in which the capacity to enter cells is blocked by a linker that can be specifically cleaved by a protease secreted by the target cells (Jiang et al. 2004).

On the other hand, the local restriction of CPPs is of great interest for the treatment of skin disorders. It has been already shown that hemagglutinin (HA) epitopes coupled to CPPs and fluorescently labeled cationic β -peptides penetrated to the deep dermis after one hour after topical application (Robbins et al. 2002; Rueping et al. 2004). Thus, pepsRNAs could be used in the treatment of psoriasis or for the study of the water-permeability barrier of the skin *in vivo*.

During the work on the pepsRNAs approach reported here, the same idea has been developed and tested by other groups. The first reports on penetratin (Davidson et al. 2004; Muratovska and Eccles 2004) and Tat or oligocarbamate-coupled siRNAs (Chiu et al. 2004a) confirm the findings presented in this work: CPP-coupled siRNAs via disulfide bonds are taken up by various kinds of mammalian cell lines and primary cells and the coupling to CPPs does not interfere with the RNAi efficiency so that significant levels of more than 99% of downregulation are already obtained in the lower nanomolar range depending on the cell type. pepsRNAs, also named V-siRNAs for vector-coupled siRNAs, are taken up by primary neurons, where they downregulate the targeted genes (Davidson et al. 2004; Schmitz et al.). It was also shown that the decrease of mRNA is preceded by a drop of protein levels due to translational inhibition (Davidson et al. 2004).

All reports on peptide-coupled siRNAs are based on compounds generated by solid phase synthesis (SPS). As thiol-modified nucleotides for SPS are readily available on the market, the synthesis of thiol-modified siRNAs is straightforward, once the technique has been established in the lab. However, siRNAs and peptides from solid phase synthesis are obtained in small amounts at comparably high costs. Therefore, the work presented here aimed at developing a strategy that allows the scale up of pepsRNA synthesis.

Large amounts of siRNAs have been obtained from recombinant organisms overexpressing hairpin-shaped RNAs. It has been demonstrated that lhrRNA recombinantly expressed in *Nicotiana tabacum* was processed into siRNAs by the host organism. These siRNAs could be applied to mammalian cells, where they down-regulated endogenous and viral target genes with an efficiency comparable to synthetic siRNAs (Zhou 2004). However, such siRNAs need to be functionalized by a subsequent step, which appears to be a non-trivial task if the modification has to be directed to the sense strand of the native siRNA.

In vitro transcription by T7 RNA polymerase (Milligan et al. 1987) is a convenient approach to generate large amounts of RNA, that has gained considerable interest for the generation of long dsRNAs and siRNAs. It bears the advantage that single stranded RNAs can be generated in separate reactions and hybridized in a subsequent step. To functionalize enzymatically generated RNAs, chemically modified nucleotides can be attached to the 3'-terminus with T4-RNA-ligase (Hausch 1997; Igloi 1996), or GMP derivatives that act as initiator nucleotides can be added to the reaction mixture to be selectively incorporated at the 5'-terminus (Seelig 1997, 1999). For the coupling of peptides to siRNAs via an *in vivo* cleavable disulfide bond, a thiol-modified initiator nucleotide is required. Although guanosine monophosphorothioate (GMPS) can be readily incorporated into RNA and used for the formation of disulfide bonds (Lorsch and Szostak 1994), the resulting phosphorothioate-sulfide compound (R-SSPO₃-RNA) is not very stable (Goody and Walker 1971; Sengle et al. 2001). 5'-Deoxy-5'-thioguanosine-monophosphorothioate (GSMP) yields 5'-thiophosphate modified RNAs that can be transformed into 5'-SH-RNAs by incubation with phosphatase (Zhang et al. 2001a). This approach brings the two oppositely charged coupling partners into close proximity, which makes interaction less likely than conjugation via a long chain flexible linker.

Although the synthesis of GSMP has been reported with yields of 35% in 4 steps (Zhang et al. 2001a), it was found difficult to reproduce. The major obstacle consisted in the purification of 5'-deoxy-5'-iodo-2',3'-O-isopropylidene-guanosine. The dried reaction mixture needs to be washed prior to column chromatography, which leads to losses due to its stickiness. The crude product is poorly soluble in the solvents required for column chromatography and tends to obstruct chromatography columns, leading to further losses. Moreover, the iodide is subject to an intramolecular cyclization reaction that has been previously described (Verheyden and Moffat 1970). Due to the high rate of this side reaction in DMSO, it is difficult to determine the purity of the product by NMR-spectroscopy. The instability of the iodide also leads to contaminations in the subsequent deprotection step.

As the cyclization requires a freely accessible purin-N3, the adjacent primary amine was protected as an imine in an additional reaction step. Thus, the nucleophilic attack of N3 on

the ribose C5' was sterically hindered, which resulted in an increase of the half-life time of the iodide by a factor of 12.

Due to its increased solubility, the protected iodide was readily purified and quantitative yields could be obtained by column chromatography. The overall yield of the additional protection reaction and the iodination (79%) was about twice as large as the yield for the unprotected iodide (39%) and even exceeded the literature yield (62%) (Zhang et al. 2001b). The protected iodide was stable even after months of storage and did not lead to any contaminations during the deprotection reaction.

As the solubility of GSMP in water is similar to that of thiophosphate, it is difficult to purify from the excess of reactant. After the first precipitation step as described by Zhang (Zhang et al. 2001b), chromatography methods have to be applied to obtain GSMP without contaminations of thiophosphate. FPLC via an anionic exchange column (DEAE-Sepharose A25), column chromatography on silica gel and reversed phase chromatography on RP-18 material were compared as purification methods. The highest yields were obtained by column chromatography on RP-18 material with gravity flow elution with water that yielded 68% of GSMP. An overall yield of 53% was obtained for the refined synthesis of GSMP in 5 steps as opposed to the reported 35% in 4 steps (Zhang et al. 2001a).

GSMP **15** was added to the *in vitro* transcription reaction for the generation of the siRNA sense strands. The reaction mixtures for the sense strand and for the antisense strand were incubated with phosphatase to liberate the thiol-group from the thiophosphate and to remove 5'-terminal triphosphates, respectively, that have been reported to induce an interferon response in mammalian cells (Kim et al. 2004). After precipitation and hybridization, modified siRNAs are obtained in a reasonable yield.

The thiol-modified siRNAs were coupled to commercially obtained biotinylated penetratin™. The reaction can be easily monitored by a yellow ring of thiopyridone at the interface of the peptide and siRNA solution at elevated concentrations. In some experiments, the formation of a precipitate due to aggregation of the oppositely charged compounds was observed, which could be redissolved by the addition of concentrated NaCl solution. Precipitation could be largely avoided if the experiment was carried out in a flow of argon and if the solution was not agitated to mix the compounds. The formation of conjugates could be confirmed by 15% SDS-PAGE and by MALDI-TOF analysis. Separate experiments under reducing and non-reducing conditions indicated, that the disulfide bond could be cleaved to release the two monomers. This demonstrated that thiol-modified siRNAs could be generated in one step by *in vitro* transcription if the modified initiator nucleotide was readily available.

Both pepsRNA and standard oligonucleotide were detected as broadened peaks. Due to the high acidity of the backbone phosphates these residues are deprotonated at neutral pH. The siRNAs bear 42 negatively charged residues and are thereby found as mixtures of sodium and potassium salts, so that broadened peaks are found. As described by Jensen (Jensen et al. 1996), the pepsRNA and reference samples were treated with ammonium acetate to exchange sodium and potassium ions for ammonium ions that dissociate to volatile NH₃ and H⁺ in the gas phase leaving behind protonated phosphate residues. The thus obtained peaks were much more focused but could still not be assigned to one distinct mass. In three

measurements of aliquots of the same sample, the value for the dsRNA peak varied between 14180 and 14649 Da corresponding to a maximum deviation of 1.8% from the average of the three measured values. This was much higher than the deviations of 0.08% reported for short model conjugates of peptides with oligodeoxynucleotides of an overall mass of 1942 to 4381 Da as determined by MALDI-MS (Jensen et al. 1996). One reason for this was the low signal to noise ratio obtained for the pepsRNAs, which led to ambiguous results in the determination of the peak maximum. Additionally, the incomplete removal of associated Na⁺ ions resulted in a mass distribution of the oligoribonucleotides, and the siRNAs might have been subject to nuclease degradation during sample preparation leading to fragments of different size. Finally, those nucleotides may result from strand termination during solid phase synthesis. Due to these results the cell culture studies must be considered with caution concerning the final concentration of the pepsRNAs estimated photometrically. The concentration for the experiments might be much lower than depicted, even though the pepsRNAs were subjected to gel filtration, due to incomplete coupling and degradation of the compounds.

The recombinant expression of CPPs is a straightforward approach towards a large-scale generation of pepsRNAs. Vectors for the expression of GST-coupled Antennapedia peptide and Tat peptide with C-terminal cysteine residues were generated by cloning the corresponding synthetic genes into a GST-expression vector. The presence of the insert was confirmed by PCR and sequencing. Unlike plain GST, the overexpressed GST-CPP fusion-proteins could not be purified by the standard protocol, as the recombinant proteins resided in the pellet. This was thought to correlate with the degree of CPP-membrane interaction, since a GST-Tat mutant (R9Q), in which one of the cationic arginine residues is replaced by a neutral glutamine residue, thus reducing the degree of electrostatic interactions, shows a higher solubility than Tat. Thus, it was necessary to develop a novel purification protocol that allowed the solubilization of GST-CPPs. It was found that increased amounts of DTT and Triton X-100, a higher pH and elevated temperatures enhanced the solubility of the recombinant protein. The yield of GST-Tat could be further increased by sonication. The yields of GST-CPPs obtained with the modified protocol correspond to those found with plain GST.

According to the design of the recombinant GST-CPPs, TEV protease was required to cleave the CPPs from the GST-tag. Recombinant vectors were generated to express GST-tagged TEV protease. The overexpressed fusion-protein resided in the insoluble fraction of the lysate. Apparently, the fusion protein did not fold back properly and formed insoluble inclusion bodies. After solubilization under denaturing conditions and dialysis against different refolding buffers no soluble native protein could be obtained. Attempts to express recombinant TEV protease with a His₆-tag led to similar results. The solubility of the recombinant protein could neither be increased by expression at lower temperatures nor by expression in different strains. The protein obtained by inclusion body preparation did not bind to the Ni-NTA resin for affinity purification.

The formation of inclusion bodies is a well-known problem in the expression of TEV protease (Kapust et al. 2001; Lucast et al. 2001). Various mutations have been tested to increase its solubility and to suppress its autoproteolysis activity. From a collaboration, a recombinant strain of *E.coli* BL21 DE3 pLysS was obtained that expressed the mutant S219Q in which an autocatalytically active residue is replaced by an inactive one (A. Ulrich, TH Karlsruhe). This mutant is also known for its improved solubility (Lucast et al. 2001). The recombinant protein could be prepared in a straightforward manner following the protocol for native preparation by Lucast (Lucast et al. 2001). The amounts of protein obtained after affinity purification on Ni-NTA were comparable to the amounts of plain GST obtained by affinity purification on glutathione sepharose. The pooled eluates were tested in a cleavage reaction with GST-Tat and GST-AntP in comparison to commercially obtained TEV protease. The used amounts of commercial and recombinantly generated protease exhibited a comparable cleavage activity in an overnight cleavage assay.

Peptide bands could not be detected by 15% SDS-PAGE, which may be explained by the weak staining of the peptide and the generally less focused peptide bands that are more difficult to detect, as known from Penetratin™ controls. As only 4% and 6% of the protein mass are made up by Tat peptide and AntP, respectively. Only small amounts of peptide are to be expected even if the full amount of GST-CPP is cleaved. Although, His₆-tagged TEV protease and free GST-tags could be removed by the corresponding affinity-resins, it is more convenient to purify the reaction mixtures by FPLC on RP-18, since both resins require different conditions to bind their substrate, and DTT needs to be removed prior to coupling of the CPP to the siRNA via a disulfide bond. Moreover, by UV-detection during elution from an RP-18 column at 280 nm the amounts of free peptide and uncleaved GST-CPP could be assessed and the purity of the peptide fractions could be monitored.

Peptides are sensitive to degradation by proteases and to oxidation, which affords great care when working with CPP-coupled substances. It also lowers the half-life of these compounds *in vivo* and reduces the fraction that reaches its target site. Moreover, peptides may be recognized as epitopes and trigger immunogenic responses. Therefore, small molecules with membrane permeating properties were developed and tested in cell culture as a future replacement of the CPP moiety for the delivery of siRNAs.

Preliminary tests with rhodamine-coupled oligoamines, indicated that spermine was a suitable candidate as a backbone for novel cell-permeating molecules, as it bears a significant potential to enter cells.

Over the last decade, conjugates of spermine or spermidine with lipids like dioctadecylaminoglycylspermine (DOGS, transfectam) have been established as transfection agents (Boletta et al. 1997; Kichler et al. 1997; Mack et al. 1994). Furthermore, spermin conjugates with cholesterol have been developed for the delivery of oligonucleotides (Guy-Caffey et al. 1995; Lee et al. 1996; Lee et al. 2004b). All of these approaches make use of the formation of non-covalent complexes of the positively charged amine with the negatively charged DNA cargo (Symons 1995). Covalent attachment of spermine has helped to target DNA-cleaving effector molecules like acridine and iron chelators to their target site (Bergeron et al. 2003; Delcros et al. 2002). Finally, covalent coupling spermine to an RNA cleaving

DNA enzyme could enhance the enzyme's activity and its affinity to the target RNA (Kubo et al. 2003).

In this work, conjugates of spermine with carboxyfluorescein and porphyrin as reporter molecules were tested in cultured mammalian cells. Porphyrin is of specific interest for the treatment of tumors in photodynamic therapy. Upon irradiation, porphyrins generate highly-reactive singlet oxygen that leads to fatal damage of the affected cell (Capella and Capella 2003; Detty et al. 2004).

Uptake experiments with fluorescein-labeled spermine in mammalian cell lines showed that the spermine conjugates were taken up in vesicular structures after 4h of incubation with 100 μ M of the compound as assessed by life microscopy. Further incubation over night, led to a distribution of these structures throughout the cell. The time-frame required for uptake and the finding of vesicular structures indicate an uptake by endocytosis followed by endosomal escape. Unmodified carboxyfluorescein was not taken up by any of the tested cell types, so that the observed phenomena must be due to the conjugation with spermine. It has been reported that conjugates of spermine with small molecules have a high affinity for the cellular polyamine transport system (PTS) (Bergeron et al. 2003; Delcros et al. 2002). However, others have found a role for endocytosis (Soulet et al. 2002), which is in agreement with the results presented here.

The same patterns were observed in the experiments with spermine-coupled porphyrin. At a concentration of 10 μ M, all cells were stained after 4h of incubation. After incubation over night, fluorescence could also be seen in the cytosol, and cellular uptake was observed for concentrations as low as 100 nM in almost all cells. Punctate fluorescent staining on the surface of fibroblasts could be even detected at concentrations of 10 nM. It is assumed that, the fluorescence intensity of the porphyrin is not sufficient to be detected after cellular uptake in low concentrations.

At concentrations of 50 and 100 μ M of conjugate, severe toxic effects were observed for all cell types. In comparison with untreated controls, over 80% of the cells had detached from the culture plate, and the remaining cells showed signs of cell death after 30 min of incubation. In the transmission mode many of the remaining fragments were fluorescent with the associated porphyrin conjugate. This effect was significantly pronounced in cells treated in daylight, while the majority of cells retained a healthy phenotype when treated in the dark. This confirms the phototoxicity of the porphyrin-derivative. The association of the spermine-coupled porphyrin with the cell surface helps to restrict this kind of light-induced damage to the site of application. In photodynamic therapy, porphyrins are used to destroy tumors by application to the affected tissue followed by irradiation at high intensities. In these applications, spermine-porphyrin conjugates may reduce systemic side effects by localizing the phototoxic compounds to the site of administration and decrease the efficient dose due to an enhanced uptake.

For future applications for the delivery of siRNAs, peptoids were selected as a peptide-mimetic with increased stability toward proteases *in vivo*. The synthesis of peptide analogs that mimic CPP function has been described by several groups (Potocky et al. 2003; Raguse et al. 2002; Rueping et al. 2002; Rueping et al. 2004; Wender et al. 2000; Wender et al. 2002). For efficient uptake, such backbone mimetics must bear a high number of positively

charged side chains that can adopt an amphipathic secondary structure in which polar and non-polar fractions of the molecule point into opposite directions.

β -peptides, the higher homologs of the α -peptides, form stable helices that are structurally more confined than those formed by α -peptides. (Rueping et al. 2004). They are stable toward degradation by proteases and their structures can be more readily predicted. β -peptides functionalized with guanidinium groups enter cultured mammalian cells with high efficiency (Wender et al. 2000). As opposed to α -peptides, the side chains in oligo-N-alkylglycines or peptoids are attached to the amine, so that the monomers can be readily synthesized from functionalized diamines (Figliozzi et al. 1996; Goff and Zuckermann 1992; Wender et al. 2000). Like β -peptides, peptoids with guanidinium-headgroups enter mammalian cells, where they have been used to mimic peptide-hormones, antibiotics, and receptor ligands (Murphy et al. 1998; Wender et al. 2000).

In this work, fluorescently labeled peptoids consisting of a polyamide backbone of varying length with amino-functionalized side chains of different side chain lengths as kindly provided by T. Schröder (Schroeder 2004) have been tested in HeLa- and COS7 cells and in primary fibroblasts.

In preliminary experiments, it was found that the presence of serum in the application medium does not interfere with the uptake of the compound. On the contrary, long incubation times in serum free medium alter the morphology of the treated cells. The artifactual redistribution of the fluorescent conjugates with localization to the nucleus, as previously described by others (Leifert et al. 2002; Lundberg et al. 2002), was confirmed by these experiments, so that further experiments were evaluated by life cell microscopy in isotonic buffer. Concentrations of 10, 50, and 100 μ M and incubation times of 4h and 16h were found as conditions under which uptake of the fluorescein-labeled peptoids could be observed in all of the treated cells.

The putative cytosolic stain was stronger for peptoids with longer chain lengths and went along with uptake into the nucleoli. Vesicular structures were less pronounced for the octamers, which exhibited the strongest staining of the cellular background. This is in agreement with reports about synthetic oligopeptides, where no uptake was observed for less than 6 amino acids and the highest efficiency was found for the octamer (Rothbard et al. 2000). The chimeric compound appeared to be entrapped in vesicular structures with markedly less diffuse fluorescence. With an increase of incubation time, vesicular structures redistributed from the proximity of the plasma membrane to the proximity of the nucleus. This tendency was markedly less pronounced for the hexamer with alternating side chain lengths than for the homohexamer.

As for the spermine conjugates, vesicular structures distributed throughout the cell and accumulated in the perinuclear region were observed in all experiments with the fluorescent peptoids, while incubation over night also led to a staining of the nucleoli. Moreover, the overall fluorescence inside the cells and the cytosolic fluorescence was markedly increased after incubation over night suggesting an escape of the labeled molecules from the vesicles into the cytosol.

Nevertheless, lysosomal markers need to be used to determine whether the components were entrapped in lysosomes or another species of transport vesicle.

Apparently, all of the synthetic positively charged small molecules were taken up by an endocytosis-related mechanism followed by endosomal release. In this, they resemble the uptake behavior of CPPs.

With 10-100 μM , the concentration range required to visualize cellular uptake of the labeled peptoids and spermine conjugates lies 2-3 orders of magnitude above the concentrations used in CPP-mediated delivery. In the experiments with the cationic amphiphilic synthetic transporters, dosages appear to be very high, especially since it is known that cationic amphiphiles are mainly stored in the lysosomes eventually leading to the disruption of the latter. It can be assumed that in agreement with other cationic amphiphiles, the peptoids as well as the polyamines or the CPPs tested in the previous sections are protonated when they reach the acid lysosome (pH 4.5). There they will interact with any kind of negatively charged lipids and might aggregate while slowly getting released into the cytosol. Since the compounds tested in these experiments are still crude after the cleavage from the resin and comprise a mixture of labeled and unlabeled peptoids the dosages have to be refined with further purified peptoids. A new synthesis of peptoids is still ongoing and the experiments will be repeated with purified peptoids and analyzed by confocal microscopy to determine the uptake kinetics.

However, these findings confirm the reports of homologous peptoid transporters that act in a similar concentration range (Yingyongnarongkul et al. 2004). Reasons for this discrepancy may lie in a weak reporter signal. Fluorescence microscopy is made difficult by rapid photobleaching of fluorescein. Similar studies have been performed on other peptoids by Wender and Bradley using confocal microscopy (Shi Kam et al. 2004; Yingyongnarongkul et al. 2004). They could show an internalization of the peptoids rather than a loose attachment of the peptoids on the cell membrane. Those studies would support our experiments.

Moreover, the tested structures are only lead-structures that are to be developed into powerful delivery agents. An elongation of spermine or the functionalization of the peptoids with arginine residues could be reasonable modifications for further investigations.

With this work, some first steps have been taken into the vast field of artificial delivery molecules. The finding that molecules that are otherwise excluded from the cells can be delivered after covalent coupling with spermine or amino-functionalized peptoids points at the potential of these compounds for the delivery of drugs and especially siRNAs. The coupling of these novel delivery molecules to siRNAs and the testing of these conjugates will be subject to future work.

5 Materials and methods

5.1 Bacteria culture

5.1.1 Culture conditions

Wild type and recombinant *E. coli* strains are grown in LB medium supplemented with the following antibiotics required for selection: 60µg/ml ampicillin, 10µg/ml tetracyclin, 50µg/ml kanamycin or 7 µg/ml gentamycin, respectively. Single colonies are incubated over night at 37°C in 20 ml LB-medium or the corresponding selection medium. These overnight cultures are used to start large-scale expression experiments (50 – 1000 ml) or to amplify plasmids. *E. coli* DH5α cells are used for plasmid amplification and *E. coli* BL21 strains for protein expression.

5.1.2 Storage

For the generation of glycerol stocks, 1 ml of the overnight culture is pelleted (15 min at 2000 rpm, RT, Microcentrifuge MiniSpin, Eppendorf). After discarding the supernatant, the cells are resuspended in 0.5 ml freezing medium (20% glycerol in LB medium) and stored at -80°C. Glycerol stocks remain functional for several years. To start an overnight culture, it is sufficient to pick some of the bacteria from the frozen glycerol culture surface using a sterile pipette tip and drop it into a flask with selection medium for inoculation.

5.1.3 Generation of competent cells

500 ml LB-Medium are inoculated with 1ml bacteria suspension and incubated at 37°C to an optical density (OD₆₀₀) of 0.5-0.7. The cell suspension is stored on ice for 30 min and pelleted by centrifugation (10 min, 4°C, 3000 rpm, Megafuge 2.0 Heraeus). Pellets are resuspended in 300 ml of sterile and cooled 0.1 M CaCl₂ solution and stored at 4°C for 1-2 days. The bacteria are pelleted as described above and resuspended in 20 ml of cold 0.1M CaCl₂ solution containing 10% glycerol. The cells are kept at 4°C for about 5 days and stored in 200 µl aliquots at -80°C for several months.

5.1.4 Transformation and selection

For the transformation of recombinant DNA into prokaryotic cells, 5 µl of the ligation sample or 5-10 ng of a purified plasmid is added to 200µl of competent cells and incubated on ice for 30 min. The cell pores are closed by heat shock (30-45 s at 42°C), and the suspension is cooled on ice for another 2 minutes. One ml of LB-medium is added to the cells, and the suspension is incubated on a shaker or overhead roller for 1 h at 37°C. After centrifugation (5 min at 5000 rpm, RT, Microcentrifuge MiniSpin, Eppendorf), 1 ml of culture medium is removed. The pellet is resuspended in the remaining medium. 50-100 µl of the suspension are plated on culture dishes with selection agar (LB medium, 1,5 % agar, 60µg/ml ampicillin, 10µg/ml tetracycline, 50µg/ml kanamycin or 7 µg/ml gentamycin, respectively) and incubated for 12-18 h at 37°C.

5.2 Cell culture techniques for mammalian cells

5.2.1 General procedures

All procedures with mammalian cells are carried out under sterile conditions.

Human fibroblasts, COS1-, COS7- and HeLa-cells are cultured in 10% DMEM (DMEM supplemented with 10% FCS, 1 u/ml streptomycin (and tylosine)). For the cultivation of murine myocytes, HAMs Nutrient Medium F-10 (E15-014, PAA-Laboratories GmbH) without glutamine supplemented with 10% FCS, 1 u/ml penicillin, and streptomycin is used. Jurkat cells are kept in RPMI 1640 with 10% FCS as a suspension culture.

Mature dendritic cells (DC 721) are kept as suspension culture in RPMI medium supplemented with 10% FCS. For immature dendritic cells VLE-RPMI containing 10% FCS is used. All cells are incubated at 37°C in a 5% CO₂ atmosphere. Adherent monolayers of cells are harvested with a trypsin/EDTA solution after removal of culture medium and washing with PBS. The process is stopped by the addition of a threefold excess of culture medium.

5.2.2 Storage of mammalian cells in liquid nitrogen

For long time storage in liquid nitrogen, the cells are kept in DMEM with 50% FCS and 9% DMSO to prevent the formation of intracellular ice crystals.

Cells are harvested as described above. The cell suspension is pelleted at 2000 rpm for 5 min (Centrifuge 5810 R, Eppendorf), the supernatant is removed, and the cells are resuspended in FCS. An equal volume of freezing medium (serum free medium with 20% DMSO) is added. 1 to 1.3 ml of cell suspension is transferred into freezing vials and deposited in a Nalgene freezing container. After storage at –80°C over night, the freezing vials are transferred into liquid nitrogen.

5.2.3 Preparation of FCS-coated cover slips

Sterile cover slips are placed into 24-wells and covered with 0.5 ml of inactivated FCS. After 2 min the FCS is removed and the cover slips are permitted to dry for 10-15 min with the lid of the culture dish open.

5.2.4 Treatment of adherent cells with pepsRNAs

Confluent cells from 75 cm² (25 cm²) dishes were harvested as described above, diluted with culture medium to 25 ml (8 ml) and plated in 6-well plates (1 ml per well) or on cover slips coated with FCS (0.5 ml per 24well). The dilution of the cells was adjusted to achieve approximately 80% confluency at the time of treatment (see Table 5-1). Plated cells are permitted to attach to the culture dish for at least 4 h or over night (18 h).

| | 6-well, 4h | 6-well, 18h | 24-well, 4h | 24-well, 18h |
|--------------------|------------|-------------|-------------|--------------|
| 25 cm ² | 4 ml | 8 ml | 8 ml | 16 ml |
| 75 cm ² | 12 ml | 25 ml | 25 ml | 50 ml |

Table 5-1 Volume of culture medium required to dilute confluent cells in order to be plated in 6-well or 24-well dishes and to achieve 80% confluency within 4 or 18 h. Volumes of cell suspension are 1 ml per 6-well and 0.5 ml per 24-well.

To avoid cross-reactions of the conjugate with free DNA, the cells are washed twice with serum free medium. The culture dishes are then filled with half the final volume of serum free medium (DMEM, 250 µl for 24well plates, 0,5 ml for 6well plates). The same amount of pepsRNA solution with a twofold concentration of conjugate in serum free medium is added in a dropwise fashion under constant rocking of the culture plate. This procedure provides an even distribution of the conjugate to all cells. After 15-30 min of incubation at 37°C the application medium is removed and replaced with growth medium (DMEM with 10% FCS).

5.2.5 Transfection of adherent cells with siRNAs

To compare pepsRNAs with conventional techniques, control experiments are carried out in which adherent cells are transfected with siRNAs using Lipofectamine 2000 (Invitrogen).

The cells are cultured in 6well-plates over night to reach a confluency of 80-90%.

Prior to treatment, 10µl of Oligofectamine are incubated for 5 min in 240 µl of OptiMEM for each sample. The siRNA stock solutions are diluted in OptiMEM to a total volume of 250 µl, added to the Oligofectamin solutions, and incubated for 20 min. In the meantime, the culture medium is removed and the cells washed twice with serum free medium. 1.5 ml of serum free medium are pipetted into each 6well-dish, and the transfection reagent is added dropwise under constant rocking of the culture plate. The cells are incubated at 37°C for 4 hours before the transfection solution is exchanged for culture medium.

5.2.6 Treatment of suspension cultures with pepsRNAs

5 ml of cell suspension (1×10^6 cells/ml) are pelleted (5 min, 1000 rpm, 20°C, Centrifuge 5810 R, Eppendorf) and the cells washed twice with serum free medium (RPMI 1640) by resuspending, centrifugation, and removal of the supernatant. The cells are then resuspended in 1 ml of serum free medium and subsequently mixed with 1 ml of 2x concentrated pepsRNA solution in serum free medium. After 20 min of incubation at 37°C, the cells are pelleted as described above and resuspended in culture medium (RPMI 1640 with 10% FCS).

5.2.7 Treatment of adherent cells with novel cell permeating molecules

One day prior to treatment, confluent cells are harvested from 25 cm² dishes by trypsin/EDTA, diluted 1:50 with culture medium and plated on cover slips coated with FCS (0.5 ml per 24well). The fluorescein or porphyrin coupled oligoamines or peptoids to be tested are dissolved in methanol to yield a 20 mM stock solution and further diluted with 10% DMEM to yield the respective application solution. To avoid differences due to a varying

content of methanol, dilutions of the stock solution in methanol are used to prepare test solutions of lower concentrations.

For treatment, the culture medium was removed and replaced by 0.5 ml of application solution. After varying incubation times at 37°C, the cells were cooled on ice and washed three times with 0.2% BSA in PBS+ and three times with PBS+. Without fixation, the cover slips were attached to the microscopy slides with 25µl of Mowiol 4-88 solution (10% in 10% glycerol 0.1M Tris), fixed with nail polish, and immediately evaluated by light and fluorescence microscopy (Zeiss Axiovert 35, 400x, filter set 15: $\lambda_{excit.} = 546nm$, $\lambda_{em} >590nm$; filter set 17: $\lambda_{excit.} = 485nm$, $\lambda_{em} = 515-565nm$).

5.2.8 Fixation of cells for microscopy

The cells are harvested one day after treatment, diluted 1:50, plated on FCS coated cover slips, and allowed to attach for at least 4 hours.

After treatment and appropriate times of incubation, the culture medium is removed and the cells thoroughly washed with pre-cooled PBS+. 0.5 ml of a 4% paraformaldehyde (PFA) solution in PBS+ is added per 24well, and the cells are incubated 30 min on ice. The PFA is quenched by incubation with a 50 mM NH₄Cl solution in PBS+ at room temperature for 5 min. The cells are washed three times with PBS+.

Alternatively, the pre-washed cells can be fixed with methanol and acetone by incubating with each pre-cooled solvent for 5 min on ice, starting with methanol. The cells are then washed three times with PBS+ to remove any solvent.

The cover slips are removed from the culture dish and attached to a microscopy slide with 25 µl of antibleach solution (25% phenylenediamine in 80% glycerol/PBS) and sealed with nail polish. The microscopy slides are stored at -20°C.

5.2.9 Preparation of cells grown on cover slips for immunofluorescence microscopy

For immunofluorescence experiments, the fixed and washed cells are washed twice with 0.2% BSA in PBS+. The BSA solution is exchanged against 1% Triton X-100 in 0.2% BSA solution, and after 10 min of incubation the cover slips are transferred into a moist chamber. The Triton/BSA solution is replaced by 25µl of primary antibody (AB1) solution in Triton/BSA and allowed to incubate at RT for 40-60 min or at 4°C overnight.

| <i>Primary antibody</i> | <i>Donor organism</i> | <i>Concentration</i> | <i>kindly provided by</i> |
|-------------------------|-----------------------|----------------------|---------------------------|
| anti-LaminA/C (human) | mouse | 1:50, 1:100 | M.Osborn, Göttingen |
| anti-HexA (human) | rabbit | 1:50, 1:100 | A.Hasilik, Marburg |
| anti-GCS (murine) | rabbit | 1:50 | R.Pagano, San Diego, USA |

Table 5-2 Antibodies used for immunofluorescence microscopy

The cover slips are washed 3x with PBS+ and 2x with 0.2% BSA solution as described above. The cells are incubated with 25-35 µl of secondary antibody (AB2) solution (anti-mouse-Alexa 688, 1:500; anti-rabbit-Alexa 688, 1:500) in Triton/BSA for 30 min excluding light to protect the dye-coupled antibody from photobleaching. The cover slips are thoroughly

washed with PBS+ and attached to a glass slide with mounting medium as described in 5.2.8.

5.3 DNA-Techniques

5.3.1 Photometric measurement of nucleic acid concentration

Concentration and purity of DNA, RNA and oligonucleotides are determined photometrically at 260 nm und 280 nm (Sambrook 1989) on SmartSpec™ 3000 Spectrophotometer (BioRad). Samples are diluted to keep the absorption in the range of $0.010 < A < 1.000$ to avoid errors due to a lack of sensitivity or saturation effects, respectively.

5.3.2 Separation of DNA by agarose gel electrophoresis

Separation by gel electrophoresis depends on different migration rates of negatively charged DNA molecules in an electric field. DNA samples are treated with a corresponding amount of 5x gel loading buffer and applied to an agarose gel (0,7-3% agarose in TAE) containing 0,1µg/ml ethidium bromide for DNA staining. Electrophoresis is performed at 10-100 mA at a voltage of about 1-5 V per cm of gel length.

Agarose gels are evaluated on a UV-transilluminator by the fluorescence of intercalated ethidium bromide. Fragment sizes are estimated in reference to a DNA-standard (1 kb ladder, Invitrogen).

5.3.3 Extraction of DNA from agarose gels

The DNA fragments of interest are excised from the gel and transferred to a microfuge tube. 300 µl of QG buffer (QIAquick gel extraction kit) are added per 100 mg of gel and the gel dissolved by heating to 50°C for 10 min. DNA-fragments >5kb are supplemented with 100µl isopropanol per 100 mg of gel, smaller fragments are directly applied to a MiniElute-column and centrifuged (1 min, 14,000 rpm, Microcentrifuge MiniSpin, Eppendorf). After washing with another 500µl of QG buffer and 750µl of pre elution buffer (PE) the columns are dried by centrifugation (1 min, 14,000 rpm), and the DNA eluted with 30 µl of EB (Elution Buffer).

5.3.4 Synthetic gene cloning

Lyophilized oligonucleotides (Sigma) are dissolved in RNase free water to yield a 25 or 100 nmol/µl solution. Equimolar amounts of complementary ssDNA solutions are pipetted together, heated to 80°C for 5 min and allowed to cool to room temperature over several hours. Oligonucleotides are designed with overlapping 12-17nt sequences of forward and reverse strands so that hybridization yields full-length double-stranded sequences that are sufficiently stable to be ligated to a vector and transformed into bacteria.

5.3.5 Enzymatic restriction of plasmids

Type II restriction endonucleases are utilized to clone DNA-fragments or to analyze recombinant vectors. Thus, the DNA is cleaved within the recognition sequence leading to

single stranded overhangs on both sides (sticky ends). Reaction conditions are adjusted according to the manufacturer's protocol for every given enzyme or set of enzymes. For analysis 1-5 µg DNA are incubated with 0.5-1 u enzyme in a total volume of 20 µl for 1-5 h at 37°C. For preparative purposes 5-10 µg DNA are cleaved with up to 20 u of enzyme in a total volume of 20-60 µl over night.

5.3.6 Ligation of DNA-fragments

The formation of phosphodiester bonds between matching sticky ends produced by a type II endonuclease is catalyzed by T4-ligase. The vector of interest is cleaved with corresponding restriction endonucleases, purified by gel electrophoresis and extracted from the gel as described in 5.3.2 and 5.3.3. 50-200 ng of the purified vector and a 2-100fold molar excess of insert-DNA with sticky ends corresponding to the cleavage sites are added together with 2 µl of 5x dilution buffer and 10 µl of ligase buffer yielding a typical volume of 18 µl. 2 µl (10u) of T4-ligase is added and the reaction mixture incubated at room temperature for 15-45 min.

5.3.7 Plasmid isolation from recombinant bacteria cells

The isolation of pure plasmid DNA is performed by alkaline lysis (Birnboim and Doly 1979) with subsequent purification by anion exchange chromatography according to the manufacturer's protocol. All reagents are taken from the QIAprep Mini Kit (QIAGEN). Bacteria from overnight culture are pelleted by centrifugation (15 min, RT, 4000 rpm, Megafuge 2.0 Heraeus) and resuspended in 0.25 ml of resuspension buffer P1. The cells are lysed by adding 0.25 ml alkaline buffer P2, and the reaction is stopped after 3-5 min by the addition of 0.35 ml neutralizing buffer N3. Precipitated proteins and chromosomal DNA are pelleted by centrifugation (10 min, RT, 14.000 rpm, Microcentrifuge MiniSpin, Eppendorf) and the plasmids purified from the supernatant by anion exchange chromatography according to the manufacturer's protocol.

5.3.8 PCR : *in vitro* amplification of DNA

PCR (polymerase chain reaction) is a method for the selective *in vitro* amplification of DNA. It is based on repeated cycles of denaturing of template DNA, annealing of sequence specific sense and antisense oligonucleotides, and elongation of the reverse strand by a thermostable DNA-polymerase from the thermophile *Thermus aquaticus* (Taq-polymerase).

| | | | |
|-------------|---------|----|------------------------|
| Mastermix 1 | 1.0 | µl | primer 1 (20 pmol) |
| | 1.0 | µl | primer 2 (20 pmol) |
| | 1 | µl | dNTP solution (10 mM) |
| | 22-23 | µl | water |
| Mastermix 2 | 0.2-1.0 | µl | template DNA (5-50 ng) |
| | 5 | µl | buffer 2 (10x) |
| | 0.5-1.0 | µl | Taq polymerase |
| | 19 | µl | water |

The mastermixes are added together on ice and placed on a thermocycler (PTC-200, Biozyme Diagnostic) to run the amplification program:

| | | | |
|-----------------|------|----------|-------------|
| hot start: | 94°C | 2:00 min | } 35 cycles |
| denaturing: | 94°C | 0:30 min | |
| annealing*: | 58°C | 0:30 min | |
| elongation: | 68°C | 2:00 min | |
| last extension: | 68°C | 5:00 min | |

The annealing temperature is chosen according to the T_m of the primer-template complex. Elongation may be extended from 0:30 to 3:00 min depending on the length of the target sequence (1min per 1000 bp). PCR-products are purified from reagents and side products by agarose gel electrophoresis and gel extraction.

5.3.9 Mutagenesis-PCR

Point mutations or single base insertions in expression vectors can be corrected by mutagenesis-PCR. Only one primer is used that comprises ~20nt of the sequence to be corrected with the appropriate base exchanged or excised. For the correction of synthetic genes the full-length oligonucleotides were used as primers.

| | | | |
|-------------------|-------|----|--------------------------------|
| reaction mixture: | 0.5-1 | µl | template vector (50-100 ng) |
| | 1 | µl | mutagenesis primer |
| | 1 | µl | dNTPs (25 mM) |
| | 5 | µl | 10x Pfu buffer |
| | 1 | µl | Turbo Pfu polymerase (2.5u/µl) |
| | 42 | µl | water |

The reaction mixture is prepared on ice and placed on a thermocycler (PTC-200, Biozyme Diagnostics) to run the mutagenesis program:

| | | | |
|-----------------|---------|-----------|-------------|
| hot start: | 95°C | 0:30 min | } 30 cycles |
| denaturing: | 95°C | 0:30 min | |
| annealing*: | 55/58°C | 1:00 min | |
| elongation: | 68°C | 10:00 min | |
| last extension: | 68°C | 10:00 min | |

Elongation is adjusted to the length of the target sequence (2min per 1000 bp). The annealing temperature has to be modified according to the primer sequence. Best results were obtained with 55°C for AntP and 58°C for Tat. PCR-products are incubated for 1h with Dpn I to degrade methylated DNA templates, and 10-20µl are immediately transformed into *E. coli* DH5α.

5.4 RNA techniques

5.4.1 Isolation of RNA

Total-RNA is isolated according to the RNeasy protocol (QIAGEN). The culture medium is removed and the cells washed twice with PBS. 600µl RTL buffer supplemented with 6µl β-mercaptoethanol are added. The cells are removed with a rubber policeman and transferred into a microfuge tube. DNA is destroyed by homogenizing the lysates 5-8 times through a G20 needle. After mixing with 600 µl of 70% ethanol, the lysates are transferred onto RNeasy microspin columns and centrifuged for 15s at 10,000 rpm (Microcentrifuge MiniSpin, Eppendorf). The flow-through is discarded and the columns washed with 700 µl of RW1 buffer by centrifugation. The collection tube is replaced and the columns are treated twice with 500 µl RPE buffer and centrifuged. The flow-through is discarded and the columns centrifuged at 14,000 rpm for 2 min to remove all residual buffer. The total RNA is eluted with 50µl RNase free water and collected in Rnase-free microfuge tubes.

5.4.2 Separation of dsRNA

RNA-molecules are separated via gel electrophoresis under RNase free conditions on 1% - 1.5% agarose in TAE with 40µl/l ethidium bromide of gel for detection (see 5.3.2).

5.4.3 RT-PCR

To obtain cDNAs from mRNA or to estimate the levels of mRNA in cells, RNA transcripts can be converted into copy-DNA (cDNA) by reverse transcriptase. In subsequent PCR steps, the cDNA strands are amplified to yield detectable levels. Prior to RT-PCR, RNA templates are heated to 75°C for 5 min to denature the RNAs, and cooled on ice to prevent re-annealing. RT-PCRs are carried out with the Titan-Kit (Roche) according to the manufacturer's protocol.

| | | | |
|--------------------|-----|----|--------------------------|
| Mastermix1: | 1 | µl | dNTPs (10 mM) |
| | 1 | µl | primer1 (25 µM) |
| | 1 | µl | primer2 (25 µM) |
| | 2.5 | µl | DTT (100 mM) |
| | 0.5 | µl | RNasin (40u/µl) |
| | 10 | µl | template RNA (100 µg/ml) |
| | 14 | µl | RNase free water |

| | | | |
|--------------------|-----|----|--------------------|
| Mastermix2: | 10 | µl | RT-PCR buffer (5x) |
| | 5 | µl | RNase free water |
| | 0.8 | µl | enzyme-mix |

The two mastermixes are combined in a 500µl tube, placed in a thermocycler (PTC-200, Biozym Diagnostics), and incubated according to the following program:

| | | | |
|------------------------|------|-----------|-----------|
| reverse transcription: | 50°C | 30:00 min | |
| denaturation: | 94°C | 00:30 min | 30 cycles |
| annealing: | 62°C | 00:45 min | |
| elongation: | 68°C | 01:00 min | |
| last extension: | 68°C | 10:00 min | |

5.4.4 *In vitro* generation of 5'-thiol-modified siRNAs with T7-polymerase

The antisense strand is generated according to the RiboMAX-protocol (Promega). To generate the 5'-thiol-modified sense strand an 8fold excess of GSMP over the non-modified NTPs is added to the reaction mixture. 1-2µl of RNasin are added to compensate for the non-RNase-free synthesis procedures. GSMP is synthesized as described in chapters 3.1.1 and 3.1.2. The purified product is dissolved in 10 mM Tris-HCl, pH 7.5. Following the *in vitro* transcription reaction, DNase is added to both reaction mixtures to degrade the DNA templates. Also, 4 µl of CIP are added to remove 5'-triphosphates and to release the thiol-function from the 5'-thiophosphate group of the sense strand. After 15 min of incubation at 37°C, the 21mers are precipitated and dried according to the manufacturer's manual. The RNA pellet is dissolved in RNase-free water, and the concentration determined photometrically. Equimolar amounts of sense and antisense strand are pipetted together, supplemented with the corresponding amount of 10x annealing buffer, heated to 75°C for 5 min, and allowed to cool to RT over several hours for hybridization.

5.4.5 Reduction of homodimers of 5'-thiol-modified siRNAs

Under oxidizing conditions, free thiol groups may react to form disulfide bonds that link two monomers together. To enable the coupling of siRNA and CPPs, these spontaneously formed homodimers have to be reduced.

Synthetic siRNA aliquots of 20 nmol are dissolved in 120 µl of RNase free 0.1 M DTT solution (Titan-Kit, Roche). Enzymatically generated siRNAs are supplemented with ¼ of the total volume of 100 mM DTT-solution (Roche). Both reaction mixtures are incubated at 37°C for at least one hour.

To remove the DTT, the reduced siRNAs are purified by gel filtration (MicroSpin™ G-25 Columns, AP-Biotech) according to the manufacturer's manual.

5.4.6 Coupling of synthetic siRNA and CPP

After over night incubation with DTT, synthetic thiol-modified siRNAs are purified by gel filtration via Microspin™ G-25 columns (AP-Biotech). In the last step of the procedure, the siRNA aliquot is eluted into an equimolar amount of the activated peptide. The reaction mixture is incubated 1 h at 37°C.

5.4.7 Coupling of enzymatically synthesized siRNA and CPP

After gel filtration of the enzymatically synthesized siRNA, the concentration is determined to avoid errors due to free nucleotides. An equimolar amount of peptide solution is diluted in EB to the same volume and both solutions are pipetted together under argon. Precipitate forming at high concentrations due to aggregation of pepsRNAs can be dissolved by the addition of NaCl-solution to a final concentration of up to 400 mM.

5.4.8 Radiolabelling of siRNAs

T4-kinase attaches the terminal phosphate residue of [³²P]- γ -ATP to free 5'-hydroxyl-groups of oligonucleotides. The lyophilized enzyme is dissolved in 25 μ l of water. After 5 min of quelling, 50-100 pmol of siRNA and water are added to yield 24 μ l. After the addition of 1 μ l of [³²P]- γ -ATP (10 mCi/ μ l) the reaction mixture is incubated at 37°C for 30 min and the reaction stopped with 5 μ l of 250 mM EDTA. Residual ATP is removed by gel filtration (MicroSpin™ G-25 Columns, AP-Biotech) according to the manufacturer's manual.

5.4.9 Analysis of siRNAs on sequencing gels

siRNAs are radioactively labeled and run on a 25 cm x 55 cm 10% TBE-urea sequencing gel of 0.1 mm thickness. The Macromould glass plate is prepared with 3 x 200 μ l of binding-silane and the thermoplate is coated with 1 ml of repel silane. Both plates are thoroughly cleaned with ethanol to remove an excess of silane.

The 12% gel is prepared by dissolving 42g of urea in 10 ml of 10x TBE and 25 ml of water by gentle heating. After cooling down, 30 ml of 40% acrylamide solution is added and the solution filtered to remove undissolved solid. For polymerization and cross-linking, 0.8 ml of APS solution and 40 μ l of TEMED are added. Prior to running, the gel is heated to 50°C via the thermoplate of the gel chamber, and 3000V/28mA are applied for 30 min to equilibrate the gel with the TBE buffer.

The 10 μ l samples are prepared by adding 10 μ l of formamide loading buffer, heating to 95°C for 5 min. The samples are placed on ice. 3-6 μ l of sample are loaded and the gel is run at 3000 V at 21-27 mA. The gel is fixed by soaking in 10% acetic acid for 30 min, washed with water for 5 min, and dried at 70°C for 45-60 min. The detection of the radioactivity is performed using a phosphorimager screen (BAS III, Fuji). Radioactivity screens are read out on a Bas reader (Fujix Bas 1000, Fuji) and the results evaluated on Tina 2.0 software.

0.5M NaOH is used to remove the gel and binding-silane from the carrier-glass plate.

5.5 Protein techniques

5.5.1 Preparation of protein samples

Protein samples from bacterial expression cultures or plated mammalian cells are prepared for SDS-PAGE in a reducing SDS-containing buffer according to Laemmli: 1 ml of suspension culture is pelleted by centrifugation (5 min, 14,000 rpm, Microcentrifuge MiniSpin,

Eppendorf) and the pellet is resuspended in 0.5 ml of 1x Laemmli buffer. Adherent cells are directly treated with 1x Laemmli buffer (0.5 ml per 6well), detached from the culture plate with a rubber policeman and transferred into a microfuge tube.

Purified protein, peptide and pepsRNA solutions are supplemented with appropriate amounts of 5x Laemmli buffer. After resuspension, the samples are boiled at 95-100°C for 5 min. To separate the proteins, 15-20 µl per sample are applied to 10-12.5% SDS-PAGE at 70-110 V.

5.5.2 SDS-PAGE

Proteins are separated in non-reducing and reducing gels (10-20%) according to Laemmli. Electrophoresis is performed in 6x8 cm vertical gels of 0.5-0.75 mm thickness in a Hoefer Minigel apparatus (Hoefer Mighty Small 250). Gels are run at 70-110 V.

| (per gel) | stacking gel, 5% | separating gel, 10% | separating gel, 12.5 % | separating gel, 20% |
|-----------------------|---------------------|------------------------|---------------------------|------------------------|
| acrylamide (31%) | 0.5 ml | 3.35 ml | 4.2 ml | 5.0 ml (40%) |
| Tris-HCl (pH 6.8, 1M) | 0.325 ml | - | - | - |
| Tris-HCl (pH 8.8, 1M) | - | 5.0 ml | 5.0 ml | 5.0 ml |
| Water | 2.06 ml | 1.5 ml | 0.64 ml | - |
| SDS (20%) | 30 µl | 0.1 ml | 0.1 ml | 0.1 ml |
| TEMED | 3 µl | 10 µl | 10 µl | 10 µl |
| APS (10mg/ml) | 30 µl | 50 µl | 50 µl | 50 µl |

5.5.3 Protein staining with Coomassie Brilliant Blue R250

For protein detection, SDS-PA gels are boiled in a 0.25 % Coomassie Brilliant Blue R250-staining solution for 2 min in a microwave or incubated at room temperature over night. Excess dye is removed by repeated boiling in water in a microwave or destaining for 4-6h using destaining solution. Gels are evaluated on a transilluminator.

5.5.4 Silver staining of protein gels

The gel is fixed in formaldehyde solution for 1-24h. After washing 3x 20min with 50% ethanol, the gel is incubated in sodium thiosulfate solution (200mg/l) for 1min and washed 3x 20s with bidistilled water. The gel is soaked 20min in silver solution and washed 2x 20s with bidistilled water. The gel is incubated in developing solution until the first protein bands can be seen, rinsed with water and soaked 10 min in stop solution. The developed gel is stored in wash solution for >20min.

5.5.5 Western blot

Protein samples are separated via SDS-PAGE and transferred to a PVDF membrane by wet blotting (Towbin et al, 1979). Before blotting, the PVDF membrane is soaked in methanol and equilibrated in transfer buffer (10 mM CAPS, pH11, 10% MeOH). The membrane is placed

on the gel and covered with filter cardboard and sponge pads both soaked in transfer buffer. The assembly is enclosed in the blotting apparatus (Mini Protean II, BioRad) filled with cooled transfer buffer. Blotting is performed for 30 min at 400mA and >100V. After the protein transfer, the PVDF membrane is saturated with 5% milk in TBS-T for 1-2h at RT or overnight at 4°C. For the identification of the proteins, the membrane is incubated in a solution of the appropriate primary antibody in milk buffer for 1h at RT or overnight at 4°C on an overhead rotor.

| <i>Primary antibody</i> | <i>Donor</i> | <i>Concentration</i> | <i>kindly provided by</i> |
|-------------------------|--------------|----------------------|---------------------------|
| anti-LaminA/C (human) | mouse | 1:1000, 1:250 (ON) | M.Osborn, Göttingen |
| Anti-Lamin A/C (murine) | rabbit | 1:1000 | M.Osborn, Göttingen |
| anti-HexA (human) | rabbit | 1:1000, 1:100 (ON) | A.Hasilik, Marburg |
| Anti-GCS-1,2 (human) | rabbit | 1:1000 | R.Pagano, San Diego, USA |

Table 5-3 Antibodies used for Western blotting (ON = incubation overnight at 4°C)

The membrane is washed 3x 10 min TBS-T and incubated with the appropriate secondary antibody (anti-mouse-HRP 1:1000, anti-rabbit-HRP, 1:10000, HRP = horse radish peroxidase) in milk buffer for 1 h at RT. After further washing steps in TBS-T, the membrane is incubated for 1 min with 1 ml of chemiluminescence substrates A und B (1:1; LumiGlo, BioRad). The chemiluminescence of the secondary antibody is detected by a photographic film (10s to 1 min depending on chemoluminescence intensity).

5.5.6 Quantitative measurement of protein concentrations

Proteins are detected by the Bradford reagent that is based on the blue stain of Coomassie blue in acidic solution upon reaction with proteins. In a range between 0.1 to 20µg/ml the protein concentration can be determined photometrically according to the Lambert-Beer law. To this means, a calibration curve is calculated from the absorptions obtained from 10 standard solutions ranging from 0.0 to 2.0 µg/ml.

20µl of standard or protein sample at varying dilutions are added to 200µl of Bradford reagent diluted 1:4 in PBS.

Absorption measurements and calculation of sample concentrations are carried out photometrically on a Multiskan Ascent readout instrument (Labsystems).

5.5.7 Protein expression in bacteria

All used expression vectors contain the promoter of the lac-operon, so that the expression of the recombinant gene can be induced by the synthetic lactose analogon IPTG (isopropyl-thio-galactopyranoside). 20 ml (400 ml) of LB are inoculated with 5 ml (20 ml) of overnight culture and grown at 37°C to an optical density of OD₆₀₀ = 0.6 to 0.7 and stored on ice for 15-30 min. Protein expression is induced by addition of 40µl (800 µl) 100 mM IPTG solution and incubated at 37°C (30, 22 or 17°C for TEV-fusion proteins). Samples are taken prior to induction, after 1, 2, and, 4 h and after incubation over night and analyzed by SDS-PAGE.

Alternatively, expression can be performed in TB or SOC medium. Lower temperatures (down to 17°C), smaller amounts of IPTG, and shorter expression times may prevent the formation of inclusion bodies.

5.5.8 Preparation of native GST-fusion proteins (pGEX protocol)

After overnight expression at 37°C, recombinant BL21 cells are harvested by centrifugation (15 min, 4000 rpm, 4°C, Megafuge 2.0, Heraeus). The supernatant is discarded and the pellets resuspended in 1ml/20ml (expression culture) of pGEX lysis buffer on ice, and 60µl of a 100 mg/ml solution of lysozyme in pGEX lysis buffer is added. After 20 min incubation on ice, 5 µl of DNase (1u/µl, Ribomax Kit, Promega) is added to degrade genomic DNA, and the cell suspensions are incubated for another 20 min. The cell suspensions are homogenized using a Potter Elvogen Homogenizer (Potter S, B. Braun Melsungen AG) and centrifuged (50 min, 14,000 rpm, 4°C, Centrifuge 5402, Eppendorf). Protein samples taken from supernatant and pellets are prepared in 5x and 1x Laemmli, respectively, for SDS-PAGE.

5.5.9 Preparation of native GST-fusion proteins (modified protocol)

After overnight expression at 37°C, recombinant BL21 cells are harvested by centrifugation (15 min, 4000 rpm, 4°C, Megafuge 2.0, Heraeus). The supernatant is discarded and the pellets resuspended in 1ml/20ml (expression culture) of pGEX lysis buffer at room temperature, and 20µl of a 100 mg/ml solution of lysozyme in pGEX lysis buffer is added. After 20 min incubation at room temperature, 6 µl of DNase (1u/µl, Ribomax Kit, Promega) is added to degrade genomic DNA, and the cell suspensions are incubated for another 20 min. The cell suspensions are homogenized using a Potter Elvogen Homogenizer (Potter S, B. Braun Melsungen AG). GST-Tat homogenates are sonicated (3x 10s-blasts, 200W, 20 MHz, 15s intervals) and incubated for 30 min at 37°C, while GST-AntP homogenates are incubated for 45 min at 37°C. After centrifugation (50 min, 14,000 rpm, 4°C, Centrifuge 5402, Eppendorf), protein samples are taken from the supernatant and pellets to be prepared in 5x and 1x Laemmli, respectively, for SDS-PAGE.

5.5.10 Preparation of native TEV-protease

Cells are grown in 20ml LB to $OD_{600} = 0.7$ and expression is induced with 80 µl of IPTG (100 mM). Expression is carried out at 37°C over night. Protein samples are taken and cells are harvested by centrifugation (20 min, 4000 rpm, 4°C, Megafuge 2.0, Heraeus). The pellets are resuspended in 1 ml of freshly prepared lysis buffer (per 20 ml of expression culture) containing DNase and lysozyme. After 30 min of incubation on ice, cells are lysed by three freeze and thaw cycles, 11 µl Triton-X 100 are added (yielding a final concentration of 1%) and the suspension is vortexed for 1 min. Alternatively, cell suspensions are homogenized using a Potter Elvogen Homogenizer (Potter S, B. Braun Melsungen AG) and centrifuged (50 min, 14,000 rpm, 4°C, Centrifuge 5402, Eppendorf). Protein samples taken from supernatant and pellets are prepared in 5x and 1x Laemmli, respectively, for SDS-PAGE (Lucast et al. 2001).

5.5.11 Preparation denaturing of TEV-protease from inclusion bodies

If the main fraction of the recombinant protein is found in the pellet, inclusion bodies have formed from which the denatured protein needs to be purified and subsequently refolded. The pelleted inclusion bodies (from 20ml of expression culture as obtained in 5.5.8, 5.5.10 or 5.5.15) are resuspended in 1 ml of denaturing resuspension buffer (per 20 ml expression culture) and heated to 65°C on a thermomixer for 15-20 min (Thermomixer 5436, Eppendorf). After centrifugation (20 min, 14,000 rpm, 4°C, Centrifuge 5402, Eppendorf) the supernatant is transferred into a dialysis chamber (cut-off = 12-14,000 Da) and dialyzed over night against pGEX-Lysis buffer or Ni-NTA lysis buffer, respectively (Lucast et al. 2001).

5.5.12 Purification of GST-fusion proteins on glutathione-sepharose

The supernatant containing the GST-fusion proteins is incubated with 25 µl (per 20 ml of expression culture) of a slurry of GST-sepharose beads equilibrated in pGEX lysis buffer. After 4 h of incubation at room temperature (or overnight incubation at 4°C, respectively), the supernatant is removed by centrifugation (5 min, 1500 rpm, Microcentrifuge MiniSpin, Eppendorf) or filtration and the beads washed with a 10x volume of pGEX pre-elution buffer to remove non-specifically bound proteins. GST-fusion proteins are obtained by eluting 3-8x with 50 µl of elution buffer.

The purity of the eluates is verified by SDS-PAGE and the protein concentration determined as in 5.5.6. Eluates containing recombinant TEV-Protease are subsequently dialyzed against TEV storage buffer.

5.5.13 Preparation of sepharose beads

GST-Sepharose beads are stored as a suspension in twice the volume of 20% ethanol. Prior to use, the resin is sedimented by 3 min centrifugation at 1500 rpm (Microcentrifuge MiniSpin, Eppendorf). The supernatant is carefully removed and the beads resuspended in the 5-10fold volume of the buffer corresponding to the protein solution to be purified. This procedure is repeated twice to ensure a sufficient buffer exchange.

5.5.14 Regeneration of GST-sepharose beads

Used GST-Sepharose resin is pooled and after removal of the supernatant buffer resuspended in a 10x volume of pGEX high-pH buffer. The buffer is removed by 3 min centrifugation at 1500 rpm and removal of the supernatant or by filtration via filter columns if larger amounts are to be regenerated. Likewise, 10 volumes of pGEX low-pH buffer are applied to the resin and the alternating treatment with both buffers is repeated twice. For storage, the last regeneration buffer is replaced by 20% ethanol in water as described under 5.5.13.

5.5.15 Native preparation of His₆-TEV from *E. coli*

After protein expression over night at 37°C, 1 ml of bacteria suspension is prepared as a control for SDS-PAGE. The remaining cells are harvested by 15 min of centrifugation at 4,000 rpm and 4°C (Megafuge 2.0, Heraeus). The supernatant is discarded and the pellet resuspended in 1 ml of native lysis buffer (per 20 ml of expression culture) on ice. 2 mg of lysozyme (or 20 µl of a 100 mg/ml solution of lysozyme in lysis buffer) and 6 µl of DNase solution (1 µg/ml, RiboMAX-Kit, Proligo) are subsequently added, and after each addition the suspension is incubated for 20 min on ice. The cell suspensions are homogenized by a bug crusher (Potter S, B. Braun Melsungen AG) and centrifuged 60 min with 14,000 rpm at 4°C (Centrifuge 5402, Eppendorf). Protein samples are taken from pellet and supernatant and analyzed by SDS-PAGE to determine which fraction contains the recombinant protein.

5.5.16 Denaturing preparation of His₆-TEV from *E. coli*

After protein expression over night at 37°C, 1 ml of bacteria suspension is prepared as a control and prepared for SDS-PAGE. The remaining cells are harvested by 15 min of centrifugation at 4,000 rpm and 4°C (Megafuge 2.0, Heraeus). The supernatant is discarded and the pellet resuspended in 1 ml of denaturing lysis buffer (per 20 ml of expression culture) and incubated for 1h on an overhead roller at room temperature. The lysate is centrifuged (50 min, 14,000 rpm, 4°C, Centrifuge 5402, Eppendorf) and protein samples are taken from pellet and supernatant.

Alternatively, the lysates are prepared according to Lucast (Lucast et al. 2001) and after centrifugation the pellets are dissolved in denaturing guanidinium chloride buffer as described for GST-TEV in 5.5.10 and 5.5.11.

5.5.17 Purification of His₆-fusion proteins on Ni-NTA-sepharose

Analytic expression (20 ml)

Ni-NTA microspin columns (QIAGEN) are equilibrated with 600 µl of lysis buffer by centrifugation (2 min, 2,000 rpm, 4°C, Centrifuge 5402, Eppendorf). 600µl of the protein containing supernatant are applied to the Ni-NTA columns up to three times until all supernatant has been passed through the columns by centrifugation (2 min, 2,000 rpm, 4°C, Centrifuge 5402, Eppendorf). 20 µl protein samples are taken from the flow-through and prepared for SDS-PAGE. The columns are washed twice with 600 µl of Ni-NTA wash buffer, and the His₆-fusion protein is eluted with 2x 50 µl of elution buffer. A dilute sample of the eluate is prepared for SDS-PAGE.

Large scale expression (120-1000 ml)

The supernatant is incubated for 4 h at room temperature or over night at 4°C with 25µl/ml of Ni-NTA slurry equilibrated in lysis buffer. The supernatant is removed by centrifugation at 1500 rpm or filtration, and the beads are washed with a 10x volume of wash buffer to remove non-specifically bound proteins. His₆-fusion proteins are obtained by eluting 3x with 50 µl of elution buffer.

The purity of the eluates is verified by SDS-PAGE and the protein concentration determined as in 5.5.6. Eluates containing recombinant TEV-Protease are subsequently dialyzed against TEV storage buffer.

5.5.18 Dialysis

Protein solutions are dialyzed against a 20-100fold volume of exchange buffer at 4°C over night. Dialysis tubing is chosen according to the size of the respective protein and prepared by boiling twice in 1l of sodium hydrogencarbonate/EDTA buffer for 10 min and rinsing extensively with distilled water to remove the buffer. Ready-to-use dialysis tubing can be stored in 50% EtOH at 4°C.

Alternatively, dialysis of small volumes can be carried out with Spin-Concentrators (Vivaspin 500 µl Concentrator, Vivascience) of varying pore sizes (GST-TEV: < 50,000 Da, His-TEV: < 10,000 Da) by centrifugation (6 min, 12,000 rpm, Centrifuge 5415 C, Eppendorf) and repeated buffer exchange.

5.5.19 Cleavage of GST-fusion peptides with TEV

300-400 µM of GST-peptide substrate in Elution buffer (10 mM glutathione, 50 mM Tris-HCl pH 8.0) are supplemented with an appropriate amount of EDTA to yield a 1 mM solution. 1.5µl 100 mM DTT, an appropriate amount of 20x TEV buffer, and either 5-10 µl of HisTEV (S219V) protease or 1 µl of AcTEV protease (invitrogen) are added. The reaction mixture is filled up with water to 100 µl and the reaction allowed to proceed at 30°C for 6-24h h. To analyze the amount of cleaved peptide, 20 µl samples are taken from the reaction mixture and analyzed by 15% SDS-PAGE. To examine the amounts of GST-CPP and GST 1ml samples are analyzed by 12% SDS-PAGE.

5.5.20 Handling of Penetratin™

Commercially available penetratin (Qbiogene) is delivered in batches of 500 µg in lyophilized form. After short centrifugation to clear the substance from the lid, 500µl of bidistilled water are added and the peptide is allowed to dissolve slowly. The 0.27 mM peptide solution is distributed into 50µl aliquots and stored at -80°C. Repeated freeze-and-thaw cycles are to be avoided. Fractions of the aliquots are taken under a stream of argon to avoid the contact of oxygen with the sensitive peptide.

5.6 Chemical syntheses

5.6.1 Thin layer chromatography

To control the completion of a reaction or to monitor column chromatography samples of the reaction mixture, chromatography fractions are analyzed by thin layer chromatography (TLC) on silicagel-aluminium plates (2.5x6.5 cm or 7x5 cm respectively). Prior to each run, the liquid phase was allowed to equilibrate in the TLC chamber to obtain an atmosphere saturated with the applied solvents. TLC plates were dried and evaluated either under UV-light or by staining with molybdophosphoric acid (10% in methanol).

5.6.2 NMR spectroscopy

All NMR-spectra were recorded on Bruker spectrometers DPX300 and DPX400 at room temperature. ^1H -spectra were obtained at 300 and 400 MHz, ^{13}C -spectra at 75 and 100 MHz, respectively. Chemical shifts are reported in parts per million [ppm] in reference to the ^1H - or ^{13}C chemical shift of tetramethylsilane (TMS). All spectra were processed with WinNMR 6.1 (Bruker). If no internal standard was used, the signal was calibrated according to the signal of DMSO ($\delta(^1\text{H}) = 2.49$ ppm, $\delta(^{13}\text{C}) = 39.7$ ppm) or DHO ($\delta(^1\text{H}) = 4.79$ ppm). The signals were assigned to protons and carbon centers according to the numeration depicted in the corresponding schemes. Multiplet structures are named with the following abbreviations: s (singlet), d (doublet), t (triplet), q (quartet), dd (doublet of doublets), td (triplet of doublets) m (multiplet), br (broadened signal). The 5'-carbon is the only secondary carbon in the guanosine system, so that only one negative signal is detected in DEPT-135 spectra, which is indicative for the success of each reaction.

5.6.3 Long-term NMR measurements

Long-term ^1H NMR experiments to estimate the rate of transformation from the 5'-iodo-guanosines to the corresponding 2,5'-cycloguanosines were carried out on a Bruker spectrometer DPX500 at 500 MHz. The dried compounds were dissolved in d_6 -DMSO immediately prior to measurement. Spectra were recorded in intervals of 30 min for 24 h. The sets of 49 spectra were phase corrected and integrated by the serial processing option of WinNMR 6.1 (Bruker). All integrals were calculated with reference to the DMSO signal. Further evaluation was carried out under Microsoft Excel 2000. The integrals of significant iodide signals, that showed no overlap with other signals over the course of the experiment, were normalized to the initial value and averaged. Correspondingly, the integrals of significant signals of the cyclized product were normalized to the end value. The averages were plotted against time with the recording of the first spectrum as $t(0)$. To estimate the rate constant k , the normalized integrals of the iodide (C_{iodide}) were plotted as their negative natural logarithm, $-\ln(C_{\text{iodide}})$, against time. k was obtained as the slope of the best fit straight line. To estimate the deviation σ from k , two more straight lines were drawn with the slopes $k+\sigma$ and $k-\sigma$ so that $\sim 2/3$ of the data points were included between these lines.

5.6.4 Mass spectroscopy

All FAB (fast atom bombardment) mass spectra were recorded in meta-nitrobenzoic acid (mNBA) matrix on a Kratos MS 50 (70 eV) instrument, Thermo Quest Finnigan MAT 95 XL. EI (electron impact ionization) spectra were recorded on a Kratos MS50 (I) instrument, ThermoQuest Finnigan MAT 95 XL (II). High-resolution (HR) masses were derived from EI spectra.

ESI (electron spray ionization) mass spectra of GSMP were measured on Micromass Q-TOF-2™ from 100 pmol/μl GSMP solutions in 99.5% methanol in the negative mode.

MALDI (Matrix assisted laser desorption ionization) spectra were obtained with a HiResMALDI FT-ICR (Ionspec, Lake Forrest, CA; 7 T magnet, pulsed laser 337 nm). pepsRNAs were measured from a matrix of trihydroxyacetophenone (THAP) in the negative mode against a standard deoxyoligonucleotide of known mass. Samples were treated with ammonium acetate prior to treatment to exchange sodium and potassium ions for ammonium ions, so that narrower peaks are obtained.

5.6.5 Anion exchange chromatography

Triethylamine bicarbonate (TEAB) buffers are obtained by dissolving the appropriate amount of HPLC grade triethylamine in bidistilled water and bubbling the cooled solutions with carbon dioxide until a pH of 7.5 is reached. Buffers have to be stored and processed at 4°C to avoid the formation of bubbles. The pH of the buffers is measured with indicator paper prior to column chromatography.

The DEAE Sephadex A-25 column (CV = 34 ml; Amersham Bioscience) is prepared by washing with at least 10 column volumes (CVs) of low salt buffer (0.01 M, pH 6.9), 7 CVs of high salt buffer (1.0 M, pH 7.5) and 10 CVs of low salt buffer. The column was built into the FPLC instrument (ÄKTA-FPLC, AP-Biotech), that is set in an air-conditioned closet at 4°C. The set-up was equilibrated with low salt buffer over night at 0.3 ml/min. The crude product was dissolved in low salt buffer and centrifuged (1min, 14 000 rpm, 4°C, Centrifuge 5402, Eppendorf) to remove any precipitate. 0.5 - 2.0 ml are loaded onto the column over a 2ml-loop and the chromatography is run according to the following program:

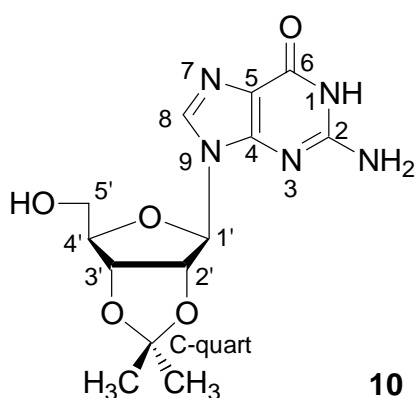
| | |
|-----------------------|------------------|
| Flow rate: | 1.0 ml/min |
| Flowthrough: | 12.5 ml |
| Loop injection: | 12.5 ml |
| Start Fractionation | |
| Fraction size: | 12.5 ml |
| Clean with: | 12.5 ml |
| Gradient length: | 20 CV |
| Target Concentration: | 60 % 1.0 M TEAB |
| Wash column with: | 100 % 1.0 M TEAB |
| | 1 CV |
| End Program | |

5.6.6 Reversed phase HPLC

The analytical RP-18 column is built into the HPLC instrument (EttanLC, Amersham Bioscience) and prepared by running a gradient from 0% to 100% methanol over 20 min, washing with methanol for 20 min, and running a gradient back to 0% methanol over 20 min at a flow rate 0.5 ml/min.

The crude product is dissolved in bidistilled water and centrifuged (1min, 14 000 rpm, 4°C, Centrifuge 5402, Eppendorf) to remove any precipitate. After preliminary experiments to determine the maximum capacity of the column, up to 0.8 ml are loaded with a 1ml loop. Due to the short elution times and the need to exchange collection vessels and store product fractions immediately on ice, the run is performed manually. After injection of the sample the auto-sampler is started and fractions of 0.2 ml collected. At flow rates of 0.8 ml/min the sample and side products are eluted with bidistilled degassed water. The run is monitored by a photocell at 280 and 260 nm, and the elution of the thiophosphate is detected by a conductivity cell. Several runs are necessary to purify 5-10 ml of crude product solution obtained from one reaction on an analytic column.

5.6.7 2',3'-O,O-Isopropylidene-guanosine, (10)

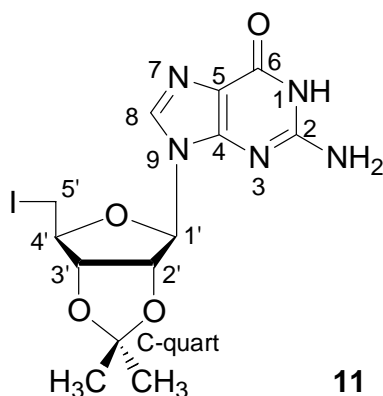


10

8.99 g (31.8 mmol) of guanosine **9** are suspended in 600 ml of acetone. 3 ml of aqueous 70% perchloric acid are added and the clear reaction mixture is stirred for 4 h at room temperature. The reaction is stopped by the addition of 3 ml of 25% aqueous ammonia solution resulting in the formation of a white precipitate. The solvent is removed under reduced pressure without previous filtration and the white residue stirred with 40 ml of water over night. The residue is filtered and thoroughly washed with cold water. After drying in

vacuo, 9.7 g (30,0 mmol; 94%) of a white powdery product are obtained. All steps are carried out under protection from light. $T_m > 200^\circ\text{C}$ - $R_f = 0.70$ (in $\text{CHCl}_3/\text{MeOH}$ 4:1 (v/v)); 0.21 (in $\text{CHCl}_3/\text{MeOH}$ 9:1 (v/v)). - ^1H NMR (400 MHz, d_6 -DMSO): δ [ppm] = 10.64 (s, 1H, NH), 7.89 (s, 1H, H-8), 6.47 (s, 2H, NH_2), 5.91 (d, $J = 2.8$ Hz, 1H, H-1'), 5.17 (dd, $J = 2.8$ Hz, 6.3 Hz, 1H, H-2'), 5.00 (t, $J = 5.3$ Hz, 1H, 5'-OH), 4.95 (dd, $J = 3.0$ Hz, 6.3 Hz, 1H, H-3'), 4.10 (dt, $J = 3.0$ Hz, 5.3 Hz, 1H, H-4'), 3.58 -3.46 (m, 2H, H-5'), 1.50 (s, 3H, CH_3), 1.30 (s, 3H, CH_3). - ^{13}C NMR (101 MHz, d_6 -DMSO): δ [ppm] = 156.8, 153.9, 150.9 (C-4, C-2, C-6), 136.0 (C-8), 116.9 (C-5), 113.2 (C-quart), 88.6, 86.8, 83.7, 81.3 (C-1' to C-4'), 61.7 (C-5'), 27.2 (CH_3), 25.4 (CH_3). FAB-MS (MeOH, mNBA): $m/z = 324$ [$\text{M}+1$]; EI (70 eV) m/z (%) = 323 (12 %) $^+$; 293 (4 %) [$\text{M}-\text{CH}_2\text{O}$] $^+$; 234 (6 %) [$\text{M}-\text{NH}_2$, $\text{CH}_3\text{C}(\text{CH}_2)\text{O}_2$] $^+$; 157 (4 %) [$\text{M}-\text{guanine}$, CH_3] $^+$; 151 (100 %) [guanine] $^+$ - HR-MS: 323.1225 (± 0.8 ppm) calculated: 323.1230.

5.6.8 2',3'-O,O-Isopropylidene-5'-deoxy-5'-iodoguanosine, (11)

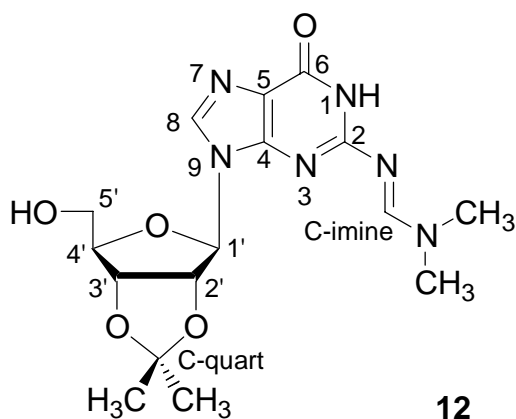


11

4.85 g (15.0 mmol) of ground **10** are resuspended in 150 ml of dried THF under argon and cooled to -70°C by a mixture of acetone and dry ice. 10.0 g (22.1 mmol; 1.5 eq) of methyltriphenoxyphosphonium iodide are added. Due to the light sensitivity of the reactant and the product all subsequent steps have to be carried out under exclusion of light. After 30 min of stirring the reaction mixture is allowed to warm to room temperature and stirred for another 4 hours. The reaction is stopped by the addition of 12 ml of methanol and the solvent is removed under reduced pressure. The residue is resuspended in a

mixture of diethyl ether and cyclohexane (1:1 (v/v)), filtered and thoroughly washed with diethylether and cyclohexane. The crude product is a bright yellow powder that is subsequently purified by column chromatography (silicagel: Merck 0.40-0.65 μm ; eluent: $\text{CHCl}_3/\text{MeOH}$ 9:1 (v/v)). After removal of the solvent, **11** is obtained as a pale yellow powder in 38% yield (0.51 g, 1.18 mmol). To avoid side reactions that lead to a cyclization, moisture has to be strictly excluded in the first steps and the product should not be exposed to polar solvents. T_m : $134\text{--}136^{\circ}\text{C}$ (degradation) - $R_f = 0.80$ (in $\text{CHCl}_3/\text{MeOH}$ 4:1 (v/v)); 0.32 (in $\text{CHCl}_3/\text{MeOH}$ 9:1 (v/v)). - ^1H NMR (300 MHz, d_6 -DMSO): δ [ppm] = 10.73 (s, 1H, NH), 7.89 (s, 1H, H-8), 6.56 (br, 2H, NH_2), 6.02 (d, $J = 2.1$ Hz, 1H, H-1'), 5.31 (dd, $J = 2.1$ Hz, 6.3 Hz, 1H, H-2'), 5.03 (dd, $J = 3.1$ Hz, 6.3 Hz, 1H, H-3'), 4.23 (ddd, $J = 3.1$ Hz, 7.6 Hz, 6.4 Hz, 1H, H-4'), 3.42 (dd, $J = 7.6$ Hz, 10.0 Hz, 1H, H-5'), 3.33 (dd, $J = 6.4$ Hz, 10.0 Hz, 1H, H-5'), 1.50 (s, 3H, CH_3), 1.31 (s, 3H, CH_3). - ^{13}C NMR (101 MHz, d_6 -DMSO): δ [ppm] = 157.5, 154.6 (C-4, C-6), 151.3 (C-2), 137.2 (C-8), 114.2 (C-5), 113.2 (C-quart), 87.3, 84.7, 84.3, 81.1 (C-1' to C-4'), 27.7 (CH_3), 26.1 (CH_3), 7.7 (C-5'). EI (70 eV) m/z (%) = 433 (1%) [$\text{M}+\text{H}$] $^+$; 305 (100%) [$\text{M}-\text{HI}$] $^+$, 290 (13%) [$\text{M}-\text{HI}-\text{CH}_3$] $^+$; 151 (20%) [guanine] $^+$, 128 (65%) [HI] $^+$, 127 (31%), [I] $^+$.

5.6.9 *N,N*-Dimethylaminomethylene-2',3'-O,O-isopropylidene-guanosine (12)



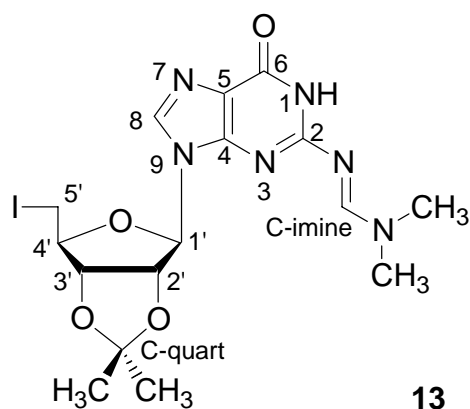
12

5.75 g (17.8 mmol) 2',3'-O,O-isopropylidene-guanosine **10** are resuspended in 60 ml of *N,N*-dimethylformamide and 8.91 ml of *N,N*-dimethylformamide dimethylacetal are added under argon to yield an orange-brown solution. The reaction mixture is stirred at 50°C for 4h. The solvent is removed under reduce pressure and at elevated temperatures ($\sim 55^{\circ}\text{C}$), and the white precipitate removed by filtration. The filtrate is dried under reduced pressure, redissolved in 25 ml of methanol yielding a

fluorescent green solution and precipitated with 50 ml of ethylacetate. After storage at 4°C over night, the residue was removed by filtration and the joined fresidues are thoroughly

washed with ethyl acetate and thoroughly dried under reduced pressure. **12** is obtained as a white powdery solid in 80% yield (5.38 g, 14.2 mmol). All steps are carried out under protection from light. $T_m > 200^\circ\text{C}$ - $R_f = 0.47$ ($\text{CHCl}_3/\text{MeOH}$ 8:1 (v/v)); 0.08 ($\text{CHCl}_3/\text{MeOH}$ 19:1 (v/v)). - ^1H NMR (400 MHz, d_6 -DMSO): δ [ppm] = 11.32 (br, 1H, NH), 8.56 (s, 1H, H-imine), 8.00 (s, 1H, H-8), 6.03 (d, $J = 3.0$ Hz, 1H, H-1'), 5.26 (dd, $J = 3.0$ Hz, 6.3 Hz, 1H, H-2'), 5.03 (dd, $J = 5.4$ Hz, 5.4 Hz 1H, 5'-OH), 4.95 (dd, $J = 2.9$ Hz, 6.3 Hz, 1H, H-3'), 4.13 (ddd, $J = 2.9$ Hz, 4.9 Hz, 4.9 Hz, 1H, H-4'), 3.59 - 3.47 (m 2H, H-5'), 3.15 (s, 3H, N-CH₃), 3.03 (s, 3H, N-CH₃), 1.53 (s, 3H, CH₃), 1.33 (s, 3H, CH₃). - ^{13}C NMR (101 MHz, d_6 -DMSO): δ [ppm] = 158.3 (C-imine), 157.6, 157.5 (C-4, C-6), 149.6 (C2), 136.0 (C-8), 119.9 (C-5), 113.2 (C-quart), 88.6, 86.4, 83.6, 81.2 (C-1' to C-4'), 61.5 (C-5'), 40.8 (N-CH₃), 34.8 (N-CH₃), 27.2 (CH₃), 25.3 (CH₃). - MS-EI (70 eV) m/z (%) = 378 (89%)⁺, 363 (6%) [M-CH]⁺, 348 (6%) [M-2CH₃]⁺, 333 (2%) [M-NH(CH₃)₂]⁺, 206 (100%) [M-DAMG]⁺, 191 (26%) [DAMG-CH₃]⁺, 176 (3%) [DAMG-2CH₃]⁺, 150 (6%) [guanine]⁺ - HR-MS: 378.1654 (± 0.0095) calculated: 378.1652 (DAMG = 2-*N,N*-dimethylaminomethylene guanine).

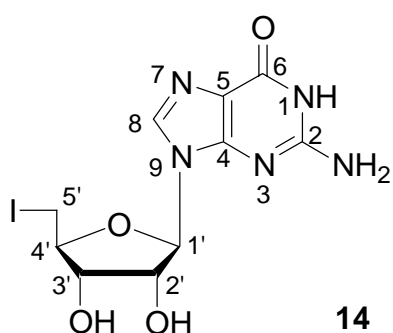
5.6.10 *N,N*-Dimethylaminomethylene-2',3'-*O,O*-isopropylidene-5'-deoxy-5'-iodoguanosine (**13**):



2.20 g (5.81 mmol) of ground **12** are resuspended in 110 ml of dried THF under argon and cooled to -70°C by a mixture of acetone and dry ice. 3.94 g (8.71 mmol; 1.5 eq) of methyl-triphenoxyphosphonium iodide are added. Due to the light sensitivity of the reactant and the product all subsequent steps have to be carried out under exclusion of light. After 30 min of stirring the reaction mixture is allowed to warm to room temperature and stirred for another 4 hours. The reaction is stopped by the addition of 5 ml of methanol

and the solvent is removed under reduced pressure. The dark red residue is dissolved in 2.5 ml methanol/chloroform (1:4 (v/v)) and 7 ml of chloroform are added. The solution of the crude product is subjected to column chromatography on silicagel (Merck 0.40-0.65 μm ; eluent: $\text{CHCl}_3/\text{MeOH}$ 9:1 (v/v)). After removal of the solvent, **12** is obtained as an orange solid in 99% yield (2.81 g, 5.75 mmol). $T_m = 95$ - 97°C - $R_f = 0.74$ ($\text{CHCl}_3/\text{MeOH}$ 5:1 (v/v)); 0.22 ($\text{CHCl}_3/\text{MeOH}$ 19:1 (v/v)). - ^1H NMR (400 MHz, d_6 -DMSO): δ [ppm] = 11.39 (br, 1H, NH), 8.58 (s, 1H, H-imine), 8.01 (s, 1H, H-8), 6.15 (d, $J = 2.1$ Hz, 1H, H-1'), 5.42 (dd, $J = 2.1$ Hz, 6.3 Hz, 1H, H-2'), 5.02 (dd, $J = 2.8$ Hz, 6.3 Hz, 1H, H-3'), 4.28 (ddd, $J = 2.8$ Hz, 5.7 Hz, 9.0 Hz, 1H, H-4'), 3.49 (dd, $J = 9.0$ Hz, 9.9 Hz, 1H, H-5'), 3.30 (dd, $J = 5.7$ Hz, 9.9 Hz, 1H, H-5'), 3.19 (s, 3H, N-CH₃), 3.04 (s, 3H, N-CH₃), 1.53 (s, 3H, CH₃), 1.35 (s, 3H, CH₃). - ^{13}C NMR (101 MHz, d_6 -DMSO): δ [ppm] = 158.2 (C-imine), 157.7, 157.5 (C-4, C-6), 149.2 (C2), 137.9 (C-8), 120.2 (C-5), 113.5 (C-quart), 89.4, 86.4, 84.0, 83.9 (C-1' to C-4'), 41.1 (N-CH₃), 34.9 (N-CH₃), 27.2 (CH₃), 25.3 (CH₃), 6.7 (C-5') - MS-EI (70 eV) m/z = 488 (13%)⁺; 361 (7%) [M-I]⁺; 360 (35%) [M-HI]⁺; 345 (1%) [M-HI, CH₃]⁺; 206 (3%) [DAMG]⁺; 188 (2%) [DAMG-H₂O]⁺; 176 (26%) [DAMG-2CH₃]⁺; 149 (12%) [guanine-H]⁺; 128 (100%) [HI]. - HR-MS: 488.06631 calculated: 488.0669 (DAMG = 2-*N,N*-dimethylaminomethylene guanine).

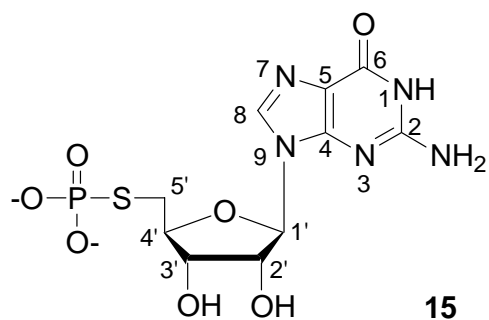
5.6.11 5'-Deoxy-5'-iodoguanosine (**14**):



14

1.20 g (2.78 mmol) of **11** (or an equivalent amount of **13**) are resuspended in 40 ml of aqueous 50% formic acid and stirred for 3 days at room temperature under protection from light. The solvent is removed under reduced pressure at room temperature and the residue, 1.07 g (2.72 mmol, 98%) of a white solid, used for the next step without further purification. $T_m = 142-145^\circ\text{C}$ (degradation) - $R_f = 0.84$ ($^i\text{PrOH}/\text{NH}_3/\text{H}_2\text{O}$, 6:3:1 (v/v/v)). - $^1\text{H NMR}$ (400 MHz, $\text{DMSO}-d_6$): δ [ppm] = 8.27 (s, 1H, NH), 7.90 (s, 1H, H-8), 6.61 (br, 2H, NH_2), 5.71 (d, $J = 5.6$ Hz, 1H, H-1'), 4.62 (dd, $J = 5.6$ Hz, 5.6 Hz, 1H, H-2'), 4.06 (dd, $J = 3.4$ Hz, 5.6 Hz, 1H, H-3'), 4.10 (ddd, $J = 3.4$ Hz, 6.5 Hz, 1H, H-4'), 3.55 (dd, $J = 6.5$ Hz, 10.4 Hz, 1H, H-5'), 3.41 (dd, $J = 6.5$ Hz, 10.4 Hz, 1H, H-5'). - $^{13}\text{C NMR}$ (101 MHz, d_6 -DMSO): δ [ppm] = 157.9, 154.3, 151.8 (C-2, C-4, C-6), 136.1 (C-8), 117.1 (C-5), 87.0, 86.4, 84.1, 83.5 (C-1' to C-4'), 8.5 (C-5'). - FAB-MS (MeOH, mNBA): $m/z = 394.1$ (6%) $[\text{M}+\text{H}]^+$ - EI-MS (70 eV) m/z (%) = 254 (12%) $[\text{I}_2]^+$, 149 (2%) $[\text{guanine}]^+$, 127.9 (100%) $[\text{HI}]^+$, 126.9 (50%) $[\text{I}]^+$ - HR-MS: no mass peak was obtained in electron ionization mode so that no high resolution mass could be determined.

5.6.12 5'-Deoxy-5'-thioguanosine-monophosphorothioate (GSMP) (**15**):

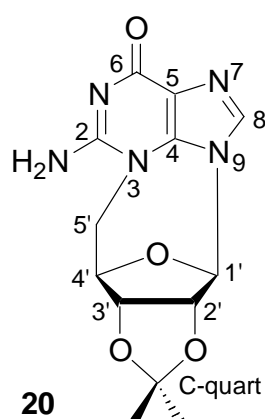


15

1.06 g (2.69 mmol) of 5'-deoxy-5'-iodoguanosine **14** are resuspended in 60 ml of degassed water and a degassed solution of 3,84 g (9.7 mmol; 3.6 eq) of trisodium thiophosphate dodecahydrate in water is added. The colorless reaction mixture is degassed three times and flooded with argon. After three days of stirring protected from light under argon, the precipitated solid is removed by filtration and the solvent is evaporated under reduced pressure at room temperature. The pale yellow residue is resuspended in 15 ml of ice-cooled degassed water, and 30 ml of methanol are added to precipitate the excess of sodium thiophosphate. The precipitate is removed by filtration and the residue washed with 10 ml of cooled methanol/water (2:1 (v/v)). The solvent is removed from the filtrate and the pale yellow solid dissolved in 14 ml of water and subjected to reverse phase chromatography (RP-18, eluent: water). The elution of GSMP is monitored by TLC. Molybdophosphate in methanol (10%) stains GSMP in a weak blue that appears with a latency of several minutes and is easily overseen. The thiophosphate contamination is easily detected by this method. GSMP can be visualized on fluorescent TLC paper under UV illumination, so that a combination of both methods may be used to distinguish GSMP fractions with a thiophosphate contamination from the pure GSMP. The product fractions are pooled and after photometric determination of the concentration split into aliquots that can be directly

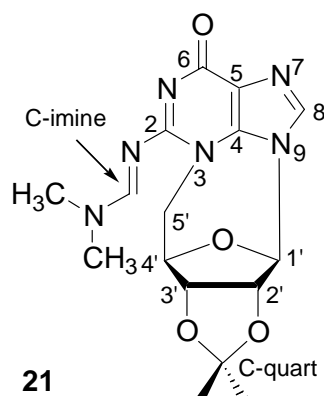
used for in vitro transcription. GSMP is lyophilized and stored at -20°C under argon. Yield = 68% (0,69 g, 1.83 mmol) - $T_m = 100^{\circ}\text{C}$ (degradation) - $R_f = 0.26$ (iPrOH/NH₃/H₂O, 6:3:1 (v/v/v)). - ^1H NMR (400 MHz, D₂O): δ [ppm] = 8.12 (s, 1H, H-8), 5.97 (d, $J = 5.4$ Hz, 1H, H-1'), 4.89 (dd, $J = 5.4$ Hz, 5.4 Hz, 1H, H-2'), 4.58 (dd, $J = 4.1$ Hz, 5.4 Hz, 1H, H-3'), 4.44 (dt, $J = 4.1$ Hz, 6.2 Hz, 1H, H-4'), 3.27 - 3.10 (m, 2H, H-5'). ^{31}P NMR (162 MHz, D₂O) = 19.0 ppm. - ^{13}C NMR (101 MHz, D₂O): δ [ppm] = 161.5, 156.4, 154.2 (C-2, C-4, C-6), 140.4 (C-8), 119.0 (C-5), 89.8, 87.2, 75.9, 74.7 (C-1' to C-4'), 34.5 (C-5'). - ESI-MS (negative mode, MeOH): 400 (2%) [M - 2H + Na]⁻, 378 (100%) [M-H]⁻, - HR-MS: 378.04 calculated: 378.027.

5.6.13 2',3'-O,O-Isopropylidene-3,5'-C- cycloguanosine (20)



After 24 h at RT in d₆-DMSO, **11** has been completely converted into its cyclized form **20** in an intramolecular reaction. ^1H NMR (300 MHz, d₆-DMSO): δ [ppm] = 8.62 (br, 1H, NH₂), 8.07 (s, 1H, H-8), 6.52 (s, 1H, H-1'), 5.01 (d, $J = 5.8$ Hz, 1H, H-2'), 4.92 (t, $J = 2.6$ Hz, 1H, H-4'), 4.74 (dd, $J = 2.6$ Hz, 14.1 Hz, 1H, H-5'), 4.55 (d, $J = 5.8$ Hz, 1H, H-3'), 3.98 (dd, $J = 14.1$ Hz, 2.6 Hz, 1H, H-5'), 1.45 (s, 3H, CH₃), 1.24 (s, 3H, CH₃). - ^{13}C NMR (101 MHz, d₆-DMSO): δ [ppm] = 155.5, 153.6 (C-4, C-6), 140.6 (C-2), 136.9 (C-8), 112.8 (C-5), 113.2 (C-quart), 90.7, 85.5, 83.5, 80.7 (C-1' to C-4'), 55.3 (C-5'), 26.1 (CH₃), 24.7 (CH₃).

5.6.14 N,N-Dimethylaminomethylene-2',3'-O,O-isopropylidene-3,5'-C-cycloguanosine (21)



After 10 days at RT in d₆-DMSO, **13** has been completely converted into its cyclized form **21** in an intramolecular reaction. ^1H NMR (300 MHz, d₆-DMSO): δ [ppm] = 8.39 (br, 1H, H-imine), 8.13 (s, 1H, H-8), 6.55 (s, 1H, H-1'), 5.30 (dd, $J = 15.0$ Hz, 2.7 Hz, 1H, H-5'), 4.90 (dd, $J = 2.7$ Hz, 2.7 Hz, 1H, H-4'), 4.88 (d, $J = 5.8$ Hz, 1H, H-2'), 4.51 (d, $J = 5.8$ Hz, 1H, H-3'), 3.83 (dd, $J = 15.0$ Hz, 2.7 Hz; 1H, H-5'), 3.31 (s, 3H, N-CH₃), 3.20 (s, 3H, N-CH₃), 1.45 (s, 3H, C-CH₃), 1.23 (s, 3H, C-CH₃). - ^{13}C NMR (101 MHz, d₆-DMSO): δ [ppm] = 159.8 (C-imine), 156.1, 155.3 (C-4, C-6), 141.1 (C-2), 137.3 (C-8), 121.9 (C-5), 112.8 (C-quart), 90.9, 85.7, 84.1, 80.7 (C-1' to C-4'), 54.1 (C-5'), 42.1 (N-CH₃), 36.2 (N-CH₃), 26.2 (C-CH₃), 24.8 (C-CH₃).

5.7 Buffers and solutions

5.7.1 Cell culture

10% DMEM

| | | |
|----|------|--------------|
| 10 | % | FCS |
| 1 | u/ml | streptomycin |
| 1 | u/ml | tylosin |

antibleach

| | | |
|----|----|--------------------|
| 20 | mg | p-phenylenediamine |
| 2 | ml | PBS+ |
| 8 | ml | glycerol |

PBS (pH 7.4)

| | | |
|-----|----|----------------------------------|
| 140 | mM | NaCl |
| 3 | mM | KCl |
| 16 | mM | Na ₂ HPO ₄ |
| 1.5 | mM | KH ₂ PO ₄ |

in bidistilled water

PBS+

| | | |
|-----|----|-------------------|
| 1.0 | mM | MgCl ₂ |
| 0.1 | mM | CaCl ₂ |

in PBS

Mowiol

| | | |
|-----|----|----------------------|
| 2.4 | g | Mowiol 4-88 |
| 6 | g | glycerol |
| 6 | ml | water |
| 12 | ml | Tris (0.2 M, pH 8.5) |

heat to 50°C to dissolve compounds;
remove remaining particles by
centrifugation; store at -20°C

T/E

| | | |
|------|----|---------|
| 0.05 | % | trypsin |
| 0.53 | mM | EDTA |

5.7.2 Protein expression

IPTG 100 mM in water

LB-medium 20 % LB in water

SOB-medium

| | | |
|------|----|-------------------|
| 2 | % | trypton |
| 0.5 | % | yeast-extrakt |
| 0.05 | % | NaCl |
| 10 | mM | MgCl ₂ |
| 10 | mM | MgSO ₄ |

SOC-medium

| | | |
|----|----|------------|
| 1x | | SOB-medium |
| 20 | mM | glucose |

Supermedium

| | | |
|-----|---|---------------|
| 3.0 | % | NaCl |
| 1.5 | % | yeast-extract |
| 3.0 | % | trypton |

Terrific broth medium

| | | |
|------|---|---------------------------------|
| 12 | % | trypton |
| 24 | % | yeast-extract |
| 4 | % | glycerol |
| 0,17 | M | KH ₂ PO ₄ |
| 0,72 | M | K ₂ HPO ₄ |

Trypton, yeast extract and glycerol are filled up to 90% of the total volume with water and autoclaved. The phosphate solution (10% of total volume) is sterilized separately and added when both solutions are cooled down.

5.7.3 Protein purification

Bradford reagent

0.01 % Serva Blue
0.8 M ethanol (96%)
1.6 M phosphoric acid (85%)

HEPES-stock solution

0.5 M HEPES (pH 7.0)

Inclusion body preparation:

lysis buffer

50 mM Tris-HCl (pH 8.0)
300 mM NaCl
20 mM MgSO₄
2 mM CaCl₂

add immediately prior to use

500 µg/ml lysozyme
200 µg/ml DNase

Inclusion body preparation:

denaturing buffer

6 M urea
100 mM NaH₂PO₄
10 mM Tris-HCl (pH 8.0)

Inclusion body preparation:

resuspension buffer

6 M guanidine
100 mM NaH₂PO₄
10 mM Tris-HCl (pH 8.0)

pGEX high pH-buffer

0.1 M Tris-HCl
5.0 M NaCl
adjust to pH 8.5 with HCl

pGEX low pH-buffer

0.1 M Na-acetate
5.0 M NaCl
adjust to pH 4.5 with NaOH

pGEX-lysis buffer

20 mM HEPES (pH 7.6)
100 mM KCl
0.2 mM EDTA
20 % glycerol
1 % Triton X-100

add immediately prior to use (per 50 ml):

1.0 ml DTT (50 mM)

pGEX-pre-elution buffer

100 mM NaCl
25 mM HEPES (pH 7.0)
0,1 mM EGTA

pGEX-elution buffer

50 mM reduced glutathione
10 mM Tris-HCl, pH 8.0

Lysis buffer

50 mM Tris-HCl, pH 8.0
300 mM NaCl
500 µg/ml Lysozym
200 µg/ml DNase
20 mM MgCl₂
2 mM CaCl₂

Lysis + buffer

20 mM HEPES (pH 7.6)
100 mM KCl
0.2 mM EDTA
20 % glycerol
2 % Triton X-100
5 mM DTT

Lysis buffer A

pGEX lysis buffer supplemented with
2 % Triton X-100
10 mM DTT

Lysis buffer B

pGEX lysis buffer supplemented with
1 % Triton X-100
5 mM DTT
adjusted to pH 8.0

Lysis buffer C

pGEX lysis buffer supplemented with

1 % Triton X-100
5 mM DTT
1 M urea

Lysis buffer D

pGEX lysis buffer supplemented with

1 % Triton X-100
5 mM DTT
2 M urea

Ni-NTA-purification buffers (denaturing)

8.0 M urea
50 mM NaH_2PO_4
pH: buffer B (lysis): pH 8.0
buffer C (wash): pH 6.3
buffer E (elution): pH 4.5

Ni-NTA-purification buffers (native)

50 mM NaH_2PO_4 (pH 8.0)
300 mM NaCl

10 mM imidazol (lysis)
20 mM imidazol (wash)
250 mM imidazol (elution)

Sodium hydrogencarbonate/EDTA buffer

2 % sodium hydrogencarbonate
1 mM EDTA, pH 8.0

20x TEV buffer

1 M Tris-HCl, pH 8.0
10 mM EDTA, pH 8.0

TEV storage buffer

100 mM Tris-HCl pH 8.5
500 mM NaCl
50 % glycerol
5 mM DTT
0.5 mM EDTA

5.7.4 Gel electrophoresis

Acrylamide (AA) stock solution

38 % acrylamide
2 % bisacrylamide

Coomassie stain

0.1 % Coomassie Brilliant Blue R250
25 % methanol
10 % acetic acid

Laemmli buffer (5x)

312.5 mM Tris-HCl (pH 6.8)
2.5 % SDS
5 % β -mercaptoethanol
50 % glycerol
0.025 % Serva Blue G
in PBS

SDS-PAGE running buffer

50 mM Tris-HCl (pH 8.25)
384 mM tricin
0.2 % SDS

Silver stain formaldehyde solution

50 % methanol
12 % acetic acid
0.5 ml/l formaldehyde (37%)

Silver stain silver solution

2 g/l AgNO_3
750 $\mu\text{l/l}$ formaldehyde (37%)

Silver stain developing solution

60 g/l Na_2CO_3
500 $\mu\text{l/l}$ formaldehyde (37%)
4 mg/l $\text{Na}_2\text{S}_2\text{O}_3$

Silver stain stop solution

50 % methanol
12 % acetic acid

Silver stain wash solution

30 % methanol
3 % glycerol

2.5 g molybdophosphoric acid
1.0 g cer(IV)sulfate tetrahydrate
6.0 g conc. sulfuric acid
90.5 ml water

5.7.5 Western blotting

Triton/BSA-solution (TBS)

0.1% Triton X-100
1.0% BSA
in PBS+

TBS-T

0.1 % Triton X-100
1.0 % BSA
in PBS+
add 1.0 % Tween 20

Transfer buffer

10 mM CAPS, pH 11
10% MeOH

5.7.6 DNA/RNA techniques

Formamide loading buffer

80 % deionized formamide
10 mM EDTA
1 mg/ml bromophenol blue

TAE (50x)

2 M Tris-acetate
50 mM EDTA (pH 8.0)

TBE (10x, 1l)

108 g Tris
55 g boronic acid
40 ml EDTA

5.7.7 Synthesis

Kaegi-Miescher stain

0.5 ml anisaldehyde
1.0 ml conc. sulfuric acid
50.0 ml glacial acetic acid

Seebach reagent

5.8 Material

5.8.1 Apparatus

| | |
|---------------------------|---|
| autoclave | Integra Biosciences, Fedegari, Pavia, Italy |
| balances | BP 610, Sartorius AG, Göttingen Explorer, Ohaus, Giessen |
| centrifuges | RC5-B Sorvall-Kühlzentrifuge, Du Pont Instruments, Bad Homburg RC5-C Plus Sorvall-Kühlzentrifuge, Kendro Laboratory Products, Hanau Eppendorf-Tischzentrifuge 5415 6, Eppendorf, Hamburg Eppendorf-Tischzentrifuge MiniSpin, Eppendorf, Hamburg Eppendorf-Kühlzentrifuge 5402, Eppendorf, Hamburg Eppendorf-Kühlzentrifuge 5810 R, Eppendorf, Hamburg Kühlzentrifuge Sepatech Megafuge 2.0R Heraeus |
| chromatography columns: | Nucleosil-100, RP-18 (2mm, 25 cm, 3 µm) Anion exchange: DEAE Sephadex-A25, Amersham Bioscience |
| drier | KL 500, Heraeus, Hanau |
| evaporators | IKA-Dest, IKA-Werke GmbH & Co KG, Staufen |
| FAB-mass spectrometer: | H1, Kratos, Manchester |
| FPLC | ÅKTA-FPLC, AP Biotech, Braunschweig Software: Unicorn |
| freeze dryer | VirTis GT2, Leybold-Heraeus, Hanau |
| gel chambers | Horizontalelektrophoresessystem Horizon 11-14, 20-25, Gibco-BRL, Bethesda Research Laboratories MiniSun™ DNA Cell, BioRad, Munich Hoefer Mighty Small 250, Hoefer Scientific Instruments, San Francisco, USA Blotting instrument Firma BioRad, Munich |
| gel photography | Camera: hama® Repro Video monitor WV-BM 80, Panasonic Illumination controller: CS1, Cybertech Image Capture Computer, Cybertech printer: Video Copy Processor, Mitsubishi |
| glass tools | Schott-Duran, Jenaglas, Mainz |
| heating block | Dri-Block, DB3, Techne, Duxford, U.K. |
| homogenizer | Potter S, B.Braun Melsungen AG |
| incubators | Heraeus-Christ, Hanau; WTB Binder, Tuttlingen |
| magnetic stirrer | Ika-Combimag RCT, IKA-Werke GmbH & Co KG, Staufen |
| membrane pump | M72C, Vacubrand GmbH & Co, Wertheim |
| microscope | Wilovert S, Hund, Wetzlar Fluorescence microscope Zeiss Axiovert 35 with filters (Bp 485, Ft 510, 515-565), Oberkochen |
| microwave | Microchef FM 3915, Moulinex |
| NMR spectrometer | DPX300 (300 MHz), DPX400 (400 MHz), Bruker, Karlsruhe |
| overhead mixer | Reax 2, Heidolph, Schwabach |
| PCR thermoblock | MJ Research PTC-200 (Peltier Thermo Cycler), Biozym, Hess. Oldendorf |
| pH-meter | MP 220, Mettler Toledo, Greifensee, Switzerland |
| peristaltic pump | P1, AP Biotech, Piscataway, USA |
| phosphoimager | Bas Reader, Fujix Bas 1000, Fuji, Minami-Ashigara, Japan |
| phosphoimaging plates | Bas III, Fuji, Minami-Ashigara, Japan |
| phosphoimaging decharger: | Raytest-Isotopenmessgeräte |
| photospectrometer | Smartspec™ 3000, BioRad Laboratories, Hercules, CA, USA |

| | |
|--------------------------------|---|
| pipettors | Gilson Pipetman P20, P200, P1000 Abimed, Langenfeld Eppendorf Reference 2,5; 10; Eppendorf Research 1000, Hamburg Akkupipettierhilfe, Hirschmann, Eberstedt |
| power supplies: | LKB ECPS 3000/150, AP Biotech, Braunschweig PS 305, Gibco BRL, Life Technologies, Freiburg Power Pac 300, BioRad, Munich |
| protein quantitation rotors | Multiskan Ascent, Labsystems Typ GSA Sorvall, Du Pont, France Typ GS-3 Sorvall, Newton, USA SLA-3000 Superlite, Newton, USA Typ SS-34 Sorval, Newton, USA |
| shakers | Series 25 New Brunswick Scientific CO., Inc. , Edison, USA Multitron, Infors AG, Bottmingen, Switzerland |
| sterilbench | Biohazard, Gelaire, Mailand, Italy Heraeus-Christ, Hanau |
| sterilizer | Memmert, Schwabach Ecocell, MMM Medcenter |
| thermomixer | Eppendorf 5436, Hamburg |
| UV-transilluminator | Biometra, Göttingen |
| vortex | Vortex-2-Genie, Scientific Industries, Bohema, USA |
| water purification | Millipore-Pelicon Filtration device with polysulfone filter cassette PTGC, 10000 MW, Millipore, Molsheim, France |

5.8.2 Consumables

| | |
|--------------------|--|
| cover slips | Menzel Gläser, Breda, Netherlands |
| culture dishes: | 6-, 24-, 96-well, Costar, Cambridge, USA |
| culture tubes | Costar, USA Greiner, Nürtingen |
| filters | Schleicher und Schüll, Dassel |
| filtration columns | BioRad, Munich |
| membranes | QIAGEN, Hilden BioRad, Munich |
| microscopy slides | Superfrost Plus, Menzel Gläser, Breda, Netherlands |
| microfuge tubes | 1,5 ml, 2 ml, Eppendorf, Hamburg 0,5 ml ultra-thin, Biozym, Hess. Oldenburg 15 ml, 50 ml Falcon / Costar, GB |
| parafilm | ACC, Greenwich, USA |
| petri dishes | Ø 90 mm, Ø 135 mm, Falcon, GB |
| pipet equipment | Abimed, Langenfeld Greiner, Nürtingen |
| TLC-plates | Silicagel 60 on aluminium, Merck, Darmstadt |
| culture flasks | 25er, 75er, 162er, Costar, USA |

5.8.3 Antibodies

| | |
|----------------------------|-------------------------------|
| anti-rabbit-IgG-HRP (goat) | Cell Signalling Technologies, |
| anti-goat-IgG-AB (rabbit) | Dianova, Hamburg |
| anti-lamin A/C | M. Osborn, Göttingen |
| anti-HexA | A. Hasilik, Marburg |
| anti-GCS | R. Pagano, San Diego, USA |

5.8.4 Purification kits

| | | |
|-----------|---------------------------------|----------------|
| QIAprep | (plasmid isolation) | QIAGEN, Hilden |
| QIAquick | (gel extraction) | QIAGEN, Hilden |
| RNeasy | (RNA isolation) | QIAGEN, Hilden |
| NiNTA-kit | (purification of His6-proteins) | QIAGEN, Hilden |

5.8.5 Enzymes and markers

| | |
|----------------------------|---|
| Alkaline phosphatase (CIP) | New England Biolabs, Schwalbach |
| DNase | RiboMAX™ Large Scale RNA Production Systems – SP6 and T7, Promega, Madison, WI, USA |
| Restriction endonucleases | New England Biolabs |
| Reverse transkriptase | Titan Kit, Roche Diagnostics, Mannheim |
| RNase Inhibitor | Promega, Heidelberg |
| T4-Ligase | Rapid Ligation Kit, Roche Diagnostics, Mannheim |
| T4-Kinase | T4-Pronucleotid Kinase, Amersham Bioscience, Uppsala, Sweden |
| T7- RNA-polymerase | RiboMAX™ Large Scale RNA Production Systems – SP6 and T7, Promega, Madison, WI, USA |
| Taq-polymerase | QIAGEN, Hilden Expand-Long-Template, Roche Diagnostics, Mannheim |
| Trypsin | Paisley, Scotland, GB |
| DNA marker | 1kb ladder, Invitrogen Life Technologies, Karlsruhe |
| Protein standard | Prestained Protein Standard, Broad range, New England Biolabs, Schwalbach |

6 Oligonucleotides and Peptides

| | |
|---------------------------|---|
| synthetic siRNAs | Dharmacon Research, Lafayette, CO, USA Proligo, Boulder, CO, USA |
| biotinylated Penetratin | Qbiogene, Heidelberg |
| pGEXuni5' oligonucleotide | QIAGEN Operon Technologies, Hilden |
| DNA-Oligonucleotides | Sigma-Aldrich, Taufkirchen (custom synthesis) |

6.1.1 Radioactivity

| | |
|------------------------|--------------------------------------|
| [³² P]-ATP | Amersham Bioscience, Uppsala, Sweden |
|------------------------|--------------------------------------|

6.1.2 Bacterial Strains

Escherichia coli : DH-5 α , DH10 Bac, BL21, BL21 DE3, BL21 DE3 pLysS, BL21 RIL

6.1.3 Cell Lines

| | |
|----------|-----------------------------|
| HeLa wt | human ovary blastoma cells |
| 91/17-21 | humane fibroblasts (normal) |

| | |
|--------|--------------------------------|
| F81/23 | Nieman Pick-Type C fibroblasts |
| MEB4 | murine melanoma cells |
| COS1,7 | monkey cells |

6.1.4 Vectors

| | |
|-----------|--------------------------|
| pQE30 | QIAGEN, Hilden |
| pREP4 | QIAGEN, Hilden |
| pFASTBAC1 | GIBCOBRL, Freiburg |
| pGEX-4T2 | AP Biotech, Braunschweig |

6.1.5 Chemicals

Molecular Biology

Amersham Bioscience, Uppsala, Sweden: glutathione-sepharose, Binding Silane, Repel Silane, Sephadex A-25

Fluka, Buchs, Switzerland: ampicillin

Valeant Pharmaceuticals, Costa Mesa, CA, USA: MEM-medium

Invitrogen Life Technologies, Bethesda, USA: agar, agarose, DMEM, 1kb DNA length standard, FCS, LB Medium, Lipofectamine, MEM-Medium, OptiMEM, , penicillin/streptomycin, Select Agar, Select Yeast Extract, Select Peptone, Triton-X 100

Janssen Chimica, Beerse, Belgium: PFA

Macherey und Nagel, Düren: PVDF-membrane, pH-papers

MBI Fermentas, St. Leon-Roth: DTT, IPTG, HEPES, lysozyme, X-Gal

E. Merck, Darmstadt: amido black, bromophenol blue, disodiumhydrogen phosphate, EDTA-sodium salt, glycerol, LiChroprep RP-18 material, *N,N'*-dimethylbisacrylamide, sodium chloride, potassium acetate, potassium chloride, potassium dihydrogen phosphate, sodiumhydroxide, tris-(hydroxymethyl)-aminomethane, urea

PAA Laboratories GmbH, Pasching, Austria: FCS, HAMs Nutrient Medium F-10

Roche, Mannheim: ampicilin, dNTP-mix, Expand-Long Template, kanamycin, PMSF, rapid ligation kit, T7-polymerase, Taq-polymerase

Roth, Karlsruhe: acrylamide mix 29:1, 40%

Cambrex, Baltimore, M, USA: Seakem LE agarose

Serva, Heidelberg: acrylamide, ammonium peroxodisulfate, glucose, PVDF-membrane, Coomassie R250

Sigma-Aldrich, Taufkirchen: APS, BSA, Coomassie blue, ethidium bromide, gentamycin, β -mercaptoethanol, paraformaldehyde, p-phenylene diamine, poly-L-lysine, sodium dodecyl sulfate, Triton X-100, Tween 20, TEMED

Synthesis

Fischer, Wiesbaden: chloroform p.a.

Fluka, Buchs, Switzerland: absolute solvents over molecular sieve (dimethyl formamide, THF, pyridine), guanosine, methyltriphenoxyphosphonium iodide perchloric acid (70% puriss.), tosyl chloride, triethylamine (puriss.),

KFM optichem, Lohmar: methanol p.a.

E. Merck, Darmstadt: silica gel (40 – 65 μ m), LiChroprep RP-18 material (40-65 μ m)

Riedel de Haen, Seelze: acetic acid, formic acid, formaldehyde, hydrochloric acid

Schleicher und Schüll, Dassel: blotting papers, filter papers

Sigma-Aldrich, Taufkirchen: acetone (p.a.), trisodium thiophosphate dodecahydrate

7 References

- Abbas-Terki T, Blanco-Bose W, Deglon N, Pralong W, Aebischer P (2002) Lentiviral-mediated RNA interference. *Hum Gene Ther* 13: 2197-201
- Aboobaker AA, Blaxter ML (2003) Use of RNA interference to investigate gene function in the human filarial nematode parasite *Brugia malayi*. *Molecular & Biochemical Parasitology* 129: 41-51
- Adams RR, Maiato H, Earnshaw WC, Carmena M (2001) Essential roles of *Drosophila* inner centromere protein (INCENP) and aurora B in histone H3 phosphorylation, metaphase chromosome alignment, kinetochore disjunction, and chromosome segregation. *Journal of Cell Biology* 153: 865-879
- Akusjarvi G, Svensson C, Nygard O (1987) A mechanism by which adenovirus virus-associated RNAi controls translation in a transient expression assay. *Mol Cell Biol* 7: 549-51
- Akuta T, Eguchi A, Okuyama H, Senda T, Inokuchi H, Suzuki Y, Nagoshi E, Mizuguchi H, Hayakawa T, Takeda K, Hasegawa M, Nakanishi M (2002) Enhancement of phage-mediated gene transfer by nuclear localization signal. *Biochem Biophys Res Commun* 297: 779-86
- Amarzguioui M, Holen T, Babaie E, Prydz H (2003) Tolerance for mutations and chemical modifications in a siRNA. *Nucleic Acids Res* 31: 589-95
- Ambros V (2004) The function of animal microRNAs. *Nature* 431: 350-355
- Ambros V, Lee RC, Lavanway A, Williams PT, Jewell D (2003) MicroRNAs and Other Tiny Endogenous RNAs in *C. elegans*. *Curr Biol* 13: 807-18
- Ameri K, Lewis CE, Raida M, Sowter H, Hai T, Harris AL (2004) Anoxic induction of ATF-4 through HIF-1-independent pathways of protein stabilization in human cancer cells. *Blood* 103: 1876-82
- Amsellem S, Pflumio F, Bardin D, Izac B, Charneau P, Romeo PH, Dubart-Kupferschmitt A, Fichelson S (2003) Ex vivo expansion of human hematopoietic stem cells by direct delivery of the HOXB4 homeoprotein. *Nat Med* 9: 1423-7
- Anderson DC, Nichols E, Manger R, Woodle D, Barry M, Fritzberg AR (1993) Tumor cell retention of antibody Fab fragments is enhanced by an attached HIV TAT protein-derived peptide. *Biochem Biophys Res Commun* 194: 876-84
- Anderson J, Banerjee A, Akkina R (2003) Bispecific short hairpin siRNA constructs targeted to CD4, CXCR4, and CCR5 confer HIV-1 resistance. *Oligonucleotides* 13: 303-12
- Andino R (2003) RNAi puts a lid on virus replication. *Nat Biotechnol* 21: 629-30
- Antopolsky M, Azhayeva E, Tengvall U, Auriola S, Jaaskelainen I, Ronkko S, Honkakoski P, Urtti A, Lonnberg H, Azhayev A (1999) Peptide-oligonucleotide phosphorothioate conjugates with membrane translocation and nuclear localization properties. *Bioconjugate Chemistry* 10: 598-606
- Anwer K, Kao G, Rolland A, Driessen WH, Sullivan SM (2004) Peptide-mediated gene transfer of cationic lipid/plasmid DNA complexes to endothelial cells. *J Drug Target* 12: 215-21
- Aoki Y, Kawa S, Karasawa Y, Horiuchi A, Kiyosawa K (1998) Anti-proliferative effects of unmodified antisense oligodeoxynucleotides targeted against c-raf mRNA: use of poly (lysine/serine) copolymers or cationic lipopolyamines. *Clin Exp Pharmacol Physiol* 25: 702-5
- Aravin AA, Lagos-Quintana M, Yalcin A, Zavolan M, Marks D, Snyder B, Gaasterland T, Meyer J, Tuschl T (2003) The small RNA profile during *Drosophila melanogaster* development. *Dev Cell* 5: 337-50
- Aravind L, Koonin EV (2001) A natural classification of ribonucleases. *Methods Enzymol* 341: 3-28
- Arenz C, Schepers U (2003) RNA interference: from an ancient mechanism to a state of the art therapeutic application? *Naturwissenschaften* 90: 345-59
- Aronsohn AI, Hughes JA (1998) Nuclear localization signal peptides enhance cationic liposome-mediated gene therapy. *Journal of Drug Targeting* 5: 163-169

- Arteaga HJ, Hinkula J, van Dijk-Hard I, Dilber MS, Wahren B, Christensson B, Mohamed AJ, Smith CI (2003) Choosing CCR5 or Rev siRNA in HIV-1. *Nat Biotechnol* 21: 230-1
- Asai M, Hattori C, Szabo B, Sasagawa N, Maruyama K, Tanuma S, Ishiura S (2003) Putative function of ADAM9, ADAM10, and ADAM17 as APP alpha-secretase. *Biochemical & Biophysical Research Communications* 301: 231-235
- Askjaer P, Galy V, Hannak E, Mattaj IW (2002) Ran GTPase cycle and importins alpha and beta are essential for spindle formation and nuclear envelope assembly in living *Caenorhabditis elegans* embryos. *Molecular Biology of the Cell* 13: 4355-4370
- Astriab-Fisher A, Sergueev D, Fisher M, Shaw BR, Juliano RL (2002) Conjugates of antisense oligonucleotides with the Tat and antennapedia cell-penetrating peptides: effects on cellular uptake, binding to target sequences, and biologic actions. *Pharm Res* 19: 744-54.
- Aza-Blanc P, Cooper CL, Wagner K, Batalov S, Deveraux QL, Cooke MP (2003) Identification of modulators of TRAIL-induced apoptosis via RNAi-based phenotypic screening. *Mol Cell* 12: 627-37
- Bachelder RE, Lipscomb EA, Lin X, Wendt MA, Chadborn NH, Eickholt BJ, Mercurio AM (2003) Competing autocrine pathways involving alternative neuropilin-1 ligands regulate chemotaxis of carcinoma cells. *Cancer Res* 63: 5230-3
- Balaban TS, Goddard R, Linke-Schaetzl M, Lehn JM (2003) 2-Aminopyrimidine directed self-assembly of zinc porphyrins containing bulky 3,5-di-tert-butylphenyl groups. *J Am Chem Soc* 125: 4233-9
- Ballard JD, Collier RJ, Starnbach MN (1996) Anthrax toxin-mediated delivery of a cytotoxic T-cell epitope in vivo. *Proc Natl Acad Sci U S A* 93: 12531-12534
- Banerjea A, Li MJ, Bauer G, Remling L, Lee NS, Rossi J, Akkina R (2003) Inhibition of HIV-1 by lentiviral vector-transduced siRNAs in T lymphocytes differentiated in SCID-hu mice and CD34+ progenitor cell-derived macrophages. *Mol Ther* 8: 62-71
- Barth H, Blocker D, Behlke J, Bergsma-Schutter W, Brisson A, Benz R, Aktories K (2000) Cellular uptake of *Clostridium botulinum* C2 toxin requires oligomerization and acidification. *J Biol Chem* 275: 18704-11
- Barton GM, Medzhitov R (2002) Retroviral delivery of small interfering RNA into primary cells. *Proc Natl Acad Sci U S A* 99: 14943-5
- Bass BL (2000) Double-stranded RNA as a template for gene silencing [Review]. *Cell* 101: 235-238
- Baulcombe D (1999) Viruses and gene silencing in plants. *Archives of Virology*: 189-201
- Bellet-Amalric E, Blaudez D, Desbat B, Graner F, Gauthier F, Renault A (2000) Interaction of the third helix of Antennapedia homeodomain and a phospholipid monolayer, studied by ellipsometry and PM-IRRAS at the air-water interface. *Biochim Biophys Acta* 1467: 131-43
- Bellocq NC, Pun SH, Jensen GS, Davis ME (2003) Transferrin-containing, cyclodextrin polymer-based particles for tumor-targeted gene delivery. *Bioconjug Chem* 14: 1122-1132
- Belostotsky D (2004) mRNA turnover meets RNA interference. *Mol Cell* 16: 498-500
- Benimetskaya L, Guzzo-Pernell N, Liu ST, Lai JC, Miller P, Stein CA (2002) Protamine-fragment peptides fused to an SV40 nuclear localization signal deliver oligonucleotides that produce antisense effects in prostate and bladder carcinoma cells. *Bioconjug Chem* 13: 177-87
- Bergeron RJ, McManis JS, Franklin AM, Yao H, Weimar WR (2003) Polyamine-iron chelator conjugate. *J Med Chem* 46: 5478-83
- Berlose JP, Convert O, Derossi D, Brunissen A, Chassaing G (1996) Conformational and associative behaviours of the third helix of antennapedia homeodomain in membrane-mimetic environments. *Eur J Biochem* 242: 372-86
- Bernstein E, Caudy AA, Hammond SM, Hannon GJ (2001) Role for a bidentate ribonuclease in the initiation step of RNA interference. *Nature* 409: 363-366
- Bernstein E, Kim SY, Carmell MA, Murchison EP, Alcorn H, Li MZ, Mills AA, Elledge SJ, Anderson KV, Hannon GJ (2003) Dicer is essential for mouse development. *Nat Genet* 35: 215-7

- Billy E, Brondani V, Zhang H, Muller U, Filipowicz W (2001) Specific interference with gene expression induced by long, double-stranded RNA in mouse embryonal teratocarcinoma cell lines. *Proc Natl Acad Sci U S A* 98: 14428-33.
- Binder H, Lindblom G (2003) Charge-dependent translocation of the Trojan peptide penetratin across lipid membranes. *Biophys J* 85: 982-95
- Birnboim HC, Doly J (1979) A rapid alkaline extraction procedure for screening recombinant plasmid DNA. *Nucleic Acids Res* 7: 1513-23
- Bitko V, Barik S (2001) Phenotypic silencing of cytoplasmic genes using sequence-specific double-stranded short interfering RNA and its application in the reverse genetics of wild type negative-strand RNA viruses. *BMC Microbiol* 1: 34
- Blaszczyk J, Tropea JE, Bubunenko M, Routzahn KM, Waugh DS, Court DL, Ji XH (2001) Crystallographic and modeling studies of RNase III suggest a mechanism for double-stranded RNA cleavage. *Structure* 9: 1225-1236
- Blochlinger K, Jan LY, Jan YN (1991) Transformation of sensory organ identity by ectopic expression of *Cut* in *Drosophila*. *Genes Dev* 5: 1124-35
- Boden D, Pusch O, Lee F, Tucker L, Ramratnam B (2003a) Human immunodeficiency virus type 1 escape from RNA interference. *J Virol* 77: 11531-5
- Boden D, Pusch O, Lee F, Tucker L, Ramratnam B (2004a) Efficient Gene Transfer of HIV-1-Specific Short Hairpin RNA into Human Lymphocytic Cells Using Recombinant Adeno-associated Virus Vectors. *Mol Ther* 9: 396-402
- Boden D, Pusch O, Lee F, Tucker L, Shank PR, Ramratnam B (2003b) Promoter choice affects the potency of HIV-1 specific RNA interference. *Nucleic Acids Res* 31: 5033-8
- Boden D, Pusch O, Silbermann R, Lee F, Tucker L, Ramratnam B (2004b) Enhanced gene silencing of HIV-1 specific siRNA using microRNA designed hairpins. *Nucleic Acids Res* 32: 1154-8
- Boletta A, Benigni A, Lutz J, Remuzzi G, Soria MR, Monaco L (1997) Nonviral gene delivery to the rat kidney with polyethylenimine. *Hum Gene Ther* 8: 1243-51
- Bolton SJ, Jones DN, Darker JG, Eggleston DS, Hunter AJ, Walsh FS (2000) Cellular uptake and spread of the cell-permeable peptide penetratin in adult rat brain. *Eur J Neurosci* 12: 2847-55
- Bonci D, Cittadini A, Latronico MV, Borello U, Aycocock JK, Drusco A, Innocenzi A, Follenzi A, Lavitrano M, Monti MG, Ross J, Jr., Naldini L, Peschle C, Cossu G, Condorelli G (2003) 'Advanced' generation lentiviruses as efficient vectors for cardiomyocyte gene transduction in vitro and in vivo. *Gene Ther* 10: 630-6
- Boonyarattanakalin S, Martin SE, Dykstra SA, Peterson BR (2004) Synthetic mimics of small Mammalian cell surface receptors. *J Am Chem Soc* 126: 16379-86
- Boquet P, Duflot E (1982) Tetanus toxin fragment forms channels in lipid vesicles at low pH. *Proc Natl Acad Sci U S A* 79: 7614-8
- Bosher JM, Labouesse M (2000) RNA interference: genetic wand and genetic watchdog. *Nat Cell Biol* 2: E31-6.
- Boutla A, Delidakis C, Livadaras I, Tsagris M, Tabler M (2001) Short 5'-phosphorylated double-stranded RNAs induce RNA interference in *Drosophila*. *Curr Biol* 11: 1776-80.
- Braasch DA, Jensen S, Liu Y, Kaur K, Arar K, White MA, Corey DR (2003) RNA interference in mammalian cells by chemically-modified RNA. *Biochemistry* 42: 7967-75
- Brand AH, Perrimon N (1993) Targeted gene expression as a means of altering cell fates and generating dominant phenotypes. *Development* 118: 401-15
- Branden LJ, Christensson B, Smith CIE (2001) In vivo nuclear delivery of oligonucleotides via hybridizing bifunctional peptides. *Gene Therapy* 8: 84-87
- Brantl S (2002) Antisense-RNA regulation and RNA interference [Review]. *Biochimica et Biophysica Acta - Gene Structure & Expression* 1575: 15-25
- Braun K, Peschke P, Pipkorn R, Lampel S, Wachsmuth M, Waldeck W, Friedrich E, Debus J (2002) A biological transporter for the delivery of peptide nucleic acids (PNAs) to the nuclear compartment of living cells. *J Mol Biol* 318: 237-43
- Bremner KH, Seymour LW, Logan A, Read ML (2004) Factors influencing the ability of nuclear localization sequence peptides to enhance nonviral gene delivery. *Bioconjug Chem* 15: 152-61

- Brewis N, Phelan A, Normand N, Choolun E, O'Hare P. (2003) Particle assembly incorporating a VP22-BH3 fusion protein, facilitating intracellular delivery, regulated release, and apoptosis. *Mol Ther* 7: 262
- Bridge AJ, Pebernard S, Ducraux A, Nicoulaz AL, Iggo R (2003) Induction of an interferon response by RNAi vectors in mammalian cells. *Nature Genetics* 34: 263-264
- Brown AE, Bugeon L, Crisanti A, Catteruccia F (2003) Stable and heritable gene silencing in the malaria vector *Anopheles stephensi*. *Nucleic Acids Res* 31: e85
- Brown MS, Goldstein JL (1986) A receptor-mediated pathway for cholesterol homeostasis. *Science* 232: 34-47
- Brückner R (2000) Reaktionsmechanismen - Organische Reaktionen, Stereochemie, moderne Synthesemethoden. Spektrum Akad. Verlag, Heidelberg
- Brummelkamp TR, Bernards R, Agami R (2002a) Stable suppression of tumorigenicity by virus-mediated RNA interference. *Cancer Cell* 2: 243-7
- Brummelkamp TR, Bernards R, Agami R (2002b) A system for stable expression of short interfering RNAs in mammalian cells. *Science* 296: 550-3
- Brummelkamp TR, Nijman SM, Dirac AM, Bernards R (2003) Loss of the cylindromatosis tumour suppressor inhibits apoptosis by activating NF-kappaB. *Nature* 424: 797-801
- Buerger C, Groner B (2003) Bifunctional recombinant proteins in cancer therapy: cell penetrating peptide aptamers as inhibitors of growth factor signaling. *J Cancer Res Clin Oncol* 129: 669-75
- Buschle M, Schmidt W, Zauner W, Mechtler K, Trska B, Kirlappos H, Birnstiel ML (1997) Cationic polyamino acids as potent adjuvants for peptide based cancer vaccines. *Journal of Investigative Dermatology* 109: 7-7
- Butz K, Ristriani T, Hengstermann A, Denk C, Scheffner M, Hoppe-Seyler F (2003) siRNA targeting of the viral E6 oncogene efficiently kills human papillomavirus-positive cancer cells. *Oncogene* 22: 5938-45
- Calegari F, Haubensak W, Yang D, Huttner WB, Buchholz F (2002) Tissue-specific RNA interference in postimplantation mouse embryos with endoribonuclease-prepared short interfering RNA. *Proc Natl Acad Sci U S A* 99: 14236-40
- Callebaut I, Mornon JP (1997) The human EBNA-2 coactivator p100: multidomain organization and relationship to the staphylococcal nuclease fold and to the tudor protein involved in *Drosophila melanogaster* development. *Biochem J* 321 (Pt 1): 125-32
- Capella MA, Capella LS (2003) A light in multidrug resistance: photodynamic treatment of multidrug-resistant tumors. *J Biomed Sci* 10: 361-6
- Caplen NJ, Parrish S, Imani F, Fire A, Morgan RA (2001) Specific inhibition of gene expression by small double-stranded RNAs in invertebrate and vertebrate systems. *Proceedings of the National Academy of Sciences of the United States of America* 98: 9742-9747
- Capodici J, Kariko K, Weissman D (2002) Inhibition of HIV-1 infection by small interfering RNA-mediated RNA interference. *J Immunol* 169: 5196-201
- Carmell MA, Hannon GJ (2004) RNase III enzymes and the initiation of gene silencing. *Nat Struct Mol Biol* 11: 214-8
- Carmell MA, Xuan Z, Zhang MQ, Hannon GJ (2002) The Argonaute family: tentacles that reach into RNAi, developmental control, stem cell maintenance, and tumorigenesis. *Genes Dev* 16: 2733-42
- Carmell MA, Zhang L, Conklin DS, Hannon GJ, Rosenquist TA (2003) Germline transmission of RNAi in mice. *Nat Struct Biol* 10: 91-2.
- Carrington JC, Ambros V (2003) Role of microRNAs in plant and animal development. *Science* 301: 336-8
- Castro-Obregon S, Rao RV, Del Rio G, Chen SF, Poksay KS, Rabizadeh S, Vesce S, Zhang XK, Swanson RA, Bredesen DE (2004) Alternative, non-apoptotic programmed cell death: mediation by arrestin 2, ERK2 and Nur77. *J Biol Chem*
- Cattel L, Ceruti M, Dosio F (2003) From conventional to stealth liposomes: a new frontier in cancer chemotherapy. *Tumori* 89: 237-49

- Caudy AA, Ketting RF, Hammond SM, Denli AM, Bathoorn AM, Tops BB, Silva JM, Myers MM, Hannon GJ, Plasterk RH (2003) A micrococcal nuclease homologue in RNAi effector complexes. *Nature* 425: 411-4
- Caudy AA, Myers M, Hannon GJ, Hammond SM (2002) Fragile X-related protein and VIG associate with the RNA interference machinery. *Genes & Development* 16: 2491-2496
- Cegnar M, Premzl A, Zavasnik-Bergant V, Kristl J, Kos J (2004) Poly(lactide-co-glycolide) nanoparticles as a carrier system for delivering cysteine protease inhibitor cystatin into tumor cells. *Exp Cell Res* 301: 223-31
- Cerutti L, Mian N, Bateman A (2000) Domains in gene silencing and cell differentiation proteins: the novel PAZ domain and redefinition of the Piwi domain. *Trends in Biochemical Sciences* 25: 481-482
- Chang C, Mooser A, Pluckthun A, Wlodawer A (2001) Crystal structure of the dimeric C-terminal domain of TonB reveals a novel fold. *J Biol Chem* 276: 27535-40.
- Chatterjee B (2003) The role of the androgen receptor in the development of prostatic hyperplasia and prostate cancer. *Mol Cell Biochem* 253: 89-101
- Chawla JS, Amiji MM (2003) Cellular uptake and concentrations of tamoxifen upon administration in poly(epsilon-caprolactone) nanoparticles. *Aaps Pharmsci* 5: -
- Chen D, Maa YF, Haynes JR (2002a) Needle-free epidermal powder immunization. *Expert Rev Vaccines* 1: 265-76
- Chen K, Albano A, Ho A, Keaney JF, Jr. (2003) Activation of p53 by oxidative stress involves platelet-derived growth factor-beta receptor-mediated ataxia telangiectasia mutated (ATM) kinase activation. *J Biol Chem* 278: 39527-33
- Chen L, Wright LR, Chen CH, Oliver SF, Wender PA, Mochly-Rosen D (2001) Molecular transporters for peptides: delivery of a cardioprotective epsilonPKC agonist peptide into cells and intact ischemic heart using a transport system, R(7). *Chem Biol* 8: 1123-9.
- Chen YG, Lui HM, Lin SL, Lee JM, Ying SY (2002b) Regulation of cell proliferation, apoptosis, and carcinogenesis by activin. *Exp Biol Med (Maywood)* 227: 75-87
- Chiu YL, Ali A, Chu CY, Cao H, Rana TM (2004a) Visualizing a correlation between siRNA localization, cellular uptake, and RNAi in living cells. *Chem Biol* 11: 1165-75
- Chiu YL, Cao H, Jacque JM, Stevenson M, Rana TM (2004b) Inhibition of human immunodeficiency virus type 1 replication by RNA interference directed against human transcription elongation factor P-TEFb (CDK9/CyclinT1). *J Virol* 78: 2517-29
- Chiu YL, Rana TM (2002) RNAi in human cells: Basic structural and functional features of small interfering RNA. *Molecular Cell* 10: 549-561
- Chiu YL, Rana TM (2003) siRNA function in RNAi: A chemical modification analysis. *Rna-A Publication of the Rna Society* 9: 1034-1048
- Christiaens B, Grooten J, Reusens M, Joliot A, Goethals M, Vandekerckhove J, Prochiantz A, Rosseneu M (2004) Membrane interaction and cellular internalization of penetratin peptides. *Eur J Biochem* 271: 1187-97
- Christiaens B, Symoens S, Verheyden S, Engelborghs Y, Joliot A, Prochiantz A, Vandekerckhove J, Rosseneu M, Vanloo B, Vanderheyden S (2002) Tryptophan fluorescence study of the interaction of penetratin peptides with model membranes. *Eur J Biochem* 269: 2918-26
- Cioca DP, Aoki Y, Kiyosawa K (2003) RNA interference is a functional pathway with therapeutic potential in human myeloid leukemia cell lines. *Cancer Gene Therapy* 10: 125-33
- Clemens MJ (1997) Pkr - a Protein Kinase Regulated by Double-Stranded Rna. *International Journal of Biochemistry & Cell Biology* 29: 945-949
- Clemens MJ, Elia A (1997) The double-stranded RNA-dependent protein kinase PKR - structure and function [Review]. *Journal of Interferon & Cytokine Research* 17: 503-524
- Coburn GA, Cullen BR (2002) Potent and specific inhibition of human immunodeficiency virus type 1 replication by RNA interference. *J Virol* 76: 9225-31

- Cogoni C, Macino G (1997) Isolation of quelling defective (QDE) mutants impaired in posttranscriptional transgene- induced gene silencing in *Neurospora crassa*. *Proc Natl Acad Sci U S A* 94: 10233-10238
- Cogoni C, Macino G (1999a) Gene silencing in *Neurospora crassa* requires a protein homologous to RNA-dependent RNA polymerase. *Nature* 399: 166-169
- Cogoni C, Macino G (1999b) Posttranscriptional gene silencing in *Neurospora* by a RecQ DNA helicase. *Science* 286: 2342-4.
- Cogoni C, Macino G (2000) Post-transcriptional gene silencing across kingdoms. *Curr Opin Genet Dev* 10: 638-43.
- Console S, Marty C, Garcia-Echeverria C, Schwendener R, Ballmer-Hofer K (2003) Antennapedia and HIV transactivator of transcription (TAT) "protein transduction domains" promote endocytosis of high molecular weight cargo upon binding to cell surface glycosaminoglycans. *J Biol Chem* 278: 35109-14
- Couzin J (2004) RNAi Shows Cracks in Its Armor. *Science* 306: 1124-1125
- Cui Z, Hsu CH, Mumper RJ (2003) Physical characterization and macrophage cell uptake of mannan-coated nanoparticles. *Drug Dev Ind Pharm* 29: 689-700
- Cui Z, Mumper RJ (2003) The effect of co-administration of adjuvants with a nanoparticle-based genetic vaccine delivery system on the resulting immune responses. *Eur J Pharm Biopharm* 55: 11-8
- Cui ZR, Mumper RJ (2002) Plasmid DNA-entrapped nanoparticles engineered from microemulsion precursors: In vitro and in vivo evaluation. *Bioconjug Chem* 13: 1319-1327
- Cummins LL, Owens SR, Risen LM, Lesnik EA, Freier SM, McGee D, Guinosso CJ, Cook PD (1995) Characterization of fully 2'-modified oligoribonucleotide hetero- and homoduplex hybridization and nuclease sensitivity. *Nucleic Acids Res* 23: 2019-24
- Cunningham JM, Weinberg RA (1985) Ras oncogenes in human tumours: identification, mechanism of activation and cooperative role in transformation. *IARC Sci Publ*: 359-64
- Czauderna F, Fechtner M, Dames S, Aygun H, Klippel A, Pronk GJ, Giese K, Kaufmann J (2003) Structural variations and stabilising modifications of synthetic siRNAs in mammalian cells. *Nucleic Acids Res* 31: 2705-16
- Dalmay T, Hamilton A, Mueller E, Baulcombe DC (2000) Potato virus X amplicons in *Arabidopsis* mediate genetic and epigenetic gene silencing. *Plant Cell* 12: 369-379
- Dathe M, Schumann M, Wieprecht T, Winkler A, Beyermann M, Krause E, Matsuzaki K, Murase O, Bienert M (1996) Peptide helicity and membrane surface charge modulate the balance of electrostatic and hydrophobic interactions with lipid bilayers and biological membranes. *Biochemistry* 35: 12612-22
- Dave RS, Pomerantz RJ (2003) RNA interference: on the road to an alternate therapeutic strategy! *Rev Med Virol* 13: 373-85
- Davidson TJ, Harel S, Arboleda VA, Prunell GF, Shelanski ML, Greene LA, Troy CM (2004) Highly efficient small interfering RNA delivery to primary mammalian neurons induces MicroRNA-like effects before mRNA degradation. *J Neurosci* 24: 10040-6
- Dector MA, Romero P, Lopez S, Arias CF (2002) Rotavirus gene silencing by small interfering RNAs. *EMBO Rep* 3: 1175-80
- DeGrado WF (1999) Molecular design as an approach to understanding membrane protein structure and function. *Faseb Journal* 13: A1431-A1431
- Delcros JG, Tomasi S, Carrington S, Martin B, Renault J, Blagbrough IS, Uriac P (2002) Effect of spermine conjugation on the cytotoxicity and cellular transport of acridine. *J Med Chem* 45: 5098-111
- Deroanne C, Vouret-Craviari V, Wang B, Pouyssegur J (2003) EphrinA1 inactivates integrin-mediated vascular smooth muscle cell spreading via the Rac/PAK pathway. *J Cell Sci* 116: 1367-76
- Derossi D, Calvet S, Trembleau A, Brunissen A, Chassaing G, Prochiantz A (1996) Cell internalization of the third helix of the Antennapedia homeodomain is receptor-independent. *J Biol Chem* 271: 18188-93.

- Derossi D, Chassaing G, Prochiantz A (1998) Trojan Peptides - the Penetratin System for Intracellular Delivery. *Trends in Cell Biology* 8: 84-87
- Derossi D, Joliot AH, Chassaing G, Prochiantz A (1994) The third helix of the Antennapedia homeodomain translocates through biological membranes. *Journal of Biological Chemistry* 269: 10444-50
- Deshayes S, Plenat T, Aldrian-Herrada G, Divita G, Le Grimellec C, Heitz F (2004) Primary amphipathic cell-penetrating peptides: structural requirements and interactions with model membranes. *Biochemistry* 43: 7698-706
- Detty MR, Gibson SL, Wagner SJ (2004) Current clinical and preclinical photosensitizers for use in photodynamic therapy. *J Med Chem* 47: 3897-915
- Devroe E, Silver PA (2002) Retrovirus-delivered siRNA. *BMC Biotechnol* 2: 15
- Diallo M, Arenz C, Schmitz K, Sandhoff K, Schepers U (2003a) Long endogenous dsRNAs can induce a complete gene silencing in mammalian cells and primary cultures. *Oligonucleotides* 13: 381-392
- Diallo M, Arenz C, Schmitz K, Sandhoff K, Schepers U (2003b) RNA Interference: A new method to analyze the function of glycoproteins and glycosylating proteins in mammalian cells. Knockout experiments with UDP-glucose/ ceramide-glycosyltransferase. *Methods in Enzymology* 363: 173-190
- Diaz-Griffero F, Hoschander SA, Brojatsch J (2002) Endocytosis is a critical step in entry of subgroup B avian leukosis viruses. *J Virol* 76: 12866-76
- Ding D, Moskowitz SI, Li R, Lee SB, Esteban M, Tomaselli K, Chan J, Bergold PJ (2000) Acidosis induces necrosis and apoptosis of cultured hippocampal neurons. *Experimental Neurology* 162: 1-12
- Ding H, Schwarz DS, Keene A, Affar el B, Fenton L, Xia X, Shi Y, Zamore PD, Xu Z (2003) Selective silencing by RNAi of a dominant allele that causes amyotrophic lateral sclerosis. *Aging Cell* 2: 209-17
- Doench JG, Petersen CP, Sharp PA (2003) siRNAs can function as miRNAs. *Genes & Development* 17: 438-442
- Doench JG, Sharp PA (2004) Specificity of microRNA target selection in translational repression. *Genes Dev* 18: 504-11
- Doi N, Zenno S, Ueda R, Ohki-Hamazaki H, Ui-Tei K, Saigo K (2003) Short-interfering-RNA-mediated gene silencing in mammalian cells requires Dicer and eIF2C translation initiation factors. *Curr Biol* 13: 41-6
- Dom G, Shaw-Jackson C, Matis C, Bouffieux O, Picard JJ, Prochiantz A, Mingeot-Leclercq MP, Brasseur R, Rezsöházy R (2003) Cellular uptake of Antennapedia Penetratin peptides is a two-step process in which phase transfer precedes a tryptophan-dependent translocation. *Nucleic Acids Res* 31: 556-61.
- Donze O, Picard D (2002) RNA interference in mammalian cells using siRNAs synthesized with T7 RNA polymerase. *Nucleic Acids Res* 30: e46.
- Dorn G (2004) siRNA relieves chronic neuropathic pain. *Nucleic Acids Research* 32
- Douglas SJ, Davis SS, Illum L (1987) Nanoparticles in drug delivery. *Crit Rev Ther Drug Carrier Syst* 3: 233-61
- Drin G, Mazel M, Clair P, Mathieu D, Kaczorek M, Tamsamani J (2001) Physico-chemical requirements for cellular uptake of pAntp peptide. Role of lipid-binding affinity. *Eur J Biochem* 268: 1304-14
- Drin GC, Sylvine; Blanc, Emmanuelle; Rees, Anthony R.; Tamsamani, Jamal (2003) Studies on the internalization mechanism of cationic cell-penetrating peptides. *J. Biol. Chem.* 278: 31192-31201
- Dudley NR, Labbe JC, Goldstein B (2002) Using RNA interference to identify genes required for RNA interference. *Proc Natl Acad Sci U S A* 99: 4191-6.
- Dunn SJ, Khan IH, Chan UA, Scearce RL, Melara CL, Paul AM, Sharma V, Bih FY, Holzmayer TA, Luciw PA, Abo A (2004) Identification of cell surface targets for HIV-1 therapeutics using genetic screens. *Virology* 321: 260-73
- Dunne J, Drescher B, Riehle H, Hadwiger P, Young BD, Krauter J, Heidenreich O (2003) The apparent uptake of fluorescently labeled siRNAs by electroporated cells depends on the fluorochrome. *Oligonucleotides* 13: 375-80

- Duursma AM, Agami R (2003) Ras interference as cancer therapy. *Seminars in Cancer Biology* 13: 267-273
- Duxbury MS, Ito H, Benoit E, Zinner MJ, Ashley SW, Whang EE (2003) RNA interference targeting focal adhesion kinase enhances pancreatic adenocarcinoma gemcitabine chemosensitivity. *Biochem Biophys Res Commun* 311: 786-92
- Dzitoyeva S, Dimitrijevic N, Manev H (2003) Gamma-aminobutyric acid B receptor 1 mediates behavior-impairing actions of alcohol in *Drosophila*: adult RNA interference and pharmacological evidence. *Proc Natl Acad Sci U S A* 100: 5485-90
- Elbashir SM, Harborth J, Lendeckel W, Yalcin A, Weber K, Tuschl T (2001a) Duplexes of 21-nucleotide RNAs mediate RNA interference in cultured mammalian cells. *Nature* 411: 494-498
- Elbashir SM, Lendeckel W, Tuschl T (2001b) RNA interference is mediated by 21- and 22-nucleotide RNAs. *Genes & Development* 15: 188-200
- Elbashir SM, Martinez J, Patkaniowska A, Lendeckel W, Tuschl T (2001c) Functional anatomy of siRNAs for mediating efficient RNAi in *Drosophila melanogaster* embryo lysate. *EMBO Journal* 20: 6877-6888
- Elliott G, Ohare P (1997) Intercellular Trafficking and Protein Delivery by a Herpesvirus Structural Protein. *Cell* 88: 223-233
- Elmqvist A, Lindgren M, Bartfai T, Langel U (2001) VE-cadherin-derived cell-penetrating peptide, pVEC, with carrier functions. *Experimental Cell Research* 269: 237-44
- Emi N, Kidoaki S, Yoshikawa K, Saito H (1997) Gene transfer mediated by polyarginine requires a formation of big carrier-complex of DNA aggregate. *Biochem Biophys Res Commun* 231: 421-4
- Famulok M (1999) Oligonucleotide aptamers that recognize small molecules. *Current Opinion in Structural Biology*. 9: 324-329
- Farokhzad OC, Jon S, Khademhosseini A, Tran TN, Lavan DA, Langer R (2004) Nanoparticle-aptamer bioconjugates: a new approach for targeting prostate cancer cells. *Cancer Res* 64: 7668-72
- Farrow B, Rychahou P, Murillo C, O'Connor K L, Iwamura T, Evers BM (2003) Inhibition of pancreatic cancer cell growth and induction of apoptosis with novel therapies directed against protein kinase A. *Surgery* 134: 197-205
- Fawell S, Seery J, Daikh Y, Moore C, Chen LL, Pepinsky B, Barsoum J (1994) Tat-mediated delivery of heterologous proteins into cells. *Proc Natl Acad Sci U S A* 91: 664-8
- Fernandez-Carneado J, Kogan MJ, Castel S, Giralt E (2004) Potential peptide carriers: amphipathic proline-rich peptides derived from the N-terminal domain of gamma-zein. *Angew Chem Int Ed Engl* 43: 1811-4
- Figliozzi GM, Goldsmith R, Ng SC, Banville SC, Zuckermann RN (1996) Synthesis of N-substituted glycine peptoid libraries. *Methods Enzymol* 267: 437-47
- Filippov V, Solovyev V, Filippova M, Gill SS (2000) A novel type of RNase III family proteins in eukaryotes. *Gene* 245: 213-21
- Fire A, Xu SQ, Montgomery MK, Kostas SA, Driver SE, Mello CC (1998) Potent and specific genetic interference by double-stranded RNA in *Caenorhabditis elegans*. *Nature* 391: 806-811
- Fischer M, Vögtle, F (1999) Dendrimere: vom Design zu Anwendung - ein Fortschrittsbericht. *Angew. Chem.* 111: 934-955
- Fischer PM, Krausz E, Lane DP (2001) Cellular delivery of impermeable effector molecules in the form of conjugates with peptides capable of mediating membrane translocation. *Bioconjugate Chemistry* 12: 825-841
- Fischer R, Kohler K, Fotin-Mleczek M, Brock R (2004) A stepwise dissection of the intracellular fate of cationic cell-penetrating peptides. *J Biol Chem* 279: 12625-35
- Fischer R, Waizenegger T, Kohler K, Brock R (2002) A quantitative validation of fluorophore-labelled cell-permeable peptide conjugates: fluorophore and cargo dependence of import. *Biochim Biophys Acta* 1564: 365-74
- Fish RJ, Kruihof EK (2004) Short-term cytotoxic effects and long-term instability of RNAi delivered using lentiviral vectors. *BMC Mol Biol* 5: 9

- Fisher L, Soomets U, Cortes Toro V, Chilton L, Jiang Y, Langel U, Iverfeldt K (2004) Cellular delivery of a double-stranded oligonucleotide NFkappaB decoy by hybridization to complementary PNA linked to a cell-penetrating peptide. *Gene Ther* 11: 1264-72
- Fittipaldi A, Ferrari A, Zoppe M, Arcangeli C, Pellegrini V, Beltram F, Giacca M (2003) Cell membrane lipid rafts mediate caveolar endocytosis of HIV-1 Tat fusion proteins. *J Biol Chem* 278: 34141-9
- Fortin KR, Nicholson RH, Nicholson AW (2002) Mouse ribonuclease III. cDNA structure, expression analysis, and chromosomal location. *BMC Genomics* 3: 26
- Francis R, McGrath G, Zhang J, Ruddy DA, Sym M, Apfeld J, Nicoll M, Maxwell M, Hai B, Ellis MC, Parks AL, Xu W, Li J, Gurney M, Myers RL, Himes CS, Hiebsch R, Ruble C, Nye JS, Curtis D (2002) aph-1 and pen-2 are required for Notch pathway signaling, gamma-secretase cleavage of betaAPP, and presenilin protein accumulation. *Dev Cell* 3: 85-97.
- Frankel AD, Chen L, Cotter RJ, Pabo CO (1988) Dimerization of the tat protein from human immunodeficiency virus: a cysteine-rich peptide mimics the normal metal-linked dimer interface. *Proceedings of the National Academy of Sciences of the United States of America* 85: 6297-300
- Frankel AD, Pabo CO (1988) Cellular uptake of the tat protein from human immunodeficiency virus. *Cell* 55: 1189-93
- Frank-Kamenetsky (2001) Small-molecule modulators of Hedgehog signaling: identification and characterization of Smoothed agonists and antagonists. *J. Biol.* 1: 10
- Fujii G, Horvath, S., Woodward, S., Eiserling, F., and Eisenberg, D. (1992) A molecular model for membrane fusion based on solution studies of an amphiphilic peptide from HIV gp41. *Protein Sci.* 1: 1454-1464
- Futami T, Miyagishi M, Seki M, Taira K (2002) Induction of apoptosis in HeLa cells with siRNA expression vector targeted against bcl-2. *Nucleic Acids Research. Supplement*: 251-2
- Gademann K, Hintermann, T. (1999) beta-peptides: Twisting and turning. *Curr. Med. Chem.* 6: 905-925
- Garcia-Echeverria C, Ruetz S (2003) beta-Homolysine oligomers: a new class of Trojan carriers. *Bioorg Med Chem Lett* 13: 247-51
- Gardner RA, Delcros JG, Konate F, Breitbeil F, 3rd, Martin B, Sigman M, Huang M, Phanstiel Ot (2004) N1-substituent effects in the selective delivery of polyamine conjugates into cells containing active polyamine transporters. *J Med Chem* 47: 6055-69
- Gazzani S, Lawrenson T, Woodward C, Headon D, Sablowski R (2004) A link between mRNA turnover and RNA interference in Arabidopsis. *Science* 306: 1046-8
- Ge Q, McManus MT, Nguyen T, Shen CH, Sharp PA, Eisen HN, Chen J (2003) RNA interference of influenza virus production by directly targeting mRNA for degradation and indirectly inhibiting all viral RNA transcription. *Proc Natl Acad Sci U S A* 100: 2718-23
- Geller BL, Deere JD, Stein DA, Kroeker AD, Moulton HM, Iversen PL (2003) Inhibition of gene expression in Escherichia coli by antisense phosphorodiamidate morpholino oligomers. *Antimicrobial Agents and Chemotherapy* 47: 3233-3239
- Gellman SH (1998) Minimal model systems for beta sheet secondary structure in proteins. *Current Opinion in Chemical Biology* 2: 717-725
- Gil-Parrado S, Assfalg-Machleidt I, Fiorino F, Deluca D, Pfeiler D, Schaschke N, Moroder L, Machleidt W (2003) Calpastatin exon 1B-derived peptide, a selective inhibitor of calpain: enhancing cell permeability by conjugation with penetratin. *Biol Chem* 384: 395-402
- Giordano E, Rendina R, Peluso I, Furia M (2002) RNAi triggered by symmetrically transcribed transgenes in Drosophila melanogaster. *Genetics* 160: 637-48.
- Gitlin L, Andino R (2003) Nucleic acid-based immune system: the antiviral potential of mammalian RNA silencing. *J Virol* 77: 7159-65
- Gitlin L, Karelsky S, Andino R (2002) Short interfering RNA confers intracellular antiviral immunity in human cells. *Nature* 418: 430-4.

- Gittins PJ, Twyman LJ (2003) Dendrimers and supramolecular chemistry. *Supramol Chem* 15: 5-23
- Gius DR, Ezhevsky SA, Becker-Hapak M, Nagahara H, Wei MC, Dowdy SF (1999) Transduced p16INK4a peptides inhibit hypophosphorylation of the retinoblastoma protein and cell cycle progression prior to activation of Cdk2 complexes in late G1. *Cancer Res* 59: 2577-80
- Godfrey A, Laman H, Boshoff C (2003) RNA interference: a potential tool against Kaposi's sarcoma-associated herpesvirus. *Curr Opin Infect Dis* 16: 593-600
- Goff DA, Zuckermann RN (1992) Solid Phase Synthesis of Highly Substituted Peptoid 1(2H) Isoquinolinones. *Proc. Nat. Acad. Sci. USA* 60
- Gonzalez-Reyes A, Morata G (1990) The developmental effect of overexpressing a Ubx product in *Drosophila* embryos is dependent on its interactions with other homeotic products. *Cell* 61: 515-22
- Goody RS, Walker RT (1971) The preparation and properties of some cytosine derivatives. *J Org Chem* 36: 727-30
- Gratton JP, Yu J, Griffith JW, Babbitt RW, Scotland RS, Hickey R, Giordano FJ, Sessa WC (2003) Cell-permeable peptides improve cellular uptake and therapeutic gene delivery of replication-deficient viruses in cells and in vivo. *Nat Med* 9: 357-62
- Green I, Christison R, Voyce CJ, Bundell KR, Lindsay MA (2003) Protein transduction domains: are they delivering? *Trends Pharmacol Sci* 24: 213-5
- Green M, Loewenstein PM (1988) Autonomous functional domains of chemically synthesized human immunodeficiency virus tat trans-activator protein. *Cell* 55: 1179-88
- Grishok A, Mello CC (2002) RNAi (Nematodes: *Caenorhabditis elegans*). *Adv Genet* 46: 339-60
- Grishok A, Pasquinelli AE, Conte D, Li N, Parrish S, Ha I, Baillie DL, Fire A, Ruvkun G, Mello CC (2001) Genes and mechanisms related to RNA interference regulate expression of the small temporal RNAs that control *C. elegans* developmental timing. *Cell* 106: 23-34.
- Grishok A, Tabara H, Mello CC (2000) Genetic requirements for inheritance of RNAi in *C. elegans*. *Science* 287: 2494-7.
- Grunweller A, Gillen C, Erdmann VA, Kurreck J (2003) Cellular uptake and localization of a Cy3-labeled siRNA specific for the serine/threonine kinase Pim-1. *Oligonucleotides* 13: 345-52
- Grzmil M, Thelen P, Hemmerlein B, Schweyer S, Voigt S, Mury D, Burfeind P (2003) Bax inhibitor-1 is overexpressed in prostate cancer and its specific down-regulation by RNA interference leads to cell death in human prostate carcinoma cells. *Am J Pathol* 163: 543-52
- Guo F, Cen S, Niu M, Javanbakht H, Kleiman L (2003) Specific inhibition of the synthesis of human lysyl-tRNA synthetase results in decreases in tRNA(Lys) incorporation, tRNA(3)(Lys) annealing to viral RNA, and viral infectivity in human immunodeficiency virus type 1. *J Virol* 77: 9817-22
- Guo S, Kemphues KJ (1995) Par-1, a Gene Required for Establishing Polarity in *C-Elegans* Embryos, Encodes a Putative Ser/Thr Kinase That Is Asymmetrically Distributed. *Cell* 81: 611-620
- Guy-Caffey JK, Bodepudi V, Bishop JS, Jayaraman K, Chaudhary N (1995) Novel polyaminolipids enhance the cellular uptake of oligonucleotides. *J Biol Chem* 270: 31391-6
- Haag R (2001) Dendrimers and hyperbranched polymers as high-loading supports for organic synthesis. *Chem* 7: 327-35
- Haag R (2004) Supramolecular drug-delivery systems based on polymeric core-shell architectures. *Angew Chem Int Ed* 43: 278-282
- Hacein-Bey-Abina S, von Kalle C, Schmidt M, Le Deist F, Wulffraat N, McIntyre E, Radford I, Villeval JL, Fraser CC, Cavazzana-Calvo M, Fischer A (2003a) A serious adverse event after successful gene therapy for X-linked severe combined immunodeficiency. *N Engl J Med* 348: 255-6

- Hacein-Bey-Abina S, Von Kalle C, Schmidt M, McCormack MP, Wulffraat N, Leboulch P, Lim A, Osborne CS, Pawliuk R, Morillon E, Sorensen R, Forster A, Fraser P, Cohen JI, de Saint Basile G, Alexander I, Wintergerst U, Frebourg T, Aurias A, Stoppa-Lyonnet D, Romana S, Radford-Weiss I, Gross F, Valensi F, Delabesse E, Macintyre E, Sigaux F, Soulier J, Leiva LE, Wissler M, Prinz C, Rabbitts TH, Le Deist F, Fischer A, Cavazzana-Calvo M (2003b) LMO2-associated clonal T cell proliferation in two patients after gene therapy for SCID-X1. *Science* 302: 415-9
- Hahn F (2005) Festphasensynthese von Sperminderivaten als neuartige Transportermoleküle für Porphyrin und siRNAs (vorläufiger Titel). Diplomarbeit, Bonn
- Haley B, Zamore PD (2004) Kinetic analysis of the RNAi enzyme complex. *Nat Struct Mol Biol* 11: 599-606
- Hall AH, Alexander KA (2003) RNA interference of human papillomavirus type 18 E6 and E7 induces senescence in HeLa cells. *J Virol* 77: 6066-9
- Hall AH, Wan J, Shaughnessy EE, Ramsay Shaw B, Alexander KA (2004) RNA interference using boranophosphate siRNAs: structure-activity relationships. *Nucleic Acids Res* 32: 5991-6000
- Hall IM, Noma K, Grewal SI (2003) RNA interference machinery regulates chromosome dynamics during mitosis and meiosis in fission yeast. *Proc Natl Acad Sci U S A* 100: 193-8
- Hallbrink M, Floren A, Elmquist A, Pooga M, Bartfai T, Langel U (2001) Cargo delivery kinetics of cell-penetrating peptides. *Biochimica et Biophysica Acta* 1515: 101-9
- Hallbrink M, Oehlke J, Papsdorf G, Bienert M (2004) Uptake of cell-penetrating peptides is dependent on peptide-to-cell ratio rather than on peptide concentration. *Biochim Biophys Acta* 1667: 222-8
- Hamasaki K, Nakao K, Matsumoto K, Ichikawa T, Ishikawa H, Eguchi K (2003) Short interfering RNA-directed inhibition of hepatitis B virus replication. *FEBS Letters* 543: 51-54
- Hamilton A, Voinnet O, Chappell L, Baulcombe D (2002) Two classes of short interfering RNA in RNA silencing. *Embo J* 21: 4671-9
- Hamilton AJ, Baulcombe DC (1999) A species of small antisense RNA in posttranscriptional gene silencing in plants. *Science* 286: 950-2.
- Hammond SM, Bernstein E, Beach D, Hannon GJ (2000) An RNA-directed nuclease mediates post-transcriptional gene silencing in *Drosophila* cells. *Nature* 404: 293-296
- Hammond SM, Boettcher S, Caudy AA, Kobayashi R, Hannon GJ (2001) Argonaute2, a link between genetic and biochemical analyses of RNAi. *Science* 293: 1146-1150
- Han K, Jeon MJ, Kim KA, Park J, Choi SY (2000) Efficient intracellular delivery of GFP by homeodomains of *Drosophila* Fushi-tarazu and Engrailed proteins. *Mol Cells* 10: 728-32
- Hannon GJ (2002) RNA interference. *Nature* 418: 244-51.
- Harborth J, Elbashir SM, Vandeburgh K, Manninga H, Scaringe SA, Weber K, Tuschl T (2003) Sequence, Chemical, and Structural Variation of Small Interfering RNAs and Short Hairpin RNAs and the Effect on Mammalian Gene Silencing. *Antisense Nucleic Acid Drug Dev* 13: 83-105
- Hariton-Gazal E, Feder R, Mor A, Graessmann A, Brack-Werner R, Jans D, Gilon C, Loyter A (2002) Targeting of nonkaryophilic cell-permeable peptides into the nuclei of intact cells by covalently attached nuclear localization signals. *Biochemistry* 41: 9208-14
- Hasuwa H, Kaseda K, Einarsdottir T, Okabe M (2002) Small interfering RNA and gene silencing in transgenic mice and rats. *FEBS Lett* 532: 227-30.
- Hausch F, Jäschke, A (1997) Libraries of multifunctional RNA conjugates for the selection of new RNA catalysts. *Bioconj. Chem.* 8: 885
- He ML, Zheng B, Peng Y, Peiris JS, Poon LL, Yuen KY, Lin MC, Kung HF, Guan Y (2003) Inhibition of SARS-associated coronavirus infection and replication by RNA interference. *Jama* 290: 2665-6
- Heidel JD, Hu S, Liu XF, Triche TJ, Davis ME (2004) Lack of interferon response in animals to naked siRNAs. *Nat Biotechnol* 22: 1579-82

- Heidenreich O, Krauter J, Riehle H, Hadwiger P, John M, Heil G, Vornlocher HP, Nordheim A (2003) AML1/MTG8 oncogene suppression by small interfering RNAs supports myeloid differentiation of t(8;21)-positive leukemic cells. *Blood* 101: 3157-63
- Hemann MT, Fridman JS, Zilfou JT, Hernando E, Paddison PJ, Cordon-Cardo C, Hannon GJ, Lowe SW (2003) An epi-allelic series of p53 hypomorphs created by stable RNAi produces distinct tumor phenotypes in vivo. *Nat Genet* 33: 396-400
- Henry CM (2003) Method Targets Transporter Proteins To Deliver Drugs. *Chemical & Engineering News* 81: 40
- Hierholzer M (1997) Epithelien. In: Schmidt RF, Thews, G (ed) *Physiologie des Menschen*, 27 edn. Springer, Heidelberg
- Ho A, Schwarze SR, Mermelstein SJ, Waksman G, Dowdy SF (2001) Synthetic protein transduction domains: enhanced transduction potential in vitro and in vivo. *Cancer Res* 61: 474-7.
- Holen T, Amarzguioui M, Wiiger MT, Babaie E, Prydz H (2002) Positional effects of short interfering RNAs targeting the human coagulation trigger Tissue Factor. *Nucleic Acids Res* 30: 1757-66.
- Huang CY, Uno T, Murphy JE, Lee S, Hamer JD, Escobedo JA, Cohen FE, Radhakrishnan R, Dwarki V, Zuckermann RN (1998) Lipitoids--novel cationic lipids for cellular delivery of plasmid DNA in vitro. *Chem Biol* 5: 345-54
- Hunter CP (1999) Genetics: a touch of elegance with RNAi. *Curr Biol* 9: R440-2.
- Hutvagner G, McLachlan J, Pasquinelli AE, Balint E, Tuschl T, Zamore PD (2001) A cellular function for the RNA-interference enzyme Dicer in the maturation of the let-7 small temporal RNA. *Science* 293: 834-838
- Hutvagner G, Mlynarova L, Nap JP (2000) Detailed characterization of the posttranscriptional gene-silencing-related small RNA in a GUS gene-silenced tobacco. *RNA - A publication of the RNA Society* 6: 1445-1454
- Hutvagner G, Zamore PD (2002a) A MicroRNA in a Multiple-Turnover RNAi Enzyme Complex. *Science* 1: 1
- Hutvagner G, Zamore PD (2002b) RNAi: nature abhors a double-strand. *Current Opinion in Genetics & Development* 12: 225-232
- Igarashi K, Kashiwagi K (2000) Polyamines: mysterious modulators of cellular functions. *Biochem Biophys Res Commun* 271: 559-64
- Igloi GL (1996) Nonradioactive labeling of RNA. *Anal Biochem* 233: 124-9
- Ignatovich IA, Dizhe EB, Pavlotskaya AV, Akifiev BN, Burov SV, Orlov SV, Perevozchikov AP (2003) Complexes of plasmid DNA with basic domain 47-57 of the HIV-1 Tat protein are transferred to mammalian cells by endocytosis-mediated pathways. *J Biol Chem* 278: 42625-36
- Ilves H, Barske C, Junker U, Bohnlein E, Veres G (1996) Retroviral vectors designed for targeted expression of RNA polymerase III-driven transcripts: a comparative study. *Gene* 171: 203-8.
- Innis MAR, Christoph J.; Zuckermann, Ronald N.; Reinhard, Christoph J.; Jefferson, Ann B.; Beausoleil, Eric (2001) Chimeric antisense oligonucleotides and cell transfecting formulations thereof. *PCT Int. Appl.*: 37 pp
- Ishizuka A, Siomi MC, Siomi H (2002) A Drosophila fragile X protein interacts with components of RNAi and ribosomal proteins. *Genes & Development* 16: 2497-2508
- Jackson AL, Bartz SR, Schelter J, Kobayashi SV, Burchard J, Mao M, Li B, Cavet G, Linsley PS (2003) Expression profiling reveals off-target gene regulation by RNAi. *Nat Biotechnol* 21: 635-7
- Jacobsen SE, Running MP, Meyerowitz EM (1999) Disruption of an RNA helicase/RNase III gene in Arabidopsis causes unregulated cell division in floral meristems. *Development* 126: 5231-43.
- Jacobson MA (1993) Valaciclovir (BW256U87): the L-valyl ester of acyclovir. *J Med Virol Suppl* 1: 150-3
- Jacque JM, Triques K, Stevenson M (2002) Modulation of HIV-1 replication by RNA interference. *Nature* 418: 435-8.

- Janout V, Zhang LH, Staina IV, Di Giorgio C, Regen SL (2001) Molecular umbrella-assisted transport of glutathione across a phospholipid membrane. *J Am Chem Soc* 123: 5401-6.
- Jarad G, Wang B, Khan S, DeVore J, Miao H, Wu K, Nishimura SL, Wible BA, Konieczkowski M, Sedor JR, Schelling JR (2002) Fas activation induces renal tubular epithelial cell beta 8 integrin expression and function in the absence of apoptosis. *J Biol Chem* 277: 47826-33
- Jayachandran G, Fallon AM (2003) Ribosomal protein P0 from *Aedes albopictus* mosquito cells: cDNA cloning and analysis of expression. *Genetica* 119: 1-10
- Jeang KT, Xiao H, Rich EA (1999) Multifaceted activities of the HIV-1 transactivator of transcription, Tat. *J Biol Chem* 274: 28837-40
- Jennings PA, Molloy PL (1987) Inhibition of SV40 replicon function by engineered antisense RNA transcribed by RNA polymerase III. *Embo J* 6: 3043-7.
- Jensen ON, Kulkarni S, Aldrich JV, Barofsky DF (1996) Characterization of peptide-oligonucleotide heteroconjugates by mass spectrometry. *Nucleic Acids Res* 24: 3866-72
- Ji J, Wernli M, Klimkait T, Erb P (2003) Enhanced gene silencing by the application of multiple specific small interfering RNAs. *FEBS Lett* 552: 247-52
- Jia Q, Sun R (2003) Inhibition of gammaherpesvirus replication by RNA interference. *J Virol* 77: 3301-6
- Jiang M, Milner J (2003) Bcl-2 constitutively suppresses p53-dependent apoptosis in colorectal cancer cells. *Genes Dev* 17: 832-7
- Jiang T, Olson ES, Nguyen QT, Roy M, Jennings PA, Tsien RY (2004) Tumor imaging by means of proteolytic activation of cell-penetrating peptides. *Proc Natl Acad Sci U S A* 101: 17867-72
- Johnston SA, Tang DC (1993) The use of microparticle injection to introduce genes into animal cells in vitro and in vivo. *Genet Eng (N Y)* 15: 225-36
- Jones L, Ratcliff F, Baulcombe DC (2001) RNA-directed transcriptional gene silencing in plants can be inherited independently of the RNA trigger and requires Met1 for maintenance. *Curr Biol* 11: 747-57.
- July LV, Beraldi E, So A, Fazli L, Evans K, English JC, Gleave ME (2004) Nucleotide-based therapies targeting clusterin chemosensitize human lung adenocarcinoma cells both in vitro and in vivo. *Mol Cancer Ther* 3: 223-32
- Kaihatsu K, Huffman KE, Corey DR (2004) Intracellular uptake and inhibition of gene expression by PNAs and PNA-peptide conjugates. *Biochemistry* 43: 14340-7
- Kaneda Y (2000) Virosomes: evolution of the liposome as a targeted drug delivery system. *Adv Drug Deliv Rev* 43: 197-205
- Kao SC, Krichevsky AM, Kosik KS, Tsai LH (2004) BACE1 suppression by RNA interference in primary cortical neurons. *J Biol Chem* 279: 1942-9
- Kapadia SB, Brideau-Andersen A, Chisari FV (2003) Interference of hepatitis C virus RNA replication by short interfering RNAs. *Proc Natl Acad Sci U S A* 100: 2014-8
- Kapust RB, Tozser J, Fox JD, Anderson DE, Cherry S, Copeland TD, Waugh DS (2001) Tobacco etch virus protease: mechanism of autolysis and rational design of stable mutants with wild-type catalytic proficiency. *Protein Eng* 14: 993-1000
- Kasim V, Miyagishi M, Taira K (2004) Control of siRNA expression using the Cre-loxP recombination system. *Nucleic Acids Res* 32: e66
- Kaushik N, Basu A, Palumbo P, Myers RL, Pandey VN (2002) Anti-TAR polyamide nucleotide analog conjugated with a membrane-permeating peptide inhibits human immunodeficiency virus type 1 production. *J Virol* 76: 3881-91
- Kawasaki H, Taira K (2003) Short hairpin type of dsRNAs that are controlled by tRNA(Val) promoter significantly induce RNAi-mediated gene silencing in the cytoplasm of human cells. *Nucleic Acids Res* 31: 700-7
- Kelemen BR, Hsiao K, Goueli SA (2002) Selective in vivo inhibition of mitogen-activated protein kinase activation using cell-permeable peptides. *J Biol Chem* 277: 8741-8
- Kennerdell JR, Carthew RW (2000) Heritable gene silencing in *Drosophila* using double-stranded RNA. *Nature Biotechnology* 18: 896-898

- Ketting RF, Fischer SE, Bernstein E, Sijen T, Hannon GJ, Plasterk RH (2001) Dicer functions in RNA interference and in synthesis of small RNA involved in developmental timing in *C. elegans*. *Genes Dev* 15: 2654-9.
- Ketting RF, Haverkamp TH, van Luenen HG, Plasterk RH (1999) Mut-7 of *C. elegans*, required for transposon silencing and RNA interference, is a homolog of Werner syndrome helicase and RNaseD. *Cell* 99: 133-41.
- Khvorova A, Reynolds A, Jayasena SD (2003) Functional siRNAs and miRNAs exhibit strand bias. *Cell* 115: 209-16
- Kichler A, Mechtler K, Behr JP, Wagner E (1997) Influence of membrane-active peptides on lipospermine/DNA complex mediated gene transfer. *Bioconjug Chem* 8: 213-21
- Kiehl TR, Shibata H, Pulst SM (2000) The ortholog of human ataxin-2 is essential for early embryonic patterning in *C. elegans*. *J Mol Neurosci* 15: 231-41.
- Kilk K, Magzoub M, Pooga M, Eriksson LE, Langel U, Graslund A (2001) Cellular internalization of a cargo complex with a novel peptide derived from the third helix of the islet-1 homeodomain. Comparison with the penetratin peptide. *Bioconjug Chem* 12: 911-6
- Kim DH, Longo M, Han Y, Lundberg P, Cantin E, Rossi JJ (2004) Interferon induction by siRNAs and ssRNAs synthesized by phage polymerase. *Nat Biotechnol* 22: 321-5
- Kiriakidou M, Nelson PT, Kouranov A, Fitziev P, Bouyioukos C, Mourelatos Z, Hatzigeorgiou A (2004) A combined computational-experimental approach predicts human microRNA targets. *Genes Dev* 18: 1165-78
- Kirschberg TA, VanDeusen CL, Rothbard JB, Yang M, Wender PA (2003) Arginine-based molecular transporters: the synthesis and chemical evaluation of releasable taxol-transporter conjugates. *Org Lett* 5: 3459-62
- Knight SW, Bass BL (2001) A role for the RNase III enzyme DCR-1 in RNA interference and germ line development in *Caenorhabditis elegans*. *Science* 293: 2269-2271
- Kobayashi H, Kawamoto S, Saga T, Sato N, Hiraga A, Ishimori T, Konishi J, Togashi K, Brechbiel MW (2001) Positive effects of polyethylene glycol conjugation to generation-4 polyamidoamine dendrimers as macromolecular MR contrast agents. *Magn Reson Med* 46: 781-8
- Kolter T, Sandhoff K (1999) Sphingolipids - Their metabolic pathways and the pathobiochemistry of neurodegenerative diseases. *Angewandte Chemie. International Ed. in English* 38: 1532-1568
- Konnikova L, Kotecki M, Kruger MM, Cochran BH (2003) Knockdown of STAT3 expression by RNAi induces apoptosis in astrocytoma cells. *BMC Cancer* 3: 23
- Kono K, Yoshino K, Takagishi T (2002) Effect of poly(ethylene glycol) grafts on temperature-sensitivity of thermosensitive polymer-modified liposomes. *Journal of Controlled Release* 80: 321-332
- Kramer SF, Bentley WE (2003) RNA interference as a metabolic engineering tool: potential for in vivo control of protein expression in an insect larval model. *Metab Eng* 5: 183-90
- Kretz A, Wybranietz WA, Hermening S, Lauer UM, Isenmann S (2003) HSV-1 VP22 augments adenoviral gene transfer to CNS neurons in the retina and striatum in vivo. *Mol Ther* 7: 659-69
- Kreuter J, Ramge P, Petrov V, Hamm S, Gelperina SE, Engelhardt B, Alyautdin R, von Briesen H, Begley DJ (2003) Direct evidence that polysorbate-80-coated poly(butylcyanoacrylate) nanoparticles deliver drugs to the CNS via specific mechanisms requiring prior binding of drug to the nanoparticles. *Pharmaceutical Research* 20: 409-416
- Krichevsky AM, Kosik KS (2002) RNAi functions in cultured mammalian neurons. *Proceedings of the National Academy of Sciences of the United States of America* 99: 11926-11929
- Kronke J, Kittler R, Buchholz F, Windisch MP, Pietschmann T, Bartenschlager R, Frese M (2004) Alternative approaches for efficient inhibition of hepatitis C virus RNA replication by small interfering RNAs. *J Virol* 78: 3436-46

- Kubo T, Yokoyama K, Ueki R, Yano M, Anno Y, Sasaki K, Ohba H, Fujii M (2003) DNA conjugates as novel functional oligonucleotides. *Nucleosides Nucleotides Nucleic Acids* 22: 1359-61
- Kumar M, Kong X, Behera AK, Hellermann GR, Lockey RF, Mohapatra SS (2003) Chitosan IFN-gamma-pDNA Nanoparticle (CIN) Therapy for Allergic Asthma. *Genet Vaccines Ther* 1: 3
- Kunath T, Gish G, Lickert H, Jones N, Pawson T, Rossant J (2003) Transgenic RNA interference in ES cell-derived embryos recapitulates a genetic null phenotype. *Nat Biotechnol* 21: 559-61
- Kwak YD, Koike H, Sugaya K (2003) RNA interference with small hairpin RNAs transcribed from a human U6 promoter-driven DNA vector. *J Pharmacol Sci* 93: 214-7
- Lagos-Quintana M, Rauhut R, Lendeckel W, Tuschl T (2001) Identification of novel genes coding for small expressed RNAs. *Science* 294: 853-858
- Lagos-Quintana M, Rauhut R, Meyer J, Borkhardt A, Tuschl T (2003) New microRNAs from mouse and human. *Rna* 9: 175-9
- Lagos-Quintana M, Rauhut R, Yalcin A, Meyer J, Lendeckel W, Tuschl T (2002) Identification of tissue-specific microRNAs from mouse. *Current Biology* 12: 735-739
- Lai YL, Yu SC, Chen MJ (2003) RNA interference prevents lipopolysaccharide-induced preprotachykinin gene expression. *Toxicol Appl Pharmacol* 193: 47-54
- Lander ES, Linton LM, Birren B, Nusbaum C, Zody MC, Baldwin J, Devon K, Dewar K, Doyle M, FitzHugh W, Funke R, Gage D, Harris K, Heaford A, Howland J, Kann L, Lehoczky J, LeVine R, McEwan P, McKernan K, Meldrim J, Mesirov JP, Miranda C, Morris W, Naylor J, Raymond C, Rosetti M, Santos R, Sheridan A, Sougnez C, Stange-Thomann N, Stojanovic N, Subramanian A, Wyman D, Rogers J, Sulston J, Ainscough R, Beck S, Bentley D, Burton J, Clee C, Carter N, Coulson A, Deadman R, Deloukas P, Dunham A, Dunham I, Durbin R, French L, Grafham D, Gregory S, Hubbard T, Humphray S, Hunt A, Jones M, Lloyd C, McMurray A, Matthews L, Mercer S, Milne S, Mullikin JC, Mungall A, Plumb R, Ross M, Shownkeen R, Sims S, Waterston RH, Wilson RK, Hillier LW, McPherson JD, Marra MA, Mardis ER, Fulton LA, Chinwalla AT, Pepin KH, Gish WR, Chissoe SL, Wendl MC, Delehaunty KD, Miner TL, Delehaunty A, Kramer JB, Cook LL, Fulton RS, Johnson DL, Minx PJ, Clifton SW, Hawkins T, Branscomb E, Predki P, Richardson P, Wenning S, Slezak T, Doggett N, Cheng JF, Olsen A, Lucas S, Elkin C, Uberbacher E, Frazier M, et al. (2001) Initial sequencing and analysis of the human genome. *Nature* 409: 860-921.
- Lau NC, Lim LP, Weinstein EG, Bartel DP (2001) An abundant class of tiny RNAs with probable regulatory roles in *Caenorhabditis elegans*. *Science* 294: 858-62
- Lauterwasser F (2004) Dissertation, Karlsruhe
- Lee ER, Marshall J, Siegel CS, Jiang C, Yew NS, Nichols MR, Nietupski JB, Ziegler RJ, Lane MB, Wang KX, Wan NC, Scheule RK, Harris DJ, Smith AE, Cheng SH (1996) Detailed analysis of structures and formulations of cationic lipids for efficient gene transfer to the lung. *Hum Gene Ther* 7: 1701-17
- Lee J, Nam S, Hwang SB, Hong M, Kwon JY, Joeng KS, Im SH, Shim J, Park MC (2004a) Functional genomic approaches using the nematode *Caenorhabditis elegans* as a model system. *J Biochem Mol Biol* 37: 107-13
- Lee MT, Coburn GA, McClure MO, Cullen BR (2003a) Inhibition of human immunodeficiency virus type 1 replication in primary macrophages by using Tat- or CCR5-specific small interfering RNAs expressed from a lentivirus vector. *J Virol* 77: 11964-72
- Lee NS, Dohjima T, Bauer G, Li H, Li MJ, Ehsani A, Salvaterra P, Rossi J (2002) Expression of small interfering RNAs targeted against HIV-1 rev transcripts in human cells. *Nat Biotechnol* 20: 500-5.
- Lee RC, Ambros V (2001) An extensive class of small RNAs in *Caenorhabditis elegans*. *Science* 294: 862-4
- Lee Y, Ahn C, Han J, Choi H, Kim J, Yim J, Lee J, Provost P, Radmark O, Kim S, Kim VN (2003b) The nuclear RNase III Drosha initiates microRNA processing. *Nature* 425: 415-9

- Lee Y, Koo H, Lim YB, Mo H, Park JS (2004b) New cationic lipids for gene transfer with high efficiency and low toxicity: T-shape cholesterol ester derivatives. *Bioorg Med Chem Lett* 14: 2637-41
- Lee YS, Nakahara K, Pham JW, Kim K, He Z, Sontheimer EJ, Carthew RW (2004c) Distinct Roles for *Drosophila* Dicer-1 and Dicer-2 in the siRNA/miRNA Silencing Pathways. *Cell* 117: 69-81
- Leifert JA, Harkins S, Whitton JL (2002) Full-length proteins attached to the HIV tat protein transduction domain are neither transduced between cells, nor exhibit enhanced immunogenicity. *Gene Ther* 9: 1422-8
- Letoha T, Gaal S, Somlai C, Czajlik A, Perczel A, Penke B (2003) Membrane translocation of penetratin and its derivatives in different cell lines. *J Mol Recognit* 16: 272-9
- Lewin M, Carlesso N, Tung CH, Tang XW, Cory D, Scadden DT, Weissleder R (2000) Tat peptide-derivatized magnetic nanoparticles allow in vivo tracking and recovery of progenitor cells. *Nat Biotechnol* 18: 410-4
- Lewis BP, Shih IH, Jones-Rhoades MW, Bartel DP, Burge CB (2003) Prediction of mammalian microRNA targets. *Cell* 115: 787-98
- Lewis DL, Hagstrom JE, Loomis AG, Wolff JA, Herweijer H (2002) Efficient delivery of siRNA for inhibition of gene expression in postnatal mice. *Nat Genet* 32: 107-8
- Li JK, Wang N, Wu XS (1997) A novel biodegradable system based on gelatin nanoparticles and poly(lactic-co-glycolic acid) microspheres for protein and peptide drug delivery. *J Pharm Sci* 86: 891-895
- Li XP, Li G, Peng Y, Kung HF, Lin MC (2004) Suppression of Epstein-Barr virus-encoded latent membrane protein-1 by RNA interference inhibits the metastatic potential of nasopharyngeal carcinoma cells. *Biochem Biophys Res Commun* 315: 212-8
- Li Y, Rosal RV, Brandt-Rauf PW, Fine RL (2002) Correlation between hydrophobic properties and efficiency of carrier-mediated membrane transduction and apoptosis of a p53 C-terminal peptide. *Biochem Biophys Res Commun* 298: 439-49
- Lieberman J, Song E, Lee SK, Shankar P (2003) Interfering with disease: opportunities and roadblocks to harnessing RNA interference. *Trends Mol Med* 9: 397-403
- Lim LP, Glasner ME, Yekta S, Burge CB, Bartel DP (2003) Vertebrate microRNA genes. *Science* 299: 1540
- Lima RT, Martins LM, Guimaraes JE, Sambade C, Vasconcelos MH (2004) Specific downregulation of bcl-2 and XIAP by RNAi enhances the effects of chemotherapeutic agents in MCF-7 human breast cancer cells. *Cancer Gene Ther*
- Lin Q, Jo D, Greber-Amlak KD, Ruley HE (2004) Enhanced cell-permeant Cre protein for site-specific recombination in cultured cells. *BMC Biotechnol* 4: 25
- Lin SL, Chuong CM, Ying SY (2001) A novel mRNA-cDNA interference phenomenon for silencing bcl-2 expression in human LNCaP cells. *Biochemical & Biophysical Research Communications* 281: 639-644
- Lin YZ, Yao SY, Veach RA, Torgerson TR, Hawiger J (1995) Inhibition of nuclear translocation of transcription factor NF-kappa B by a synthetic peptide containing a cell membrane-permeable motif and nuclear localization sequence. *J Biol Chem* 270: 14255-8
- Lindgren M, Gallet X, Soomets U, Hallbrink M, Brakenhielm E, Pooga M, Brasseur R, Langel U (2000a) Translocation properties of novel cell penetrating transportan and penetratin analogues. *Bioconjug Chem* 11: 619-26
- Lindgren M, Hallbrink M, Prochiantz A, Langel U (2000b) Cell-penetrating peptides. *Trends in Pharmacological Sciences* 21: 99-103
- Lindgren ME, Hallbrink MM, Elmquist AM, Langel U (2004) Passage of cell-penetrating peptides across a human epithelial cell layer in vitro. *Biochem J* 377: 69-76
- Lindsay MA (2002) Peptide-mediated cell delivery: application in protein target validation. *Curr Opin Pharmacol* 2: 587-94
- Lingel A, Simon B, Izaurralde E, Sattler M (2003) Structure and nucleic-acid binding of the *Drosophila* Argonaute 2 PAZ domain. *Nature*

- Lipardi C, Wei Q, Paterson BM (2001) RNAi as random degradative PCR: siRNA primers convert mRNA into dsRNAs that are degraded to generate new siRNAs. *Cell* 107: 297-307
- Lipinski C, Lombardo, F. D, BW and Feeney, PJ (1997) Experimental and computational approaches to estimate solubility and permeability in drug discovery and development setting. *Adv Drug Deliv Rev* 23: 3-25
- Liu J, Carmell MA, Rivas FV, Marsden CG, Thomson JM, Song JJ, Hammond SM, Joshua-Tor L, Hannon GJ (2004) Argonaute2 is the catalytic engine of mammalian RNAi. *Science* 305: 1437-41
- Liu LT, Chang HC, Chiang LC, Hung WC (2003a) Histone deacetylase inhibitor up-regulates RECK to inhibit MMP-2 activation and cancer cell invasion. *Cancer Res* 63: 3069-72
- Liu MJ, Kono K, Frechet JMJ (1999) Water-soluble dendrimer-poly(ethylene glycol) starlike conjugates as potential drug carriers. *Journal of Polymer Science Part a-Polymer Chemistry* 37: 3492-3503
- Liu Q, Rand TA, Kalidas S, Du F, Kim HE, Smith DP, Wang X (2003b) R2D2, a bridge between the initiation and effector steps of the *Drosophila* RNAi pathway. *Science* 301: 1921-5
- Llave C, Xie ZX, Kasschau KD, Carrington JC (2002) Cleavage of Scarecrow-like mRNA targets directed by a class of Arabidopsis miRNA. *Science* 297: 2053-2056
- Lobo BA, Vetro JA, Suich DM, Zuckermann RN, Middaugh CR (2003) Structure/function analysis of peptoid/lipoid:DNA complexes. *J Pharm Sci* 92: 1905-18
- Lockman PR, Mumper RJ, Khan MA, Allen DD (2002) Nanoparticle technology for drug delivery across the blood-brain barrier. *Drug Dev Ind Pharm* 28: 1-13
- Lorenz K, Lohse MJ, Quitterer U (2003) Protein kinase C switches the Raf kinase inhibitor from Raf-1 to GRK-2. *Nature* 426: 574-9
- Lorsch JR, Szostak JW (1994) In vitro Selection of Rna Aptamers Specific for Cyanocobalamin. *Biochemistry* 33: 973-982
- Love R (2004) First disease model created by RNA interference. *Lancet Neurol* 3: 7
- Lu D, Benjamin R, Kim M, Conry RM, Curiel DT (1994) Optimization of methods to achieve mRNA-mediated transfection of tumor cells in vitro and in vivo employing cationic liposome vectors. *Cancer Gene Ther* 1: 245-52
- Lu S, Cullen BR (2004) Adenovirus VA1 noncoding RNA can inhibit small interfering RNA and MicroRNA biogenesis. *J Virol* 78: 12868-76
- Lucast LJ, Batey RT, Doudna JA (2001) Large-scale purification of a stable form of recombinant tobacco etch virus protease. *Biotechniques* 30: 544-6, 548, 550 passim
- Lund E, Guttinger S, Calado A, Dahlberg JE, Kutay U (2003) Nuclear Export of MicroRNA Precursors. *Science*
- Lundberg M, Wikstrom S, Johansson M (2003) Cell surface adherence and endocytosis of protein transduction domains. *Mol Ther* 8: 143-50
- Lundberg P, Magzoub M, Lindberg M, Hallbrink M, Jarvet J, Eriksson LE, Langel U, Graslund A (2002) Cell membrane translocation of the N-terminal (1-28) part of the prion protein. *Biochemical & Biophysical Research Communications* 299: 85-90
- Mack KD, Walzem R, Zeldis JB (1994) Cationic lipid enhances in vitro receptor-mediated transfection. *Am J Med Sci* 307: 138-43
- Magzoub M, Eriksson LE, Graslund A (2002) Conformational states of the cell-penetrating peptide penetratin when interacting with phospholipid vesicles: effects of surface charge and peptide concentration. *Biochim Biophys Acta* 1563: 53-63
- Magzoub M, Kilk K, Eriksson LE, Langel U, Graslund A (2001) Interaction and structure induction of cell-penetrating peptides in the presence of phospholipid vesicles. *Biochim Biophys Acta* 1512: 77-89
- Mariott J, Mottahedeh, M, Reese, CB (1990) 9-(4-Methoxyphenyl)xanthen-9-thiol: A useful reagent for the preparation of thiols. *Tetrahedron Letters* 31: 7485-7488
- Marlow L, Canet RM, Haugabook SJ, Hardy JA, Lahiri DK, Sambamurti K (2003) APH1, PEN2, and Nicastrin increase Abeta levels and gamma-secretase activity.[erratum appears in *Biochem Biophys Res Commun*. 2003 Aug 1;307(3):756]. *Biochemical & Biophysical Research Communications* 305: 502-9

- Martienssen RA (2003) Maintenance of heterochromatin by RNA interference of tandem repeats. *Nat Genet* 35: 213-4
- Martinez J, Patkaniowska A, Urlaub H, Luhrmann R, Tuschl T (2002a) Single-stranded antisense siRNAs guide target RNA cleavage in RNAi. *Cell* 110: 563-574
- Martinez MA, Clotet B, Este JA (2002b) RNA interference of HIV replication. *Trends Immunol* 23: 559-61
- Martinez MA, Gutierrez A, Armand-Ugon M, Blanco J, Parera M, Gomez J, Clotet B, Este JA (2002c) Suppression of chemokine receptor expression by RNA interference allows for inhibition of HIV-1 replication. *Aids* 16: 2385-2390
- Martins LM, Iaccarino I, Tenev T, Gschmeissner S, Totty NF, Lemoine NR, Savopoulos J, Gray CW, Creasy CL, Dingwall C, Downward J (2002) The serine protease Omi/HtrA2 regulates apoptosis by binding XIAP through a reaper-like motif. *J Biol Chem* 277: 439-44
- Marty C, Meylan C, Schott H, Ballmer-Hofer K, Schwendener RA (2004) Enhanced heparan sulfate proteoglycan-mediated uptake of cell-penetrating peptide-modified liposomes. *Cell Mol Life Sci* 61: 1785-94
- Matsuzaki K, Yoneyama S, Murase O, Miyajima K (1996) Transbilayer transport of ions and lipids coupled with mastoparan X translocation. *Biochemistry* 35: 8450-6
- Mattson MP (2003) Neurobiology: Ballads of a protein quartet. *Nature* 422: 385, 387
- Maxwell MM, Pasinelli P, Kazantsev AG, Brown RH, Jr. (2004) RNA interference-mediated silencing of mutant superoxide dismutase rescues cyclosporin A-induced death in cultured neuroblastoma cells. *Proc Natl Acad Sci U S A* 101: 3178-83
- May S, Ben-Shaul A (2000) A molecular model for lipid-mediated interaction between proteins in membranes. *Physical Chemistry Chemical Physics* 2: 4494-4502
- McCaffrey AP, Meuse L, Pham TTT, Conklin DS, Hannon GJ, Kay MA (2002) Gene expression - RNA interference in adult mice. *Nature* 418: 38-39
- McCaffrey AP, Nakai H, Pandey K, Huang Z, Salazar FH, Xu H, Wieland SF, Marion PL, Kay MA (2003) Inhibition of hepatitis B virus in mice by RNA interference. *Nat Biotechnol* 21: 639-44
- McKenzie DL, Smiley E, Kwok KY, Rice KG (2000) Low molecular weight disulfide cross-linking peptides as nonviral gene delivery carriers. *Bioconjug Chem* 11: 901-9.
- McManus MT, Petersen CP, Haines BB, Chen J, Sharp PA (2002) Gene silencing using micro-RNA designed hairpins. *Rna* 8: 842-50.
- Mei ZN, Chen HB, Weng T, Yang YJ, Yang XL (2003) Solid lipid nanoparticle and microemulsion for topical delivery of triptolide. *European Journal of Pharmaceutics and Biopharmaceutics* 56: 189-196
- Meister G, Landthaler M, Dorsett Y, Tuschl T (2004) Sequence-specific inhibition of microRNA- and siRNA-induced RNA silencing. *Rna* 10: 544-50
- Mette MF, Matzke AJ, Matzke MA (2001) Resistance of RNA-mediated TGS to HC-Pro, a viral suppressor of PTGS, suggests alternative pathways for dsRNA processing. *Curr Biol* 11: 1119-23.
- Mi Z, Mai J, Lu X, Robbins PD (2000) Characterization of a class of cationic peptides able to facilitate efficient protein transduction in vitro and in vivo. *Mol Ther* 2: 339-47
- Mian IS (1997) Comparative Sequence Analysis of Ribonucleases Hii, Iii, Ii Ph and D. *Nucleic Acids Research* 25: 3187-3195
- Michienzi A, Castanotto D, Lee N, Li S, Zaia JA, Rossi JJ (2003) RNA-mediated inhibition of HIV in a gene therapy setting. *Ann N Y Acad Sci* 1002: 63-71
- Miller VM, Xia H, Marrs GL, Gouvion CM, Lee G, Davidson BL, Paulson HL (2003) Allele-specific silencing of dominant disease genes. *Proc Natl Acad Sci U S A* 100: 7195-200
- Milligan JF, Groebe DR, Witherell GW, Uhlenbeck OC (1987) Oligoribonucleotide synthesis using T7 RNA polymerase and synthetic DNA templates. *Nucleic Acid Research* 15: 8783-8798
- Milner J (2003) RNA interference for treating cancers caused by viral infection [Review]. *Expert Opinion on Biological Therapy* 3: 459-467

- Misquitta L, Paterson B (2000) Targeted disruption of Gene function by RNA interference. Cold Spring Harbor Press, Cold Spring Harbor, NY
- Mitchell DJ, Kim DT, Steinman L, Fathman CG, Rothbard JB (2000) Polyarginine enters cells more efficiently than other polycationic homopolymers. *J Pept Res* 56: 318-25
- Miyagishi M, Taira K (2002) U6 promoter driven siRNAs with four uridine 3' overhangs efficiently suppress targeted gene expression in mammalian cells. *Nat Biotechnol* 20: 497-500.
- Mochizuki K, Fine NA, Fujisawa T, Gorovsky MA (2002) Analysis of a piwi-related gene implicates small RNAs in genome rearrangement in tetrahymena. *Cell* 110: 689-99
- Montgomery MK, Fire A (1998) Double-stranded RNA as a mediator in sequence specific genetic silencing and co-suppression. *Trends in Genetics* 14: 255-258
- Montgomery MK, Xu SQ, Fire A (1998) RNA as a target of double-stranded RNA-mediated genetic interference in *Caenorhabditis elegans*. *Proceedings of the National Academy of Sciences of the United States of America* 95: 15502-15507
- Moon C, Kang WS, Jeong DC, Jin JY (2003) Distribution of adenoviral vector in brain after intravenous administration. *J Korean Med Sci* 18: 108-11
- Morgan JR, Cloninger, M. J. (2002) Heterogeneously functionalized dendrimers. *Current Opinion in Drug Discovery & Development* 5: 966-973
- Morris MC, Depollier J, Mery J, Heitz F, Divita G (2001) A peptide carrier for the delivery of biologically active proteins into mammalian cells. *Nat Biotechnol* 19: 1173-6.
- Morris MC, Vidal P, Chaloin L, Heitz F, Divita G (1997) A new peptide vector for efficient delivery of oligonucleotides into mammalian cells. *Nucleic Acids Res* 25: 2730-6
- Mortlock A, Low W, Crisanti A (2003) Suppression of gene expression by a cell-permeable Tet repressor. *Nucleic Acids Res* 31: e152
- Mourelatos Z, Dostie J, Paushkin S, Sharma A, Charroux B, Abel L, Rappsilber J, Mann M, Dreyfuss G (2002) miRNPs: a novel class of ribonucleoproteins containing numerous microRNAs. *Genes Dev* 16: 720-8
- Mourrain P, Beclin C, Elmayan T, Feuerbach F, Godon C, Morel JB, Jouette D, Lacombe AM, Nikic S, Picault N, Remoue K, Sanial M, Vo TA, Vaucheret H (2000) Arabidopsis SGS2 and SGS3 genes are required for posttranscriptional gene silencing and natural virus resistance. *Cell* 101: 533-42.
- Mulders P, Pang S, Dannull J, Kaboo R, Hinkel A, Michel K, Tso CL, Roth M, Beldegrun A (1998) Highly efficient and consistent gene transfer into dendritic cells utilizing a combination of ultraviolet-irradiated adenovirus and poly(L-lysine) conjugates. *Cancer Res* 58: 956-61
- Muratovska A, Eccles MR (2004) Conjugate for efficient delivery of short interfering RNA (siRNA) into mammalian cells. *FEBS Lett* 558: 63-8
- Muro S, Cui X, Gajewski C, Murciano JC, Muzykantov VR, Koval M (2003) Slow intracellular trafficking of catalase nanoparticles targeted to ICAM-1 protects endothelial cells from oxidative stress. *Am J Physiol Cell Physiol* 285: C1339-47
- Murphy JE, Uno T, Hamer JD, Cohen FE, Dwarki V, Zuckermann RN (1998) A combinatorial approach to the discovery of efficient cationic peptoid reagents for gene delivery. *Proc Natl Acad Sci U S A* 95: 1517-22
- Murray D, Arbuzova A, Hangyas-Mihalyne G, Gambhir A, Ben-Tal N, Honig B, McLaughlin S (1999) Electrostatic properties of membranes containing acidic lipids and adsorbed basic peptides: theory and experiment. *Biophys J* 77: 3176-88
- Myers JW, Jones JT, Meyer T, Ferrell JE, Jr. (2003) Recombinant Dicer efficiently converts large dsRNAs into siRNAs suitable for gene silencing. *Nat Biotechnol* 21: 324-8
- Nagahara H, Vocero-Akbani AM, Snyder EL, Ho A, Latham DG, Lissy NA, Becker-Hapak M, Ezhevsky SA, Dowdy SF (1998) Transduction of full-length TAT fusion proteins into mammalian cells: TAT-p27Kip1 induces cell migration. *Nat Med* 4: 1449-52.
- Nagashima K, Endo A, Ogita H, Kawana A, Yamagishi A, Kitabatake A, Matsuda M, Mochizuki N (2002) Adaptor protein Crk is required for ephrin-B1-induced membrane ruffling and focal complex assembly of human aortic endothelial cells. *Mol Biol Cell* 13: 4231-42

- Napoli C, Lemieux C, Jorgensen R (1990) Introduction of a Chimeric Chalcone Synthase Gene into *Petunia* Results in Reversible Co-Suppression of Homologous Genes in trans. *Plant Cell* 2: 279-289.
- Nekhotiaeva N, Elmquist A, Rajarao GK, Hallbrink M, Langel U, Good L (2004) Cell entry and antimicrobial properties of eukaryotic cell-penetrating peptides. *Faseb J* 18: 394-6
- Ngo H, Tschudi C, Gull K, Ullu E (1998) Double-stranded RNA induces mRNA degradation in *Trypanosoma brucei*. *PNAS* 95: 14687-14692
- Nicholson RH, Nicholson AW (2002) Molecular characterization of a mouse cDNA encoding Dicer, a ribonuclease III ortholog involved in RNA interference. *Mamm Genome* 13: 67-73.
- Nitin N, LaConte LE, Zurkiya O, Hu X, Bao G (2004) Functionalization and peptide-based delivery of magnetic nanoparticles as an intracellular MRI contrast agent. *J Biol Inorg Chem* 9: 706-12
- Niu Q, Perruzzi C, Voskas D, Lawler J, Dumont DJ, Benjamin LE (2004) Inhibition of Tie-2 Signaling Induces Endothelial Cell Apoptosis, Decreases Akt Signaling, and Induces Endothelial Cell Expression of the Endogenous Anti-Angiogenic Molecule, Thrombospondin-1. *Cancer Biol Ther* 3
- Noguchi H, Kaneto H, Weir GC, Bonner-Weir S (2003) PDX-1 protein containing its own antennapedia-like protein transduction domain can transduce pancreatic duct and islet cells. *Diabetes* 52: 1732-7
- Novina CD, Murray MF, Dykxhoorn DM, Beresford PJ, Riess J, Lee SK, Collman RG, Lieberman J, Shankar P, Sharp PA (2002) siRNA-directed inhibition of HIV-1 infection. *Nat Med* 8: 681-6.
- Nykänen A, Haley B, Zamore PD (2001) ATP requirements and small interfering RNA structure in the RNA interference pathway. *Cell* 107: 309-321
- Ojcius DM, Young JD (1991) Cytolytic pore-forming proteins and peptides: is there a common structural motif? *Trends Biochem Sci* 16: 225-9
- Okamura K, Ishizuka A, Siomi H, Siomi MC (2004) Distinct roles for Argonaute proteins in small RNA-directed RNA cleavage pathways. *Genes Dev* 18: 1655-66
- Olsen PH, Ambros V (1999) The *lin-4* regulatory RNA controls developmental timing in *Caenorhabditis elegans* by blocking LIN-14 protein synthesis after the initiation of translation. *Developmental Biology* 216: 671-680
- Omi K, Tokunaga K, Hohjoh H (2004) Long-lasting RNAi activity in mammalian neurons. *FEBS Lett* 558: 89-95
- Oshima K, Kawasaki H, Soda Y, Tani K, Asano S, Taira K (2003) Maxizymes and small hairpin-type RNAs that are driven by a tRNA promoter specifically cleave a chimeric gene associated with leukemia in vitro and in vivo. *Cancer Res* 63: 6809-14
- Ou J, Geiger T, Ou Z, Ackerman AW, Oldham KT, Pritchard KA, Jr. (2003) AP-4F, antennapedia peptide linked to an amphipathic alpha helical peptide, increases the efficiency of Lipofectamine-mediated gene transfection in endothelial cells. *Biochem Biophys Res Commun* 305: 605-10
- Paddison PJ, Caudy AA, Bernstein E, Hannon GJ, Conklin DS (2002a) Short hairpin RNAs (shRNAs) induce sequence-specific silencing in mammalian cells. *Genes & Development* 16: 948-958
- Paddison PJ, Caudy AA, Hannon GJ (2002b) Stable suppression of gene expression by RNAi in mammalian cells. *Proceedings of the National Academy of Sciences of the United States of America* 99: 1443-1448
- Paddison PJ, A.; Hannon, G. J. (2002) Stable suppression of gene expression by RNAi in mammalian cells. *PNAS* 99: 1443-1448
- Pal-Bhadra M, Bhadra U, Birchler JA (2002) RNAi related mechanisms affect both transcriptional and posttranscriptional transgene silencing in *Drosophila*. *Mol Cell* 9: 315-27.
- Panyam (2003) Fluorescence and electron microscopy probes for cellular and tissue uptake of poly (D, L-lactide-co-glycolide) nanoparticles,. *J. Int. Pharm.* 262: 1-11

- Park W, Li J, Song R, Messing J, Chen X (2002) CARPEL FACTORY, a Dicer homolog, and HEN1, a novel protein, act in microRNA metabolism in *Arabidopsis thaliana*. *Curr Biol* 12: 1484-95
- Park WS, Hayafune M, Miyano-Kurosaki N, Takaku H (2003) Specific HIV-1 env gene silencing by small interfering RNAs in human peripheral blood mononuclear cells. *Gene Ther* 10: 2046-50
- Parkhurst SM, Bopp D, Ish-Horowicz D (1990) X:A ratio, the primary sex-determining signal in *Drosophila*, is transduced by helix-loop-helix proteins. *Cell* 63: 1179-91
- Parrish S, Fleenor J, Xu S, Mello C, Fire A (2000) Functional anatomy of a dsRNA trigger: differential requirement for the two trigger strands in RNA interference. *Mol Cell* 6: 1077-87.
- Patri AKM, Istvan J.; Baker, James R. (2002) Dendritic polymer macromolecular carriers for drug delivery. *Current Opinion in Chemical Biology* 6: 466-471
- Paul CP, Good PD, Winer I, Engelke DR (2002) Effective expression of small interfering RNA in human cells. *Nat Biotechnol* 20: 505-8.
- Peitz M, Pfannkuche K, Rajewsky K, Edenhofer F (2002) Ability of the hydrophobic FGF and basic TAT peptides to promote cellular uptake of recombinant Cre recombinase: a tool for efficient genetic engineering of mammalian genomes. *Proc Natl Acad Sci U S A* 99: 4489-94.
- Pekarik V, Bourikas D, Miglino N, Joset P, Preiswerk S, Stoeckli ET (2003) Screening for gene function in chicken embryo using RNAi and electroporation. *Nat Biotechnol* 21: 93-6
- Pepinsky RB, Androphy EJ, Corina K, Brown R, Barsoum J (1994) Specific inhibition of a human papillomavirus E2 trans-activator by intracellular delivery of its repressor. *DNA Cell Biol* 13: 1011-9
- Peretto I, Sanchez-Martin RM, Wang XH, Ellard J, Mittoo S, Bradley M (2003) Cell penetrable peptoid carrier vehicles: synthesis and evaluation. *Chem Commun (Camb)*: 2312-3
- Perez D, White E (2003) E1A sensitizes cells to tumor necrosis factor alpha by downregulating c-FLIP S. *J Virol* 77: 2651-62
- Persson D, Thoren PE, Herner M, Lincoln P, Norden B (2003) Application of a novel analysis to measure the binding of the membrane-translocating peptide penetratin to negatively charged liposomes. *Biochemistry* 42: 421-9
- Persson D, Thoren PE, Lincoln P, Norden B (2004) Vesicle membrane interactions of penetratin analogues. *Biochemistry* 43: 11045-55
- Petersen L, de Koning MC, van Kuik-Romeijn P, Weterings J, Pol CJ, Platenburg G, Overhand M, van der Marel GA, van Boom JH (2004) Synthesis and in vitro evaluation of PNA-peptide-DETA conjugates as potential cell penetrating artificial ribonucleases. *Bioconjug Chem* 15: 576-82
- Pham JW, Pellino JL, Lee YS, Carthew RW, Sontheimer EJ (2004) A Dicer-2-Dependent 80S Complex Cleaves Targeted mRNAs during RNAi in *Drosophila*. *Cell* 117: 83-94
- Pitulle C, Kleinedam, RC, Sproat, B, Krupp, G (1992) Initiator oligonucleotides for the combination of chemical and enzymatic RNA synthesis. *Genet Vaccines Ther.* 112: 101
- Plasterk RHA (1999) The year of the worm [Review]. *Bioessays* 21: 105-109
- Plasterk RHA (2002) RNA silencing: The genome's immune system. *Science* 296: 1263-1265
- Poenaru S, Lamas JR, Folkers G, Lopez de Castro JA, Seebach D, Rognan D (1999) Nonapeptide analogues containing (R)-3-hydroxybutanoate and beta-homoalanine oligomers: synthesis and binding affinity to a class I major histocompatibility complex protein. *J Med Chem* 42: 2318-31
- Polato L, Benedetti LM, Callegaro L, Couvreur P (1994) In vitro evaluation of nanoparticle formulations containing gangliosides. *J Drug Target* 2: 53-9
- Polyakov V, Sharma V, Dahlheimer JL, Pica CM, Luker GD, Piwnica-Worms D (2000) Novel Tat-peptide chelates for direct transduction of technetium-99m and rhenium into human cells for imaging and radiotherapy. *Bioconjug Chem* 11: 762-71

- Ponting CP (1997) Evidence for PDZ domains in bacteria, yeast, and plants. *Protein Sci* 6: 464-8
- Pooga M, Hallbrink M, Zorko M, Langel U (1998a) Cell penetration by transportan. *FASEB Journal* 12: 67-77
- Pooga M, Kut C, Kihlmark M, Hallbrink M, Fernaeus S, Raid R, Land T, Hallberg E, Bartfai T, Langel U (2001) Cellular translocation of proteins by transportan. *FASEB J* 15: 1451-3
- Pooga M, Lindgren M, Hallbrink M, Brakenhielm E, Langel U (1998b) Galanin-based peptides, galparan and transportan, with receptor-dependent and independent activities. *Annals of the New York Academy of Sciences* 863: 450-3
- Pooga M, Soomets U, Hallbrink M, Valkna A, Saar K, Rezaei K, Kahl U, Hao JX, Xu XJ, Wiesenfeld-Hallin Z, Hokfelt T, Bartfai T, Langel U (1998c) Cell penetrating PNA constructs regulate galanin receptor levels and modify pain transmission in vivo. *Nat Biotechnol* 16: 857-61
- Potocky TB, Menon AK, Gellman SH (2003) Cytoplasmic and nuclear delivery of a TAT-derived peptide and a beta-peptide after endocytic uptake into HeLa cells. *J Biol Chem* 278: 50188-94
- Potter H (1988) Electroporation in biology: methods, applications, and instrumentation. *Anal Biochem* 174: 361-73
- Prochiantz A (1996) Getting Hydrophilic Compounds into Cells - Lessons from Homeopeptides - Commentary. *Current Opinion in Neurobiology* 6: 629-634
- Provost P, Dishart D, Doucet J, Frenthewey D, Samuelsson B, Radmark O (2002) Ribonuclease activity and RNA binding of recombinant human Dicer. *Embo J* 21: 5864-74.
- Pugsley AP (1996) Bacterial toxins deliver the goods. *Proc Natl Acad Sci U S A* 93: 8155-6
- Qin L, Xiong B, Luo C, Guo ZM, Hao P, Su J, Nan P, Feng Y, Shi YX, Yu XJ, Luo XM, Chen KX, Shen X, Shen JH, Zou JP, Zhao GP, Shi TL, He WZ, Zhong Y, Jiang HL, Li YX (2003) Identification of probable genomic packaging signal sequence from SARS-CoV genome by bioinformatics analysis. *Acta Pharmacol Sin* 24: 489-96
- Ragin AD, Chmielewski J (2004) Probing essential residues for cellular uptake with a cationic nuclear localization signal sequence. *J Pept Res* 63: 155-60
- Raguse TL, Lai JR, Gellman SH (2003) Environment-independent 14-helix formation in short beta-peptides: striking a balance between shape control and functional diversity. *J Am Chem Soc* 125: 5592-3
- Raguse TL, Porter EA, Weisblum B, Gellman SH (2002) Structure-activity studies of 14-helical antimicrobial beta-peptides: probing the relationship between conformational stability and antimicrobial potency. *J Am Chem Soc* 124: 12774-85
- Rajewsky N, Socci ND (2004) Computational identification of microRNA targets. *Dev Biol* 267: 529-35
- Rand TA, Ginalski K, Grishin NV, Wang X (2004) Biochemical identification of Argonaute 2 as the sole protein required for RNA-induced silencing complex activity. *Proc Natl Acad Sci U S A* 101: 14385-9
- Reich SJ, Fosnot J, Kuroki A, Tang W, Yang X, Maguire AM, Bennett J, Tolentino MJ (2003) Small interfering RNA (siRNA) targeting VEGF effectively inhibits ocular neovascularization in a mouse model. *Mol Vis* 9: 210-6
- Reinhart BJ, Bartel DP (2002) Small RNAs correspond to centromere heterochromatic repeats. *Science* 297: 1831.
- Reinhart BJ, Slack FJ, Basson M, Pasquinelli AE, Bettinger JC, Rougvie AE, Horvitz HR, Ruvkun G (2000) The 21-nucleotide let-7 RNA regulates developmental timing in *Caenorhabditis elegans*. *Nature* 403: 901-6
- Reinhart BJ, Weinstein EG, Rhoades MW, Bartel B, Bartel DP (2002) MicroRNAs in plants. *Genes Dev* 16: 1616-26.
- Reynolds A, Leake D, Boese Q, Scaringe S, Marshall WS, Khvorovova A (2004) Rational siRNA design for RNA interference. *Nat Biotechnol*

- Richard JP, Melikov K, Vives E, Ramos C, Verbeure B, Gait MJ, Chernomordik LV, Lebleu B (2003) Cell-penetrating peptides. A reevaluation of the mechanism of cellular uptake. *Journal of Biological Chemistry* 278: 585-90
- Riss D, Jin L, Qian X, Bayliss J, Scheithauer BW, Young WF, Jr., Vidal S, Kovacs K, Raz A, Lloyd RV (2003) Differential expression of galectin-3 in pituitary tumors. *Cancer Res* 63: 2251-5
- Ritter U, Damm-Welk C, Fuchs U, Bohle RM, Borkhardt A, Woessmann W (2003) Design and evaluation of chemically synthesized siRNA targeting the NPM-ALK fusion site in anaplastic large cell lymphoma (ALCL). *Oligonucleotides* 13: 365-73
- Robbins PB, Oliver SF, Sheu SM, Goodnough JB, Wender P, Khavari PA (2002) Peptide delivery to tissues via reversibly linked protein transduction sequences. *Biotechniques* 33: 190-2
- Robertson HD, Webster RE, Zinder ND (1968) Purification and properties of ribonuclease III from *Escherichia coli*. *J Biol Chem* 243: 82-91.
- Robinson KA, Beverley SM (2003) Improvements in transfection efficiency and tests of RNA interference (RNAi) approaches in the protozoan parasite *Leishmania*. *Molecular & Biochemical Parasitology* 128: 217-228
- Rogers FA, Manoharan M, Rabinovitch P, Ward DC, Glazer PM (2004) Peptide conjugates for chromosomal gene targeting by triplex-forming oligonucleotides. *Nucleic Acids Res* 32: 6595-604
- Roignant JY, Carre C, Mugat B, Szymczak D, Lepesant JA, Antoniewski C (2003) Absence of transitive and systemic pathways allows cell-specific and isoform-specific RNAi in *Drosophila*. *Rna* 9: 299-308
- Romaniuk PJ, Uhlenbeck OC (1983) Joining of RNA molecules with RNA ligase. *Methods Enzymol* 100: 52-9
- Ross MF, Murphy MP (2004) Cell-penetrating peptides are excluded from the mitochondrial matrix. *Biochem Soc Trans* 32: 1072-4
- Rossjohn J, Feil SC, McKinstry WJ, Tweten RK, Parker MW (1997) Structure of a cholesterol-binding, thiol-activated cytolysin and a model of its membrane form. *Cell* 89: 685-92
- Rothbard JB, Garlington S, Lin Q, Kirschberg T, Kreider E, McGrane PL, Wender PA, Khavari PA (2000) Conjugation of arginine oligomers to cyclosporin A facilitates topical delivery and inhibition of inflammation. *Nature Medicine* 6: 1253-7
- Rothbard JB, Kreider E, VanDeusen CL, Wright L, Wylie BL, Wender PA (2002) Arginine-rich molecular transporters for drug delivery: role of backbone spacing in cellular uptake. *Journal of Medicinal Chemistry* 45: 3612-8
- Rotondo G, Frendewey D (1996) Purification and Characterization of the Pac1 Ribonuclease of *Schizosaccharomyces Pombe*. *Nucleic Acids Research* 24: 2377-2386
- Rousselle C, Clair P, Tamsamani J, Scherrmann JM (2002) Improved brain delivery of benzylpenicillin with a peptide-vector-mediated strategy. *J Drug Target* 10: 309-15.
- Rousselle C, Smirnova M, Clair P, Lefauconnier JM, Chavanieu A, Calas B, Scherrmann JM, Tamsamani J (2001) Enhanced delivery of doxorubicin into the brain via a peptide-vector-mediated strategy: saturation kinetics and specificity. *J Pharmacol Exp Ther* 296: 124-31.
- Rubinson DA, Dillon CP, Kwiatkowski AV, Sievers C, Yang L, Kopinja J, Rooney DL, Ihrig MM, McManus MT, Gertler FB, Scott ML, Van Parijs L (2003) A lentivirus-based system to functionally silence genes in primary mammalian cells, stem cells and transgenic mice by RNA interference. *Nat Genet* 33: 401-6
- Rudin CM, Marshall JL, Huang CH, Kindler HL, Zhang C, Kumar D, Gokhale PC, Steinberg J, Wanaski S, Kasid UN, Ratain MJ (2004) Delivery of a liposomal c-raf-1 antisense oligonucleotide by weekly bolus dosing in patients with advanced solid tumors: a phase I study. *Clin Cancer Res* 10: 7244-51
- Rueping M, Mahajan Y, Sauer M, Seebach D (2002) Cellular uptake studies with beta-peptides. *Chembiochem* 3: 257-9

- Rueping M, Mahajan YR, Jaun B, Seebach D (2004) Design, synthesis and structural investigations of a beta-peptide forming a 314-helix stabilized by electrostatic interactions. *Chemistry* 10: 1607-15
- Ruiz MT, Voinnet O, Baulcombe DC (1998) Initiation and maintenance of virus-induced gene silencing. *Plant Cell* 10: 937-46
- Rutjes SAB, Piter J.; Rohn, Jennifer L.; Noteborn, Mathieu H. M.; Wesseling, John G. (2003) Induction of insolubility by herpes simplex virus VP22 precludes intercellular trafficking of N-terminal Apoptin-VP22 fusion proteins. *Journal of Molecular Medicine* 81: 558-565
- Rutz S, Scheffold A (2004) Towards in vivo application of RNA interference - new toys, old problems. *Arthritis Res Ther* 6: 78-85
- Ruzza P, Donella-Deana A, Calderan A, Brunati A, Massimino ML, Elardo S, Mattiazzo A, Pinna LA, Borin G (2001) Antennapedia/HS1 chimeric phosphotyrosyl peptide: conformational properties, binding capability to c-Fgr SH2 domain and cell permeability. *Biopolymers* 60: 290-306
- Ryser HJ (1967) A membrane effect of basic polymers dependent on molecular size. *Nature* 215: 934-6
- Ryser HJ, Mandel R, Hacopian A, Shen WC (1988) Methotrexate-poly(lysine) as a selective agent for mutants of Chinese hamster ovary cells defective in endocytosis. *J Cell Physiol* 135: 277-84
- Saalik P, Elmquist A, Hansen M, Padari K, Saar K, Viht K, Langel U, Pooga M (2004) Protein cargo delivery properties of cell-penetrating peptides. A comparative study. *Bioconjug Chem* 15: 1246-53
- Sadler K, Eom KD, Yang JL, Dimitrova Y, Tam JP (2002) Translocating proline-rich peptides from the antimicrobial peptide bactenecin 7. *Biochemistry* 41: 14150-7
- Salamon Z, Lindblom G, Tollin G (2003) Plasmon-waveguide resonance and impedance spectroscopy studies of the interaction between penetratin and supported lipid bilayer membranes. *Biophysical Journal* 84: 1796-1807
- Sambrook J, Fritsch, EF, Maniatis, T (1989) *Molecular Cloning - A Laboratory Manual*, 2nd edn. Cold Spring Harbor Laboratory Press, New York
- Sanborn TJ, Wu CW, Zuckermann RN, Barron AE (2002) Extreme stability of helices formed by water-soluble poly-N-substituted glycines (polypeptoids) with alpha-chiral side chains. *Biopolymers* 63: 12-20
- Sandhoff K, Conzelmann E, Nehrkorn H (1977) Specificity of human liver hexosaminidases A and B against glycosphingolipids GM2 and GA2. Purification of the enzymes by affinity chromatography employing specific elution. *Hoppe Seylers Z Physiol Chem* 358: 779-87
- Sandoval RM, Molitoris BA (2004) Gentamicin traffics retrograde through the secretory pathway and is released in the cytosol via the endoplasmic reticulum. *Am J Physiol Renal Physiol* 286: F617-24
- Sandvig K, van Deurs B (2000) Entry of ricin and Shiga toxin into cells: molecular mechanisms and medical perspectives. *Embo J* 19: 5943-50
- Santra S, Yang H, Dutta D, Stanley JT, Holloway PH, Tan W, Moudgil BM, Mericle RA (2004) TAT conjugated, FITC doped silica nanoparticles for bioimaging applications. *Chem Commun (Camb)*: 2810-1
- Sasaki T, Shiohama A, Minoshima S, Shimizu N (2003) Identification of eight members of the Argonaute family in the human genome. *Genomics* 82: 323-330
- Saxena S, Jonsson ZO, Dutta A (2003) Small RNAs with imperfect match to endogenous mRNA repress translation. Implications for off-target activity of small inhibitory RNA in mammalian cells. *J Biol Chem* 278: 44312-9
- Schafer FQ, Buettner GR (2001) Redox environment of the cell as viewed through the redox state of the glutathione disulfide/glutathione couple. *Free Radic Biol Med* 30: 1191-212
- Schafer R, Abraham D, Paulus P, Blumer R, Grimm M, Wojta J, Aharinejad S (2003) Impaired VE-cadherin/beta-catenin expression mediates endothelial cell degeneration in dilated cardiomyopathy. *Circulation* 108: 1585-91

- Schaschke N, Deluca D, Assfalg-Machleidt I, Hohneke C, Sommerhoff CP, Machleidt W (2002) Epoxysuccinyl peptide-derived cathepsin B inhibitors: modulating membrane permeability by conjugation with the C-terminal heptapeptide segment of penetratin. *Biol Chem* 383: 849-52
- Schauer SE, Jacobsen SE, Meinke DW, Ray A (2002) DICER-LIKE1: blind men and elephants in Arabidopsis development. *Trends in Plant Science* 7: 487-491
- Schepers U (2004) RNA interference in practice, 1 edn. Wiley-VCH, Weinheim
- Schepers U, Kolter T (2001) RNA Interference: A New Way to Analyze Protein Function. *Angew Chem Int Ed Engl* 40: 2437-2439
- Scherr M, Battmer K, Blomer U, Schiedlmeier B, Ganser A, Grez M, Eder M (2002) Lentiviral gene transfer into peripheral blood-derived CD34+ NOD/SCID-repopulating cells. *Blood* 99: 709-12
- Scherr M, Morgan MA, Eder M (2003) Gene silencing mediated by small interfering RNAs in mammalian cells. *Curr Med Chem* 10: 245-56
- Schiffelers RM, Ansari A, Xu J, Zhou Q, Tang Q, Storm G, Molema G, Lu PY, Scaria PV, Woodle MC (2004) Cancer siRNA therapy by tumor selective delivery with ligand-targeted sterically stabilized nanoparticle. *Nucleic Acids Res* 32: e149
- Schirmbeck R, König-Merediz SA, Riedl P, Kwissa M, Sack F, Schroff M, Junghans C, Reimann J, Wittig B (2001) Priming of immune responses to hepatitis B surface antigen with minimal DNA expression constructs modified with a nuclear localization signal peptide. *J Mol Med* 79: 343-50
- Schmidt RF (1999) Physiologie kompakt, 3 edn. Springer, Berlin, Heidelberg
- Schmidt Y (2004) Festphasensynthese von Spermin-Konjugaten und ihre Funktion als molekulare Transporter. Diplomarbeit, Bonn
- Schmitz K (2002) Herstellung von Peptid-RNA-Konjugaten für die RNA-Interferenz in Säugerzellen. Diplomarbeit, Bonn
- Schmitz K, Diallo M, Mundegar R, Schepers U (submitted) pepsRNAs for RNAi in mammals.
- Schreiber JV, Frackenpohl J, Moser F, Fleischmann T, Kohler HP, Seebach D (2002) On the biodegradation of beta-peptides. *Chembiochem* 3: 424-32
- Schroeder T (2004) Synthese neuer fluoreszenzmarkierter Peptide als selektive zelldurchgängige Transporter. Diplomarbeit, Bonn
- Schuette CG, Pierstorff B, Huettler S, Sandhoff K (2001) Sphingolipid activator proteins: proteins with complex functions in lipid degradation and skin biogenesis. *Glycobiology* 11: 81R-90R.
- Schwarz DS, Hutvagner G, Du T, Xu Z, Aronin N, Zamore PD (2003) Asymmetry in the assembly of the RNAi enzyme complex. *Cell* 115: 199-208
- Schwarz DS, Tomari Y, Zamore PD (2004) The RNA-Induced Silencing Complex Is a Mg(2+)-Dependent Endonuclease. *Curr Biol* 14: 787-91
- Schwarze SR, Dowdy SF (2000) In vivo protein transduction: intracellular delivery of biologically active proteins, compounds and DNA. *Trends in Pharmacological Sciences* 21: 45-48
- Schwarze SR, Ho A, Vocero-Akbani A, Dowdy SF (1999) In vivo protein transduction: Delivery of a biologically active protein into the mouse. *Science* 285: 1569-1572
- Schwarze SR, Hruska KA, Dowdy SF (2000) Protein transduction: unrestricted delivery into all cells? *Trends Cell Biol* 10: 290-5.
- Seelig B, Jäschke, A (1997) Site-specific modification of enzymatically synthesized RNA: transcription initiation and Diels-Alder reaction,. *Tetrahedron Letters* 38: 7729-7732
- Seelig B, Jäschke, A (1999) Ternary conjugates of guanosine monophosphate as initiator nucleotides for the enzymatic synthesis of 5'-modified RNAs. *Bioconj. Chem.* 10: 371-378
- Seggerson K, Tang LJ, Moss EG (2002) Two genetic circuits repress the *Caenorhabditis elegans* heterochronic gene *lin-28* after translation initiation. *Developmental Biology* 243: 215-225
- Sen A, Steele R, Ghosh AK, Basu A, Ray R, Ray RB (2003) Inhibition of hepatitis C virus protein expression by RNA interference. *Virus Res* 96: 27-35

- Sengle G, Eisenfuhr A, Arora PS, Nowick JS, Famulok M (2001) Novel RNA catalysts for the Michael reaction. *Chemistry & Biology* 8: 459-473
- Shen WC, Ryser HJ (1978) Conjugation of poly-L-lysine to albumin and horseradish peroxidase: a novel method of enhancing the cellular uptake of proteins. *Proc Natl Acad Sci U S A* 75: 1872-6
- Sherman MP, Schubert U, Williams SA, de Noronha CM, Kreisberg JF, Henklein P, Greene WC (2002) HIV-1 Vpr displays natural protein-transducing properties: implications for viral pathogenesis. *Virology* 302: 95-105
- Shi Kam NW, Jessop TC, Wender PA, Dai H (2004) Nanotube molecular transporters: internalization of carbon nanotube-protein conjugates into Mammalian cells. *J Am Chem Soc* 126: 6850-1
- Shlomai A, Shaul Y (2003) Inhibition of hepatitis B virus expression and replication by RNA interference. *Hepatology* 37: 764-70
- Shlomai A, Shaul Y (2004) RNA interference--small RNAs effectively fight viral hepatitis. *Liver Int* 24: 526-31
- Shultz LG, Zimmermann S.C. (1999) Dendrimers: potential drugs and drug delivery agents. *Pharm News* 6: 25-29
- Siegmund D, Hadwiger P, Pfizenmaier K, Vornlocher HP, Wajant H (2002) Selective inhibition of FLICE-like inhibitory protein expression with small interfering RNA oligonucleotides is sufficient to sensitize tumor cells for TRAIL-induced apoptosis. *Mol Med* 8: 725-32
- Sijen T, Fleenor J, Simmer F, Thijssen KL, Parrish S, Timmons L, Plasterk RH, Fire A (2001a) On the role of RNA amplification in dsRNA-triggered gene silencing. *Cell* 107: 465-76.
- Sijen T, Vijn I, Rebocho A, van Blokland R, Roelofs D, Mol JN, Kooter JM (2001b) Transcriptional and posttranscriptional gene silencing are mechanistically related. *Curr Biol* 11: 436-40.
- Silhol M, Tyagi M, Giacca M, Lebleu B, Vives E (2002) Different mechanisms for cellular internalization of the HIV-1 Tat-derived cell penetrating peptide and recombinant proteins fused to Tat. *European Journal of Biochemistry* 269: 494-501
- Simeoni F, Morris MC, Heitz F, Divita G (2003) Insight into the mechanism of the peptide-based gene delivery system MPG: implications for delivery of siRNA into mammalian cells. *Nucleic Acids Research* 31: 2717-2724
- Simeonova M, Velichkova R, Ivanova G, Enchev V, Abrahams I (2003) Poly(butylcyanoacrylate) nanoparticles for topical delivery of 5-fluorouracil. *Int J Pharm* 263: 133-140
- Simmer F, Tijsterman M, Parrish S, Koushika SP, Nonet ML, Fire A, Ahringer J, Plasterk RH (2002) Loss of the putative RNA-directed RNA polymerase RRF-3 makes *C. elegans* hypersensitive to RNAi. *Curr Biol* 12: 1317-9
- Siprashvili Z, Scholl FA, Oliver SF, Adams A, Contag CH, Wender PA, Khavari PA (2003) Gene transfer via reversible plasmid condensation with cysteine-flanked, internally spaced arginine-rich peptides. *Hum Gene Ther* 14: 1225-33
- Skelly PJ, Da'dara A, Harn DA (2003) Suppression of cathepsin B expression in *Schistosoma mansoni* by RNA interference. *Int J Parasitol* 33: 363-9
- Slack FJ, Basson M, Liu Z, Ambros V, Horvitz HR, Ruvkun G (2000) The lin-41 RBCC gene acts in the *C. elegans* heterochronic pathway between the let-7 regulatory RNA and the LIN-29 transcription factor. *Mol Cell* 5: 659-69
- Sledz CA, Holko M, de Veer MJ, Silverman RH, Williams BR (2003) Activation of the interferon system by short-interfering RNAs. *Nat Cell Biol* 5: 834-9
- Smalheiser NR, Manev H, Costa E (2001) RNAi and brain function: was McConnell on the right track? *Trends in Neurosciences* 24: 216-218
- Smardon A, Spoerke JM, Stacey SC, Klein ME, Mackin N, Maine EM (2000) EGO-1 is related to RNA-directed RNA polymerase and functions in germ-line development and RNA interference in *C. elegans*. *Curr Biol* 10: 169-78.
- Snove O, Jr., Holen T (2004) Many commonly used siRNAs risk off-target activity. *Biochem Biophys Res Commun* 319: 256-63

- Sohail M, Doran G, Riedemann J, Macaulay V, Southern EM (2003) A simple and cost-effective method for producing small interfering RNAs with high efficacy. *Nucleic Acids Res* 31: e38
- Song E, Lee SK, Wang J, Ince N, Ouyang N, Min J, Chen J, Shankar P, Lieberman J (2003a) RNA interference targeting Fas protects mice from fulminant hepatitis. *Nat Med* 9: 347-51
- Song JJ, Liu J, Tolia NH, Schneiderman J, Smith SK, Martienssen RA, Hannon GJ, Joshua-Tor L (2003b) The crystal structure of the Argonaute2 PAZ domain reveals an RNA binding motif in RNAi effector complexes. *Nat Struct Biol* 10: 1026-1032
- Song JJ, Smith SK, Hannon GJ, Joshua-Tor L (2004) Crystal structure of Argonaute and its implications for RISC slicer activity. *Science* 305: 1434-7
- Soughayer JS, Wang Y, Li H, Cheung SH, Rossi FM, Stanbridge EJ, Sims CE, Allbritton NL (2004) Characterization of TAT-mediated transport of detachable kinase substrates. *Biochemistry* 43: 8528-40
- Soulet D, Covassin L, Kaouass M, Charest-Gaudreault R, Audette M, Poulin R (2002) Role of endocytosis in the internalization of spermidine-C(2)-BODIPY, a highly fluorescent probe of polyamine transport. *Biochem J* 367: 347-57
- Soutschek J, Akinc A, Bramlage B, Charisse K, Constien R, Donoghue M, Elbashir S, Geick A, Hadwiger P, Harborth J, John M, Kesavan V, Lavine G, Pandey RK, Racie T, Rajeev KG, Rohl I, Toudjarska I, Wang G, Wuschko S, Bumcrot D, Kotliansky V, Limmer S, Manoharan M, Vornlocher HP (2004) Therapeutic silencing of an endogenous gene by systemic administration of modified siRNAs. *Nature* 432: 173-8
- Sprong H, Degroote S, Claessens T, van Drunen J, Oorschot V, Westerink BH, Hirabayashi Y, Klumperman J, van der Sluijs P, van Meer G (2001) Glycosphingolipids are required for sorting melanosomal proteins in the Golgi complex. *J Cell Biol* 155: 369-80.
- Stark A, Brennecke J, Russell RB, Cohen SM (2003) Identification of Drosophila MicroRNA Targets. *PLoS Biol* 1: E60
- Stark GR, Kerr IM, Williams BR, Silverman RH, Schreiber RD (1998) How cells respond to interferons. *Annu Rev Biochem* 67: 227-64
- Stein P, Svoboda P, Anger M, Schultz RM (2003) RNAi: Mammalian oocytes do it without RNA-dependent RNA polymerase. *Rna-A Publication of the Rna Society* 9: 187-192
- Stein S, Weiss A, Adermann K, Lazarovici P, Hochman J, Wellhoner H (1999) A disulfide conjugate between anti-tetanus antibodies and HIV (37-72)Tat neutralizes tetanus toxin inside chromaffin cells. *FEBS Lett* 458: 383-6
- Stenmark H, Moskaug JO, Madhus IH, Sandvig K, Olsnes S (1991) Peptides fused to the amino-terminal end of diphtheria toxin are translocated to the cytosol. *J Cell Biol* 113: 1025-32
- Stewart SA, Dykxhoorn DM, Palliser D, Mizuno H, Yu EY, An DS, Sabatini DM, Chen IS, Hahn WC, Sharp PA, Weinberg RA, Novina CD (2003) Lentivirus-delivered stable gene silencing by RNAi in primary cells. *Rna* 9: 493-501
- Stolzenberger S, Haake M, Duschl A (2001) Specific inhibition of interleukin-4-dependent Stat6 activation by an intracellularly delivered peptide. *Eur J Biochem* 268: 4809-4814
- Stroh C, Held J, Samraj AK, Schulze-Osthoff K (2003) Specific inhibition of transcription factor NF-kappaB through intracellular protein delivery of I kappaBalpha by the Herpes virus protein VP22. *Oncogene* 22: 5367-73
- Subramanian T, Chinnadurai G (2003) Pro-apoptotic activity of transiently expressed BCL-2 occurs independent of BAX and BAK. *Journal of Cellular Biochemistry* 89: 1102-1114
- Sui G, Soohoo C, Affar el B, Gay F, Shi Y, Forrester WC (2002) A DNA vector-based RNAi technology to suppress gene expression in mammalian cells. *Proc Natl Acad Sci U S A* 99: 5515-20.
- Sullenger BA, Gallardo HF, Ungers GE, Gilboa E (1990) Overexpression of TAR sequences renders cells resistant to human immunodeficiency virus replication. *Cell* 63: 601-8.
- Sun B, Nishihira J, Suzuki M, Fukushima N, Ishibashi T, Kondo M, Sato Y, Todo S (2003) Induction of macrophage migration inhibitory factor by lysophosphatidic acid: relevance to tumor growth and angiogenesis. *Int J Mol Med* 12: 633-41

- Sunaga N, Miyajima K, Suzuki M, Sato M, White MA, Ramirez RD, Shay JW, Gazdar AF, Minna JD (2004) Different roles for caveolin-1 in the development of non-small cell lung cancer versus small cell lung cancer. *Cancer Res* 64: 4277-85
- Symons MC (1995) Polyamines to target drugs to DNA. *Free Radic Res* 22: 1-9
- Tabara H, Grishok A, Mello CC (1998) RNAi in *C. elegans*: soaking in the genome sequence. *Science* 282: 430-1.
- Tabara H, Hill RJ, Mello CC, Priess JR, Kohara Y (1999a) pos-1 encodes a cytoplasmic zinc-finger protein essential for germline specification in *C. elegans*. *Development* 126: 1-11
- Tabara H, Sarkissian M, Kelly WG, Fleenor J, Grishok A, Timmons L, Fire A, Mello CC (1999b) The rde-1 gene, RNA interference, and transposon silencing in *C. elegans*. *Cell* 99: 123-32.
- Tabara H, Yigit E, Siomi H, Mello CC (2002) The dsRNA binding protein RDE-4 interacts with RDE-1, DCR-1, and a DEXH- box helicase to direct RNAi in *C. elegans*. *Cell* 109: 861-71.
- Tachibana R, Harashima H, Ide N, Ukitsu S, Ohta Y, Suzuki N, Kikuchi H, Shinohara Y, Kiwada H (2002) Quantitative analysis of correlation between number of nuclear plasmids and gene expression activity after transfection with cationic liposomes. *Pharm Res* 19: 377-81
- Tahbaz N, Kolb FA, Zhang H, Jaronczyk K, Filipowicz W, Hobman TC (2004) Characterization of the interactions between mammalian PAZ PIWI domain proteins and Dicer. *EMBO Rep* 5: 189-94
- Takasugi N, Tomita T, Hayashi I, Tsuruoka M, Niimura M, Takahashi Y, Thinakaran G, Iwatsubo T (2003) The role of presenilin cofactors in the gamma-secretase complex. *Nature* 422: 438-41
- Tanaka Y, Gavrielides MV, Mitsuuchi Y, Fujii T, Kazanietz MG (2003) Protein kinase C promotes apoptosis in LNCaP prostate cancer cells through activation of p38 MAPK and inhibition of the Akt survival pathway. *J Biol Chem* 278: 33753-62
- Tang GL, Reinhart BJ, Bartel DP, Zamore PD (2003) A biochemical framework for RNA silencing in plants. *Genes Dev* 17: 49-63
- Taverna SD, Coyne RS, Allis CD (2002) Methylation of histone h3 at lysine 9 targets programmed DNA elimination in tetrahymena. *Cell* 110: 701-11
- Tavernarakis N, Wang SL, Dorovkov M, Ryazanov A, Driscoll M (2000) Heritable and inducible genetic interference by double-stranded RNA encoded by transgenes. *Nat Genet* 24: 180-3.
- Terrone D, Sang SL, Roudaia L, Silviu JR (2003) Penetratin and related cell-penetrating cationic peptides can translocate across lipid bilayers in the presence of a transbilayer potential. *Biochemistry* 42: 13787-99
- Thilo L, Stroud E, Haylett T (1995) Maturation of early endosomes and vesicular traffic to lysosomes in relation to membrane recycling. *J Cell Sci* 108 (Pt 4): 1791-803
- Thoren PE, Persson D, Isakson P, Goksor M, Onfelt A, Norden B (2003) Uptake of analogs of penetratin, Tat(48-60) and oligoarginine in live cells. *Biochem Biophys Res Commun* 307: 100-7
- Thyberg (2002) *Histochem. Cytochem.*
- Tien ES, Davis JW, Vanden Heuvel JP (2004) Identification of the CBP/p300 interacting protein CITED2 as a PPARalpha coregulator. *J Biol Chem*
- Tijsterman M, Ketting R, Fischer S, Simmer F, Sijen T, Okihara K, Tops B, Vastenhouw N, Plasterk R (2002) The mechanism of RNA interference and the transposon silencing in *Caenorhabditis elegans*. *ScientificWorldJournal* 2: 3-4
- Tilly G, Chapuis J, Vilette D, Laude H, Vilotte JL (2003) Efficient and specific down-regulation of prion protein expression by RNAi. *Biochemical & Biophysical Research Communications* 305: 548-551
- Timmons L, Fire A (1998) Specific Interference by Ingested dsRNA. *Nature* 395: 854
- Tiscornia G, Singer O, Ikawa M, Verma IM (2003) A general method for gene knockdown in mice by using lentiviral vectors expressing small interfering RNA. *Proc Natl Acad Sci U S A* 100: 1844-8

- Tomar RS, Matta H, Chaudhary PM (2003) Use of adeno-associated viral vector for delivery of small interfering RNA. *Oncogene* 22: 5712-5715
- Tomari Y, Du T, Haley B, Schwarz DS, Bennett R, Cook HA, Koppetsch BS, Theurkauf WE, Zamore PD (2004) RISC assembly defects in the Drosophila RNAi mutant armitage. *Cell* 116: 831-41
- Torchilin VP (2002) TAT peptide-modified liposomes for intracellular delivery of drugs and DNA. *Cell Mol Biol Lett* 7: 265-7
- Torchilin VP, Levchenko TS (2003) TAT-liposomes: a novel intracellular drug carrier. *Curr Protein Pept Sci* 4: 133-40
- Torchilin VP, Rammohan R, Weissig V, Levchenko TS (2001) TAT peptide on the surface of liposomes affords their efficient intracellular delivery even at low temperature and in the presence of metabolic inhibitors. *Proc Natl Acad Sci U S A* 98: 8786-91
- Trehin R, Krauss U, Muff R, Meinecke M, Beck-Sickinger AG, Merkle HP (2004) Cellular internalization of human calcitonin derived peptides in MDCK monolayers: a comparative study with Tat(47-57) and penetratin(43-58). *Pharm Res* 21: 33-42
- Trulzsch B, Davies K, Wood M (2004) Survival of motor neuron gene downregulation by RNAi: towards a cell culture model of spinal muscular atrophy. *Brain Res Mol Brain Res* 120: 145-50
- Tseng YL, Liu JJ, Hong RL (2002) Translocation of liposomes into cancer cells by cell-penetrating peptides penetratin and tat: a kinetic and efficacy study. *Mol Pharmacol* 62: 864-72
- Turk MJ, Waters DJ, Low PS (2004) Folate-conjugated liposomes preferentially target macrophages associated with ovarian carcinoma. *Cancer Lett* 213: 165-72
- Twyman LJ, Beezer AE, Esfand R, Hardy MJ, Mitchell JC (1999) The synthesis of water soluble dendrimers, and their application as possible drug delivery systems. *Tetrahedron Letters* 40: 1743-1746
- Uhrich KE, Cannizzaro SM, Langer RS, Shakesheff KM (1999) Polymeric systems for controlled drug release. *Chem Rev* 99: 3181-98
- Ulrich AS (2002) Biophysical aspects of using liposomes as delivery vehicles. *Biosci Rep* 22: 129-50
- Umezawa N, Gelman MA, Haigis MC, Raines RT, Gellman SH (2002) Translocation of a beta-peptide across cell membranes. *J Am Chem Soc* 124: 368-9
- Uno T, Beausoleil E, Goldsmith RA, Levine BH, Zuckermann RN (1999) New submonomers for poly N-substituted glycines (peptoids). *Tetrahedron Letters* 40: 1475-1478
- Usui I, Imamura T, Huang J, Satoh H, Olefsky JM (2003) Cdc42 is a Rho GTPase family member that can mediate insulin signaling to glucose transport in 3T3-L1 adipocytes. *J Biol Chem* 278: 13765-74
- van der Aa MA, Koning GA, d'Oliveira C, Oosting RS, Wilschut KJ, Hennink WE, Crommelin DJ (2004) An NLS peptide covalently linked to linear DNA does not enhance transfection efficiency of cationic polymer based gene delivery systems. *J Gene Med*
- Venter JC, Adams MD, Myers EW, Li PW, Mural RJ, Sutton GG, Smith HO, Yandell M, Evans CA, Holt RA, Gocayne JD, Amanatides P, Ballew RM, Huson DH, Wortman JR, Zhang Q, Kodira CD, Zheng XH, Chen L, Skupski M, Subramanian G, Thomas PD, Zhang J, Gabor Miklos GL, Nelson C, Broder S, Clark AG, Nadeau J, McKusick VA, Zinder N, Levine AJ, Roberts RJ, Simon M, Slayman C, Hunkapiller M, Bolanos R, Delcher A, Dew I, Fasulo D, Flanigan M, Florea L, Halpern A, Hannerhalli S, Kravitz S, Levy S, Mobarry C, Reinert K, Remington K, Abu-Threideh J, Beasley E, Biddick K, Bonazzi V, Brandon R, Cargill M, Chandramouliswaran I, Charlab R, Chaturvedi K, Deng Z, Di Francesco V, Dunn P, Eilbeck K, Evangelista C, Gabrielian AE, Gan W, Ge W, Gong F, Gu Z, Guan P, Heiman TJ, Higgins ME, Ji RR, Ke Z, Ketchum KA, Lai Z, Lei Y, Li Z, Li J, Liang Y, Lin X, Lu F, Merkulov GV, Milshina N, Moore HM, Naik AK, Narayan VA, Neelam B, Nusskern D, Rusch DB, Salzberg S, Shao W, Shue B, Sun J, Wang Z, Wang A, Wang X, Wang J, Wei M, Wides R, Xiao C, Yan C, et al. (2001) The sequence of the human genome. *Science* 291: 1304-51.
- Verdel A, Jia S, Gerber S, Sugiyama T, Gygi S, Grewal SI, Moazed D (2004) RNAi-mediated targeting of heterochromatin by the RITS complex. *Science* 303: 672-6

- Verheyden JPH, Moffat JG (1970) Halo Sugar Nucleosides. I. Iodination of the Primary Hydroxyl Groups of Nucleosides with Methyltriphenoxyphosphonium Iodide. *J. Org. Chem.* 35: 2319-2326
- Villa R, Folini M, Lualdi S, Veronese S, Daidone MG, Zaffaroni N (2000) Inhibition of telomerase activity by a cell-penetrating peptide nucleic acid construct in human melanoma cells. *FEBS Letters* 473: 241-248
- Violini S, Sharma V, Prior JL, Dyszlewski M, Piwnica-Worms D (2002) Evidence for a plasma membrane-mediated permeability barrier to Tat basic domain in well-differentiated epithelial cells: lack of correlation with heparan sulfate. *Biochemistry* 41: 12652-61
- Vives E (2003) Cellular uptake [correction of utake] of the Tat peptide: an endocytosis mechanism following ionic interactions. *J. Mol. Recognition* 16: 265-271
- Vives E, Brodin P, Lebleu B (1997a) A truncated HIV-1 Tat protein basic domain rapidly translocates through the plasma membrane and accumulates in the cell nucleus. *J Biol Chem* 272: 16010-7
- Vives E, Charneau P, van Rietschoten J, Rochat H, Bahraoui E (1994) Effects of the Tat basic domain on human immunodeficiency virus type 1 transactivation, using chemically synthesized Tat protein and Tat peptides. *J Virol* 68: 3343-53
- Vives E, Granier C, Prevot P, Lebleu B (1997b) Structure-activity relationship study of the plasma membrane translocating potential of a short peptide from HIV-1 Tat protein. *Letters in Peptide Science* 4: 429-436
- Vives E, Lebleu B (1997) Selective coupling of a highly basic peptide to an oligonucleotide. *Tetrahedron Letters* 38: 1183-1186
- Vives E, Lebleu B (2003) One-pot labeling and purification of peptides and proteins with fluorescein maleimide. *Tetrahedron Letters* 44: 5389-5391
- Vives E, Richard JP, Rispal C, Lebleu B (2003) TAT peptide internalization: seeking the mechanism of entry. *Current Protein & Peptide Science* 4: 125-32
- Vocero-Akbani AM, Heyden NV, Lissy NA, Ratner L, Dowdy SF (1999) Killing HIV-infected cells by transduction with an HIV protease-activated caspase-3 protein.[comment]. *Nat Med* 5: 29-33
- Voet D, Voet JG (1998) *Biochemistry*, 2 edn. John Wiley & Sons, New York
- Voinnet O (2001) RNA silencing as a plant immune system against viruses. *Trends Genet* 17: 449-59
- Volpe T, Schramke V, Hamilton GL, White SA, Teng G, Martienssen RA, Allshire RC (2003) RNA interference is required for normal centromere function in fission yeast. *Chromosome Research* 11: 137-146
- Volpe TA, Kidner C, Hall IM, Teng G, Grewal SIS, Martienssen RA (2002) Regulation of heterochromatic silencing and histone H3 lysine-9 methylation by RNAi. *Science* 297: 1833-1837
- Wadia JS, Dowdy SF (2002) Protein transduction technology. *Current Opinion in Biotechnology* 13: 52-6
- Wadia JS, Stan RV, Dowdy SF (2004) Transducible TAT-HA fusogenic peptide enhances escape of TAT-fusion proteins after lipid raft macropinocytosis. *Nat Med* 10: 310-5
- Wall NR, Shi Y (2003) Small RNA: can RNA interference be exploited for therapy? *Lancet* 362: 1401-3
- Walters DK, Jelinek DF (2002) The effectiveness of double-stranded short inhibitory RNAs (siRNAs) may depend on the method of transfection. *Antisense Nucleic Acid Drug Dev* 12: 411-8
- Wang Y, Decker SJ, Sebolt-Leopold J (2004) Knockdown of Chk1, Wee1 and Myt1 by RNA Interference Abrogates G(2) Checkpoint and Induces Apoptosis. *Cancer Biol Ther* 3
- Wassenegger M, Heimes S, Riedel L, Sanger HL (1994) RNA-directed de novo methylation of genomic sequences in plants. *Cell* 76: 567-76
- Weber A, Casini A, Heine A, Kuhn D, Supuran CT, Scozzafava A, Klebe G (2004) Unexpected nanomolar inhibition of carbonic anhydrase by COX-2-selective celecoxib: new pharmacological opportunities due to related binding site recognition. *J Med Chem* 47: 550-7

- Wender PA, Jessop TC, Pattabiraman K, Pelkey ET, VanDeusen CL (2001) An efficient, scalable synthesis of the molecular transporter octaarginine via a segment doubling strategy. *Org Lett* 3: 3229-32.
- Wender PA, Mitchell DJ, Pattabiraman K, Pelkey ET, Steinman L, Rothbard JB (2000) The design, synthesis and evaluation of molecules that enable or enhance cellular uptake: Peptoid molecular transporters. *Proc. Natl. Acad. Sci. USA* 97: 13003-13008
- Wender PA, Rothbard JB, Jessop TC, Kreider EL, Wylie BL (2002) Oligocarbamate molecular transporters: design, synthesis, and biological evaluation of a new class of transporters for drug delivery. *Journal of the American Chemical Society* 124: 13382-3
- Wianny F, Zernicka-Goetz M (2000) Specific interference with gene function by double-stranded RNA in early mouse development. *Nature Cell Biology* 2: 70-75
- Wienholds E, Van Eeden F, Kusters M, Mudde J, Plasterk RH, Cuppen E (2003) Efficient Target-Selected Mutagenesis in Zebrafish. *Genome Res* 13: 2700-2707
- Wilda M, Fuchs U, Wossmann W, Borkhardt A (2002) Killing of leukemic cells with a BCR/ABL fusion gene by RNA interference (RNAi). *Oncogene* 21: 5716-24
- Wolff JA, Herweijer H (2003) Nonviral vectors for cardiovascular gene delivery. *Ernst Schering Res Found Workshop*: 41-59
- Wong FM, MacAdam SA, Kim A, Oja C, Ramsay EC, Bally MB (2002) A lipid-based delivery system for antisense oligonucleotides derived from a hydrophobic complex. *J Drug Target* 10: 615-23
- Wu H, Xu H, Miraglia LJ, Crooke ST (2000) Human RNase III is a 160-kDa protein involved in preribosomal RNA processing. *J Biol Chem* 275: 36957-65
- Wu HY, Guy JS, Yoo D, Vlasak R, Urbach E, Brian DA (2003) Common RNA replication signals exist among group 2 coronaviruses: evidence for in vivo recombination between animal and human coronavirus molecules. *Virology* 315: 174-83
- Xia H, Mao Q, Paulson HL, Davidson BL (2002) siRNA-mediated gene silencing in vitro and in vivo. *Nat Biotechnol* 20: 1006-10
- Xia XG, Zhou H, Ding H, Affar el B, Shi Y, Xu Z (2003) An enhanced U6 promoter for synthesis of short hairpin RNA. *Nucleic Acids Res* 31: e100
- Yakymovych I, Engstrom U, Grimsby S, Heldin CH, Souchelnytskyi S (2002) Inhibition of transforming growth factor-beta signaling by low molecular weight compounds interfering with ATP- or substrate-binding sites of the TGF beta type I receptor kinase. *Biochemistry* 41: 11000-11007
- Yamada T, Morishita S (2004) Accelerated off-target search algorithm for siRNA. *Bioinformatics*
- Yamamoto T, Omoto S, Mizuguchi M, Mizukami H, Okuyama H, Okada N, Saksena NK, Brisibe EA, Otake K, Fujii YR (2002) Double-stranded nef RNA interferes with human immunodeficiency virus type 1 replication. *Microbiology & Immunology* 46: 809-817
- Yan KS, Yan S, Farooq A, Han A, Zeng L, Zhou MM (2003) Structure and conserved RNA binding of the PAZ domain. *Nature*
- Yang D, Lu H, Erickson JW (2000) Evidence that processed small dsRNAs may mediate sequence-specific mRNA degradation during RNAi in *Drosophila* embryos. *Curr Biol* 10: 1191-200.
- Yang WW, Q et al (2004) ADAR1 RNA Deaminase Limits siRNA Efficacy in Mammalian Cells. *JBC*
- Yang Y, Nishimura I, Imai Y, Takahashi R, Lu B (2003) Parkin suppresses dopaminergic neuron-selective neurotoxicity induced by Pael-R in *Drosophila*. *Neuron* 37: 911-24
- Yi CE, Bekker JM, Miller G, Hill KL, Crosbie RH (2003) Specific and Potent RNA Interference in Terminally Differentiated Myotubes. *J Biol Chem* 278: 934-939.
- Yin JQ, Gao J, Shao R, Tian WN, Wang J, Wan Y (2003a) siRNA agents inhibit oncogene expression and attenuate human tumor cell growth. *J Exp Ther Oncol* 3: 194-204
- Yin MJ, Shao L, Voehringer D, Smeal T, Jallal B (2003b) The serine/threonine kinase Nek6 is required for cell cycle progression through mitosis. *J Biol Chem* 278: 52454-60
- Ying C, De Clercq E, Neyts J (2003) Selective inhibition of hepatitis B virus replication by RNA interference. *Biochem Biophys Res Commun* 309: 482-4

- Yingyongnarongkul BE, Howarth M, Elliott T, Bradley M (2004) DNA transfection screening from single beads. *J Comb Chem* 6: 753-60
- Yoshinari K, Miyagishi M, Taira K (2004) Effects on RNAi of the tight structure, sequence and position of the targeted region. *Nucleic Acids Res* 32: 691-9
- Yu JY, DeRuiter SL, Turner DL (2002) RNA interference by expression of short-interfering RNAs and hairpin RNAs in mammalian cells. *Proceedings of the National Academy of Sciences of the United States of America* 99: 6047-6052
- Zamore PD (2001) Thirty-three years later, a glimpse at the ribonuclease III active site. *Molecular Cell* 8: 1158-1160
- Zamore PD, Tuschl T, Sharp PA, Bartel DP (2000) RNAi: Double-stranded RNA directs the ATP-dependent cleavage of mRNA at 21 to 23 nucleotide intervals. *Cell* 101: 25-33
- Zangemeister-Wittke U (2003) Antisense to apoptosis inhibitors facilitates chemotherapy and TRAIL-induced death signaling. *Ann N Y Acad Sci* 1002: 90-4
- Zanta MA, Belguise-Valladier P, Behr JP (1999) Gene delivery: A single nuclear localization signal peptide is sufficient to carry DNA to the cell nucleus. *Proceedings of the National Academy of Sciences of the United States of America* 96: 91-96
- Zaro JL, Shen WC (2003) Quantitative comparison of membrane transduction and endocytosis of oligopeptides. *Biochemical and Biophysical Research Communications* 307: 241-247
- Zavaglia D, Normand N, Brewis N, O'Hare P, Favrot MC, Coll JL (2003) VP22-mediated and light-activated delivery of an anti-c-raf1 antisense oligonucleotide improves its activity after intratumoral injection in nude mice. *Mol Ther* 8: 840-5
- Zeng Y, Cullen BR (2002) RNA interference in human cells is restricted to the cytoplasm. *Rna* 8: 855-60.
- Zeng Y, Cullen BR (2003) Sequence requirements for micro RNA processing and function in human cells. *Rna-A Publication of the Rna Society* 9: 112-123
- Zhang BL, Cui ZY, Sun LL (2001a) Synthesis of 5'-deoxy-5'-thioguanosine-5'-monophosphorothioate and its incorporation into RNA 5'-termini. *Organic Letters* 3: 275-278
- Zhang G, Budker V, Wolff JA (1999) High levels of foreign gene expression in hepatocytes after tail vein injections of naked plasmid DNA. *Hum Gene Ther* 10: 1735-7
- Zhang H, Kolb FA, Brondani V, Billy E, Filipowicz W (2002) Human Dicer preferentially cleaves dsRNAs at their termini without a requirement for ATP. *Embo J* 21: 5875-85.
- Zhang H, Kolb FA, Jaskiewicz L, Westhof E, Filipowicz W (2004a) Single processing center models for human Dicer and bacterial RNase III. *Cell* 118: 57-68
- Zhang J, Hua ZC (2004) Targeted Gene Silencing by Small Interfering RNA-Based Knock-Down Technology. *Curr Pharm Biotechnol* 5: 1-7
- Zhang L, Sun LL, Cui ZY, Gottlieb RL, Zhang BL (2001b) 5'-sulfhydryl-modified RNA: Initiator synthesis, in vitro transcription, and enzymatic incorporation. *Bioconjugate Chemistry* 12: 939-948
- Zhang L, Yang N, Mohamed-Hadley A, Rubin SC, Coukos G (2003) Vector-based RNAi, a novel tool for isoform-specific knock-down of VEGF and anti-angiogenesis gene therapy of cancer. *Biochem Biophys Res Commun* 303: 1169-78
- Zhang X, Shan P, Jiang D, Noble PW, Abraham NG, Kappas A, Lee PJ (2004b) Small interfering RNA targeting heme oxygenase-1 enhances ischemia-reperfusion-induced lung apoptosis. *J Biol Chem* 279: 10677-84
- Zhang Y, Li T, Fu L, Yu C, Li Y, Xu X, Wang Y, Ning H, Zhang S, Chen W, Babiuk LA, Chang Z (2004c) Silencing SARS-CoV Spike protein expression in cultured cells by RNA interference. *FEBS Lett* 560: 141-6
- Zhao M, Kircher MF, Josephson L, Weissleder R (2002) Differential conjugation of tat peptide to superparamagnetic nanoparticles and its effect on cellular uptake. *Bioconjug Chem* 13: 840-4
- Zhou Y, Chan, J. etc (2004) Transgenic plant-derived siRNAs can suppress propagation of influenza virus in mammalian cells. *FEBS Letters* 577: 345-350

- Ziegler A, Blatter XL, Seelig A, Seelig J (2003) Protein transduction domains of HIV-1 and SIV TAT interact with charged lipid vesicles. Binding mechanism and thermodynamic analysis. *Biochemistry* 42: 9185-94
- Zimmer A, Mutschler E, Lambrecht G, Mayer D, Kreuter J (1994) Pharmacokinetic and pharmacodynamic aspects of an ophthalmic pilocarpine nanoparticle-delivery-system. *Pharm Res* 11: 1435-42
- Zippo A, De Robertis A, Bardelli M, Galvagni F, Oliviero S (2004) Identification of Flk-1-target genes in vasculogenesis: Pim-1 is required for endothelial and mural cell differentiation in vitro. *Blood*
- Zuckermann RN, Martin EJ, Spellmeyer DC, Stauber GB, Shoemaker KR, Kerr JM, Figliozzi GM, Goff DA, Siani MA, Simon RJ, et al. (1994) Discovery of nanomolar ligands for 7-transmembrane G-protein-coupled receptors from a diverse N-(substituted)glycine peptoid library. *J Med Chem* 37: 2678-85

Summary

In recent years, RNA interference has gained a lot of importance as a tool for posttranscriptional silencing of genes due to its high specificity, efficiency and ease of application. Treatment of cells with double-stranded RNA leads to the degradation of homologous, endogenous mRNA and hence to the downregulation of the corresponding gene product. In mammalian cells, RNAi can be achieved with 21 bp short dsRNAs, so-called short interfering RNAs (siRNAs). Numerous studies indicate the great potential of RNAi in the therapy of viral infections and inherited diseases. However, the application of RNAi is severely limited by the delivery issue, as conventional transfection methods cannot be applied to a number of primary and non-dividing cells or even fully-grown organisms.

Cell-penetrating peptides (CPPs) are one means to overcome these limitations. These short positively charged amino acid sequences are internalized by cells, where they can be detected in the endosomes, lysosomes, but also in the cytosol. If attached to CPPs, large cargo molecules can be taken up with a high efficiency that surpasses that of most conventional transfection methods.

In the work presented here, peptide-coupled siRNAs (pepsiRNAs) have been developed as a novel tool for transient RNAi in mammalian cells. To covalently attach the peptide with the siRNA, a disulfide bond was used, that is cleaved under the reducing conditions of the cytosol and thus releases the siRNA cargo.

PepsiRNAs are readily taken up by many cell types that are difficult to address by conventional transfection methods, and siRNA-induced downregulation of the targeted genes is observed at concentrations between 10 and 100 nM.

For the scale up of the pepsRNA approach, an enzymatic method has been modified to yield siRNAs with a 5'-thiol modification upon their sense-strand. To this means, the synthesis protocol of a thiol-modified nucleotide has been optimized. For the recombinant generation of cell-penetrating peptides, vectors for the expression of GST-tagged AntP and Tat peptide have been cloned, and the standard purification protocol was improved to account for the strong membrane interaction of the GST-tagged CPPs. Recombinant TEV protease was expressed to cleave the CPPs from the fusion-tag and the cleavage activity was assessed by comparison with commercially obtained. Thus, alternative routes to the building blocks for pepsRNAs have been provided to scale up the amount of the conjugates.

Finally, small molecules with cell-penetrating properties have been developed as a future replacement of the peptide moiety. Fluorescently labeled peptoids of differing length with amine-functionalized side chains have been shown to enter different mammalian cells lines at concentrations in the lower micromolar range by an endocytosis dependent mechanism. Cationic molecules as small as spermine attached to fluorescein are able to enter fibroblasts HeLa- and COS7 cells also by an endocytosis-related mechanism. They have been shown to deliver bulky cargo molecules like porphyrins into the interior of the cells, where they exhibited a cytotoxic effect upon illumination. Thus spermine-coupled porphyrins may constitute a novel drug for photodynamic therapy.

Tabellarischer Lebenslauf

Katja Schmitz

*1978 in Andernach

Kontakt

email: katja.schmitz@uni-bonn.de

Ausbildung

| | |
|----------------------|--|
| 16.09.2002 | Beginn der Doktorarbeit betreut von Prof. Dr. K. Sandhoff und Dr. U. Schepers an der Universität Bonn: "Entwicklung neuer <i>Delivery</i> -Strategien für siRNAs Von zellpenetrierenden Peptiden zu Peptoiden und Polyaminen als neuartige molekulare Transporter " |
| 31.07.2002 | Diplom |
| Jan 2002 - Jul 2002 | Diplomarbeit in Chemie in betreut von Prof. Dr. K. Sandhoff und Dr. U. Schepers an der Universität Bonn: "Herstellung von RNA-Peptid-Konjugaten für die RNA Interferenz in Säugerzellen" |
| Feb 2000 - Aug 2000 | 6monatiger Studienaufenthalt in der Gruppe von Dr. Peter Hore am Physical and Theoretical Chemistry Laboratory in Oxford, GB |
| 18.08.1999 | Vordiplom |
| Okt 1997 – Jul 2002 | Chemiestudium an der Universität Bonn |
| Sept 1988 - Jun 1997 | Bertha-von-Suttner Gymnasium, Andernach |
| Aug 1984 – Jun 1988 | Grundschule St. Stephan, Andernach |

Stipendien

| | |
|-------------|--|
| 2003-2005 | ideelle Förderung der Studienstiftung des deutschen Volkes |
| 2003 – 2004 | Doktorandenstipendium des Fonds der Chemischen Industrie |
| 2001 – 2002 | Stipendium der Theodor-Laymann-Stiftung |
| 2000 – 2002 | Stipendium der Fritz-ter-Meer-Stiftung |
| 1996 – 2002 | Stipendium der Studienstiftung des deutschen Volkes |